Hashemite Kingdom of Jordan

Jordan Journal of Biological Sciences

An International Peer-Reviewed Scientific Journal

Financed by the Scientific Research and Innovation Support Fund

This title is indexed in Scopus

http://jjbs.hu.edu.jo/

المجلة الأردنية للعلوم الحياتية
Jordan Journal of Biological Sciences (JJBS)
http://jjbs.hu.edu.jo

Jordan Journal of Biological Sciences (JJBS) (ISSN: 1995–6673 (Print); 2307-7166 (Online)):

An International Peer- Reviewed Open Access Research Journal financed by the Scientific Research and Innovation Support Fund, Ministry of Higher Education and Scientific Research, Jordan and published quarterly by the Deanship of Scientific Research , The Hashemite University, Jordan.

Submission Address

The Hashemite University
P.O. Box 330127, Zarqa, 13115, Jordan
Phone: +962-5-3903333 ext.
E-Mail: jjbs@hu.edu.jo

المجلة الاردنية للعلوم الحياتية
Jordan Journal of Biological Sciences (JJBS)
http://jjbs.hu.edu.jo

International Advisory Board (Arranged alphabetically)

Instructions to Authors

Scopes

Study areas include cell biology, genomics, microbiology, immunology, molecular biology, biochemistry, embryology, immunogenetics, cell and tissue culture, molecular ecology, genetic engineering and biological engineering, bioremediation and biodegradation, bioinformatics, biotechnology regulations, gene therapy, organismal biology, microbial and environmental biotechnology, marine sciences. The JJBS welcomes the submission of manuscript that meets the general criteria of significance and academic excellence. All articles published in JJBS are peer-reviewed. Papers will be published approximately one to two months after acceptance.

Type of Papers

The journal publishes high-quality original scientific papers, short communications, correspondence and case studies. Review articles are usually by invitation only. However, Review articles of current interest and high standard will be considered.

Submission of Manuscript

Manuscript, or the essence of their content, must be previously unpublished and should not be under simultaneous consideration by another journal. The authors should also declare if any similar work has been submitted to or published by another journal. They should also declare that it has not been submitted/ published elsewhere in the same form, in English or in any other language, without the written consent of the Publisher. The authors should also declare that the paper is the original work of the author(s) and not copied (in whole or in part) from any other work. All papers will be automatically checked for duplicate publication and plagiarism. If detected, appropriate action will be taken in accordance with International Ethical Guideline. By virtue of the submitted manuscript, the corresponding author acknowledges that all the co-authors have seen and approved the final version of the manuscript. The corresponding author should provide all co-authors with information regarding the manuscript, and obtain their approval before submitting any revisions. Electronic submission of manuscripts is strongly recommended, provided that the text, tables and figures are included in a single Microsoft Word file. Submit manuscript as e-mail attachment to the Editorial Office at: JJBS@hu.edu.jo. After submission, a manuscript number will be communicated to the corresponding author within 48 hours.

Peer-review Process

It is requested to submit, with the manuscript, the names, addresses and e-mail addresses of at least 4 potential reviewers. It is the sole right of the editor to decide whether or not the suggested reviewers to be used. The reviewers' comments will be sent to authors within 6-8 weeks after submission.
Manuscripts and figures for review will not be returned to authors whether the editorial decision is to accept, revise, or reject. All Case Reports and Short Communication must include at least one table and/ or one figure.

Preparation of Manuscript

The manuscript should be written in English with simple lay out. The text should be prepared in single column format. Bold face, italics, subscripts, superscripts etc. can be used. Pages should be numbered consecutively, beginning with the title page and continuing through the last page of typewritten material.

The text can be divided into numbered sections with brief headings. Starting from introduction with section 1. Subsections should be numbered (for example 2.1 (then 2.1.1, 2.1.2, 2.2, etc.), up to three levels. Manuscripts in general should be organized in the following manner:

Title Page

The title page should contain a brief title, correct first name, middle initial and family name of each author and name and address of the department(s) and institution(s) from where the research was carried out for each author. The title should be without any abbreviations and it should enlighten the contents of the paper. All affiliations should be provided with a lower-case superscript number just after the author's name and in front of the appropriate address.
The name of the corresponding author should be indicated along with telephone and fax numbers (with country and area code) along with full postal address and e-mail address.

Abstract

The abstract should be concise and informative. It should not exceed **350 words** in length for full manuscript and Review article and **150 words** in case of Case Report and/ or Short Communication. It should briefly describe the purpose of the work, techniques and methods used, major findings with important data and conclusions. No references should be cited in this part. Generally non-standard abbreviations should not be used, if necessary they should be clearly defined in the abstract, at first use.

Keywords

Immediately after the abstract, **about 4-8 keywords** should be given. Use of abbreviations should be avoided, only standard abbreviations, well known in the established area may be used, if appropriate. These keywords will be used for indexing.

Abbreviations

Non-standard abbreviations should be listed and full form of each abbreviation should be given in parentheses at first use in the text.

Introduction

Provide a factual background, clearly defined problem, proposed solution, a brief literature survey and the scope and justification of the work done.

Materials and Methods

Give adequate information to allow the experiment to be reproduced. Already published methods should be mentioned with references. Significant modifications of published methods and new methods should be described in detail. Capitalize trade names and include the manufacturer's name and address. Subheading should be used.

Results

Results should be clearly described in a concise manner. Results for different parameters should be described under subheadings or in separate paragraph. Results should be explained, but largely without referring to the literature. Table or figure numbers should be mentioned in parentheses for better understanding.

Discussion

The discussion should not repeat the results, but provide detailed interpretation of data. This should interpret the significance of the findings of the work. Citations should be given in support of the findings. The results and discussion part can also be described as separate, if appropriate. The Results and Discussion sections can include subheadings, and when appropriate, both sections can be combined

Conclusions

This should briefly state the major findings of the study.

Acknowledgment

A brief acknowledgment section may be given after the conclusion section just before the references. The acknowledgment of people who provided assistance in manuscript preparation, funding for research, etc. should be listed in this section.

Tables and Figures

Tables and figures should be presented as per their appearance in the text. It is suggested that the discussion about the tables and figures should appear in the text before the appearance of the respective tables and figures. No tables or figures should be given without discussion or reference inside the text.

Tables should be explanatory enough to be understandable without any text reference. Double spacing should be maintained throughout the table, including table headings and footnotes. Table headings should be placed above the table. Footnotes should be placed below the table with superscript lowercase letters. Each table should be on a separate page, numbered consecutively in Arabic numerals.

Each figure should have a caption. The caption should be concise and typed separately, not on the figure area. Figures should be self-explanatory. Information presented in the figure should not be repeated in the table. All symbols and abbreviations used in the illustrations should be defined clearly. Figure legends should be given below the figures.

References

References should be listed alphabetically at the end of the manuscript. Every reference referred in the text must be also present in the reference list and vice versa. In the text, a reference identified by means of an author's name should be followed by the year of publication in parentheses (e.g.(Brown,2009)). For two authors, both authors' names followed by the year of publication (e.g.(Nelson and Brown, 2007)). When there are more than two authors, only the first author's name followed by "*et al*." and the year of publication (e.g. (Abu-Elteen *et al*., 2010)). When two or more works of an author has been published during the same year, the reference should be identified by the letters "a", "b", "c", etc., placed after the year of publication. This should be followed both in the text and reference list. e.g., Hilly, (2002a, 2002b); Hilly, and Nelson, (2004). Articles in preparation or submitted for publication, unpublished observations, personal communications, etc. should not be included in the reference list but should only be mentioned in the article text (e.g., Shtyawy,A., University of Jordan, personal communication). Journal titles should be abbreviated according to the system adopted in Biological Abstract and Index Medicus, if not included in Biological Abstract or Index Medicus journal title should be given in full. The author is responsible for the sccuracy and completeness of the references and for their correct textual citation. Failure to do so may result in the paper being withdraw from the evaluation process. Example of correct reference form is given as follows:-

Reference to a journal publication:

Bloch BK. 2002. Econazole nitrate in the treatment of *Candida vaginitis*. *S Afr Med J.* , **58**:314-323.

Ogunseitan OA and Ndoye IL. 2006. Protein method for investigating mercuric reductase gene expression in aquatic environments. *Appl Environ Microbiol*., **64**: 695-702.

Hilly MO, Adams MN and Nelson SC. 2009. Potential fly-ash utilization in agriculture. *Progress in Natural Sci.*, **19**: 1173-1186.

Reference to a book:

Brown WY and White SR.1985. **The Elements of Style**, third ed. MacMillan, New York.

Reference to a chapter in an edited book:

Mettam GR and Adams LB. 2010. How to prepare an electronic version of your article. In: Jones BS and Smith RZ (Eds.), **Introduction to the Electronic Age**. Kluwer Academic Publishers, Netherlands, pp. 281–304.

Conferences and Meetings:

Embabi NS. 1990. Environmental aspects of distribution of mangrove in the United Arab Emirates. Proceedings of the First ASWAS Conference. University of the United Arab Emirates. Al-Ain, United Arab Emirates.

Theses and Dissertations:

El-Labadi SN. 2002. Intestinal digenetic trematodes of some marine fishes from the Gulf of Aqaba. MSc dissertation, The Hashemite University, Zarqa, Jordan.

Nomenclature and Units

Internationally accepted rules and the international system of units (SI) should be used. If other units are mentioned, please give their equivalent in SI.

For biological nomenclature, the conventions of the *International Code of Botanical Nomenclature, the International Code of Nomenclature of Bacteria,* and the *International Code of Zoological Nomenclature* should be followed.
Scientific names of all biological creatures (crops, plants, insects, birds, mammals, etc.) should be mentioned in parentheses at first use of their English term.

Chemical nomenclature, as laid down in the *International Union of Pure and Applied Chemistry* and the official recommendations of the *IUPAC-IUB Combined Commission on Biochemical Nomenclature* should be followed. All biocides and other organic compounds must be identified by their Geneva names when first used in the text. Active ingredients of all formulations should be likewise identified.

Math formulae

All equations referred to in the text should be numbered serially at the right-hand side in parentheses. Meaning of all symbols should be given immediately after the equation at first use. Instead of root signs fractional powers should be used. Subscripts and superscripts should be presented clearly. Variables should be presented in italics. Greek letters and non-Roman symbols should be described in the margin at their first use.

To avoid any misunderstanding zero (0) and the letter O, and one (1) and the letter l should be clearly differentiated. For simple fractions use of the solidus (/) instead of a horizontal line is recommended. Levels of statistical significance such as: $^{*}P < 0.05$, $^{**}P < 0.01$ and $^{***}P < 0.001$ do not require any further explanation.

Copyright

Submission of a manuscript clearly indicates that: the study has not been published before or is not under consideration for publication elsewhere (except as an abstract or as part of a published lecture or academic thesis); its publication is permitted by all authors and after accepted for publication it will not be submitted for publication anywhere else, in English or in any other language, without the written approval of the copyright-holder. The journal may consider manuscripts that are translations of articles originally published in another language. In this case, the consent of the journal in which the article was originally published must be obtained and the fact that the article has already been published must be made clear on submission and stated in the abstract. It is compulsory for the authors to ensure that no material submitted as part of a manuscript infringes existing copyrights, or the rights of a third party.

Ethical Consent

All manuscripts reporting the results of experimental investigation involving human subjects should include a statement confirming that each subject or subject's guardian obtains an informed consent, after the approval of the experimental protocol by a local human ethics committee or IRB. When reporting experiments on animals, authors should indicate whether the institutional and national guide for the care and use of laboratory animals was followed.

Plagiarism

The JJBS hold no responsibility for plagiarism. If a published paper is found later to be extensively plagiarized and is found to be a duplicate or redundant publication, a note of retraction will be published, and copies of the correspondence will be sent to the authors' head of institute.

Galley Proofs

The Editorial Office will send proofs of the manuscript to the corresponding author as an e-mail attachment for final proof reading and it will be the responsibility of the corresponding author to return the galley proof materials appropriately corrected within the stipulated time. Authors will be asked to check any typographical or minor clerical errors in the manuscript at this stage. No other major alteration in the manuscript is allowed. After publication authors can freely access the full text of the article as well as can download and print the PDF file.

Publication Charges

There are no page charges for publication in Jordan Journal of Biological Sciences, except for color illustrations,

Reprints

Ten (10) reprints are provided to corresponding author free of charge within two weeks after the printed journal date. For orders of more reprints, a reprint order form and prices will be sent with article proofs, which should be returned directly to the Editor for processing.

Disclaimer

Articles, communication, or editorials published by JJBS represent the sole opinions of the authors. The publisher shoulders no responsibility or liability what so ever for the use or misuse of the information published by JJBS.

Indexing

JJBS is indexed and abstracted by:

DOAJ (Directory of Open Access Journals)	CABI
Google Scholar	EBSCO
Journal Seek	CAS (Chemical Abstract Service)
HINARI	ETH- Citations
Index Copernicus	Open J-Gat
NDL Japanese Periodicals Index	SCImago
SCIRUS	Clarivate Analytics (Zoological Abstract)
OAJSE	Scopus
ISC (Islamic World Science Citation Center)	AGORA (United Nation's FAO database)
Directory of Research Journal Indexing (DRJI)	SHERPA/RoMEO (UK)
Ulrich's	

المجلة الأردنية للعلوم الحياتية
Jordan Journal of Biological Sciences (JJBS)
ISSN 1995- 6673 (Print), 2307- 7166 (Online)
http://jjbs.hu.edu.jo

The Hashemite University

Deanship of Scientific Research

TRANSFER OF COPYRIGHT AGREEMENT

Journal publishers and authors share a common interest in the protection of copyright: authors principally because they want their creative works to be protected from plagiarism and other unlawful uses, publishers because they need to protect their work and investment in the production, marketing and distribution of the published version of the article. In order to do so effectively, publishers request a formal written transfer of copyright from the author(s) for each article published. Publishers and authors are also concerned that the integrity of the official record of publication of an article (once refereed and published) be maintained, and in order to protect that reference value and validation process, we ask that authors recognize that distribution (including through the Internet/WWW or other on-line means) of the authoritative version of the article as published is best administered by the Publisher.

To avoid any delay in the publication of your article, please read the terms of this agreement, sign in the space provided and return the complete form to us at the address below as quickly as possible.

Article entitled:----------

Corresponding author: ----------

To be published in the journal: Jordan Journal of Biological Sciences (JJBS)

I hereby assign to the Hashemite University the copyright in the manuscript identified above and any supplemental tables, illustrations or other information submitted therewith (the "article") in all forms and media (whether now known or hereafter developed), throughout the world, in all languages, for the full term of copyright and all extensions and renewals thereof, effective when and if the article is accepted for publication. This transfer includes the right to adapt the presentation of the article for use in conjunction with computer systems and programs, including reproduction or publication in machine-readable form and incorporation in electronic retrieval systems.
Authors retain or are hereby granted (without the need to obtain further permission) rights to use the article for traditional scholarship communications, for teaching, and for distribution within their institution.

☐ **I am the sole author of the manuscript**

☐ **I am signing on behalf of all co-authors of the manuscript**

☐ **The article is a 'work made for hire' and I am signing as an authorized representative of the employing company/institution**

Please mark one or more of the above boxes (as appropriate) and then sign and date the document in black ink.

Signed:_____ **Name printed:** _____
Title and Company (if employer representative) : _____
Date: _____

Data Protection: By submitting this form you are consenting that the personal information provided herein may be used by the Hashemite University and its affiliated institutions worldwide to contact you concerning the publishing of your article.

Please return the completed and signed original of this form by mail or fax, or a scanned copy of the signed original by e-mail, retaining a copy for your files, to:

Hashemite University
Jordan Journal of Biological Sciences
Zarqa 13115 Jordan
Fax: +962 5 3903338
Email: jjbs@hu.edu.jo

EDITORIAL PREFACE

Jordan Journal of Biological Sciences (JJBS) is a refereed, quarterly international journal financed by the Scientific Research and Innovation Support Fund, Ministry of Higher Education and Scientific Research in cooperation with the Hashemite University, Jordan. JJBS celebrated its 12th commencement this past January, 2020. JJBS was founded in 2008 to create a peer-reviewed journal that publishes high-quality research articles, reviews and short communications on novel and innovative aspects of a wide variety of biological sciences such as cell biology, developmental biology, structural biology, microbiology, entomology, molecular biology, biochemistry, medical biotechnology, biodiversity, ecology, marine biology, plant and animal biology, plant and animal physiology, genomics and bioinformatics.

We have watched the growth and success of JJBS over the years. JJBS has published 11 volumes, 45 issues and 479 articles. JJBS has been indexed by SCOPUS, CABI's Full-Text Repository, EBSCO, Clarivate Analytics- Zoological Record and recently has been included in the UGC India approved journals. JJBS Cite Score has improved from 0.18 in 2015 to 0.58 in 2019 (Last updated on 16 March, 2020) and with Scimago Institution Ranking (SJR) 0.21 (Q3) in 2018.

A group of highly valuable scholars have agreed to serve on the editorial board and this places JJBS in a position of most authoritative on biological sciences. I am honored to have six eminent associate editors from various countries. I am also delighted with our group of international advisory board members coming from 15 countries worldwide for their continuous support of JJBS. With our editorial board's cumulative experience in various fields of biological sciences, this journal brings a substantial representation of biological sciences in different disciplines. Without the service and dedication of our editorial; associate editorial and international advisory board members, JJBS would have never existed.

In the coming year, we hope that JJBS will be indexed in Clarivate Analytics and MEDLINE (the U.S. National Library of Medicine database) and others. As you read throughout this volume of JJBS, I would like to remind you that the success of our journal depends on the number of quality articles submitted for review. Accordingly, I would like to request your participation and colleagues by submitting quality manuscripts for review. One of the great benefits we can provide to our prospective authors, regardless of acceptance of their manuscripts or not, is the feedback of our review process. JJBS provides authors with high quality, helpful reviews to improve their manuscripts.

Finally, JJBS would not have succeeded without the collaboration of authors and referees. Their work is greatly appreciated. Furthermore, my thanks are also extended to The Hashemite University and the Scientific Research and Innovation Support Fund, Ministry of Higher Education and Scientific Research for their continuous financial and administrative support to JJBS.

March, 2020

JJBS

Volume 13, Number 1, March .2020
ISSN 1995-6673

Jordan Journal of Biological Sciences

CONTENTS

Original Articles

Short Communication

JJBS

Jordan Journal of Biological Sciences

Volume 13, Number 1,March 2020
ISSN 1995-6673
Pages 1 - 6

Determining the Response to Statins in Rat Aorta Using High Fat Diet

Nurullahoglu-Atalik KE[1*], Yerlikaya Humeyra[2], Oz Mehmet[3] and Esen Hasan[4]

Department of [1]Pharmacology, [2] Biochemistry and [4] Pathology Meram Faculty of Medicine, University of Necmettin Erbakan, Konya, 42080, [3]Veterinary, İstanbul, Turkey

Received March 13, 2019; Revised April 10, 2019; Accepted April 18, 2019

Abstract

Atorvastatin and rosuvastatin, statins, inhibitors of 3-hydroxy-3-methylglutaryl-coenzyme A reductase are widely prescribed as lipid-lowering drugs. They also inhibit the RhoA-Rho-associated kinase pathway in vascular smooth muscle cells and inhibit smooth muscle function. It remains presently unknown whether vascular reactivity is influenced with a high fat diet. This study aimed to investigate the vascular responses to statins when rats were fed high fat diet. Adult rats were fed a normal diet or a high-fat diet (HFD) for four weeks. The relaxant effects of atorvastatin and rosuvastatin (10^{-9}-10^{-3} M) were tested against serotonin (5-HT; 10^{-6} M)-induced tone. To analyze the role of nitric oxide on the responses to statins, the concentration-response curves were also obtained in the presence of nitric oxide synthase inhibitor L-NAME (10^{-4} M). Statins, concentration-dependently relaxed aorta rings compared to control and fed a high-fat diet. The pIC_{50} values of aortas from rats fed a high fat diet to both atorvastatin and rosuvastatin were significantly lower than control groups. Preincubation with L-NAME significantly decreased the sensitivity to both statins. This finding suggests that acute vascular relaxant effects of these statins are importantly related with endothelial nitric oxide. Compared to the control group, high fat diet significantly reduced the luminal area of the aorta. Furthermore, the aorta wall thickness was significantly increased in high fat diet group. The results indicate that high fat diet affects vascular sensitivity to statins and morphology in rat aorta.

Keywords: Atorvastatin, High fat diet, Nitric oxide, Rat aorta, Rosuvastatin.

1. Introduction

High fat diet-induced hyperlipidemia is one of the most common risk factors worldwide associated with the development of atherosclerosis and coronary heart disease. Statins are the most widely prescribed medications for treatment of hyperlipidemia for over 20 years (Izadpanah and Schächtele, 2015).

Statins also have effects on vascular wall independent of their cholesterol lowering properties. Among the many effects attributed to statins, increased nitric oxide synthesis, vascular dilatation, anti-inflammatory and antithrombotic effects were described. Early findings obtained from clinical trials and experimental studies revealed that their beneficial effects are due to restoration of endothelial function (Beckman and Creager, 2006; Adam and Laufs, 2008). In vitro findings strongly suggested that increased bioavailability of, by upregulating and activating endothelial nitric oxide synthase or by decreasing its oxidative inactivation, mediate direct vasculoprotective effects of statins (Wagner *et al.,* 2000; Bonetti *et al*., 2003). A recent study showed that lovastatin and pravastatin stimulated endothelial nitric oxide production in bovine aortic endothelial cells (Datar *et al.,* 2010).

Lopez *et al* (2008) reported that, rosuvastatin, like other statins (Uydes-Dogan *et al.,* 2005), has vasodilator properties in rat aortic rings. Although, it is known that arteriosclerosis is closely associated with endothelial dysfunction and the consequent reduced production of its relaxant factors, especially nitric oxide, there is no report related to the role of high fat diet on rat aortic responses to statins. The investigators (Lopez-Canales *et al.,* 2015) also reported that vasorelaxant response to rosuvastatin was significantly greater in endothelium-intact than denuded aortic rings, which suggests that endothelium plays an important role in the vasorelaxant effect produced by rosuvastatin. Moreover, the fact that the vasorelaxant response to rosuvastatin was significantly greater in aortic rings from rats with a standard diet than in aortic rings from rats with a cafeteria-style (CAF) diet suggests that endothelial dysfunction could be involved in the inhibitory effect produced by a CAF diet. Moreover, Qin *et al* (2018) reported that high fat diet induced significant attenuation in the nitric oxide-dependent relaxation to acetylcholine of rat aortic rings. The investigators also suggested that nitric oxide produced by endothelium was inhibited by high-fat diet. However, no study has yet analysed the effect of high fat diet on the statins-induced vascular responses.

Although statins have some pleiotropic effects on vascular wall, and these nonlipid-properties might be important to prevent some cardiovascular events, there is no study on how high-fat diets affect the direct vascular responses to these drugs. Therefore, in this study we aimed

* Corresponding author e-mail: esraatalik@hotmail.com.

to investigate whether high fat diet has effects on atorvastatin and rosuvastatin-induced vasodilation in thoracic aorta rings of high fat diet-treated rats.

2. Materials and Methods

2.1. Drugs

Serotonin chloride, N^G nitro-L-arginine methyl ester, acetylcholine chloride (dissolved in distilled water) and atorvastatin, rosuvastatin (dissolved in dimethyl sulphoxide) were used. The concentration of dimethyl sulphoxide in the tissue bath was always kept below 0.4%. Serotonin chloride, N^G nitro-L-arginine methyl ester and acetylcholine chloride were obtained from Sigma (St. Louis, MO, USA). Atorvastatin and rosuvastatin were kindly provided by Abdi İbrahim Drug Industry (Istanbul, Turkey).

2.2. Animals and preparation of aortic rings

Fourteen male Wistar rats, weighing 259,36 ± 28,3 g and aged 8-12 weeks, were obtained from Necmettin Erbakan University Experimental Medicine Research and Application Center (Konya, Turkey). The rats were housed in a climate controlled room (22 ± 2 °C temperature and 50 ± 5% humidity) on a 12/12 h light/dark cycle (lights on between 07:00 and 19:00), with ad libitum food and fresh water. The experimental animals were randomly divided into two groups (n=7 for each group) and fed with either standard rat chow, or high-fat diet (Bravo *et al.,* 2014), for a period of 4 weeks. The caloric value of food intake was determined on the basis of 35% of total calorie intake for the high fat diet group rats (Table 1). Body weights before and after four weeks were recorded (Table 2). All animals were sacrificed after an overnight fasting by cervical dislocations.

Prior permission for animal experimentation was obtained from the Experimental Medicine Research and Application Center Ethics Committee of Necmettin Erbakan University (15-020).

2.3. Experimental design

Rats were sacrificed by cervical dislocations. The descending thoracic aorta was quickly isolated, cleaned and sectioned into 3- to 4-mm-long rings. The rings were then placed in organ baths containing 15 m l Krebs-Henseleit solution (KHS, mM: NaCl 119, KCl 4.70, $MgSO_4$ 1.50, KH_2PO_4 1.20, $CaCl_2$ 2.50, $NaHCO_3$ 25, Glucose 11), which were thermoregulated at 37 ºC and aerated (95% O_2 and 5% CO_2).

Changes in isometric tension of aortic rings were recorded using a four-channel force-displacement transducer (BIOPAC MP36, Santa Barbara, California, USA) connected through amplifiers to a ITBS08 Integrated Tissue Bath System (Commat, Ankara, Turkey). Endothelium intact rings were used. After the stabilization period, isometric contraction was induced by serotonin (5-hydroxytryptamine, 5-HT) (10^{-6} M) and acetylcholine (ACh, 10^{-6} M) was added to verify the integrity of the endothelium. The vascular endothelium was considered complete when the aortic rings showed relaxation ≥ 50%. Then, the rings were washed and rested; to evaluate the effect of atorvastatin or rosuvastatin on vascular tension, rat aorta rings from seven different preparations were exposed to 5-HT (10^{-6} M) to induce constriction. Atorvastatin or rosuvastatin (10^{-9}-10^{-3} M) was added after the maximal vasoconstrictive response to 5-HT had been achieved. T o determine the role of nitric oxide, the relaxant effect of atorvastatin or rosuvastatin was investigated in the presence of nitric oxide synthase inhibitor N^G nitro-L-arginine methyl ester (L-NAME, 10^{-4} M). L-NAME had been added to the organ bath 20 min before statin concentration-response curves were obtained.

In another part of the study, the same procedure was repeated in the aortas from HFD-treated rats in the absence and presence of L-NAME (10^{-4} M).

2.4. Analysis of blood parameters

Blood was immediately collected at the end of experiment and centrifuged at 3000 rpm for 15 min at 4 °C. Serum was stored at -70 °C until used in assays. Serum triglyceride (TG), cholesterol (Chol) and HDL levels were determined using commercial kits (Table 2).

2.5. Histological morphometric analysis of thoracic aorta

Thoracic aorta samples were obtained after rats were sacrificed at the end of experiment. After formaldehyde fixation, the entire thoracic aorta was sectioned at 5 segments of 4 mm each. Tissues were embedded in paraffin, cut into 4-6 µm thick sections and stained by Hematoxylin and Eosin. Measurements of the thoracic aorta cross-sectional area, were made in a single-blind fashion by pathologist.

Morphometric measurements on all five segments of aorta were performed by using the Image Analysis System (BAB Bs200ProP Image Processing and Analysis System, Ankara, Turkey). The luminal area (μm^2) and wall thickness (µ) were calculated from the perimeter of the luminal border. The luminal area and wall thickness for each thoracic aorta were obtained by averaging these measurements. The mean ± SE value for a p articular vessel, after averaging five consecutive thoracic aorta segment values for cross-sectional area, was obtained.

2.6. Statistical analysis

Relaxation responses to atorvastatin or rosuvastatin were expressed as percentages of the 5-HT (10^{-6} M) induced contraction. Concentrations of atorvastatin or rosuvastatin causing 50% of the maximal response (IC_{50}) were calculated from each individual concentration-response curves; pIC_{50} values were determined as -log IC_{50}.

Statistical analysis was performed by using Mann-Whitney U and unpaired Student's t-test where appropriate. Statistical significance was set at $P < 0.05$. All the data were expressed as mean ± SEM.

3. Results

3.1. Body weights and plasma lipid profile of rats fed a standard or high-fat diet

The effect of a high fat diet on body weight and the serum lipid profile levels in male rats is shown in Table 2. A modest nonsignificant increase in body weight was observed in rats fed a high-fat diet for a period of four weeks compared with rats fed a s tandard diet. A significantly higher level of plasma cholesterol and triglyceride levels were observed in rats fed with a high fat

diet ($P < 0.05$). No difference was observed in high-density lipoprotein (HDL) levels between groups ($P > 0.05$).

3.2. Effect of atorvastatin on 5-HT-precontracted rat aortic rings

Figure 1 shows the effects of cumulative addition of atorvastatin on 5-HT-pre-contracted aortic rings from rats with either a standard diet or a high fat diet. In all animals, (10^{-9}-10^{-3} M) atorvastatin elicited concentration-dependent vasorelaxation in aortic rings, regardless of whether the animals were fed a standard diet or a high fat diet. The pIC_{50} value in 5-HT-precontracted aortic rings from rats given a standard diet was 5.27 ± 0.20. Pre-treatment with nitric oxide synthase inhibitor L-NAME (10^{-4} M) produced a rightward shift of the atorvastatin curve in control group (pIC_{50} value was 4.77 ± 0.15). In aortas from rats fed high fat diet the pIC_{50} value (4.60 ± 0.10) was significantly lower than control group. In high fat diet group, pre-incubation with L-NAME significantly decreased the pIC50 value to atorvastatin (4.24 ± 0.20, Table 3).

3.3. Effect of rosuvastatin on 5-HT-precontracted rat aortic rings

As shown in Figure 2, the effect of cumulative addition of rosuvastatin on 5 -HT-precontracted aortic rings from rats with either a standard diet or a high fat diet. In all animals, rosuvastatin (10^{-9}-10^{-3} M) elicited concentration-dependent vasorelaxation of aortic rings, regardless of whether the animals were fed a standard diet or a high fat diet. In control rats the pIC_{50} value was 5.82 ± 0.10. L-NAME- pretreatment significantly decreased the sensitivity to rosuvastatin in control group (Table 3). In rats fed high fat diet, the pIC_{50} value was significantly lower than control (4.95 ± 0.23, $p < 0.05$). The pIC_{50} value (4.29 ± 0.16) of aortic rings after L-NAME treatment significantly reduced in high fat diet rats. These results demonstrate that inhibition of nitric oxide synthesis significantly decreased the sensitivity of aorta to rosuvastatin in both control and high fat diet rats.

3.4. Analysis of aorta wall thickness and lumen diameter

The mean values for the measurements of aortic wall thickness and lumen diameter were analysed statistically; confidence interval was assessed at 95%. The aorta wall thickness was significantly increased in high fat diet group (99.3 ± 2.8 µm) compared to control (88.0 ± 2.6 µm) ($P < 0.05$). The average luminal areas of rat aorta were found to be 1612290.0 ± 18090.4 μm^2 in control and 1501073.0 ± 26016.2 μm^2 in high fat diet group (Figure 3). The luminal area of the high fat diet group decreased significantly compared to the control ($P < 0.05$).

Table 1. Compositions and energy loads of the diets.

	Standard		High Fat	
	% of weight	% of total energy	% of weight	% of total energy
Casein	20	25.6	20	22.5
Starch	63	59.4	51.3	42.5
Vegetable oil/tallow*	7	15	18.7	35
Fibers	5	-	5	-
Vitamin and mineral mix	4.5	-	4.5	-
Total energy (gross kcal/g)	4.4	-	5	-

*Vegetable oil was used in the standard diet, whereas in the high-fat diet tallow was used.

Table 2. Characteristics of rats after four weeks of normal (control) and high-fat diet (HFD).

	Control	HFD
Triglyceride (mg/dl)	60.71 ± 5.8	93.57 ± 9.6*
Cholesterol (mg/dl)	53.85 ± 2.6	60.71 ± 1.5*
HDL (mg/dl)	32.67 ± 2.1	33.72 ± 1.2
Initial body weight (g)	267.43 ± 11.2	265.00 ± 9.9
Final body weight (g)	339.14 ± 16.9	343.86 ± 11.7
Weight gain (g)	71.71 ± 21.6	78.85 ± 17.6

Values are means ± SD. Each value is derived from seven rats. *$P < 0.05$, significant difference.

Table 3. pIC_{50} (- log IC_{50}) values for atorvastatin and rosuvastatin (10^{-9}- 10^{-3}M) in 10^{-6} M 5-HT-precontracted aortas from control, L-NAME-incubated, HFD-treated and L-NAME-incubated HFD-treated rats.

	pIC_{50}	
	Atorvastatin	Rosuvastatin
Control	5.27 ± 0.20	5.82 ± 0.10
L-NAME	4.77 ± 0.15*	4.95 ± 0.23*
HFD	4.60 ± 0.10*	4.54 ± 0.25*
HFD-L-NAME	4.24 ± 0.20**	4.29 ± 0.16**

Values are mean ± SD. Each value is derived from seven experiments.

*Statistically significant ($P < 0.05$) compared with control.

** Statistically significant ($P < 0.05$) compared with HFD.

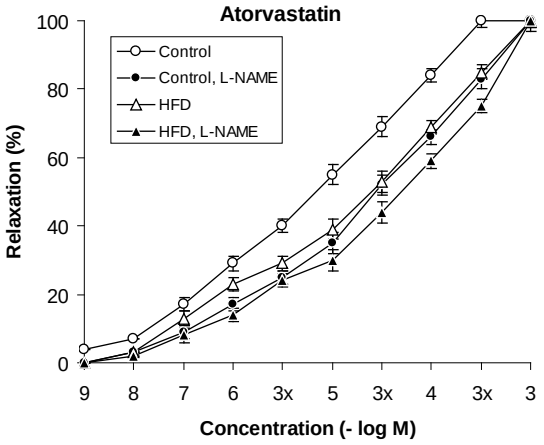

Figure 1. Concentration-response curves showing relaxations induced by atorvastatin (10^{-9}- 10^{-3} M) in 5-HT-precontracted rat thoracic aortas from control, L-NAME-incubated, HFD-treated and L-NAME-incubated HFD-treated rats. Each point represents the mean ± SD expressed as percentage of the tension developed by 10^{-6} M 5-HT. Each value is derived from seven experiments.

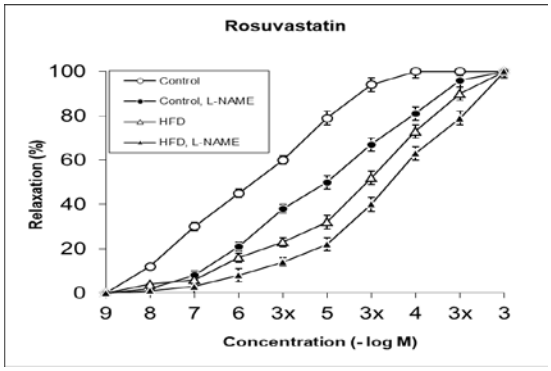

Figure 2. Concentration-response curves showing relaxations induced by rosuvastatin (10^{-9}- 10^{-3} M) in 5-HT-precontracted rat thoracic aortas from control, L-NAME-incubated, HFD-treated and L-NAME-incubated HFD-treated rats. Each point represents the mean ± SD expressed as percentage of the tension developed by 10^{-6} M 5-HT. Each value is derived from seven experiments.

Figure 3 A. Luminal area in control rat aorta.

Figure 3 B. Luminal area in high fat diet treated rat aorta.

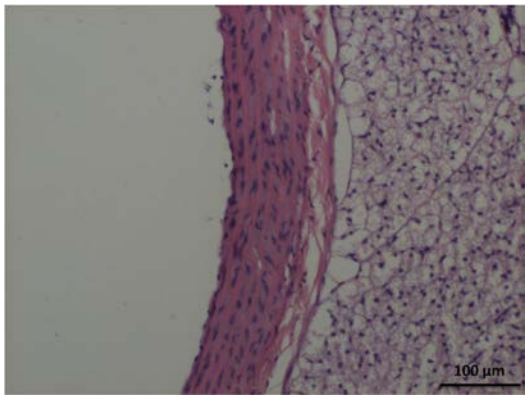

Figure 4 A. Wall thickness in control aorta.

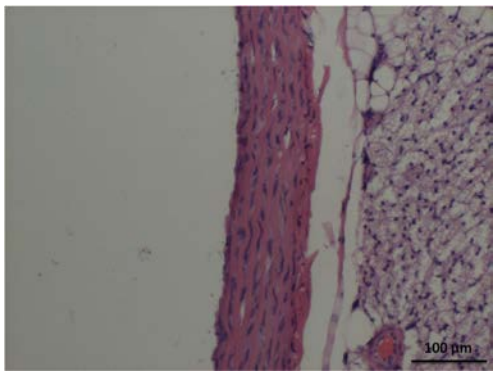

Figure 4 B. Wall thickness in high fat diet treated aorta.

4. Discussion

Atorvastatin and rosuvastatin have acute relaxant effect on rat thoracic aorta smooth muscle, which is in agreement with previous reports evaluating the vascular effects of different statins on isolated rat aortic rings (Lopez *et al.,* 2008). Furthermore, the principal finding of this study was high-fat diet could influence the responses to statins in vascular smooth muscle. We observed that the sensitivities to both atorvastatin and rosuvastatin were decreased in rats fed with a high fat diet. Overall, this study indicates that high fat diet for 4 weeks promotes vascular and histologic alterations.

Statins induce acute vasorelaxation that is independent of their lipid-lowering action which may contribute to the overall benefits of these drugs in the treatment of cardiovascular disease (Sun *et al.,* 2009; Qin *et al.,* 2018). It has even been reported that the effects of statins appear to be diverse and depend upon the vasculature studied (Corsini *et al.,* 1998; John *et al.,* 2001). Our results indicate that both atorvastatin and rosuvastatin-induced concentration-dependent relaxation of 5-HT-contracted rat aortas. Furthermore, the potencies of both statins were similar in each groups. 5-HT induces smooth muscle contraction and 5-HT2A, a G protein-coupled receptor, mediates 5-HT contractions in rat thoracic aorta (Banes *et al.,* 1999). It activates phospholipase C via Gq resulting in IP_3 and DAG formation, which induces protein kinase C and Ca^{2+} entry through voltage-operated Ca^{2+} channels. In the present study, atorvastatin and rosuvastatin both inhibited the contractions induced by 5-HT in a concentration-dependent manner. This result suggests that atorvastatin and rosuvastatin can inhibit the vasocontraction induced by extracellular Ca^{2+} entry via the voltage-operated Ca^{2+} channel pathway. The result of the present study is in agreement with previous reports evaluating the vascular effects of different statins on isolated rat aortic rings (Uydes-Dogan *et al.,* 2005; López *et al*., 2008; Lopez-Canales *et al*., 2015; Nurullahoglu-Atalik *et al.,* 2017). Furthermore, in this study both atorvastatin and rosuvastatin produced similar responses.

It is known that endothelial nitric oxide is important for vasodilation, and it has been well established that statins improve the endothelial function, especially by enhancing nitric oxide production in a manner not only dependent on but also independent of its cholesterol-lowering effect in humans and animal models (Bellosta *et al.,* 2000; Lefer *et al.,* 2001). In this study we have shown that incubation with the nitric oxide synthase inhibitor, L-

NAME, abolished the vascular smooth muscle relaxation elicited by atorvastatin and rosuvastatin in control rings. Similarly, Uydes-Dogan *et al* (2005) reported that incubation of the aortic rings with nitric oxide synthase inhibitor L-NOARG significantly attenuated the acute vasorelaxation induced by pravastatin, atorvastatin and cerivastatin on isolated rat aorta. Furthermore, lovastatin (Bravo and Herrera, 1998), serivastatin (Mukai *et al.,* 2003) and fluvastatin (Yaktubay-Dondas *et al.,* 2011) also produced vascular relaxations on isolated vessel rings; however, a significant differential was observed in their response profile in terms of endothelium dependency. Bravo and Herrera (1998) reported that lovastatin is capable of relaxing the rat aorta independently of the presence of endothelium. On the other hand, we previously observed that rosuvastatin induced endothelium-dependent relaxations in calf cardiac vein (Nurullahoglu-Atalik *et al.,* 2015). Likewise, in this study, our findings suggested that both atorvastatin and rosuvastatin-induced responses were, partly nitric oxide-dependent.

In the present study, the high fat diet produced a rightward shift in atorvastatin and rosuvastatin concentration-response curves with no suppression of maximum effect. Although, it is known that endothelial dysfunction often accompanies the hyperlipidemic state, there is no in vitro report related to the role of high fat diet on rat aortic responses to statins. In literature, the effects of high fat diet on vascular responses to different agents were investigated in statin-treated rats for a while (Choi *et al.,* 2016; Xu *et al.,* 2014), but in this study direct effects of statins in aortas from rats fed with high fat diet those pre-contracted with 5-HT were analyzed. Therefore, to the best of our knowledge, this is the first study that suggested the direct vascular effects of atorvastatin and rosuvastatin in rats fed with high fat diet for four weeks.

Changes in the aorta wall thickness are significantly associated with serum lipid profiles and hypertension, which begins in childhood and may develop into cardiovascular disease (Davis *et al.,* 2001; McGill *et al.,* 2001). Atherosclerotic plaque formation in the vessel causes increased wall thickness. In this study, the aorta wall thickness was only slightly increased in high fat diet group than control. This suggests that high fat diet treatment may have led to the development of atherosclerotic plaques. Our results also demonstrate that rats fed with high fat diet decreased the luminal areas of rat aortas compared to the control groups. To the best of our knowledge, the results are the first demonstration that high fat diet-treatment significantly affected the aortic morphology and relaxations induced by atorvastatin and rosuvastatin in rats but we have no explanation for this phenomenon. The results of this study also showed an increase in vessels wall thickness, as Pashaie *et al.*(2017) reported in aortas from rats fed with a high cholesterol diet for six months.

5. Conclusion

In the present study, we demonstrated that atorvastatin and rosuvastatin can acutely induce vasorelaxation on precontracted aortic rings via nitric oxide-dependent mechanisms. The results indicate that high fat diet treatment affects vascular sensitivity and morphology in rat aorta.

Conflict of interest

The Authors declare that there is no conflict of interest with this work and the preparation of the paper.

References

Adam O and Laufs U. 2008. Antioxidative effects of statins. *Arch Toxicol.,* **82**:885-892.

Banes A, Florian JA and Watts SW. 1999. Mechanisms of 5-hydroxytryptamine (2A) receptor activation of the mitogen-activated protein kinase pathway in vascular smooth muscle. *J Pharmacol Exp The.,* **291**:1179-1187.

Beckman JA and Creager MA. 2006.The nonlipid effects of statins on endothelial function. *Trends Cardiovasc Med.*, **16**: 156-162.

Bellosta S, Ferri N, Bernini F, Paoletti R and Corsini A. 2000. Non-lipid-related effects of statins. *Ann Med.*, **32**:164-176.

Bonetti PO, Lerman LO, Napoli C and Lerman A. 2003. Statin effects beyond lipid lowering-are they clinically relevant? *Eur Heart J.*, **24**:225-248.

Bravo L and Herrera MD.1998. Cardiovascular effects of lovastatin in normotensive and spontaneously hypertensive rats. *Gen Pharm.,* **30**:331-336.

Bravo R, Cubero J, Franco L, Mesa M, Galan C and Rodriguez AB. 2014. Body weight gain in rats by a high-fat diet produces chrono disruption in activity/inactivity circadian rhythm. *Chronobiol Int.,* **3**1:363-370.

Choi HK, Won EK and Choung SY. 2016. Effect of Coenzyme Q10 Supplementation in Statin-Treated Obese Rats. *Biomol Ther. (Seoul),* **24**:171-177.

Corsini A, Franco P, Lorenzo A, Pascal P, Fumagalli R, Paoletti R and Sirtori CR. 1998. Direct effects of statins on the vascular wall. *J Cardiovasc Pharmacol.*, **31**:773-778.

Datar R, Kaesemeyer WH, Chandra S, Fulton DJ and Caldwell RW. 2010. Acute activation of eNOS by statins involves scavenger receptor-B1, G protein subunit Gi, phospholipase C and calcium influx. *Br J Pharmacol.,* **160**:1765-1772.

Davis PH, Dawson JD, Riley WA and Lauer RM. 2001. Carotid intimal-medial thickness is related to cardiovascular risk factors measured from childhood through middle age: The Muscatine study. *Circulation*, **104**:2815-2819.

Izadpanah R and Schächtele DJ. 2015. The impact of statins on biological characteristics of stem cells provides a novel explanation for their pleiotropic beneficial and adverse clinical effects. *Am J Physiol Cell Physiol.,* **309**:522-531.

John S, Delles H, Jacobi J, Schlaich MP, Schneider M, Schmitz G and Schmieder RE. 2001.Rapid improvement of nitric oxide bioavailability after lipid-lowering therapy with cerivastatin within two weeks. *J Am Coll Cardiol.,* **37**:1351-1358.

Lefer AM, Scalia R and Lefer DJ. 2001.Vascular effects of HMG CoA-reductase inhibitors (statins) unrelated to cholesterol lowering: new concepts for cardiovascular disease. *Cardiovasc Res.*, **49**:281-287.

López J, Mendoza R, Cleva Villanueva G, Martínez G, Castillo EF and Castillo C. 2008 . Participation of K^+ channels in the endothelium-dependent and endothelium-independent components of the relaxant effect of rosuvastatin in rat aortic rings. *J. Cardiovasc Pharmacol Ther.*, **13**:207-213.

López-Canales JS, Lozano-Cuenca J, López-Canales OA, Aguilar-Carrasco JC, Aranda-Zepeda L, López-Sánchez P, Castillo-Henkel EF, López-Mayorga RM and Valencia-Hernández I. 2015. Pharmacological characterization of mechanisms involved in the vasorelaxation produced by rosuvastatin in aortic

rings from rats with a cafeteria-style diet. *Clin Exp Pharmacol Physiol.,* **42**:653-661.

McGill HC, McMahan CA, Zieske AW, Malcom GT, Tracy RE and Strong JP. 2001. Effects of nonlipid risk factors on atherosclerosis in youth with a favorable lipoprotein profile. *Circulation,* **103**:1546-1550.

Mukai Y, Shimokawa H, Matoba T, Hiroki J, Kunihiro I and Fujiki T. 2003. Acute vasodilator effects of HMG-CoA reductase inhibitors: Involvement of PI3-kinase/Akt pathway and Kv channels. *J Cardiovasc Pharmacol.,* **43**:118-124.

-Nurullahoglu-Atalik KE, Kutlu S, Solak H and Koca RO. 2017. Cilostazol enhances atorvastatin-induced vasodilation of female rat aorta during aging. *Physiol Int.,* **104**:226-234.

Nurullahoglu-Atalik KE, Oz M and Shafiyi A. 2015. Rosuvastatin-induced responses in calf cardiac vein. *Bratisl Lek Listy*,.**116**:494-498.

Pashaie B, Hobbenaghi R and Malekinejad H. 2017. Anti-atherosclerotic effect of *Cynodon dactylon* extract on experimentally induced hypercholesterolemia in rats. *Vet Res Forum,* **8**:185-193.

Qin L , Zhao Y , Zhang B and Li Y. 2018. Amentoflavone improves cardiovascular dysfunction and metabolic abnormalities in highfructose and fat diet-fed rats. *Food Func.*, **9**:243-252.

Sun YM, Tian Y ,Li X, Liu YY, Wang LF, Li J, Li ZQ and Pan W. 2009.Effect of atorvastatin on expression of IL-10 and TNF-alpha mRNA in myocardial ischemia-reperfusion injury in rats. *Biochem Biophys Res Commun.*, **382**:336-340.

Uydes-Dogan S, Topal G, Takir S and Ozdemir O. 2 005. Relaxant effects of pravastatin, atorvastatin and cerivastatin on isolated rat aortic rings. *Life Sci.*, **76**:1771-1786.

Wagner AH, Köhler T, Rückschloss U, Just I and Hecker M. 2000. Improvement of nitric oxide-dependent vasodilatation by HMG-CoA reductase inhibitors through attenuation of endothelial superoxide anion formation. *Arteriosclerosis, Thrombosis and Vasc Biol.*, **20**:61-69.

Xu QY, Liu YH, Zhang Q, Ma B, Yang ZD, Liu L, Yao D, Cui GB, Sun JJ and Wu ZM. 2014. Metabolomic analysis of simvastatin and fenofibrate intervention in high-lipid diet-induced hyperlipidemia rats. *Acta Pharmacol Sin.*, **35**:1265-1273.

Yaktubay Dondaş N, Sucu N, Coskun Yilmaz B, Kaplan HM, Ozeren M, Karaca MK, Vezir O and Singirik E. 2011.Molecular mechanism of vasorelaxant and antiatherogenic effects of the statins in the human saphenous vein graft. *Eur J Pharmacol.*, **666**:150-157.

JJBS
Jordan Journal of Biological Sciences

Volume 13, Number 1,March 2020
ISSN 1995-6673
Pages 7 - 12

Evaluation of Putative Inducers and Inhibitors toward Tyrosinase from two *Trichoderma* species

Hamed M. El-Shora[1*] and Reyad M. El-Sharkawy[2]

[1]*Botany Department, Faculty of Science, Mansoura University, Dakahlia;* [2]*Botany and Microbiology Department, Faculty of Science, Benha University, Al Qaliobia, Egypt*

Received January22, 2019; Revised April 13, 2019; Accepted April 24, 2019

Abstract

The present investigation deals with the purification of extracellular tyrosinase produced by *Trichoderma reesei* and *Trichoderma harzianum* and the characterization of putative inducers and inhibitors on the enzyme activity. Tyrosinase enzyme from *T. reesei* and *T. harzianum* was purified to homogeneity using ammonium sulphate precipitation (85%) followed by DEAE-cellulose, and phenyl Sepharose. SDS-PAGE exhibited a single band of 45 and 65 kDa for the purified tyrosinase from *T. reesei* and *T. harzianum*, respectively. The influence of guaiacol, catechol, vanillin, caffeic acid, syringaldazine and *p*-coumaric acid on purified enzyme was tested. Tyrosinase produced by the two Trichoderma species displayed a dose-dependent response toward all tested inducers. The effect of kojic acid, cinnamic acid, sodium azide, benzaldehyde and potassium cyanide was assayed at pH 5.0 in presence of monophenolic substrate (*p*-coumaric acid) and diphenolic substrate (caffeic acid). KCN and kojic acid were the powerful inhibitors on the tyrosinase-monophenolase and diphenolase activities from the investigated *Trichoderma*, respectively. The rate of tyrosinase activity showed a pseudo-first-order reaction kinetics and was proportional to the inhibitor concentration. The results reveal the possibility of using the inducers of tyrosinase to increase its activity.

Keywords: *Trichoderma*, Tyrosinase, SDS-PAGE, Inducers, Inhibitors.

1. Introduction

Tyrosinases (EC 1.14.18.1) are binuclear metallo-enzymes containing copper. Tyrosinases catalyze two different oxidation reactions through performing two functionality enzyme activities. Firstly, monophenols oxidize to *o*-diphenols (monophenolase activity). Secondly, *p*-substituted *o*-diphenols are oxidized to the *o*-quinones (diphenolase activity). In both oxidation reactions, oxygen acts as a terminal electron acceptor with the concomitant reduction to water and the formation of free radicals (El-Shora and Metwally, 2008; Fairhead and Thony-Meyer, 2012; Pretzler *et al*., 2017; Wang *et al*., 2018).

Tyrosinases as common enzymes in nature are widely distributed among plants, animals and microbes (Chang, 2009; Nawaz *et al*., 2017). It can perform various functions for plants, like production of lignin, tannins and flavonoids compounds as well as control of redox potential in plant respiration process (Marusek *et al*., 2006; Selinheimo *et al*., 2007a) and for humans, like melanin production (Zaidi *et al*., 2014; Wang *et al*., 2018). The majority of fungal tyrosinases are intracellular enzymes (Kong *et al*. 2000; Nakamura *et al*. 2000; Nawaz *et al*., 2017). However, the extracellular fungal tyrosinases have also been characterized (Montiel *et al*., 2004). The best characterized intracellular tyrosinase is derived from *A. bisporus* and *Neurospora crassa* (Ismaya *et al*., 2011), while the best characterized extracellular enzyme is derived from *Trichoderma reesei* (Selinheimo *et al*., 2006).

Several compounds may elicit a p ositive effect on tyrosinase production. These compounds are called inducers which include phenolic, aromatic compounds and metal ions. Substrates-specificity range varies from one type of tyrosinase to another. The variation of tyrosinase physiological functions may be the result of substrate specificity of tyrosinase. Tyrosinases are capable of oxidizing an extensive range of phenolic compounds. Tyrosinases can also oxidize peptide- and protein-containing a tyrosyl residues (Gasowska *et al*. 2004; Halaouli *et al*. 2005; Selinheimo *et al*. 2007a,b).

Endogenous tyrosinase oxidizes the phenolic compounds found in fruit and vegetables tissues. Tyrosinase-catalyzed browning reaction cause harmful changes in food appearance and properties (Lertsiri *et al*., 2003; Nawaz *et al*., 2017). Browning reactions cause a subsequent shortening of a product's shelf life. Anti-browning agents offer protection for the plant parts against toxic phenolic compounds. They may be either enzyme inhibitors or reducing agents. The elementary step in oxidation reaction of a phenolic compounds by tyrosinase can be suppressed or prevented by various enzyme inhibitors (Seo *et al*. 2003; Kim and Uyama 2005; Chang, 2009).

* Corresponding author e-mail: shoraem@yahoo.com.

Since there is little information about tyrosinase, particularly from *Trichoderma harzianum*, the present work focused on the purification and evaluation of the substrate-specificity of tyrosinase obtained from *Trichoderma reesei* and *Trichoderma harzianum*. In addition, the effects of various putative inhibitors on *Trichoderma* tyrosinase were evaluated.

2. Materials and Methods

2.1. Chemicals

All products were of analytical grade and obtained from different companies such as Sigma-Aldrich, Fluka and Merk.

2.2. Microorganism and culture maintenance

The investigated two fungi, *Trichoderma reesei* and *Trichoderma harzianum*, were provided from the Culture Collection and Identification Unit at the Regional Center for Mycology and Biotechnology, Al- Azhar University, Egypt. Fungal strains were grown on malt extract broth supplemented with phenol (pH 7.0). Cultures were inoculated in 100 mL medium and incubated for 3 days at 27 °C with shaking at 180 rpm. For extended periods of storage, fungi were sub-cultured periodically on malt extract agar plates.

2.3. Enzyme preparation

Fungal mycelium (30g) was collected through filtration using Whatman filter paper No. 1 (Whatman, Piscataway, NJ, USA). Mycelium debris was removed through centrifugation for 10 min at 10,000 rpm under 4 °C. The resulting clear supernatant was pooled, representing the cell free extract and stored at -20 °C for further work (Selinheimo *et al*., 2006).

2.4. Enzyme assay

Tyrosinase activity was measured with 2 mL L-tyrosine as the substrate (Ikehata and Nicell, 2000). Activity assays were proceeding in 50 M potassium phosphate buffer (pH 7.0) at 25 °C. The crude tyrosinase extract (1 mL) was added to reaction mixture. After incubation for 10 min at temperature of 25 ° C, the absorbance was assayed spectrophotometrically at 505 nm. One activity unit was expressed as the amount of enzyme oxidizing 1 µmol of the L-tyrosine using the standard assay conditions (Selinheimo *et al*., 2009).

2.5. Protein determination

The enzyme protein content was determined by the method of Lowry *et al*. (1951).

2.6. Enzyme purification

Tyrosinase purification was carried out according to Munjal and Sawhney (2002). Crude culture supernatant was resuspended in 50 mM of Tris-HCl buffer (pH 7.5). NH_4 $(SO_4)_2$ was added to the cell free extract to different 40-90% saturations with gentle stirring for 1 h and centrifuged for 30 min at 10,000 g. The precipitate was dialyzed overnight in dialysis bag against 50 mM Tris-buffer (pH 7.5) prepared with 0.15 M NaCl.

The concentrated enzyme preparation was deposited onto a DEAE-cellulose column with flow rate: 17.5 by 1.6 cm, 1 mL min^{-1}, pre-equilibrated with Tris-HCl buffer (100 mM, pH 6.5) and bound protein was then eluted with Tris-buffer (100 mM, pH 6.5) supplemented with 0.1-0.5 M NaCl gradient. Active fractions exhibiting tyrosinase activity were collected, dialyzed and equilibrated with the same buffer prepared with Tris-buffer (100 mM, pH 6.5). The active fractions with the highest enzyme activity were separated by loading onto a Phenyl-Sepharose column, pre-equilibrated with Tris-buffer (100 mM, pH 6.5) and later used for assay.

2.7. SDS-PAGE of purified enzyme

The molecular homogeneity of the purified tyrosinase was detected by one dimensional SDS-PAGE and gel was stained with Coomassie blue (Zaidi *et al*., 2014).

2.8. Tyrosinase induction

A variety of chemical compounds was examined for the substrate-specificity of tyrosinase from *T. reesei* and *T. harzianum*. Guaiacol, catechol, vanillin, caffeic acid, syringaldazine and *P*-coumaric acid were investigated for their capacity to induce tyrosinase activity. The compounds were sterilized by filtration using a Millipore membrane (0.45µm) and added aseptically into flasks. The concentration of the inducers was 0.1, 0.5 and 1 mM. One control was used without the addition of any inducer compound.

2.9. Tyrosinase enzyme inhibition

The inhibition of tyrosinase by kojic acid, cinnamic acid, sodium azide, benzaldehyde and potassium cyanide was analyzed. Putative inhibitors were simultaneously dissolved with substrate in Na phosphate buffer (50 M, pH 7.0). The inhibitory effect was carried out after 10 min incubation at 37 °C. The residual activity of tyrosinase was estimated using assay methods described before (Duarte *et al*., 2012).

2.10. Statistical analysis

All experiments were performed in three replicates and presented as their mean values with their SD, standard deviation.

3. Results

The results of tyrosinase purification are summarized in Table 1. The purification procedure included NH_4 $(SO_4)_2$ precipitation, 85%, followed by DEAE-cellulose, and phenyl Sepharose. The purification of tyrosinase demonstrated a specific activity of 69.39 and 65.11 U mg^{-1} protein from *T. reesei* and *T. harzianum*, respectively. The obtained values of the purification fold were 21.09 and 14.93 for the two tested fungal species mentioned previously in the same order. Subsequently, tyrosinase purification to homogeneity was detected by SDS-PAGE analysis, which showed a single band of 45 and 65 kDa (Figure 1) for *T. reesei* and *T. harzianum*, respectively.

Table 1. Overall purification profile of tyrosinase from two *Trichoderma* sp.

Fungi	Purification step	Total protein (mg)	Total activity (U)	Specific activity (U/mg)	Purification fold	Yield (%)
Trichoderma reesei	Crude extract	45.6	150.2	3.29	1	100
	Amm. Sulphate	16.7	127.5	7.63	2.32	84.89
	DEAE-Cellulose	0.985	30.2	30.66	9.32	20.11
	Phenyl Sepharose	0.183	12.7	69.39	21.09	8.46
Trichoderma harzianum	Crude extract	55.4	240.2	4.36	1	100
	Amm. Sulphate	18.9	139.1	7.36	1.69	57.91
	DEAE-Cellulose	0.970	40.5	41.75	9.58	16.86
	Phenyl Sepharose	0.235	15.3	65.11	14.93	6.37

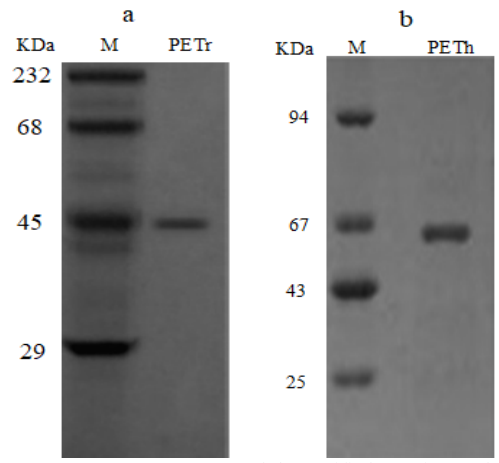

Figure 1. SDS-PAGE pattern of the purified tyrosinase obtained from *T. reesei* and *T. harzianum*. Lane M: molecular mass of marker protein; Lane PETr: purified tyrosinase from *T. reesei* (a) and Lane PETh: purified tyrosinase from *T. harzianum* (b).

The effects of various inducer compounds, monophenolic and diphenolic substrates, on t yrosinase enzyme activity were studied. Control media, without the inducer factor, were considered as 100%. The two *Trichoderma* species showed a dose-dependent response of tyrosinase activity toward all of the examined inducers. The higher the inducer concentration, the higher the induction effect on t yrosinase biosynthesis investigated. All of the inducers clearly pronounced tyrosinase activity. Among the studied diphenolic inducers, caffeic acid at 1mM was more efficient than the other tested inducers by 227% increase in tyrosinase activity in case of *T. reesei* and 184% in case of *T. harzianum*. However, *P*-coumaric acid at 1mM showed the strongest induction effects on *T. reesei*-tyrosinase (254%) and *T. harzianum*-tyrosinase (218%) among the tested monophenolic substrates. It was observed that guaiacol, catechol, vanillin and syringaldazine were less efficient inducer substrate for *T. reesei* tyrosinase and increased the percentage of tyrosinase activity, providing 180, 119, 155 and 181%, respectively (Table 2). Meanwhile, tyrosinase from *T. harzianum* showed less response towards guaiacol (122%), catechol (114%), vanillin (103%), and syringaldazine (137%).

Table 2. Effect of different monophenolic and diphenolic inducers on tyrosinase activity.

Fungi	*Trichoderma reesei*		*Trichoderma harzianum*	
	Activity (U ml^{-1})	%	Activity (U/mg)	%
Control	12.7	100	15.3	100
Guaiacol				
0.1 mM	20.0± 0. 4	157±2.1	17.4±0.6	133±2.9
0.5 mM	22.5±0.5	177±2.3	18.1±0.5	118±1.9
1 mM	22.9±0.7	180±2.2	18.8± 0.6	122±1.8
Catechol				
0.1 mM	11.5±0.3	91.6±1.7	15.0±0.6	98.0±1.9
0.5 mM	14.0± 0.8	11.7±0.3	16.1±0.5	105±1.1
1 mM	15.1±0.5	119±1.6	17.4±0.7	114±1.5
Vanillin				
0.1 mM	18.5±0.6	146±0.5	14.8±0.3	97.0±1.4
0.5 mM	19.5±0.5	154±1.7	15.3±0.5	100
1 mM	19.7±0.4	155±1.9	15.0± 0.5	103±1.5
Caffeic acid				
0.1 mM	28.3±0.4	222±2.5	25.5±0.6	167±1.8
0.5 mM	28.7±0.6	225±2.7	27.8±0.5	182±2.0
1 mM	28.9±0.4	227±2.8	28.1±0.6	184±1.7
Syringaldazine				
0.1 mM	22.0±0.5	173±1.4	19.2±0.6	125±1.8
0.5 mM	22.5±0.4	177±1.3	20.1±0.5	131±1.8
1 mM	23.1±0.7	181±1.8	21.0±0.4	137±1.9
***P*-Coumaric acid**				
0.1 mM	31.2±0.8	210±2.3	27.5±0.6	197±2.4
0.5 mM	37.2±0.7	234±2.7	30.1±0.8	207±2.8
1 mM	39.4±0.9±	254±2.8	35.2±0.9	218±2.5

Several compounds may elicit a n egative effect on tyrosinase activity. Tyrosinase enzyme activity was assayed in the existence of kojic acid, cinnamic acid, sodium azide, benzaldehyde and potassium cyanide at pH 5.0. The type of potential inhibition was investigated in the presence of monophenolic substrate like *p*-coumaric acid and diphenolic substrate, caffeic acid (Table 3) according to the above determination assay. A control sample was used without the addition of any inhibitor compounds. KCN was the most powerful inhibitor for tyrosinase enzyme from *T. reesei* and *T. harzianum*-monophenolase activity with 47.5 and 49.0%, respectively. In addition, sodium azide and cinnamic acid also showed significant inhibition toward tyrosinase enzyme from *T. reesei* and *T. harzianum* with 63.2, 74.1 and 60.2, 77.5% residual activity, respectively. Furthermore, the other remaining

substances had less significant inhibitory effect on t he monophenolase activity of tyrosinase.

Under the same tested conditions, the response of the diphenolase activity of tyrosinase derived from the tested *Trichoderma* sp. toward the tested putative inhibitors was investigated. Kojic acid was the strongest inhibitor on the diphenolase activity of *Trichoderma*-tyrosinase, followed by potassium cyanide, sodium azide, cinnamic acid and benzaldehyde.

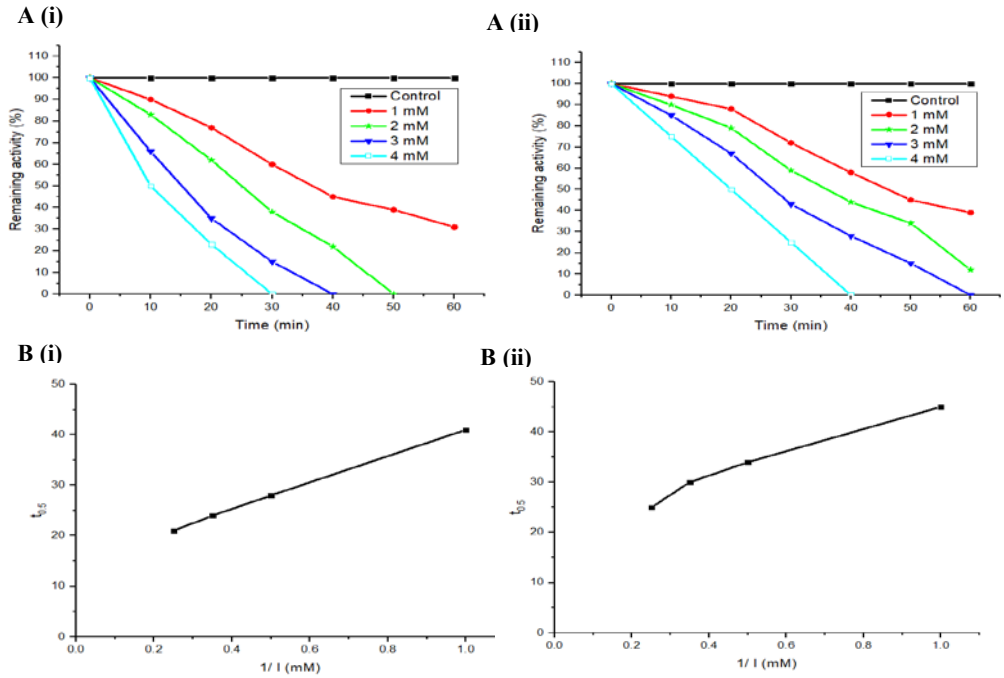

Figure 2. A:.Inactivation of monophenolase activity of tyrosinase produced by *T. reesei* (i) and *T. harzianum* (ii) using potassium cyanide, **B**: relation between $t_{0.5}$ and reciprocal of inhibitor concentration by *T. reesei* (i) and *T. harzianum* (ii).

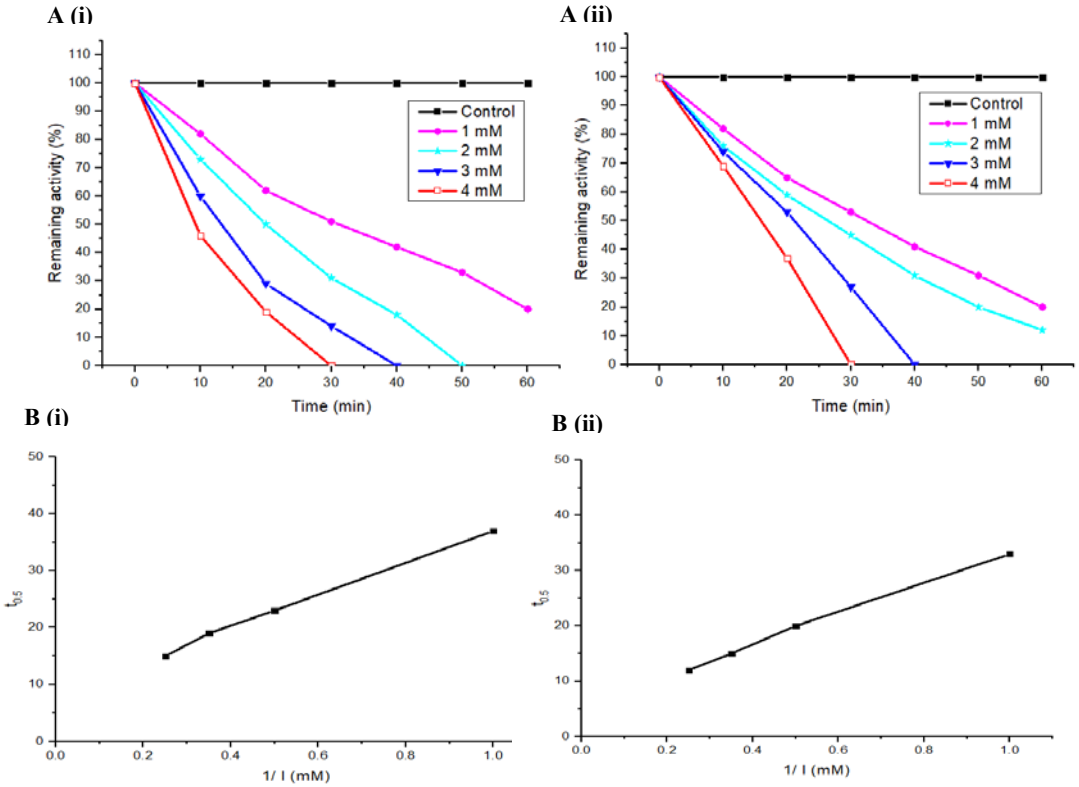

Figure 3. A: Inactivation of diphenolase activity of tyrosinase produced by *T. reesei* (i) and *T. harzianum* (ii) using kojic acid, **B**: relation between $t_{0.5}$ and reciprocal of inhibitor concentration by *T. reesei* (i) and *T. harzianum* (ii).

Table 3.Influence of different inhibitors on mono- and di-phenolase activity of tyrosinase enzyme obtained from two *Trichoderma* sp.

	Residual activity (%) towards *p*-coumaric acid	
	Trichoderma reesei	*Trichoderma harzianum*
Control	100	100
Kojic acid	59.3±1.6	59.1±1.2
Cinnamic acid	74.1±1.5	77.5±1.1
Sodium azide	63.2±1.0	60.2±1.0
Benzaldehyde	80.2±0.9	82.4±1.1
Potassium cyanide	52.5±0.7	51.0±0.8
	Residual activity (%) towards caffeic acid	
	Trichoderma reesei	*Trichoderma harzianum*
Control	100	100
Kojic acid	50.2±0.9	54.5±0.8
Cinnamic acid	79.7±1.0	81.3±1.0
Sodium azide	75.9±1.2	67.5±1.1
Benzaldehyde	99.4±1.5	99.9±1.4
Potassium cyanide	61.5±0.9	57.1±0.9

The rate of tyrosinase activity followed a pseudo-first-order reaction kinetics under the conditions of the inactivation toward mono- and di-phenolase activity by potassium cyanide (Figure 2 A,B) and kojic acid (Figure 3 A,B), respectively. Furthermore, it was observed that the rate of tyrosinase activity was proportional to the inhibitor concentration (Figure 2A, 3A) during the inactivation treatment. The rate constant for potassium cyanide inactivation of tyrosinase was calculated from the slope (Figure2B) as 0.02 and 0.03 μM^{-1} min^{-1}, from *T. reesei* and *T. harzianum*, respectively. However, the rate constant for tyrosinase inhibition from *T. reesei* and *T. harzianum* using caffeic acid was 0.027 and 0.033 μM^{-1} min^{-1} as calculated from the slope of figure 3B, respectively.

4. Discussions

In the present investigation *Trichoderma reesei* and *Trichoderma harzianum* produced appreciable activities of tyrosinase. Well-characterized extracellular tyrosinases were isolated from the fungal strains *T. reesei* (Selinheimo *et al*., 2006) and *Amylomyces rousii* (Montiel *et al*., 2004).

The purification steps included ammonium sulphate (85%), DEAE-cellulose, and phenyl Sepharose. Purified tyrosinase exhibited a final specific activity 69.39 and 65.11 U/mg protein and purification fold of 21.09 and 14.93 for *T. reesei* and *T. harzianum*, respectively. The purity of tyrosinase derived from *T. reesei* and *T. harzianum* was determined by SDS-PAGE analysis, which showed a single band of 45 kDa and 65 KDa (Selinheimo *et al*., 2006; Kawamura-Konishi *et al*., 2007).

The purified tyrosinases were tested in terms of substrate affinity and inhibition. Six compounds were investigated for their capacity to increase tyrosinase enzyme activity; guaiacol, catechol, vanillin, caffeic acid, syringaldazine and *P*-coumaric acid. The control without any inducer showed a low tyrosinase activity. Caffeic acid exhibited the most inductive effect on diphenolase activity of tyrosinase enzyme. However, the other reagents have less inductive effect on tyrosinase activity. In addition, *P*-coumaric acid as monophenolic inducer substrate displayed the highest inductive effect on tyrosinase from the tested two fungal strains. It was found that tyrosinase enzyme exhibited a m ore activity with increasing the reagents concentration in the culture medium. Tyrosinase enzyme obtained from *T. reesei* showed a remarkable difference in the enzyme–substrate specificity (Selinheimo *et al*., 2009; Fan and Flurkey, 2004). This may be attributed to the variation in binding capability of different substrates toward the binuclear-copper site of tyrosinase (Lim *et al*., 1999; Kubo *et al*., 2004; Selinheimo *et al*., 2009).

Tyrosinase-catalyzed browning reactions of vegetables and fruits are accompanying with shortening of shelf life. Therefore, inhibition of tyrosinase is of great benefit. The inhibition of tyrosinase by cinnamic acid, kojic acid, sodium azide, benzaldehyde and potassium cyanide was analyzed in the presence of monophenolic substrate (*p*-coumaric acid) and diphenolic substrate (caffeic acid). The reaction mixture includes1.0 mM inhibitor and 1.0 mM substrate in phosphate buffer (0.1 M, pH 5.0) and incubated at 25 ºC. Under the tested conditions, the inhibitory action of the investigated inhibitors on the monophenolase activity of tyrosinase from *Trichoderma* sp. showed the subsequent order: KCN> kojic acid >Na azide >cinnamic acid > benzaldehyde. However, the effect of the tested inhibitors on the diphenolase activity was ranking as follows: kojic acid > p otassium cyanide> sodium azide >cinnamic acid > benzaldehyde.

The inhibitory effect on t yrosinase activity can be speculated with relation to three possible reasons. First, the length of the lag period correlated to the oxidation reaction catalyzed by tyrosinase was significantly extended by inhibitor molecules (Selinheimo *et al*., 2009). Second, mono- and di-phenolase activity of tyrosinase showed various responses to kojic acid and potassium cyanide as inhibitor. Third, phenolic substrates were variably bound to the tyrosinase-active site. The active site of tyrosinase showed that kojic acid binds to CuB while monophenols bind to CuA (Sendovski *et al*. 2011). Indeed, both kojic acid and caffeic acid contest to CuB on tyrosinase active site. On the other hand, the CuA on tyrosinase active site was occupied by *p*-coumaric acid (Selinheimo *et al*., 2009).

The inhibition of tyrosinase activity was further analyzed with potassium cyanide as monophenolase tyrosinase inhibitors. The activity rate for two *Trichoderma* sp. was determined, with the data plotted as the tyrosinase residual activity versus incubation time. The rate of tyrosinase activity exhibited a p seudo-first-order reaction kinetics and was with linear proportion to the inhibitor concentration.

5. Conclusions

Till now there are no sufficient studies concerning inducers and inhibitors of fungal tyrosinase, accordingly our main purpose in this research aimed to determine the response of tyrosinase from two *Trichoderma* sp. toward various putative inducer substrates and inhibitors. Extracellular tyrosinase was purified by ammonium sulphate precipitation (85%), DEAE-cellulose and phenyl Sepharose from *T. reesei* and *T. harzianum*. SDS-PAGE confirmed the purity of tyrosinase produced by *T. reesei* and *T. harzianum* to homogeneity, exhibiting a single band

of 45 a nd 65 k Da, respectively. The tested inducer substrates showed a concentration dependent on tyrosinase activity, especially monophenolic substrate as *p*-coumaric acid and diphenolic substrate as caffeic acid as diphenolic substrate. Among the tested inhibitors, KCN and kojic acid had the highest inhibitory effect against the tyrosinase activities from the two investigated *Trichoderma*; monophenolase and diphenolase activities, respectively. The remaining enzyme activity was proportional to the inhibitor concentration with a pseudo-first-order reaction kinetics. Therefore, inducers can be used for increasing the efficiency of tyrosinase.

References

Chang T. 2009. An updated review of tyrosinase inhibitors. *Int J Mol Sci*, **10**: 2440-2475.

Duarte L, Tiba J, Santiago M, Garcia T and Maria T. 2012. Production and characterization of tyrosinase activity in *Pycnoporus sanguineus* cct4518 crude extract. *Braz J of Micro,* **4**: 21-29.

El-Shora H and Metwally M. 2008. Use of tyrosinase enzyme from *Bacillus thuringiensis* for the decontamination of water polluted with phenols. *Biotechnol.* **7(2)**: 305-310.

Fairhead M and Thony-Meyer L. 2012. Bacterial tyrosinases: old enzymes with new relevance to biotechnology. *New Biotechnol*, **29(2)**: 183-199.

Fan Y and Flurkey W. 2004. Purification and characterization of tyrosinase from gill tissue of Portabella mushroom. *Phytochem*, **65**: 671–678.

Gasowska B, Kafarski P and Wojtasek H. 2004. Interaction of mushrCoom tyrosinase with aromatic amines, *o*-diamines and *o*-aminophenols. *Biochim Biophys Acta*, **1673**(3): 170–177.

Halaouli S, Asther M, Kruus K, Guo L, Hamdi M, Sigoillot JC, Asther M and Lomascolo A. 2005. Characterization of a new tyrosinase from *Pycnoporus* species with high potential for food technological applications. *J Appl Microbiol*, **98**(2): 332–343.

Ikehata K and Nicell JA. 2000. Color and toxicity removal following tyrosinase-catalyzed oxidation of phenols. *Biotechnol Prog,***16**: 533-540.

Ismaya W, Rozeboom H, Weijn A, Mes J, Fusetti F, Wichers J and Dijkstra W. 2011. Crystal structure of *Agaricus bisporus* mushroom tyrosinase: identity of the tetramer subunits and interaction with tropolone. *Biochem*, **50**: 5477–5486.

Kong K, Hong M, Choi S, Kim Y and Cho S. 2000. Purification and characterization of a highly stable tyrosinase from *Thermomicrobium roseum*. *Biotechnol Appl Biochem*, **31**: 113–118.

Kim Y and Uyama H. 2005. Tyrosinase inhibitors from natural and synthetic sources: structure, inhibition mechanism and perspective for the future. *Cell Mol Life Sci*, **62**: 1707–1723.

Kawamura-Konishi Y, Tsuji M, Hatana S, Asanuma M, Kakuta D, Kawano T, Mukouyama E, Goto H and Suzuki H. 2007. Purification, Characterization, and Molecular Cloning of Tyrosinase from *Pholiota nameko*. Biosci. *Biotechnol Biochem*, **71**: 1752–1760.

Kubo I, Nihei K and Tsujimoto K. 2004. Methyl *p*-coumarate, a melanin formation inhibitor in B16 mouse melanoma cells. *Bioorg Med Chem,* **12**:5349–54.

Lertsiri S, Phontree K, Thepsingha W and Bhumiratana A. 2003. Evidence of enzymatic browning due to laccase-like enzyme during mash fermentation in Thai soybean paste. *Food Chem*, **80**: 171–176.

Lim JY, Ishiguro K and Kubo I. 1999. Tyrosinase inhibitory *p*-coumaric acid from ginseng leaves. *Phytother Res*, **13**: 371–375.

Lowry OH, Rosenbough NJ, Farr AL and Randall RJ. 1951. Protein measurement with the folin phenol reagent. *J Biol Chem*, **193**: 265- 275.

Marusek CM, Trobaugh NM, Flurkey WH and Inlow JK. 2006. Comparative analysis of polyphenol oxidase from plant and fungal species. *J Inorg Biochem*, **100**: 108–123.

Montiel AM, Fernandez FJ, Marcial J, Soriano J, Barrios-Gonzalez J and Tomasini A. 2004. A fungal phenoloxidase (tyrosinase) involved in pentachlorophenol degradation. *Biotechnol Lett*, **26**: 1353–1357.

Munjal N and Sawhney SV. 2002. Stability and properties of mushroom tyrosinase and trapped in alginate and polyacrylamide and gelatin gels. *Enz Microb Technol*, **30**: 613-619.

Nawaz A, Taha Shafi, Abdul Khaliq, Hamid Mukhtar and Ikram ul Haq. 2017. Tyrosinase: Sources, Structure and Applications. *Int J Biotech Bioeng*. **3**:142-148.

Nakamura M, Nakajima T, Ohba Y, Yamauchi S, Lee BR and Ichishima E. 2000. Identification of copper ligands in *Aspergillus oryzae* tyrosinase by site-directed mutagenesis. *Biochem J*, **350**: 537–545.

Pretzler M, Aleksandar B and Rompel A. 2017. Heterologous expression and characterization of functional mushroom tyrosinase (AbPPO4). *Sci Rep*, **7:** 1810-1822.

Selinheimo E, Saloheimo M, Ahola E, Westerholm-Parvinen A, Kalkkinen N, Buchert J and Kruus K. 2006. Production and characterization of a s ecreted, C-terminally processed tyrosinase from the filamentous fungus *Trichoderma reesei*. *FEBS J*, **273**(18): 4322–4335.

Selinheimo E, Autio K, Kruus K and Buchert J. 2007a. Elucidating the mechanism of laccase and tyrosinase in wheat bread making. *J Agric Food Chem*, **55:** 6357–6365.

Selinheimo E, NiEidhin D, Steffensen C, Nielsen J, Lomascolo A, Halaouli S, Record E, O'Beirne D, Buchert J and Kruus K. 2007b. Comparison of the characteristics of fungal and plant tyrosinases. *J Biotechnol*, **130**: 471–480.

Selinheimo E, Gasparetti C, Mattinen M, Steffensen CL, Buchert J and Kruus K. 2009. Comparison of substrate specificity of tyrosinases from *Trichoderma reesei* and *Agaricus bisporus*, *Enzyme Microb. Technol*., **44:** 1–10.

Seo SY, Sharma VK and Sharma N. 2003. Mushroom tyrosinase: recent prospects. *J Agric Food Chem*, **51**: 2837–2853.

Sendovski M, Kanteev M, Ben-Yosef VS, Adir N and Fishman A. 2011. First structures of an active bacterial tyrosinase reveal copper plasticity. *J Mol Biol.,* **405**: 227–237.

Zaidi KU, Ali AS and Ali SA. 2014. Purification and characterization of melanogenic enzyme tyrosinase from button mushroom. *Hindawi Publishing Corporation Enzyme Research*, 6 pages.

Wang Y, Hu G, Zhang Q, Yang Y, Li Q, Hu Y, Chen H and Yang F. 2018. Screening and characterizing tyrosinase inhibitors from *Salvia miltiorrhiza* and *Carthamus tinctorius* by spectrum-effect relationship analysis and molecular docking. *J Analy Meth Chem*, Article ID 2141389, 10 pages.

JJBS

Volume 13, Number 1,March 2020
ISSN 1995-6673
Pages 13 - 17

Jordan Journal of Biological Sciences

Impact of Nanoparticles on Genetic Integrity of Buckwheat (*Fagopyrum esculentum* Moench)

Girjesh Kumar, Akanksha Srivastava and Rajani Singh*

Plant Genetics Laboratory, Department of Botany, University of Allahabad, Prayagraj 211002, India

Received April 7, 2019; Revised April 16, 2019; Accepted April 24, 2019

Abstract

Nanomaterials are increasingly produced over the last decades and are expected to play an increasing role in future science, technology and medicine. These Nanoparticles (NPs) are particles between 1 and 100 nm in size. The present paper deals with the effect of copper and silver NPs on somatic cells of *Fagopyrum esculentum* Moench. For this, graded concentrations of silver and copper NPs *viz*., 18µg/mL, 36µg/mL and 54µg/mL were used for treatment along with control. Mitotic study was observed to be quite normal in case of control. An inverse relationship between the active mitotic index (AMI %) and concentrations of NPs was scored. However, as a result of the treatment on root tip cells, various chromosomal anomalies were induced such as stickiness, fragmentation, precocious movement, C-metaphase, bridge and unorientation, etc. The stickiness was found to be the predominant abnormality in both treatments. The total abnormality percentage (TAB %) was recorded higher in copper NPs as compared to silver NPs. Root length was also measured, which depicted a substantial effect of NPs on the root growth. On the basis of this result, it could be concluded that the copper NPs are more cytotoxic than silver NPs.

Keywords: AMI%, Cytotoxity, *Fagopyrum esculentum* Moench, Nanoparticles, TAB%,

1. Introduction

Buckwheat (*Fagopyrum esculentum* Moench) belongs to family polygonaceae, and contains a glucoside called rutin, a phytochemical that strengthens capillary walls. A dried buckwheat leaf has been manufactured in Europe under the brand name "Fagorutin" for use as herbal tea. Similar effects are associated with the inclusion of resistant starch in diet, which help to prevent colon cancer. These beneficial traits may be positively regulated using nanotechnology because this science has opened new vistas in the field of plant sciences, and interest for its exploration is increasing nowadays. Nanotechnology has large potential to provide an opportunity for the researchers of plant science and other fields, and to develop new tools for incorporation of NPs into plants that augment existing function and new ones (Cossins 2014). Nanoparticles (NPs) are wide class of materials that include particulate substances, which have one dimension less than 100 nm at least (Laurent *et al*., 2010). Pesticides and herbicides are usually used in agriculture to get better crop yield and efficiency. But nowadays, severe debate is going on the negative effect of conventional pesticides and herbicides on the environment. Random usage of pesticides increases pathogen and pest resistance, reduces soil biodiversity, decreases nitrogen fixation, contributes to bioaccumulation of pesticides, leads to pollinator decline, and destroys habitat for birds. When NPs are applied with herbicide, low amount of herbicide is required to achieve the weed eradication. NPs owing to their size can freely enter into the cells and can imply significant influences on the cellular function. These unique features make them highly attractive for implementation in products for wide application (Benn *et al*., 2010). NPs have unique physiochemical properties and the potential to boost the plant metabolism (Giraldo *et al.,* 2014). The literature on the ecotoxicity of NPs and Nanomaterials as well as the chemistry of both manufactured and natural NPs is summarised in recent reports (Handy *et al*., 2008). Treatment of *Arabidopsis thaliana* plants with 1 or 2.5 mg/L of AgNPs was found to increase seedling biomass, whereas treatment with higher concentrations was found to decrease seedling biomass (Kaveh *et al.,* 2013). Another study by Zafar *et al*., (2016) demonstrated effects of NPs on germination and shoot growth of *Brassica nigra.* Compared to fine particles, NPs are highly insoluble in water and culture media and show strong genotoxicity in the aqueous environment (Horie *et al*., 2013).

The two NPs selected for the present appraisal are silver and copper NPs. Cupric oxide II is an important inorganic compound with the formula CuO. A black solid, it is one of the two stable oxides of copper, the other being Cu_2O or cuprous oxide. Copper (II) oxide belongs to the monoclinic crystal system. The copper atom is coordinated by 4 oxygen atoms in an approximately square planar configuration. Halder *et al.,* (2015) reported that copper (Cu) and cadmium sulphide (CdS) NPs induce stable and heritable phenotypic changes in *Macrotyloma uniflorum* (Lam.) Verdc (Family: Leguminosae). The bio uptake of copper NPs into the cell causes generation of reactive oxygen species (ROS). Silver nitrate is an inorganic compound with chemical formula $AgNO_3$. It was once called lunar caustic with antiseptic activity. Silver nitrate can potentially be used as antifungal and antibacterial agent. The penetration of silver NPs causing chromosomal aberrations in *Allium cepa* root tips was reported by Kumari *et al.,* (2009) and Panda *et al*., (2011). Within the cell, the integration of silver creates a low molecular weight region

* Corresponding author e-mail:singh.rajani1995@gmail.com.

where the DNA condenses (Sobha *et al*., 2010). Studies performed in a v ariety of organisms indicate AgNP toxicity, which may be ascribed to different mechanisms, including the disruption of the integrity of the cell membrane and binding of the proteins and DNA (Arora *et al*., 2009).

There is a scarcity of scientific data describing the dose-response relationship with respect to their cytogenetic toxicity of NPs in plant systems. Plants are the important component in ecological system and may serve as a potential pathway for NPs transport and a route for bioaccumulation into the food chain (Zhu *et al*., 2008). The present study aims to investigate the mutagenecity and genotoxicity of silver and copper NPs as a function of mitotic index, chromosomal aberrations and mitotic behaviour. The testing material used in this study is *Fagopyrum esculentum* Moench (2n =16), commonly known as Buckwheat. It is categorized as a p seudocereal; the crop is not a cereal, but the seeds (strictly achenes) are usually classified among the cereal grains because of their similar usage.

As a result of detailed literature study, this work represents a study on t his subject being an implication of NPs on buckwheat that will prove to be useful for future studies.

2. Material and Methodology

2.1. Seed procurement

The seeds of *Fagopyrum esculentum* Moench variety-VL-7 were collected from National Bureau of Plant Genetics Resources (NBPGR), Shimla, Phagli, India.

2.2. Seed treatment

Fresh seeds of buckwheat were pre-soaked in distilled water for 12 hours. Then the seeds were treated with various concentrations of NPs i.e. 18µg/mL, 36µg/mL and 54µg/mL, suspension for 3 hr s along with control by dilution method. After treatment, the seeds were washed and left for recovery. These seeds were placed in sterilized Petriplates, kept in seed germinator for germination at 25±2°C with humidity 60-80%. After seed germination, the root length was measured at various concentrations.

Treated germinated seeds of each concentration were fixed in Carnoy's fixative [glacial acetic acid: absolute alcohol, (1:3)] along with control set. After 24 hours, all of them were removed from fixative and transferred into bottles containing only 90% alcohol.

2.3. Mitotic preparation

The control and treated root tips were excised, processed and hydrolysed in 1N HCl by adjusting water bath at 60°C for 1-2 minutes so that tissues of root tips get soften. Then they were washed under running water to remove excess HCl and allowed to keep on blotting paper for dehydration. Dried root tips were stained with 2% acetocarmine for 30 m inutes. By using squash technique, mitotic slides were prepared and observed cells were snapped under Nikon Research Electron Microscope using Olympus PCTV Vision Software. Approx. 10 microscopic field views were recorded from each slide.

2.4. Formula used for scoring of data

The array of mitotic indices and various abnormalities were screened out by applying the formula below:

Active mitotic index (AMI) % = (Total number of dividing cells/Total number of observed cells)*100

Total abnormality percentage (TAB) % =(Total number of abnormal cells/Total number of observed cells)*100

2.5. Statistical analysis

The data obtained was analysed using statistical software, SPSS 16 and means were compared using Duncan's Multiple Range Test (DMRT) ($P \leq 0.05$). All the results were expressed in form of Mean ± Standard Error. The graph was plotted by using Sigmaplot 10.00 software.

3. Results

3.1. Effect of NPs on the germination & root growth of the plant

NPs are found very effective for the germination of plant. At 54 µg/ml concentration of silver NPs, the seed germination of buckwheat was found quite well (Figure 1 A, B). Efficacy of NPs depends on their concentration and varies from plant to plant. According to Suriyaprabha *et al*. (2012), silicon NPs increased seed germination in maize by providing better nutrients availability, optimum pH and conductivity to the growing medium. The silver NPs are more efficiently utilized by plants than the copper NPs. In copper NPs, the seed germination was comparatively less, indicating that copper NPs are more toxic than silver NPs. In silver NPs treated seeds, the root length was also recorded to be increased in comparison to control.

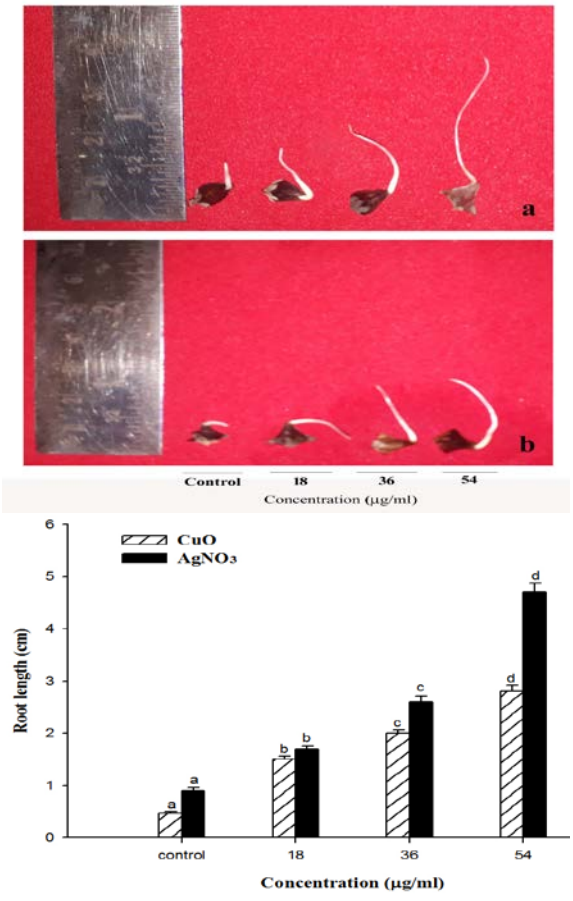

Figure 1A and B. Effect of Nanoparticles on root length of *Fagopyrum esculentum* Moench (a- $AgNO_3$ & b-CuO)

3.2. Effect of NPs on AMI% & TAB%

The data scored after NPs treatment was documented in form of Table 1. The computed AMI% for varying copper and silver concentrations divulges an inverse association between respective concentrations and AMI%. AMI% in case of control was calculated to be 11.94±0.18[a]. In comparison to control, AMI% was seen to decline with respect to increase in both the NPs. The reduced AMI% may occur due to breakdown of plant self-protection system and further inhibition of cell DNA replication, transcription and protein synthesis (Liu *et al*., 2015). The reduction is also because of slower transition of cells from S phase to M phase of cell cycle. In case of silver NPs, it declines from 11.57±0.12[b] to 8.90±0.05[d], whereas in case of copper NPs the decline from 10.80±0.57[b] to 7.85±0.22[d] was observed. On the other hand, it was observed that the TAB% shows direct correlation with increasing concentration of NPs. As at the highest concentration i.e. 54µg/ml, the TAB% was increased up to 4.50±0.57 ($AgNO_3$) and 7.16±0.33 (CuO). But it was comparatively lower in case of silver NPs treatment set; henceforth, higher dose of NPs has proved to be more chromotoxic and mitodepressive. It was also observed that the metaphasic and anaphasic abnormalities are almost equal at 18µg/ml (Figures 2 and 3), but as the concentration increases the anaphasic abnormalities were found to be more as compared to metaphasic abnormalities in copper NPs treatment. But in case of silver NPs metaphasic abnormalities were found more than the anaphasic abnormalities. Induction of various chromosomal aberrations also occurred. Kumari *et al*., (2011) reported that ZnO NPs exert cytotoxic and genotoxic effects, including lipid peroxidation, decreasing the mitotic index, increasing micronuclei and chromosomal aberration indices on r oot cells of *Allium cepa*.

Table 1. A Comparative account of Cytological abnormalities induced by Nanoparticles ($AgNO_3$ and CuO) in root meristems of *Fagopyrum esculentum* Moench

Treatment	Conc. (µg/ml)	AMI (%) (Mean±S.E.)	Metaphasic Abnormalities (%) (Mean±S.E.)					Anaphasic Abnormalities (%) (Mean±S.E.)					TAB (%) (Mean±S.E.)
			Cm	Sc	Pr	St	Un	Br	Lg	St	Un	Oth	
	Control	11.94 ± 0.18[a]	-	-	-	-	-	-	-	-	-	-	-
Silver Nanoparticle ($AgNO_3$)	18	11.57 ± 0.12[b]	0.25 ± 0.12	0.35 ± 0.20	-	0.74 ± 0.03	-	-	-	0.62 ± 0.13	0.11 ± 0.10	0.25±0.12	2.30 ± 0.10
	36	10.58 ± 0.83[c]	0.52 ± 0.01	-	-	0.51 ± 0.28	-	-	0.17 ± 0.17	0.69 ± 0.15	-	1.05±0.30	2.76 ± 0.37
	54	8.90 ± 0.05[d]	0.17 ± 0.16	0.13 ± 0.13	0.47 ± 0.03	0.65 ± 0.20	0.47 ± 0.29	0.51 ± 0.30	0.82 ± 0.20	-	0.30 ± 0.15	0.47±0.03	4.50 ± 0.57
	Control	11.94 ± 0.18[a]	-	-	-	-	-	-	-	-	-	-	-
Copper Nanoparticle (CuO)	18	10.80 ± 0.57[b]	0.49 ± 0.26	0.13 ± 0.13	0.40 ± 0.69	0.67 ± 0.06	0.90 ± 0.97	-	-	0.51 ± 0.20	0.26 ± 0.20	0.34 ± 0.18	3.30 ± 0.58
	36	9.11 ± 0.28[c]	0.63 ± 0.15	0.59 ± 0.74	-	0.59 ± 0.31	0.36 ± 0.18	-	-	1.63 ± 0.48	0.12 ± 0.13	0.74 ± 0.80	4.67 ± 0.12
	54	7.85 ± 0.22[d]	0.33 ± 0.26	0.82 ± 0.20	0.66 ± 0.21	1.25 ± 0.39	-	0.61 ± 0.12	1.42 ± 0.44	0.53 ± 0.53	0.45 ± 0.24	0.44 ± 0.24	7.16 ± 0.33

Where:**Conc-** Concentration, **Cm-** C- metaphase, **Sc-** Scattering, **Pr-** Precocious movement **, St-** Stickiness, **Un-** Un-orientation, **Br-** Bridge formation, **Lg-** Laggard formation, **Oth-**Others.

Means followed by lowercase letter are statistically significant at $p < 0.05$ in Duncan's Multiple Range Test

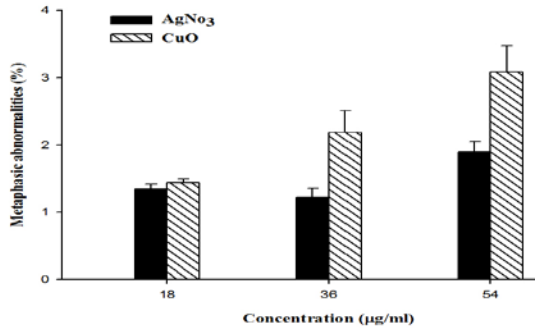

Figure 2. Comparative account of metaphasic abnormalities (%) induced by Nanoparticles ($AgNO_3$ and CuO) in the root meristems of *Fagopyrum esculentum* Moench.

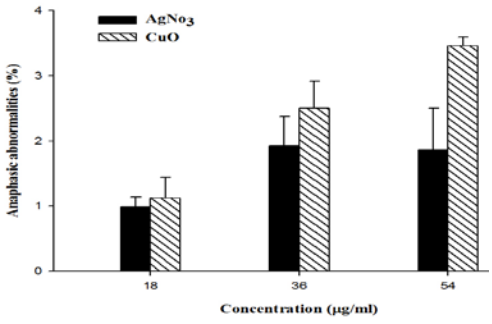

Figure 3. Comparative account of anaphasic abnormalities (%) induced by Nanoparticles ($AgNO_3$ and CuO) in the root meristems of *Fagopyrum esculentum* Moench.

3.3. Cytological impact of NPs

The cytological appraisal of the NPs shows a noteworthy impact on the cytology of root meristems of *Fagopyrum esculentum* Moench. Control seeds showed a normal mitotic behaviour, perfect alignment of chromosomes on equatorial plate at metaphase (2n=16) (Figure 4A) and 16:16 pole ward separation during anaphase (Figure 4B). However, the root tips treated with silver and copper NPs solution showed various types of chromosomal abnormalities such as metaphasic plate distortion, unorientation at metaphase, breaking of chromosomes, fragmentation, spindle dysfunctioning, stickiness, scattering, precocious movement at metaphase, laggard, bridge formation, unequal segregation and tripolarity, etc. NPs are capable of entering the nucleus, and directly or indirectly interacting with nuclear material, leading to alterations in DNA integrity (Kruszewski *et al*., 2011; Asare *et al*., 2012).

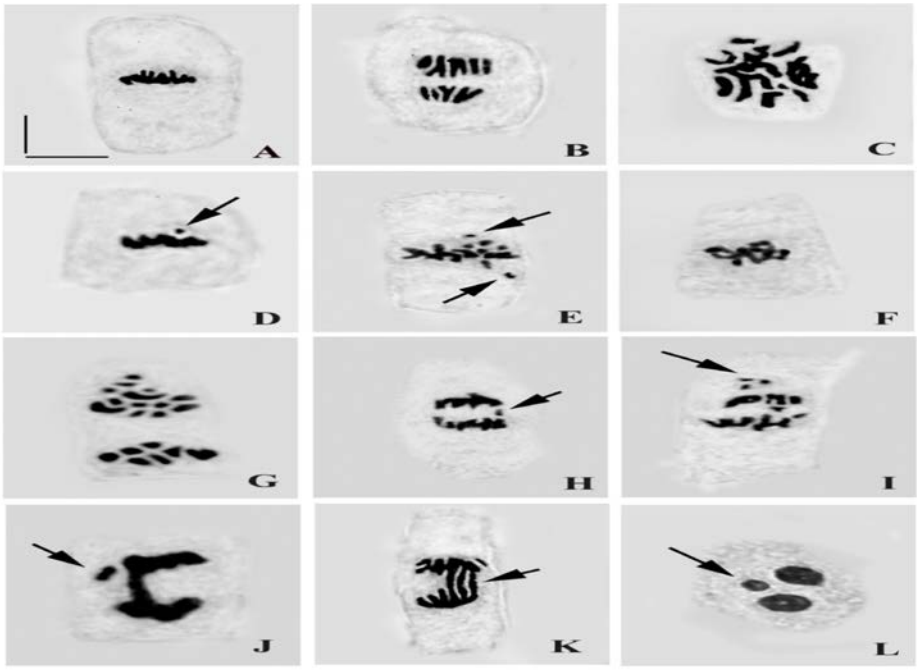

Figure 4. Different types of chromosomal aberrations induced by Nanoparticles in *Fagopyrum esculentum* Moench**:** A. Normal Metaphase (2n=16) B. Normal anaphase (16:16 separation), C. C-metaphase, D. One precocious chromosome with sticky metaphase, E. Two Precocious chromosome at metaphase, F. Loop formation at metaphase G. Scattering at anaphase, H. Laggard formation at anaphase, I. Laggard with forward movement at anaphase, J. Laggard with bridge formation at anaphase, K. Triple Bridge formation with forward movement at anaphase, L. Micronuclei formation at telophase [Scale bar: Length 6.28µm, Width- 7.52µm]

4. Discussion

Studies conducted to increase information on genotoxic risks related to exposure to emerging nanomaterials are of increasing interest (Landsiedel *et al*., 2009). Ghosh *et al.* (2010) have shown that TiO2 NPs (~100 nm) are able to induce significant increases in genetic damage in *Allium cepa* and *Nicotiana tabacum* when they used the comet assay for testing genotoxic effect. The effect of ZnO-NPs at elevated concentrations (10–2000 mg/L) revealed a biomass drop, damaged root surface cells, and induced abnormal defence system against ROS (Lee *et al*., 2016).

Disruption of spindle fibers causes scattered condensed chromosome leads to the formation of C-metaphase (Figure 4 C). Precocious movement (Figure 4 D,E) of chromosomes observed during the present study might have occurred due to disturbed homology for chromosome pairing, disturbed spindle mechanism or inactivation of spindle mechanism (Agarwal and Ansari, 2001). The loop formation (Figure 4 F) might have originated due to failure of kinetochores to attach with spindles and leading to the joining of ends forming loops (Kumar and Pandey 2016). Unorientation and scattering of chromosomes at anaphase (Figure 4.G) may be due either to the inhibition of spindle formation or destruction of spindle fibres formed (Kumar and Rai 2007). Laggards (Figure 4 H, I) in the present study have been attributed to delayed terminalisation and /or failures of chromosomal movement following spindle fiber discrepancies. The fragments which appeared on the breakage of bridges as a result of spindle fibers functioning to pull the chromosomes towards poles, formed laggards (Kumar and Gupta, 2009). Stickiness was found in both metaphase and anaphase of mitosis. Chromosome stickiness (Figure 4 J) leads to inactivation of DNA replication, increases chromosomal contraction and condensation or nucleoproteins probably leading to cell death (Khanna and Sharma, 2013). Stickiness was found to be most dominant chromosomal aberration recorded in the metaphase and anaphase of mitosis. At the higher concentrations, different abnormalities were observed viz. bridges, micronuclei etc. which was not found at the lower concentration. According to Liu *et al*.(2015), the chromosome bridge might have resulted due to enhanced activity of UV-B radiations, making chromosome breaks, and then the two chromosome sides are respectively healed, producing with double centromere chromosomes, i.e. “chromosome bridges” (Figure 4 J, K). Micronuclei (Figure 4 L) may arise mostly from acentric fragments or lagging chromosome (Fenech 2000). Cellular interaction of NPs, which leads to the generation of ROS, has been shown to be related to the physicochemical characteristics of NPs: size, coating, shape and surface charge (Carlson *et al*., 2008; Kim and Ryu 2013).

5. Conclusion

Based on previous study, it has been reported that Zn and ZnO NPs affected the growth of radish, rape, and ryegrass, but neither supernatant from centrifugation nor

filtrated Zn and ZnO solutions showed significant phytotoxic effects (Lin and Xing 2007). The present study clearly shows the chromotoxic effect of NPs. The lower concentration of NPs is beneficial for plant, but at the higher concentration it shows chromosomal aberrations. It is evident from compiled information that effect of NPs depends on their mode of application, size, and concentrations. So, in the near future NPs act as a light for farmers to induce or enhance the productivity of crops, but when its fine or good concentration is used.

Acknowledgement

The author is thankful to Laser Spectroscopy and Nanomaterials Laboratory, Department of Physics, University of Allahabad for providing NPs and is also highly obliged to National Bureau of Plant Genetics Resources (NBPGR), Shimla, Phagli, India for providing the inbred seeds of buckwheat.

References

Agarwal R and Ansari MYK. 2001. The effect of aniline on root tip cells of *Vicia faba* L. *J Cytol Genet* **2**:129-134.

Arora S, Jain J, Rajwade JM and Paknikar KM. 2009. Interactions of silver nanoparticles with primary mouse fibroblasts and liver cells. *Toxicol Appl Pharmacol.,* **236(3):**310-318.

Asare N, Instanes C, Sandberg WJ, Refsnes M, Schwarze P, Kruszewski M and Brunborg G 2012. Cytotoxic and genotoxic effects of silver nanoparticles in testicular cells. *Toxicol.,* **291**:65-72.

Benn T, Cavanagh B, Hristovski K, Posner JD, and Westerhoff P. 2010. The release of nanosilver from consumer products used in the home. *J Environ Quality* **39(6):**1875-1882.

Carlson C, Hussain SM, Schrand AM, K Braydich-Stolle, Hess KL, Jones RL and Schlager JJ. 2008. Unique cellular interaction of silver nanoparticles: size-dependent generation of reactive oxygen species. *J Physi Chem., B* **112(43):**13608-13619.

Cossins D. 2014. Next generation: nanoparticles augment plant functions. The incorporation of synthetic nanoparticles into plants can enhance photosynthesis and transform leaves into biochemical sensors. S*ci, News Opinion March* **16.**

Fenech M, 2000. The in vitro micronucleus technique. *Mutat Res* **455**: 81–95.

Ghosh M, Bandyopadhyay M, and Mukherjee A. 2010. Genotoxicity of titanium dioxide (TiO2) nanoparticles at two trophic levels: plant and human lymphocytes. *Chemosphere* **81(10):**1253-1262.

Giraldo JP, Landry MP, Faltermeier SM, McNicholas TP, Iverson NM, Boghossian AA, Reuel NF, Hilmer AJ, Sen F, Brew JA and Strano MS. 2014. Plant nanobionics approach to augment photosynthesis and biochemical sensing. *Nature Materials,* **13(4):**400.

Halder S, Mandal A, Das D, Datta AK, Chattopadhyay AP, Gupta S, and Kumbhakar DV. 2015. Effective potentiality of synthesised CdS nanoparticles in inducing genetic variation on *Macrotyloma uniflorum* (Lam.) Verdc. *Bio Nano Sci.,* **5(3):**171-180.

Handy RD, Owen R and Valsami-Jones E. 2008. The ecotoxicology of nanoparticles and nanomaterials: current status, knowledge gaps, challenges, and future needs. *Ecotoxicol.,* **17(5):**315-325.

Horie M, N ishio K, Endoh S, Kato H, Fujita K, Miyauchi A, Nakamura A, Kinugasa S, Yamamoto K, Niki E and Yoshida Y. 2013. Chromium (III) oxide nanoparticles induced remarkable oxidative stress and apoptosis on culture cells. *Environ Toxicol.,* **28(2):**61-75.

Kaveh R, Li YS, Ranjbar S, Tehrani R, Brueck CL and Van Aken B. 2013. Changes in *Arabidopsis thaliana* gene expression in response to silver nanoparticles and silver ions. *Environ Sci Technol.,* **47(18):**10637-10644.

Khanna, N. and Sharma S. 2013. *Allium Cepa* Root Chromosomal Aberration Assay: A Review. *Indian J Pharma Biol Res (IJPBR)* **1**,105-119.

Kim S and Ryu DY. 2013. Silver nanoparticle-induced oxidative stress, genotoxicity and apoptosis in cultured cells and animal tissues. *J Appl Toxicol.,* **33(2):**78-89.

Kruszewski M, Brzoska K, Brunborg G, Asare N, Dobrzyńska M, Dušinská M, Fjellsbø LM, Georgantzopoulou A, Gromadzka-Ostrowska J, Gutleb AC and Lankoff A. 2011. Toxicity of silver nanomaterials in higher eukaryotes. *Advances Molec Toxicol.,* **5**: 179-218.

Kumar, G and Pandey, A. 2016. Clastogenic and aneugenic responses of supplemental UV-B radiation on root meristems of Lentil. *Inter J Life Sci Res.,* **4(1):**1-8.

Kumar G and Gupta P. 2009. Induced karyomorphological variations in three phenodeviants of *Capsicum annuum* L. *Turkish J Biol.,* **33(2):**123-128.

Kumar G and Rai PK. 2007. EMS induced karyomorphological variations in maize (*Zea mays* L.) inbreds. *Turkish J Biology* **31 (4):**187-195.

Kumari M, Khan SS, Pakrashi S, Mukherjee A and Chandrasekaran N 2011. Cytogenetic and genotoxic effects of zinc oxide nanoparticles on root cells of *Allium cepa. J Hazardous Materials,* **190**:613-621.

Kumari M, Mukherjee A and Chandrasekaran N. 2009. Genotoxicity of silver nanoparticles in *Allium cepa*. *Sci Total Environ.,* **407(19):**5243-5246.

Landsiedel R, Kapp MD, Schulz M, Wiench K and Oesch F. 2009. Genotoxicity investigations on nanomaterials: methods, preparation and characterization of test material, potential artifacts and limitations—many questions, some answers. *Mut Res/Rev Mut Re.,* **681(2):**241-258.

Laurent S, Forge D, Port M, Roch A, Robic C, Vander Elst L and Muller R N. 2010 Magnetic iron oxide nanoparticles: synthesis, stabilization, vectorization, physicochemical characterizations, and biological applications, *Chem Rev*., **110**:2574–2574

Lee SH, Wang TY, Hong JH, Cheng TJ and Lin CY. 2016. NMR-based metabolomics to determine acute inhalation effects of nano- and fine-sized ZnO particles in the rat lung. *Nanotoxicol.,* **10 (7):** 924-934.

Lin D, Xing B. 2007.Phytotoxicity of nanoparticles: Inhibition of seed germination and rootgrowth. *Environ Pollut.,* **150(2):**243–250.

Liu F, Chen H and Han R. 2015. Different doses of the enhanced UV-B radiation effects on wheat somatic cell division. *Cell Bio.,* **4 (2):**30.

Panda KK, Achary VMM, Krishnaveni R, Padhi BK, Sarangi SN, Sahu SN and Panda BB. 2011. In vitro biosynthesis and genotoxicity bioassay of silver nanoparticles using plants. *Toxicol in vitro,* **25(5):**1097-1105.

Sobha K, Surendranath K, Meena V, Jwala TK, Swetha N and Latha KSM. 2010. Emerging trends in nanobiotechnology. *Biotechnol Molec Biol Rev.,* **4(1):**1-12.

Suriyaprabha R, Karunakaran G, Yuvakkumar R, Rajendran V and Kannan N. 2012. Silica nanoparticles for increased silica availability in maize (*Zea mays* L.) seeds under hydroponic conditions. *Current Nanosci.,* **8(6):**902-908.

Zafar H, Ali A, Ali JS, Haq IU and Zia M. 2016. Effect of ZnO nanoparticles on *Brassica nigra* seedlings and stem explants: growth dynamics and antioxidative response. *Frontiers Plant Sci.,* **7**: 535.

Zhu H, Han J, Xiao JQ and Jin Y. 2008. Uptake, translocation, and accumulation of manufactured iron oxide nanoparticles by pumpkin plants. *J Environ Monitoring,* **10 (6):** 713-717.

JJBS
Jordan Journal of Biological Sciences

Volume 13, Number 1,March 2020
ISSN 1995-6673
Pages 19 - 28

Chitinase of Marine *Penicillium chrysogenum* MH745129: Isolation, Identification, Production and Characterization as Controller for Citrus Fruits Postharvest Pathogens

Sherien M.M. Atalla[1], Nadia G. EL Gamal[2] and Hassan M. Awad[1,*]

[1]*Chemistry of Natural and Microbial Products Dept., Pharmaceutical and Drug Industries Research Div.,* [2]*Plant Pathology Department, Agricultural and Biological Research Division, National Research Centre, Dokki, Giza, Egypt, 12622*

Received February 18, 2019; Revised April 4, 2019; Accepted April 24, 2019

Abstract

Marine waste is one of the most environmental problems. Chitinase is essential in decomposition of chitin, resulting in the utilization of chitin as a renewable resource. Marine fungi *Penicillium chrysogenum* MH745129 was isolated from red sea water and identified by 18S rRNA. It was selected for chitinase production from medium containing different chitin waste sources as shrimp shell powder, fish shell powder, chitin, sawdust and alginate. Addition of dextrose to fermentation media containing shrimp shell powder increases the enzyme activity to 78.2U/mL. The optimum reaction mixture conditions of partially purified chitinase activity was obtained using 60% acetone at 40 °C, pH 6.0 at 40 min, and it was stable at 50°C for 60 min. The kinetic constants K_m and V_{max} determined for chitinase with colloidal chitin as substrate was 6.26 mg/ml and 68.5 U/ml, respectively. The chitinase molecular weight was found to be 42 kDa. In vitro partially purified chitinase was significant in reduction, reduced the linear mycelial growth of both *P. digitatum* and *P. italicum*. Also in vivo all treatments reduced significantly postharvest disease incidence of Valencia orange and Lime fruits compared to the control. After 20 days storage period, 100% of control fruit developed green and blue mold in Valencia orange and lime fruits.

Keywords: Marine fungi isolation and identification, Marine wastes, Chitinase, Partial purification, Biocontrol.

1. Introduction

Chitin, α-1, 4-connected a polymer of N-acetyl-D-Glucosamine, is the second most bounteous poly-saccharide in nature alongside cellulose, and to a great extent it exists in squanders from handling of marine nourishment items (crab, shrimp and krill shells just as fish scales) (Pointing and Hyde, 2001).

Marine squanders are viewed as the extraordinary wellsprings of chitin. Rinaudo (2006) referenced that more than 80,000 tons of chitin were created from marine squanders each year, which should be all the more viably used to keep away from the destructive effect on nature. The waste created from the overall generation and preparing of shellfish and fish scales is a difficult issue of developing greatness. This rich waste may present ecological danger because of the simple disintegration (Mejia-Saules *et al*., 2006; Darwesh *et al.,* 2018a).

Chitinases (EC 3.2.1.14) having a place with the group of glycosyl hydrolases, catalyze the hydrolysis of chitin, (GlcNAc) residues (Taib, *et al*., 2005). Chitinases are recorded as Glycosyl Hydrolases (GH) family-18 and GH family-19. Family 19 is commonly profoundly preserved and contains primarily plant chitinases. Family 18 incorporates countless developed chitinases from plants, animals, bacteria and fungi (Zees *et al*., 2005).

Interest for industrial enzymes, especially of microbial inception, is consistently expanding inferable from their applications in a wide assortment of procedures. Among the microorganisms, filamentous fungi are especially fascinating because of their simple cultivation and generation of extracellular enzymes of industrial potential, i.e. textile, animal feed, baking, pulp and paper industries, leather, chemical and biomedical industry, agriculture, food technology, pharmaceuticals, medicine (Falch, 1999; Hasanin *et al.*, 2018; Hasanin *et al.*, 2019), estimation of fungal biomass (Miller *et al*., 1998), mosquito control (Mendonsa *et al.,* 1996) and waste-management industry (Usai, *et al.,* 1987; Darwesh *et al.,* 2019).

Chitinases utilized likewise, in the biocontrol of irritations that assault diverse plantations, causing financial misfortune around the world, diminishing or killing the utilization of pesticides, and limiting the negative effect on nature. What is more, these enzymes can be utilized for the segregation of protoplasts from fungus and yeasts, for the arrangement of single-cell protein, and for the treatment of chitinous waste from the fishery business (Rathore and Gupta 2015). Chitinases produced N-acetyl-D-Gluco-samine as imperative remedial operator in the treatment of osteoarthritis and bioactive chit-oligosaccharides as vital antitumor mediators (Lodhi *et al*., 2014).

Antifungal chitinases have additionally been investigated by Berini *et al.* (2017). Chitinases serve to

* Corresponding author e-mail: awadmhassan@yahoo.com.

assault fungal pathogens that comprehend chitinous ingredients for self-defense in plants (Singh *et al*., 2007). Accordingly, chitinases are increasing much consideration around the world. Marine fungi turned out to be a rich wellspring of new biologically active ordinary products (Ghanem *et al*., 2010, Gomes *et al*., 2001). The vast majority of these microorganisms cultivate in an interesting and extraordinary environment and in this way they have the ability to deliver exceptional and unordinary secondary metabolites (Fang *et al*., 2005). Shrimp shell waste is tried basically for the generation of bioactive saccharides (Das, Neeraja *et al*., 2012), for example, N-acetylglucosamine which is utilized for the creation of beautifiers and nutritious enhancements (Chen *et al*., 2010).

In Egypt, the citrus business relies upon manufactured fungicides as ordinary repetition for the control of post-gather citrus organic product rots. Loss of viability of few fungicides, expanding good and steady evaluating of buildup limits, is difficulties for the industry. There is a developing need to create elective methodologies for controlling post-harvest rot pathogens. Post-collect rot of citrus organic product brought about by *Penicillium (p.) digitatum* (green fungus), *Penicillium italicum* Whemer (Blue shape) and *Geotrichum candidum* (Bitter rot) have been accounted for everywhere throughout the world and denotes to real losses in production throughout harvest, packing and exportation (Joseph and Korsten, 2003).

This study describes the isolation, identification of fungal strain as well as the production and characterization of an extracellular chitinase under submerged fermentation using shrimp shell wastes as an inducer. Moreover, the antimicrobial potential and in vivo experiment of the chitinase were also evaluated, the efficiency of partially pure enzymes on the mycelial growth of some plant pathogens and their efficacy in the control of citrus molds under storage conditions.

2. Materials and Methods

2.1. Microorganisms

2.1.1. Producer strain

The marine fungal strain *Penicillium chrysogenum* MH 745129 isolated from red sea water and identified by18S rRNA.

2.1.2. Test strains

Penicilium digitatum and *Penicilium italicum* were isolated from rotting citrus fruit and morphology identified according to Simmsons (2007) at Plant Pathology Department, National Research Centre, Giza, Egypt. These isolates were kept on potato dextrose medium and stored at 4°C until used.

2.2. Fungal strain isolation and medium used

Isolation and purification of fungi were carried out using single spore and hyphal tips technique and individually transferred to Glucose peptone medium (GPM) agar slants (Atalla and Nour El-Din, 1993). The medium was composed of (800 mL sea water and 200 mL distilled water): Glucose 1.0 g/L, peptone 0.5 g/L, yeast extract 0.1 g/L, agar 15 g/L, (Jenkins *et al*., 1998)**.** The strain was kept and stored at 4°C.

2.3. Molecular identification of fungal isolate

2.3.1. DNA isolation

DNA extraction was done by using the protocol of Gene Jet genomic DNA purification Kit (Thermo# K0791) as follows manufacture of the kit.

2.3.2. PCR amplification and Sequencing

The PCR amplification of 18S rDNA region was carried out following the manufacture of Maxima Hot Start PCR Master Mix (Mix (Thermo) #K0221). The 18srDNA was amplified by polymerase chain reaction (PCR) using primers designed to amplify a 1500 bp fragment of the 18SrDNA region. The ITS1–5.8S–ITS2 genomic region was amplified from genomic DNA using the forward primer ITS1 (5-TCCGTAGGTGAACCTGCGG-3) and the reverse primer ITS4 (5-TCCTCCGCTTATTGATATGC-3) (Elshahawy *et al*., 2018).

The PCR reaction was performed with 10µl of genomic DNA as the template, 1µL of 18SrRNA Forward primer, 1µL of 18SrRNA reverse primer 13 µL Water, nuclease-free and 25 µL Maxima® Hot Start PCR Master Mix (2X) in a 50µL reaction mixture as follows: activation of Taq polymerase at 95 °C for 10 minutes, 35 cycles of initial den. 95°C for 10 min, dent. 95°C for 30 sec, annealing 55°C for 1 min, extension 72°C for 1min, final extension 72°C for 15min. After completion, the PCR products were electrophoresed on 1% agarose gels, containing ethidium bromide (10 mg/mL), to ensure that a fragment of the correct size had been amplified.

The amplification products were purified with K0701 Gene JET™ PCR Purification Kit (Thermo**).** Afterward, the samples became ready for sequencing in ABI Prism 3730XL DNA sequencer and analysis on G ATC Company.

2.3.3. Phylogenetic analysis and tree construction

Phylogenetic data were obtained by aligning the nucleotides of different 18S rRNA retrieved from a BLAST algorithm (www.ncbi.nlm.nih.gov/BLAST), using the CLUSTAL W program version 1.8 with standard parameters. Phylogenetic and molecular evolutionary analyses were conducted using Mega 6 program (Barakat *et al.,* 2017). All analyses were performed on a bootstrapped data set containing 100 replicates (generated by the program).

2.4. Preparation of sea wastes substrates

Fish and shrimp shells were collected, washed with tap water and dried in oven at 70 °C. The dried shells were ground into fine powder added and mixed by shaking. Shrimp-shell powder and fish shell powder were added separately to the fermentation medium in comparison with chitin powder, sawdust and alginate as substrate.

2.5. Fermentation condition

Fermentation was carried out in 250 mL Erlenmeyer flask each containing 50 ml of fermentation medium consist of (g/L): Different chitin sources, 20.0; Sodium nitrate 2.0; K_2HPO_4, 1.0; $MgSO_4$, 0.5; KCl, 0.5; $FeSO_4.7H_2O$, 0.01 and autoclaved at 121°C for 15 min. One ml of 10^6 spore suspension of *Penicillium chrysogenum* MH745129 was inoculated in each flask and incubated at 28-30 °C for 7 days at 150 rpm. The enzyme activity was

determined under the standard conditions mentioned in chitinase assay.

2.6. Chitinase assay

Colloidal chitin was prepared from chitin powder (Sigma-Aldrich Corp. St. Louis, MO USA) according to the method described by Reid and Ogryd-Ziak (1981). Determination of enzyme activity was carried out according to the method of Reid and Ogryd-Ziak (1981). Take 1 mL of 1% colloidal chitin in citrate phosphate buffer (pH 6.6) in test tubes, one ml of culture filtrate was added and mixed by shaking. Tubes were incubated in a water bath at 37°C for 60 minutes, then cooled and centrifuged before assaying. Reducing sugars were determined in 1ml of the supernatant by 3, 5-dinitrosalysilic acid (DNS). Optical density was measured at 540 nm.

2.7. Optimization of medium composition on chitinase production

2.7.1. Effect of different chitin sources

The chitinase production was carried out by using different polysaccharides from marine origin: shrimp-shell powder and fish shell powder in comparison with chitin powder, sawdust and alginate. One ml of 10^6 spore suspension of *Penicillium chrysogenum* MH745129 was inoculated in each flask and incubated at 28-30 °C for 7 days at 150 r pm. The enzyme activity was determined under the standard conditions mentioned in chitinase assay.

2.7.2. Effect of different concentrations of shrimp shell

Fifty mL of sterile fermentation media prepared with shrimp shell powder at different concentration ranged from 10 to 50 g/L. The enzyme activity was determined under the standard conditions mentioned in chitinase assay.

2.7.3. Effect of different carbon sources

The effect of additional different carbon sources (glucose, lactose, fructose, xylose, dextrose and sucrose), supplemented in medium at a concentration of 1% was tested for their ability to enhancement of chitinase activity. The inoculated flasks were incubated at 28-30 °C for 7 days at 150 rpm. C hitinase assay was measured as mentioned above.

2.7.4. Effect of nitrogen sources

The influence of using various nitrogen sources on the chitinase production was investigated. Different nitrogen sources such as sodium nitrate, potassium nitrate, ammonium nitrate and yeast were used in comparing with medium free of nitrogen source. The inoculated flasks were incubated at 28±2 °C for 7 days at 150 rpm, and then chitinase assay was detected.

2.7.5. Effect of different incubation period

The production medium was inoculated by the selected strain and incubated at different incubation periods (3, 5 and 7 da ys). Chitinase activity and mycelium dry weight were determined by filtering the mycelial mat on pre-weighted filter paper (e.g. Whatman No.1) that has been set to dry at 105°C until constant weight and weight it again.

2.8. Characterization of partially purified chitinase enzyme

2.8.1. Partial purification of chitinase

The crude enzyme obtained from *Penicillium chrysogenum* MH745129 culture was precipitated by adding 4:1 cooled acetone to stirred supernatant as described by Darwesh *et al.* (2019). The mixture was centrifuged at 10,000 rpm for 15 m in at 4°C and the precipitated proteins were resuspended in the suitable amount of buffer.

2.8.2. The protein content measurement

The protein content was estimated by using the Lowry *et al*. [26] with bovine serum albumin (BSA), (1mg/mL) as standard.

2.8.3. Effect of different pH values, temperatures and reaction time on chitinase activity

The activity of the partially purified chitinase enzyme was measured at different pH values (3.6-7.0). The enzyme activity was determined at different temperatures of the reaction mixture (10-60 °C) and different reaction times (10-60 min).

2.8.4. Determination of thermal temperature stability of chitinase activity

Thermal chitinase stability was determined by incubating the enzyme at different temperature levels ranging 10-70 °C for 10-60 min; residual enzyme activity was measured at slandered conditions.

2.8.5. Determination of kinetic parameters (Km and Vmax) using Lineweaver-Burk plots

The kinetic parameters (*Km* and *Vmax*) were determined for the partially purified chitinase and calculated from Lineweaver –Burk plots (1934).

2.8.6. Polyacrylamide gel electrophoresis

The molecular weight of purified chitinase was estimated using a sodium dodecylsulphate polyacrylamide gel electrophoresis (12%SDS–PAGE) according to Laemmli (1970). After running at 120 V and 40 mA for 45 min, the gel was stained using Coomassie blue-silver. The Precision Plus Protein™ (Bio-Rad®) (10–250 kDa) was used as molecular mass marker (Darwesh *et al*., 2018b).

2.9. In vitro: Antifungal activity of partially purified chitinase

Antifungal activity of the partially purified enzyme obtained from *Penicillium chrysogenum* MH745129 on shrimp shell waste was studied by determining their inhibitory effect on l inear growth of *Penicilium (P.) digitatum* and *P. italicum* on PDA medium using the well-plate diffusion method as described by Marrez *et al.* (2019). Pathogenic fungi over laid on PDA plate and after 30 min three wells (5mm. in diameter) were made in each plate and inoculated with 20 µL of partially purified enzyme in contrast with the same volume of water as a control. The plates were kept for 2 h at 4°C then incubated at 28°C for 5 da ys. Diameter of linear growth and reduction was measured.

2.10. Management of green and blue mold disease of orange and lime fruits during storage

Commercially harvested navel oranges (*Citrus sinensis* L. Osbeck) and Lime (*Citrus aurantifolia* F. Muell), with a healthy appearance from citrus orchards, were used in this experiment. Highly aggressive isolates of *Penicillium digitatum* and *Penicillium italicum* originally isolated from the rotted citrus fruit were used as pathogenic fungi. Isolates were grown on potato dextrose agar (PDA) at 25°C for 7 days. Spore suspension (10^6 spores /mL) was obtained by flooding 7th day old cultures of the pathogen with sterile distilled water containing 0.01% (v/ v) Tween 80 (Zhang, 2013).

The citrus fruits were coated with either partially pure chitinase enzyme. The efficacy of coated citrus and/or lime fruits against mold incidence under stress of artificial infestation was evaluated during storage conditions. Fruits were surface sterilized by dipping them into 1% (v: v) sodium hypochlorite for 3 min. Then, fruits were rinsed 3 times with sterile distilled water and blotted dry on sterile filter paper.

The fruits were wounded by a sterilized needle at one marked point and dipped individually into partially purified enzyme; then the treated fruits were artificially inoculated by spraying with tested fungi (having a mean of 10^6 spores/mL). Thereafter, all treated fruits were air dried, placed into carton boxes (46x23x30 cm) with a capacity of 15 fruits/box, covered with plastic sheets to maintain a relative humidity–RH (90–95%), and stored in a fruit store at 20±2°C for 4 weeks. Five boxes as replicates were used for each treatment as well as the control. Decayed fruits were counted periodically every week. The percentage of total disease incidence was calculated at the end of the storage period.

2.11. Statistical analyses

Statistical analyses were performed with descriptive statistics (mean) and inferential tests (ANOVA followed by Turkey test) to determine statistically significant differences ($P < 0.05$) between treatments with Sigma Stat Software (Neler, *et al*., 1985).

3. Results and Discussion

3.1. Fungal strains isolation and selection the promising isolate

A total of 25 marine fungal isolates were tested for their ability of chitinase production. Out of them, RSW_SEP2 isolate was the most promising and selected for fully identification, production, characterization and biocontrol applications.

3.2. Molecular identification of the isolate

3.2.1. DNA isolation and PCR amplification

The genomic DNA of RSW_SEP2 isolate was applied to PCR using general primers to amplify the ITS1 and ITS4 region between the tiny and great nuclear rDNA, counting the 18S rDNA. These primers amplified a DNA fragment of about 579 bp. The outcome was in accordance with (Freeman, *et al.,* (2000); Rasu, *et al.,* 2012) who denoted that these primers are accurate for fungi and amplified a DNA fragment of about 560 bp using some fungi.

The nucleotide sequence (579 bp) of strain *Penicillium chrysogenum* RSW_SEP2 was blasted with the available Gen Bank resources using NCBI-BLAST search (www.ncbi.nlm.nih.gov/BLAST) to contest the RSW_ SEP2 isolate with those of *Penicillium chrysogenum* strains. The results displayed the great sequence similarity species (99%) with *P. chrysogenum* strains.

3.2.2. Alignment, phylogenetic tree construction and GC%

The phylogenetic tree (Figure 1) showed that strain RSW_SEP2 is greatest intimately correlated to *Penicillium chrysogenum*. Consequently, it was suggested a name of *P. chrysogenum* RSW_SEP2. The percent of Guanidine + Cytosine is individual of various universal features used to identify organism genomes. The G+C content of the genomic DNA was 58% mol% for RSW_SEP2 strain was achieved from the phylogenetic examination. The results were in agreement with those by Storck (1966) and Nakase (1971) who indicated the GC content of fungi ranges from 31.5 to 63% based on each class. The compositional variety also decreases from classes and subclasses to genera and species.

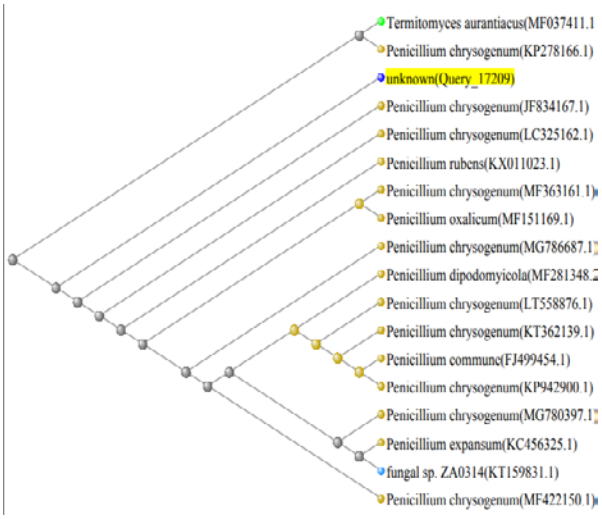

Figure 1. Phylogentic relationships of *Penicillium chrysogenum* isolate and closely related species from the GenBank database, according to 18S rDNA sequence similarity.

3.2.3. Nucleotide sequence ID

The nucleotide sequences of 18S rRNA gene of *Penicillium chrysogenum* RSW_SEP2 has been deposited in GenBank under accession number**:** MH745129.

3.3. Optimization of medium composition on chitinase production

3.3.1. Effect of different sources of chitin on chitinase activity

Determination of chitinase activity was measured using shrimp-shell powder, fish shell powder, chitin powder, sawdust and alginate as different sources of chitin. The results in Figure 2 showed maximum chitinase activity of 71.4 U/mL using shrimp shell powder followed by chitin powder of 60.7 U/mL. These results were coincided with Farag *et al*. (2014) who found that maximum chitinase activity obtained from *A. terreus* in fermentation medium containing shrimp shell powder as a chitin source. In addition, Rattanakit *et al*. (2007) and Krishnaveni and Ragunathan (2014) obtained the maximal chitinase production from fish-scales by *A. terreus* and shell fish

wastes by *Bionectria* CBNR BKRR, respectively. On the other hand, these results were constricted with Maria *et al*. (2009) and Sharmistha *et al*. (2012) who found that chitinolytic fungi produce maximum chitinase activity from colloidal chitin.

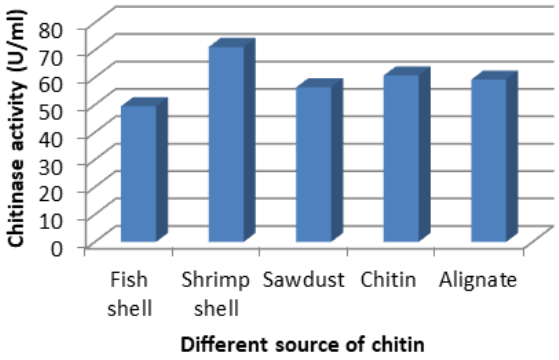

Figure 2. Effect of different source of chitin on chitinase production by *Penicillium chrysogenum* MH 745129.

3.3.2. Effect of different concentrations of shrimp shell powder

Optimization of shrimp shell powder concentration was carried out using different concentration of chitin ranged from (10-50) g/L. The results in Figure 3 s howed the highest activity of 76.8 U/mL was achieved at 20 g/L of shrimp shell followed 75.4 U/ml using 30 g /L then the activity gradually decreased. These results were not in harmony with Jesus *et al*. (2006) who found that the 60 g/L of shrimp shell powder gave the maximum chitinase activity from *Serratia marcescens*.

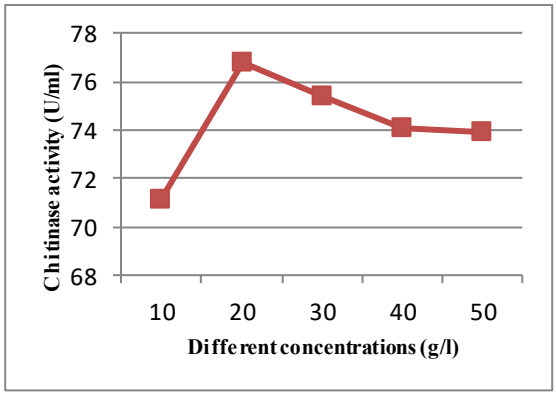

Figure 3. Effect of different concentration of shrimp shell on chitinase activity by *Penicillium chrysogenum* MH 745129.

3.3.3. Effect of different carbon source

The results in Figure 4 indicated that the maximal chitinase activity was 78.2 U/mL in presence of dextrose followed by xylose and fructose. These results were in agreement with several authors such as Sandhya *et al.* (2005); Nawani *et al.* (2002) and Farag *et al*. (2014) they reported that the addition of different sugars to the production medium increased the chitinase activity by different strains as *Trichoderma harzianum* and *A. terreus*. In contrast, Sharmistha *et al*. (2012) found that the addition of maltose, sucrose, xylose, lactose, glucose and fructose decreased chitinase production from *Serratia marcescens*.

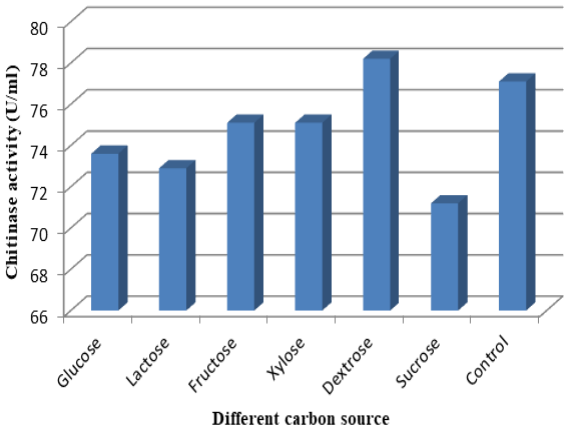

Figure 4. Effect of different carbon source on chitinase by *Penicillium chrysogenum* MH 745129.

3.3.4. Effect of different nitrogen source

The results in Figure 5 showed that the maximal chitinase activity of 92.4 U/mL was obtained from medium containing potassium nitrate using shrimp shell as substrate followed by sodium nitrate and ammonium nitrate.

These results counteracted with several authors who mentioned that 1% of ammonium sulphate were most suitable for chitinase production from *A. terreus* and (Farag *et al*., 2014). Also, the addition of 1% yeast extract increased the chitinase activity by *S. marcescens*, *Alcaligenes xylosoxydans* and *Paenibacillus Sabina* JD2 strains (Ulhoa and Peberdy, 1993 and Sharmistha *et al*., 2012).

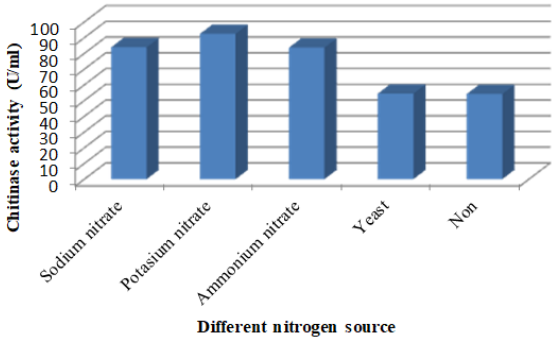

Figure 5. Effect of different nitrogen source on chitinase activity by *Penicillium chrysogenum* MH 745129.

3.3.5. Effect of different incubation period

Effect of different incubation time and mycelium dry weight was evaluated after (3, 5, 7 a nd 10 days). The results in Table 1 showed that chitinase activity increased gradually till reached its maximum activity of 78.20 U/mL on the fifth day in fermentation medium containing dextran then the enzyme activity gradually decreased by increasing the incubation period. The highest mycelium dry weight was 1.91 g/L at the same time. The outcome of these results was in agreement with Krishnaveni and Ragunathan (2014) who indicated that the maximum chitinase activity from *F. solani* CBNR BKRR was 5 days. On the contrary, the maximum chitinase activity was found 3 and 4 days from *Oidium caricae* and *Tichoderma harziaum*, respectively (Synowiecki and Al- Khateeb, 2003 and Ghanem *et al*., 2011).

Table 1. Effect of different incubation period on chitinase activity by *Penicillium chrysogenum* MH 745129.

Different incubation period (days)	Chitinase activity (U/mL)	Mycelium dry weight (g)
3	40.02	0.88
3D	42.50	0.90
5	76.40	1.49
5D	78.20	1.91
7	52.51	1.51
7D	46.09	1.88
10	42.17	1.23
10D	36.48	1.42

D = with dextran

3.4. Characterization of partially purified chitinase

The crude enzyme obtained from the harvested culture was precipitated by adding to 60% saturation of acetone. The enzyme activity was 50.33 U/mL, the total protein 19.78 U/mg and the specific activity 2.54U/mg protein.

3.4.1. Different reaction temperature

The partially purified chitinase was measured in different temperature (10-60°C) of reaction mixture to select the optimum reaction temperature. The results in Figure 6 showed that the 40 °C was optimized for chitinase activity. These results were close to that obtained from Ekundayo *et al*. (2016) who found that 50 °C had the optimal chitinase activity from *T. viride*; while Badiaa *et al*. (2010) found that the optimum reaction temperature for the chitinase produced from *P. rifitoensis* strain M2-26 was at 70°C.

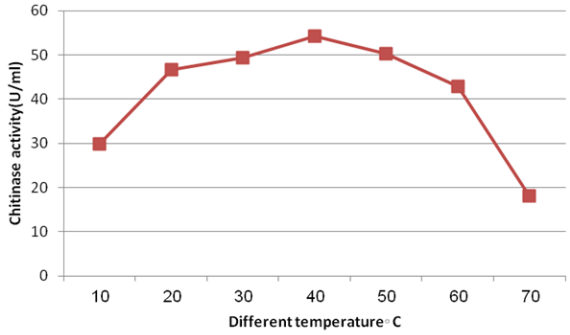

Figure 6. Effect of different temperatures on chitinase activity by *Penicillium chrysogenum* MH 745129.

3.4.2. Different pH values

The influence of different pH values ranging from (3.6-7.0) on chitinase activity was carried out. The results in Figure 7 showed that the enzyme activity increased till reaching its maximum activity of 4.97 U/mL at pH 6.0 then the enzyme activity decreased with the increasing of pH value. These results were almost near to the results that obtained by Hammami *et al*. (2013) who mentioned that the optimum pH value of the partially purified chitinase from *B. Cereus* was pH 6.5. On the contrary, pH value ranged from 4.5-5.0 was the most suitable for chitinase activity from different strains as *T. lanuginosus* SY2 and *T. viride* (Guo *et al*., 2008; Mendana *et al*., 2011 and Ekundayo *et al*., 2016).

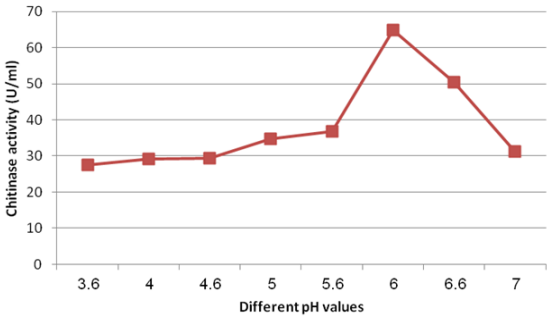

Figure 7. Effect of different pH values on chitinase activity by *Penicillium chrysogenum* MH 745129

3.4.3. Different reaction times

Different reaction mixture time (10 - 60 min) was investigated to select the best reaction time. The maximal chitinase activity of 65.11 U/mL was obtained at 40 min of reaction time as shown in Figure 8. On the other hand, the enzyme activity above and below 40 min activity decreased. These results were closer to those obtained by Farag *et al*. (2014) and Masilamani *et al*. (2012) who found the maximum chitinase activity of *A. terreus* and *Metapenaeus dobsonii* at 30 min.

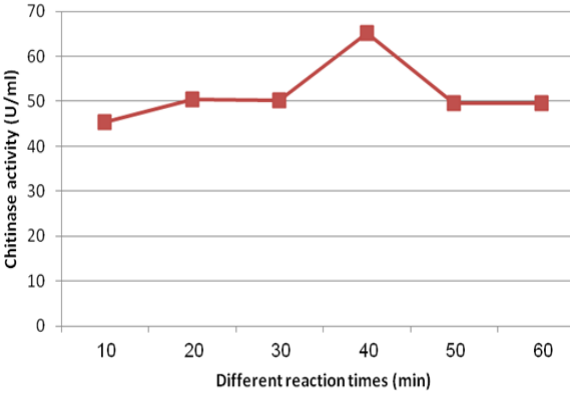

Figure 8. Effect of different reaction times (min) on chitinase activity by *Penicillium chrysogenum* MH 745129.

3.4.4. Thermal stability

The results in Table 2 showed that the enzyme activity was stable at 50 °C temperature for 60 min, and then the chitinase activity decreased with the increasing of the temperature. The obtained results were in agreement with Ekundayo *et al*. (2016) who found that the chitinase activity of *Trichoderma viride* culture was stable at temperature ranged from 40-50 °C. On the other hand, these results were contracted with Nampoothiri *et al*. (2004) and Jenifer *et al*. (2014) who observed that the optimal chitinase activity was 40 °C was optimal the relative chitinase activity.

Table 2. Thermal stability of chitinase from *Penicillium chrysogenum* MH 745129.

Temp °C	Chitinase activity (U/mL)					
min	20	30	40	50	60	70
10	47.87	46.41	46.45	47.45	49.59	44.52
20	46.96	47.09	42.00	49.19	49.66	45.04
30	46.17	47.61	43.60	48.71	49.70	47.66
40	46.10	46.81	46.87	48.56	49.91	42.04
50	46.06	45.89	44.92	48.41	50.53	37.60
60	45.24	44.84	44.21	47.99	49.66	37.27

3.4.5. Determination of kinetic parameters (Km and V max) by Lineweaver –Burk plots

The kinetic characters of the partially purified enzyme using chitin as substrate were determined and calculated from Lineweaver–Burk plots (1934). The estimated K_m and V_{max} values of the chitinase acting on chitin as substrate were 6.26 mg/ml and 68.5 U/mL (Figure 9). The K_m value (6.26 mg/mL) was greater than that obtained for the chitinase from *G. catenulatum* (Ma *et al*., 2012) but lower than those obtained for the chitinases from *T. harzianum* CECT 2413 (3.6 mg/mL) and *Serratia marcescens* B4A (8.3 mg/ml) (De La Cruz *et al*., 1992 ; Zarei *et al*., 2011).

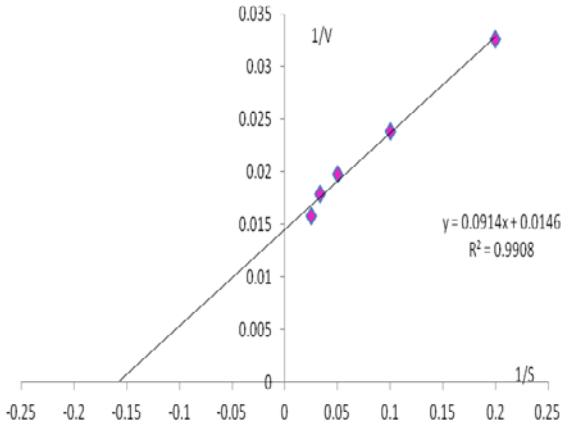

Figure 9. Lineweaver-Burk plot relating *Penicillium chrysogenum* MH745129 chitinase reaction velocity to chitinase concentration.

3.4.6. Determination of chitinase molecular weight

The molecular weight of chitinase was found to be 42 kDa estimated by 12% SDS-PAGE (Figure 10). This value was near to the value estimated for the chitinases produced from *A. niger* LOCK 62 and *A. fumigatus* YJ-407, with a molecular weight of 43 kDa and 46 kDa (Swiontek Brzezinska and Jankiweicz, 2012; Xia *et al.,* 2001). Rattanakit *et al*. (2007) purified 3 chitinases from *Aspergillus* sp. with molecular weights of 45, 51, and 73 kDa. In addition, the diverse chitinases produced by NRRL 2129 s train and *A. terreus* showed molecular weights of 82.7, 44.6, 28.2, 26 k Da and 60 k Da respectively (Farag *et al*., 2016; Binod *et al*., 2005). Furthermore, this value lay in the range in which diverse molecular weight (27-190 kDa) has been stated for other fungal chitinases (Nagpure and Gupta, 2012; Saraswathi and Ravuri, 2013; Li, 2006).

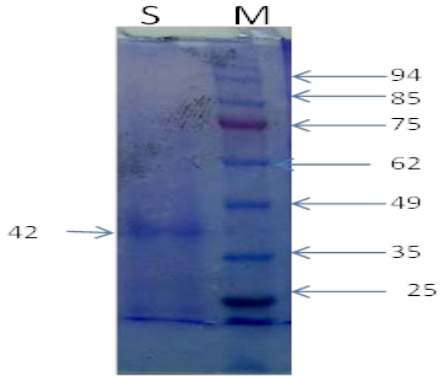

Figure 10. Molecular weight of partially purified chitinase from *Penicillium chrysogenum* MH 745129 by SDS page

3.5. In vitro: antifungal activity of partially purified enzyme on linear growth of P. digitatum and P.italicum

The *in vitro* suppressive effect of partially purified enzyme from marine fungal strain *Penicillium chrysogenum* MH745129 against the linear mycelial growth of *P. digitatum* and *P. italicum* are shown in Table (3). The results indicated that the partially pure enzyme significantly reduced the linear mycelial growth of both *P. digitatum* and *P. italicum* compared with control.

Table 3. Reduction in fungal growth in response to partially pure enzyme on linear growth (mm) and reduction of *P. digitatum* and *P. italicum* in vitro conditions.

	Penicilium digitatum		*Penicilium italicum*	
Treatment	Growth	%Reduction	Growth	%Reduction
Partially pure enzyme	27b	70	25b	72.2
Control	90a	-----	90a	-----

Data in each column with the same letter is not significantly different (P=0.05) according to Tukey test (Neter *et al.,* 1985).

3.6. In vivo: protective effect of partially purified enzyme on postharvest diseases of Valencia orange and Lime fruits

The results in Table 4 showed that in vivo t he protective effect of partially purified enzyme against postharvest diseases of Valencia Orange and Lime fruits caused by *P. digitatum* and *P. italicum* as disease incidence (%) after 20 days of treatment and inoculation, when the fruit was stored at 20±2 °C. Results indicated that all treatments significantly reduced postharvest disease incidence (%) of Valencia Orange and Lime fruits compared to the control. After 20 da ys storage period, 100% of control fruit developed green and blue molds in Valencia orange and Lime fruits.

The deterioration of chitin, an essential piece of the worldwide carbon and nitrogen cycles, depends basically on microbiological cultivations. Chitin can be utilized by microbial populaces as the sole wellspring of these 2 components thought about basic waste, shrimp squander is prepared for animal feed and is likewise utilized in farming as a shoddy normal nitrogen compost.

Table 4. Protective effect of partially pure enzyme against postharvest diseases of Valencia orange and lime fruits.

Treatments	Valencia orange fruits		Lime fruits	
	Green mold	Blue mold	Green mold	Blue mold
Partially pure enzyme	7.0b	10.0b	9.0b	12.0b
Control	100a	100a	100a	100a

Data in each column with the same letter is not significantly different (P=0.05) according to Turkey test (Neter *et al*., 1985).

Moreover, Rattanakit *et al*. (2007) illustrated that *Aspergillus* sp. cultivated on m edium containing shrimp waste, blends the equivalent or higher measures of chitinolytic enzymes than when cultivated on medium enhanced with colloidal chitin.

The most vital plant pathogens include: Fusarium, Penicillium, Alternaria, Botrytis, Ramularia, Monilinia, Cladosporium and Aspergillus. These molds assault numerous agricultural plants, including vegetables, fruit, and pretty flowers. So as to ensure the harvests individuals apply distinctive kinds of product assurance synthetic fungicides prepared by chemical combination. There are likewise numerous biotic mediators' fighting fungal pathogens, comprising different bioactive compounds of microbiological source, e.g. chitinases (CHIs). The capacities of microorganisms to deliver antifungal CHIs have been investigated. The enzymes created by the family of storing fungi named *Trichoderma* are of significant biotechnological importance (Benitez *et al*., 2004).

Utilization of arrangements containing this fungus in biological control of fungi improvement is conceivable because of the generation of such enzymes as CHIs or glucanases. The Exo-α-1.3glucanase could tie to cell walls of different phytopathogenic organisms, for example *Aspergillus niger* and *Rhizoctonia solani.* The CHI viably restrains the development of *R. solani, Marchophominia phaseolina, Fusarium* sp (Monteiro *et al*., 2010).

Various investigations showed the likelihood of utilizing them in chitinolytic enzymes production with fungal action against some phytopathogenic fungi. In biological control of fungal phytopathogens, utilization of agents containing different metabolites of microorganisms, including chitinases, has all the earmarks of being the more efficient, since they show more grounded fungicidal action than purified chitinases. The use of agents creating a consortium of chitinolytic producers seems to obtain better results in the fight against phytopathogenic fungi.

Acknowledgment

The authors thank the National Research Centre at Dokki, Cairo, Egypt for laboratory assistance.

References

Atalla, MM and Nour El-Din, K. 1993. Isolation and identification of fungi associated with feed stuffs and determination of mycotoxin producing ability. *Egypt J Microbiol*, **28**: 193-205.

Badiaa, E, Mustapha, R, Abdellatif, B, Haissam, J and Najla SZ. 2010. Production and partial characterization of chitinase from a halotolerant *Planococcus rifitoensis* strain M2-26. *WJ Microbiol and Biotechnol*, **26**:977–984

Benitez T, Rincon AM, Limon MC and Codon AC. 2004. Biocontrol mechanisms of *Trichoderma* strains. *Int Microbiol*, **7**:249–260

Berini F, Presti I, Beltrametti F, Pedroli M, Varum KM, Pellegioni L, Sjöling S, Marinelli F. 2017. Production and characterization of a novel antifungal chitinase identified by functional screening of a suppressive-soil metagenome. *Microb Cell Fact*, **16**:16. DOI 10.1186/s12934-017-0634-8

Binod P, Pusztahely T, Nagy V, Sandhya C, Szaka´cs, G, Po´ csi I and Pandey A. 2005. Production and purification of extracellular chitinases from *Penicillium aculeatum* NRRL 2129 under solid state fermentation. *Enzyme Microb Technol*, **36**: 880–887

Chen JK, Shen CR and Liu CL. 2010. N-Acetylglucosamine: production and applications. *Mar Drugs*, **8**:2493–2516.

Das SN, Neeraja Ch, Sarma PVSRN, Madhu Prakash J, Purushotham P, Kaur M, Dutta S, Podile AR. 2012. Microbial chitinases for chitin waste management. *Microorg Environ Manag,* **Chap: 6:** 135–150.

De La Cruz J, Hidalgo-Gallego A, Lora JM, Benitez T, Pintor-Toro JA, Llobell A. 1992. Isolation and characterization of three chitinases from *Trichoderma harzianum. Eur J Biochem*, **206:** 859–867.

Diaa A Marrez, Ahmed E Abdelhamid and Osama M Darwesh. 2019. Eco-friendly cellulose acetate green synthesized silver nano-composite as antibacterial packaging system for food safety. *Food Packaging and Shelf Life*, **20:** 100302: 1-8. https://doi.org/10.1016/j.fpsl.2019.100302.

Ekundayo EA, Ekundayo FO and Bamidele F. 2016. Production, partial purification and optimization of a chitinase produced from *Trichoderma viride*, an isolate of maize cob. *Mycosphere*, **7**: 786–793

Falch EA. 1991. Industrial enzymes - developments in production and application. *Biotechnol Adv*, **9**: 643-658.

Fang, W, Leng B, Xiao Y, Jin K, Ma J, Fan Y, Feng J, Yang X, Zhang J, and Pei Y. 2005. Cloning of *Beauveria bassiana* chitinase gene Bbchit1 and its application to improve fungal strain virulence. *Appl Environ Microbiol*, **71**: 363–370.

Farag AM., Abd-Elnabey HM, Ibrahim HAH and El-Shenawy M 2016. Purification, characterization and antimicrobial activity of chitinase from marine-derived *Aspergillus terreus*. *Egyptian J Aqu Res*., **42**: 185–192

Farag MA and Al-Nusarie, ST. 2014. Production, optimization, characterization and antifungal activity of chitinase produced by *Aspergillus terrus. African J Biotechnol,* **13**:1567-1578.

Freeman S, Minz D, Jurkevitch E, Maymon M, ShabiE. 2000. Molecular analyses of Colletotrichum species from almond and other fruits. *Phytopathol*, **90**: 608-614.

Ghanem KM, Al-Garni SM and Al-Makishah NH. 2010. Statistical optimization of cultural conditions for chitinase production from fish scales waste by *Aspergillus terreus. African J Biotechnol*, **9**: 5135-5146.

Ghanem KM, Fahad A Al-Fassin and Reem MF. 2011. Statistical optimization of cultural conditions for chitinase production from shrimp shellfish waste by *Alternaria alternate. African J Biotechnol*, **5**: 1649-1659.

Gomes RC, Semedo LTAS, Soares RMA, Linhares LF, Ulhoa CJ, Alviano CS, and Coelho RRR. 2001. Purification of a thermostable endochitinase from *Streptomyces* RC1071 isolated from a cerrado soil and its antagonism against phytopathogenic fungi. *J Appl Microbiol*., **90**: 653-661.

Guo RF, Shi BS, Li DC, Ma W, and Wei Q. 2008. Purification and characterization of a novel thermostable chitinase from *Thermomyces lanuginosus* SY2 and cloning of its encoding Gene. *Agr Sci*, **7**: 1458–1465.

Hammami R, Siala M, Jridi N, Ktari M, Nasri and Triki MA. 2013. Partial purification and characterization of chiIO8, a novel antifungal chitinase produced by *Bacillus cereus* IO8. *J Appl Microbiol*., **115**: 358—366.

Elshahawy I, Abouelnasr H M, Lashin S M and Darwesh O M. 2018. First report of *Pythium aphanidermatum* infecting tomato in Egypt and its control using biogenic silver nanoparticles. *J Plant Prot Res*, **15(2):** 137–151.

Jenifer S, Jeyasree J, Laveena DK and Manikandan K. 2014. Purification and characterization of chitinase from *Trichoderma virid*en and its antifungal activity against phytopathogenic fungi. *W J Pharm and Pharmaceut Sci*, **3**: 1604–1611.

Jenkins KM, Toske SG, Jensen PR, and Fenical W. 1998. Solanapyrones E-G, Antigalmetabolities produced by marine fungus. *Phytochem*, **49**(8): 2299-2304.

Jesus, E Mejia-Saule, Krzysztof, N Waliszewski, Miguel A, Garciaand Ramon Cruz-Camarillo. 2 006. The use of crude shrimp shell powder for chitinase production by *Serratia marcescens* WF. *Food Technolnol and Biotechnol,* **44**: 95–100

Joseph O and Koresten L 2003. Integrated control of citrus green and blue mold using Bacillus subtilis in combination with sodium bicarbonate or hot-water. *Postharvest Biol Technol.,* **28(1):**187-194.

Khouloud M Barakat, Sahar WM Hassan, Osama M Darwesh. 2017. Biosurfactant production by haloalkaliphilic *Bacillus* strains isolated from Red Sea, Egypt. *Egypt J Aquat Res,* **43:** 205–211

Krishnaveni B and Ragunathan R. 2014. Chitinase production from seafood wastes by plant pathogen Bionectria CBNR BKRR sps and its application in bioremediation studies. *Int Res J Med Sci*, **2**:15-19.

Laemmli UK, 1970. Cleavage of structural protein during the assembly of heat of bacteriophage T4. *Nature (London)* **227**: 680–685.

Li DC. 2006. Review of fungal chitinases. *Mycopatholo*, **161:**345–360.

Lineweaver H and Burk D. 1934. The determination of enzyme dissociation constant. *J Am Chem Soc*, **56**: 658- 666.

Lodhi G, Kim YS, Hwang JW, Kim SK, Jeon YD, Je JY, Ahn BB, Moon SH, Jeon BT and Park PJ. 2014. Chitooligosaccharide and its derivatives: preparation and biological applications. *Biomed Res Int*, **2014**:1–13.

Lowry OH, Rosebrough NN, Farr AL, Randall RY. 1951. Protein measurement with the folin phenol reagent. *J Biol Chem*, **193:** 265– 75.

Ma GZ, Gao HN, Zhang YH, Li SD, Xie SD, Wu SJ. 2012. Purification and characterization of chitinase from *Gliocladium catenulatum* strain HL-1-1. *African J Microbiol Res,* **6:** 4377–4383.

Mendana Z, Saeed A, Hossein Z, Alireza S, Morteza D, Kambiz AN, Ahmad G, and Abbasali M. 2011. Characterization of a chitinase with antifungal from a native *Serratia marcescens* B4A. *Brazil J Microbial,* **42**: 1017-1029.

Maria SB, Maciej W, Elżbieta LP, and Wojciech D. 2009. Utilization of shrimp-shell waste as a substrate for the activity of chitinases produced by microorganisms. *Pol J Environ Stud,* **19**(1):177-182.

Masilamani R, Ramachandran S, and Annaian S. 2012. Production and characterization of chitinase from *Vibrio* species, a head waste of shrimp *Metapenaeusdobsonii* (Miers, 1878) and chitin of *Sepiellainermis* Orbigny, 1848. *Adv in Biosci* and *Biotechnol,* **3**: 392-397.

Mejia-Saules JM, Waliszewski KN, Garcia MA, and Cruz-Camarillo R. 2006. The use of crude shrimp shell powder for chitinase production by *Serratia marcescens* WF. *Food Technol Biotechnol*, **44**: 646-651

Mendonsa ES, Vartak PH, Rao JU, and Deshpande MV. 1996. An enzyme from *Myrothecium verrucaria* that degrades insect cuticle for biocontrol of *Aedes aegypti* mosquito. *Biotechnol Lett*, **18**: 373-376.

Miller M, Palofarvi A, Rangger A, Reeslev M, and Kjoller A. 1998. The use of fluorogenic substrates to measure fungal presence and activity in soil. *Appl Environ Microbiol*, **64**: 613-617.

Hasanin M S, Mostafa A M, Mwafy E A and Darwesh OM. 2018. Eco-friendly cellulose nano fibers via first reported Egyptian *Humicola fuscoatra* Egyptia X4: Isolation and characterization. *Environ. Nanotechnol Monit Manag,* **10***:* 409–418.

Hasanin M S, Darwesh O M, Matter I A and El-Saied H. 2019. Isolation and characterization of non-cellulolytic *Aspergillus flavus* EGYPTA5 exhibiting selective ligninolytic potential. *Biocat* and *Agric Biotechnol*, **17**: 160–167.

Monteiro VN, Silva RN, Steindorff AS, Costa FT, Noronha EF, Ricart SAO Sousa MV, Vainstein MH, Ulhoa CJ. 2010. New insights in *Trichoderma harzianum* antagonism of fungal plant pathogens by secreted protein analysis. *Curr Microbiol*, **61**:298–305.

Nagpure and Gupta, 2012. Purification and characterization of an extracellular chitinase from antagonistic *Streptomyces violaceusniger. J Basic Microbiol*, **52**: 1–11.

Nakase T, Komagata K. 1971. DNA base composition of some species of yeasts and yeast-like fungi. *J Gen Appl Microbiol,* **17**: 363-369

Nampoothiri MK, Baiju TV, Sandhya C, Sabu A, Szakacs G, Ashok Pandey A. 2004. Process optimization for antifungal chitinase production by *Trichoderma harzianum. Proc Biochem,* **39**:1583-1590.

Nawani NN, Kapadnis BP, Das AD, Rao AS and Mahajan SK. 2002. Purification and characterization of a thermophilic and acidophilic chitinase from *Microbispora*sp. V2. *J Appl Microbiol*, **93**: 965-975

Neler J, Wassermann J, Kutner M.H. 1985. **Applied Linear Statistical Models, Regression, Analysis of Variance and Experimental Design**. 2nd edn. Homewood, Illinois: Richard D. Irw

Obagwu J and Korsten L. 2003. Control of citrus green and blue molds with garlic extracts. *Eur. J Plant Pathol,* **109**: 221–225, 2003.

Darwesh OM, Matter I A and Eida M F. 2019. Development of peroxidase enzyme immobilized magnetic nanoparticles for bioremediation of textile wastewater dye. *J Environ Chem Engin,* **7(1)**: 102805, 1-7.

Darwesh OM, Sultan Y Y, Seif M M and Marrez D A. 2018a. Bio-evaluation of crustacean and fungal nano-chitosan for applying as food ingredient. *Toxicol Rep,* **5:** 348–356.

Darwesh OM, Eida M F and Matter I A. 2018b. Isolation, screening and optimization of L-asparaginase producing bacterial strains inhabiting agricultural soils. *Bios Res,* **15(3):** 2802-2812.

Pointing SB and Hyde KD. 2001. Bio-Exploitation of Filamentous Fungi. *Fung Diver Res Ser*, **6**: 1- 467.

Rasul MG, Hiramatsu M and Okubo H. 2007. Genetic relatedness (diversity) and cultivar identification by randomly amplified polymorphic DNA (RAPD) markers in teasle gourd (Momordicadioica Roxb). *Sci Hortic,* **111**: 271-279.

Rathore AS and Gupta RD. 2015. Chitinases from bacteria to human: properties applications, and perspectives. *Enz Res*, **2015**:1– 8.

Rattanakit, N, Yano, S, Plikomol, A., Wakayama, M and Tachiki, T. 2007. Purification of *Aspergillus* sp. S1-13 chitinases and their role in saccharification of chitin in mash of solid-state culture with shellfish waste. *J Biosci and Bioeng*, **103**: 535-541.

Reid JD and Ogryd-Ziak, DM. 1981.Chitinase over producing mutant of *Serratia marcens. Appl and Environ of Microbiol*, **41**: 664 – 669.

Rinaudo M. 2006. Chitin and chitosan: properties and applications. *Prog Polym Sci,* **31:**603–632.

Sandhya C, Binod P, Nampoothiri, KM, Szakacs G and Pandey A. 2005. Microbial synthesis of chitinase in solid cultures and its potential as a biocontrol agent against phytopathogenic fungus *Colletotrichum gloeosporioides*. *Appl Biochem and Biotechnol*., **127**: 1-15.

Saraswathi M, Ravuri JM. 2013. Production and purification of chitinase by *Trichoderma harzianum* for control of *Sclerotium rolfsii*. *Int J Appl Nat Sci* , **2** (5): 65–72.

Sharmistha, C, Sourav B and Arijit D. 2012.Optimization of process parameters for chitinase production by a marine isolate of *Serratia marcescens*. *Int J Pharma and Bio Sci*.**,** **2**:8-20.

Simmons W K, Ramjee V, Beauchamp MS, McRae K, Martin A, and Barsalou LW. 2007. A common neural substrate for perceiving and knowing about color. *Neuropsychologia*, **45**: 2802-2810.

Singh RP, Dhania, G, Sharma A and Jaiwal PK, 2007. Biotechnological approaches to improve phytoremediation efficiency for environment contaminants. In: Environmental bioremediation technologies, Singh SN, Tripahti RD. (Eds) Springer, 223-258.

Storck R, 1966. Nucleotide Composition of Nucleic Acids of Fungi II. Deoxyribonucleic Acids. *J of Bacteriol*, **91:(1):**227–230

Swiontek Brzezinska M, and Jankiweicz U, 2012. Production of chitinase by *Aspergillus niger* LOCK 62 and Its potential role in the biological control.. *Curr Microbiol*, **65:**666–672.

Synowiecki J and Al-Khateeb, NA. 2003. Production, properties and some new applications of chitin and its derivatives. *Crit Rev Food sci.*, **43**:145-171.

Taib M, Pinney, JW, Westhead, DR, McDowall, KJ, and Adams, DJ. 2005. Differential expression and extent of fungal/plant and fungal/bacterial chitinases of *Aspergillus fumigatus. Arch Microbiol*, **184**: 78-81.

Tamura K, Stecher G, Peterson D, Filipski A, and Kumar S. MEGA6: Molecular Evolutionary Genetics Analysis Version 6.0 2013. *Mol Biol Evol*, **30**:2725–2729

Ulhoa CJ and Peberdy JF. 1993. Effect of carbon sources on chitobiase production by *Trichoderma harzianum. Mycol Res*, **97**: 45-48.

Usai T, Hayashi Y, Nanjo F, Sakai K and Ishido Y. 1987. Transglycosylation reaction of a chitinase purified from *Nocardia orientails*. *Biochem Biophys Acta*, **923**: 302- 309.

White TJ, Bruns T, Lee S, Taylor JW. 1990. Amplification and direct sequencing of fungal ribosomal RNA genes for phylogenetics. *In*: Innis MA, Gelfand DH, Sninsky JJ and White TJ, (Eds). **PCR Protocols: A Guide to Methods and Applications**. New York: Academic Press Inc., pp. 315–322.

Xia W, Liu P, Zhang J, Chen J, 2011. Biological activities of chitosan and chitooligosaccharides. *Food Hydrocoll*, **25**, 170–179

Zheng X, Yu T, Chen R, Huang B and Chi-Hua WV, 2007. Inhibiting *Penicillium expansum* infection on pear fruit by *Cryptococcus laurentii and cytokinin*. *Postharvest Biol Technol* **45:**221–227.

ZareiI M , Aminzadeh S, Zolgharnein H, Safahieh A, DaliriI M, NoghabiI KA, GhoroghiI A and MotallebiI A. 2011. Characterization of a chitinase with antifungal activity from a native *Serratia marcescens* B4A. *Braz J Microbiol*, **42:** 1017-1029

Zees AC, Pyrpassopoulos S, Vorgias CE. 2009. Insights into the role of the (alpha+beta) insertion in the TIM-barrel catalytic domain, regarding the stability and the enzymatic activity of chitinase A from *Serratia marcescens*. *Biochim Biophys Acta,* **1794**:23-31.

JJBS

Volume 13, Number 1,March 2020
ISSN 1995-6673
Pages 29 - 34

Jordan Journal of Biological Sciences

Studying the Association of Genetic Polymorphism in *FTO* Gene with Maternal Obesity and Metabolic Phenotypes in a Sample of Iraqi Pregnant Women

Shahla O. Al-Ogaidi[1*], Sura A. Abdulsattar[2] and Hameed M. J. Al-Dulaimi[3]

[1]*Department of Chemistry, College of Science,* [2]*College of Medicine, Mustansiriyah University, P.O.Box14022, Waziriya.* [3]*College of Biotechnology, Al-Nahrain University, Baghdad, Iraq.*

Received February 8, 2019; Revised April 13, 2019; Accepted May 6, 2019

Abstract

The prevalence of overweight and obesity is rising worldwide, particularly among women of reproductive age. The fat mass and obesity-associated protein (*FTO*) gene is known to be linked with obesity. The goal of this study was to investigate whether the *FTO* rs1421085 genetic polymorphism is a predictor for maternal obesity and to evaluate its association with obesity–related metabolic phenotypes in a sample of Iraqi pregnant women. Group of 62 overweight/obese and 32 healthy non-obese pregnant women were included in this study. Genotyping of *FTO* rs1421085 gene variant was determined by tetra-primer amplification refractory mutation system-polymerase chain reaction (Tetra-primer ARMS–PCR). Metabolic phenotypes included fasting glucose (FG), glycated hemoglobin (HbA1c), lipid profile, fasting insulin, leptin (LEP), leptin receptor (LEPR), LEP/LEPR ratio, and Homeostatic Model Assessment of Insulin Resistance (HOMA-IR). Statistical analysis revealed that participants with CC and CT genotypes increase the odds of being overweight/obese (odds ratio, OR: 5.232, confidence interval, CI 95% 1.467-18.659, *P*= 0.011) and (OR: 3.006, 95% CI: 1.034-8.742, *P*= 0.043) respectively. Furthermore, each copy of the risk allele (C) increased the odds of being overweight/obese (OR: 3.3051, 95% CI: 1.697-6.437, *P*= 0.0004). Analysis also revealed that *FTO* rs1421085 polymorphism was associated with higher levels of TC, LDL-C, LEP and LEP/LEPR ratio and decreased FG levels across the study population.

Keywords: Maternal obesity, *FTO*, Phenotype, Gene polymorphism, Tetra-primer ARMS–PCR, Iraq

1. Introduction

A major public health challenge in the 21st century is the epidemic of obesity across all spectrums of age groups (Desai *et al.*, 2013), particularly among women of reproductive age. Obesity is a major risk factor for the development of cardiovascular disease (CVD), a leading cause of death (Ugwuja *et al.*, 2013). As for maternal overweight and obesity, they are well-known risk factors for pregnancy complications (Leddy *et al.*, 2008), high birth weight and of an infant being large for gestational age (Tanvig *et al.*, 2013). In Iraq, the number of obese and overweight people has markedly increased. In 2015, Iraqi Ministry of Health estimated that 30.6% of Iraqi adult females were overweight, while 42.6% of adult females were obese **(**Iraqi Ministry of Health, Annual Statistical Report, 2016).

The susceptibility to obesity is thought to result from a combination of genes, behavior, and environment (Tanvig, 2014). Hundreds of genes were found to be as contributing to obesity (Butler, 2016). The fat mass and obesity associated (*FTO*) gene is one of these genes that is mainly expressed in the hypothalamus (Gerken *et al.*, 2007; Hsiao and Lin, 2016). It codes alpha-ketoglutarate dependent dioxygenas (*AlkB*), which is a nuclear protein of the *AlkB* related non-haem iron and 2-oxoglutarate-dependent oxygenase superfamily (Sanchez-Pulido and Andrade-Navarro, 2007). The variant rs1421085 of the *FTO* gene were first identified by Dina *et al.* (2007) as potentially functional single nucleotide polymorphism (SNP) of the *FTO* gene that was consistently strongly associated with early-onset and severe obesity for the C allele. Variants in the fat mass and obesity-associated (*FTO*) gene have been associated with obesity and obesity-related phenotypes in different populations.

Although data from different populations including Europeans found the strongest association between signal in the first intron of the *FTO* gene for SNP rs1421085 with early-onset and morbid adult obesity (Meyre *et al.* 2009), the presence of this variant in Iraqi population has not been examined.

The aim of this study was to perform a case–control association study and evaluate the association between the *FTO* rs1421085 polymorphism and the susceptibility to obesity for a sample of Iraqi pregnant women. We also undertook an analysis to provide a quantitative assessment of *FTO* rs1421085 polymorphism association with metabolic biomarkers that are known from epidemiological studies to be associated with higher body mass index (BMI) and an increased risk of type 2 diabetes and cardiovascular disease, and insulin resistance (Freathy

* Corresponding author e-mail: shahla_aleqdei@yahoo.com.

et al., 2008). Alteration of hormones involved in appetite and energy homeostasis is associated with disturbances of eating behavior and obesity (Chearskul *et al.*, 2012). Insulin and leptin (LEP) are two of the most commonly identified hormones in the regulatory control of food intake, body weight and metabolism (Benyshek, 2007).

These obesity related metabolic biomarkers include fasting glucose (FG), glycated hemoglobin (HbA1c), lipid profile, two obesity related hormones (insulin and LEP), leptin receptor (LEPR), and homeostasis model assessment-insulin resistance (HOMA-IR).

2. Materials and Methods

2.1. Study population

The Scientific Committee of Chemistry Department, College of Science at Mustansiriyah University and the Ethics Committee of Al-Eluia Teaching Hospital for Birth in Baghdad, Iraq approved the current study (approval number 3355/21/MG). The objectives and methodologies were explained to all participants and verbal consent had been taken. The study included 94 pregnant women enrolled at Al-Eluia Teaching Hospital in Baghdad, Iraq for delivery between February and May 2017. Participants (from the same ethnicity) with normal pregnancy were selected, under supervision of obstetrician, based on their weight. All participants are residents of Baghdad, Iraq. Medical records were reviewed to obtain medical history and to determine eligibility pertaining to maternal age, obstetric complications during pregnancy. Gestational age (number of completed weeks of pregnancy) was estimated based on ultrasound scans. Women were excluded if the pregnancy was complicated by medical conditions such as hypertension, diabetes, infection diseases or smoking or if they were taking any medications that could affect their weight.

Two main groups included, 32 pregnant women ageing 18-35 years, with a normal BMI (below 25 kg/m^2) served as controls and 62 pregnant women ageing 18-49 years with abnormal BMI (greater than or equal to 25 kg/m^2) served as patients (Overweight/Obese) group. Both groups were matched in gestational age (37-39 weeks); however, they differed in age.

2.2. Anthropometric measurements

Weight and height, were taken by a nurse for further BMI calculation. Women were weighed after delivery with a well-calibrated digital scale. All participants were barefooted with minimal clothes. Weight was measured in kilograms with an accepted error of 0.1 kg. Height was measured in centimeters with tape measures in standing position. BMI was defined as weight in kilograms divided by the square of height in meters (World Health Organization, 2018).

2.3. Samples collection

Fasting blood samples (10 mL) were obtained from each mother just before delivery by venipuncture using disposable syringe. Whole blood (5 mL) was placed in ethylene diamine tetra-acetic acid (EDTA)-coated tubes for genomic DNA extraction and for measurement of HbA1c. Another 5 mL of blood was placed into gel tubes and left for at least 15 min at room temperature. Then, it was centrifuged at 3000 ×g for 10 min to collect sera. The serum was divided into aliquots in Eppendorf tubes and stored at -20 Cº until use for metabolic measurements.

2.4. Metabolic measurements

Quantitative measurement of HbA1c was performed by fluorescence immunoassay (FIA) system with iCHROMA^{TM} Reader. FG was determined by colorimetric enzymatic method **(**ECM) using kit supplied by Biosystems, Spain. Lipid profile (total cholesterol TC, triglycerides TG, high-density lipoprotein-cholesterol (HDL-C) was determined by ECM using kits supplied by Linear Chemicals S.L, Spain. Low-density lipoprotein-cholesterol LDL-C and very low-density lipoprotein-cholesterol (VLDL-C) were estimated using the Friedewald equation (Friedewald *et al.*, 1972). Quantitative measurement of human serum levels of LEP, insulin, and LEPR was performed using an ELISA kits supplied by KOMA BIOTECH INC. Korea, Monobind Inc., USA and My Biosource, USA respectively. HOMA-IR is a method used to quantify insulin resistance calculated from FG and insulin using Matthew's formula (Matthews *et al.*, 1985).

2.5. Genotyping

Genomic DNA was isolated from EDTA whole blood samples using the gSYNC™ DNA Extraction Kit provided by Geneaid Biotech Ltd, Taiwan according to the manufacturer's protocol and stored at –20 °C. DNA concentration was quantified with the NanoDrop (BioDrop, United Kingdom). Genotyping of *FTO* rs1421085 SNP was performed by using the tetra-primer amplification refractory mutation system–PCR (ARMS–PCR). This method uses four primers in a single PCR to determine the genotype; two non-allele-specific primers which amplify the region that comprises the SNP named outer primers, and two allele-specific primers (inner primers) which will produce the allele-specific fragments (Ahlawat *et al.*, 2014). The primers designed in this study for genotyping of *FTO* gene rs1421085 are shown in Table 1.

PCR reaction was performed in a total volume of 10 µL containing 1 µ L genomic DNA, GoTaq® G2 Green Master Mix, 2X (Promega, USA). GoTaq®G2 DNA Polymerase is supplied in 2X Green GoTaq®G2 Reaction Buffer (pH 8.5), 400µM dATP, 400µM dGTP, 400µM dCTP, 400µM dTTP and 3mM $MgCl_2$. 10 pmol of each inner and outer primers (BIONEER, Korea) and PCR graded water (Promega, USA).

The thermocycling protocol: Initial denaturation at 95ºC for 2 min followed by 35 cycles of 30 sec at 95ºC, 30 sec at 51.6ºC, and 1 min at 72ºC followed by a final extension for 2 min at 72ºC. Products were run on a 2% agarose gel stained with ethidium bromide against 5µL of 25-2000 bp DNA ladder (BIONEER, Korea).

Table 1. The primers designed for genotyping of *FTO* gene rs1421085

Gene, SNP	Primers	Primer Sequences 5'-3'	Tm (°C)	Length (bp)	Primer Conc. (Pmol)	Ta (°C)	Expected Amplicons (bp)
FTO gene rs1421085	outer forward, OF	GGTTGTAATGAAGTTTTAGGCCTCA	58.5	25	10	51.6	450, internal standard
	outer reverse, OR	AGCCATCCATCAGGTTAAATAAATG	56.7	25	10		
	inner forward IF,T-allele	TAGCAGTTCAGGTCCTAAGGCATTAT	60.6	26	10		213, T allele
	inner reverse IR, C-allele	CAAATTCTCATCAGACACTTAATCAC TG	58.1	28	10		291, C allele

Tm Melting Temperature; **Ta** Annealing Temperature**; bp** base pair

2.6. Statistical analysis

Statistical Package for Social Sciences (SPSS Inc. Chicago, IL, USA, version 19.0) was used for data analysis. The quantitative variables (measured parameters) were expressed as means ± standard deviation (SD), whereas qualitative variables (genetic polymorphisms) were expressed as absolute numbers and frequencies. Genotype and allele frequency distributions were compared among patients and control groups using the Chi-square ($\chi 2$) test or fisher exact test assuming codominant, dominant, and recessive models of inheritance. Data was also analyzed to calculate the odds ratio (OR) and 95% confidence interval (CI) to determine the risk of obesity associated with the risk allele. General linear model (GLM) was conducted to analyze the impact (partial eta-squared η_p^2) of the *FTO* gene SNP on anthropometric and metabolic traits. This test was performed while controlling for age factor. A value of ($\eta_p^2 = 0.01$) defines small, ($\eta^2 = 0.06$), defines medium, and ($\eta^2 = 0.14$) defines large effects (Lakens, 2013). As a significant age differences were detected between groups, all analyses were adjusted for age. A value of ≤0.05 was considered statistically significant. Web-ASSOTEST - a web-based version of ASSOTEST available on www.ekstroem.com (Wrzosek *et al.*, 2016) - was used to determine whether observed genotype frequencies are consistent with Hardy Weinberg equilibrium (HWE) test.

3. Results

The Tetra-ARMS PCR product of *FTO* (rs1421085) gene polymorphism was analyzed by agarose gel electrophoresis. T allele generated 213 bp product-size and C allele generated 291 bp product-size, while two outer primers generated a product size of 450 b p which represents the internal standard. Results are demonstrated in Figure 1.

For the control samples, the genotype distribution for the *FTO* rs1421085 SNP was in HWE ($P>0.05$) (Salanti *et al.*, 2005). However, for patients, the genotype distribution for *FTO* rs1421085 SNP showed significant deviations ($P < 0.05$) from HWE.

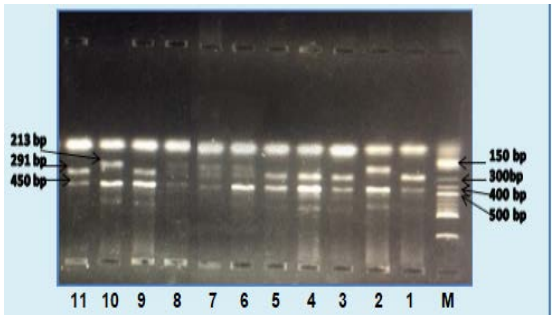

Figure 1. Genotyping of *FTO* gene polymorphism (rs1421085) by Tetra-ARMS PCR on 2%agarose gel electrophoresis. Lanes M: DNA Marker. Lanes 1,3, 4,5, 9 and 11: CC genotype. Lanes: 2 and 10: TT genotype. Lanes, 6,7and 8: CT genotype.

The OR (adjusting for age) and their 95% confidence interval (CI), and corresponding *p*-value with genotypes and alleles frequencies for *FTO* rs1421085 gene polymorphism as well in control and patients females are presented in Table 2.

Table 2: Alleles and genotypes frequencies of the *FTO* rs1421085 gene variant with odd ratio (OR) values among control and over-weight/ obese patients.

Model	Control n (%)	Patient n (%)	OR (CI 95%)	*P*- value
Genotype				
TT	20 (62.5%)	19 (30.6%)	Reference	-
CT	8 (25.0%)	21 (33.9%)	3.006 (1.034-8.742)	0.043*
CC	4 (12.5%)	22 (35.5%)	5.232 (1.467-18.659)	0.011*
Dominant				
TT	20 (62.5%)	19 (30.6%)	Reference	-
CC/CT	12 (37.5%)	43 (69.4%)	3.772 (1.485-9.584)	0.005**
Recessive				
TT/CT	28 (87.5%)	40 (64.5%)	Reference	-
CC	4 (12.5%)	22 (35.5%)	3.344 (1.010-11.076)	0.048*
C/T Allele				
T Allele	48	59	Reference	-
C Allele	16 (25%)	65(52.42%)	3.3051 (1.697-6.437)	0.0004**

*$P < 0.05$, **$P < 0.01$, OR: is the odds ratio after adjustment for age between the control and patients females. CI: 95% confidence interval.

The frequencies distribution of rs1421085 genotypes in patients group was 19 (30.6%) for TT, 21(33.9%) for CT, and 22 (35.5%) for CC. In control group, the distribution of genotypes was 20 (62.5%) for TT, 8 (25.0%) for CT, 4 (12.5%) for CC. Statistical analysis revealed that participants with the homozygous mutant (CC) genotype significantly increased the odds of being overweight/obese (OR: 5.232, CI 95% 1.467-18.659, *P*= 0.011), while heterozygous (CT) genotype was associated with increased risk for obesity (OR: 3.006, 95% CI: 1.034-8.742, *P*= 0.043). It was observed that the presence of risk allele (C) had significantly higher odds of being overweight/obese (OR: 3.3051, 95% CI: 1.697-6.437, *P*=0.0004) than females with the T allele only. The statistical analysis also revealed that both dominant and recessive models of rs1421085 significantly increased the odds of overweight/obese (OR: 3.772, 95% CI: 1.485-9.584, *P*= 0.005) (OR: 3.344, 95% CI: 1.010-11.076, *P*= 0.048) respectively.

The association between the *FTO* rs1421085 SNP and metabolic traits across study population was determined by a comparison study using codominant (genotype test) and dominant (increased risk in CC or CT *vs.* TT) models of inheritance of the *FTO* rs1421085 polymorphism and presented in Table 3.

Table 3. Impact of the *FTO* rs1421085 genetic polymorphism on maternal characteristics assuming different models of inheritance across the study population.

Parameter	TT	TC	CC	P^a value	Dominant Model (CT+CC vs. TT)	P^b value
BMI kg/m^2	26.77±4.81	28.94±4.94	30.49±4.58	0.018*	29.67±4.79	0.006*
HbA1C %	5.25±0.36	5.19±0.36	5.29±0.35	0.715	5.24±0.36	0.788
FG mg/dl	95.01±23.08	80.91±21.70	92.19±30.85	0.054	86.22±26.74	0.027*
TC mg/dl	146.84±34.76	163.6±44.41	172.93±44.93	0.065	167.99±44.45	0.025*
TG mg/dl	136.82±56.34	134.56±41.92	155.38±65.34	0.422	144.36±54.66	0.603
HDL-C mg/dl	52.08±14.55	51.29±13.84	49.95±13.13	0.422	50.66±13.39	0.603
VLDL-C mg/dl	27.36±11.27	26.91±8.38	31.07±13.07	0.840	28.87±10.93	0.638
LDL-C mg/dl	67.399±32.69	85.39±44.98	91.90±38.29	0.051	88.45±41.68	0.017*
LEP ng/mL	22.27±10.28	27.44±7.75	28.10±7.24	0.029*	27.74±7.45	0.008*
LEPR ng/mL	36.36±12.99	34.95±12.63	39.58±14.25	0.563	37.08±13.46	0.914
LEP/LEPR	0.62±0.318	0.87±0.38	0.828±0.431	0.022*	0.85±0.40	0.006*
Insulin µIU/mL	8.18±3.83	8.65±6.49	11.497±7.27	0.103	9.96±6.94	0.189
HOMA-IR	2.02±1.40	1.85±1.62	2.55±1.86	0.316	2.17±1.76	0.705

a. *P* value obtained by age adjusted multiple comparisons (TT/AA/AT). b: *P* value obtained by age adjusted comparing the women of the TT Vs. AT+AA genotypes. * *P* significant at the 0.05 level, ** *P* significant at the 0.01 level

Women carrying the C risk allele CT+CC of rs1421085 have a significantly (*P*<0.05) higher BMI, TC, LDL-C, LEP and LEP/LEPR ratio compared to TT genotypes carriers. FG significantly decreased in CT+CC carriers vs. TT. On the other hand, there were no associations between *FTO* rs1421085 polymorphism and HbA1C, TG, HDL-C, VLDL-C, LEPR, and HOMA-IR among the entire study group.

Further analysis was conducted to assess whether the *FTO* rs1421085 SNP is correlated with obesity-related traits across patients (overweight/obese) group. Statistical analysis revealed (data not shown) that rs1421085 SNP only significantly associated with increased TC, LDL levels, and decreased levels of FG and HOMA-IR, while no significant effect of this SNP was observed on BMI, LEP/LEPR ratio, HbA1C, LEP, insulin, LEPR, TG, VLDL-C, and HDL-C among patients group.

Assuming co-dominant model of inheritance revealed that the SNP has a significant medium impact on BMI (ηp^2=**0**.085, p <0.05), FG (ηp^2=0.070, p <0.05), LEP (ηp^2=0.085, p <0.05), and LEP/LEPR (ηp^2=0.091, p <0.05). When assuming the dominant model (CT+CC), however, it was found that the SNP has a significant medium impact on BMI (ηp^2=0.079, p <0.05), LDL-C (ηp^2=0.067, p <0.05), LEP (ηp^2=0.085, p <0.05), and LEP/LEPR (ηp^2=0.089, p <0.05), and a significant, yet small, impact on both TC and FG (ηp^2=0.059, p <0.05) each.

4. Discussion

In general, the HWE test assumes that the genotypes are sampled from the general population, and therefore the HWE tests are performed based on the controls (Feng *et al.*, 2014). Wittke-Thompson *et al.* (2005) suggest that if a deviation from HWE in cases or in both cases and controls is detected, it does not necessarily imply genotyping errors. Therefore, to detect any genotyping errors, we randomly selected 24% of the samples to re-genotype. The obtained results were 100% identical. Thus, we believe that the deviation from HWE in cases cannot be attributed to the genotyping errors. There are many possible factors for disequilibrium, which may cause significant deviations from HWE, either by influencing the distribution of genes in the population or by altering the gene frequencies. These factors include gene flow, small population size, and non-random mating (Turnpenny and Ellard, 2016). Disequilibrium can also arise from population substructure or inbreeding (Graffelman and Weir, 2016). All that could provide an explanation for the deviations from HWE.

In recent decades, obesity has become a global health epidemic. It is increasingly recognized to have the potential to influence the next generation through effects on women of reproductive age (Black *et al.*, 2013*;* Ng *et al.*, 2013). The *FTO* gene leads to an increased risk of obesity by influencing a central regulation of food intake (Hsiao and Lin, 2016). Some reports suggest that it affects food intake, as carriers of the risk allele tend to choose high energy and palatable food (Almen *et al.*, 2013). FTO was previously studied across Iraqi diabetic patients and reported an association of variants in exon 2 with diabetes. (Ramadhanzaidan *et al.,* 2011). In our study, we found that *FTO* rs1421085 polymorphism was associated with increased risk for maternal obesity, higher levels of TC, LDL-C, LEP and LEP/LEPR ratio and decreased FG levels across the study population. Among overweight/ obese women, however, the SNP only associated with increased TC, LDL levels, and decreased levels of FG and HOMA-IR. Interestingly, this leads to an idea that presence of this variation may have a protective role against FG elevation and eventually against developing type 2 diabetes (Janghorbani and Amini, 2012). These results were inconsistent to Attaoua *et al.*, (2009) who reported that genotypes of *FTO* were correlated with insulin resistance, and homozygous C/C was positively

correlated with an increase in insulin resistance over the value predicted by the increase in BMI.

Although, these findings partially deviate from the previous comparative studies of (Solak *et al.*, 2014; Abdel Rahman *et al.*, 2018), they reported that no significant association was found when comparing the rs1421085 genotypes in terms of BMI measurements among obese subjects.

Recent evidence suggested that *FTO* variants directly affect adipocyte function through targeting IRX3 and IRX5 (Sobalska-Kwapis *et al.*, 2017). Compared with risk-allele carriers (C), non-risk-allele carriers (T) exhibited reduction in IRX3 and IRX5 expression. These results showed that *FTO* gene mutations promote increased expression of IRX3 and IRX5 (Yang *et al.*, 2017). In a study examining the mechanistic basis of the association between the *FTO* region and obesity, Claussnitzer *et al.* (2015) found that the rs1421085 T-C alteration disrupts a conserved motif for the regulatory gene ARID5B repressor. This can cause depression of a potent preadipocyte enhancer that ultimately alters the function of adipocytes, which shift from energy-dissipating beige adipocytes to energy-storing white adipocytes with a 5-fold reduction in mitochondrial thermogenesis. This process results in imbalance of body energy, lipid accumulation and subsequent obesity without a change in physical activity or appetite (Yang *et al.*, 2017). Claussnitzer *et al.* (2015) concluded that the *FTO* SNP rs1421085 represents the causal variant that disrupts a pathway for adipocyte thermogenesis involving ARID5B, IRX3, and IRX5, providing a mechanistic basis for the genetic association between *FTO* and obesity.

Other potentially modifiable factors that cause overweight and obesity are lifestyle factors such as physical inactivity and eating habits (Mogre *et al.,* 2014). These factors could not be controlled and might cause bias.

It is noteworthy that the current study is the first study that examines the associations between rs1421085 polymorphism and obesity represented by BMI and related metabolic phenotypes represented by elevation in TC, LDL, and LEP/LEPR in a s ample of Iraqi female population. Finally, it is important to point out to the limitations of the study like generalizability as the samples were collected from one hospital only; therefore, further investigations in other regions of Iraq are necessary to generalize these results among Iraqi female population.

5. Conclusion

No data on t he relation between *FTO* rs1421085 polymorphism and obesity in Iraqi population is available. Thus, our findings provide the first evidence about the association of the rs1421085 SNP, found in first intron of *FTO*, with maternal obesity elevated metabolic phenotypes including TC, LDL-C, LEP and LEP/LEPR ratio and decreased levels of FG in a sample of Iraqi female population. The findings from our study have an important health implication. It may be speculated that Iraqi females of reproductive age may be at risk of CVD, considering that obesity and overweight are accompanied by unfavorable blood lipids patterns, Thus, weight lessening is necessary and desirable to reduce comorbidities that might later need a very intensive medical treatment, leading to rising health care costs. As *FTO* rs1421085 SNP is associated with decreased levels of FG among study population and decreased levels of FG and HOMA-IR among overweight/obese group, presence of this variation may, therefore, play a protective role against diabetes.

Acknowledgment

The authors are grateful to all the women who agreed to participate in this study.

Funding

This study was funded by the authors.

References

Abdel Rahman, A, Megied A, Baz RE, Wafa A, and Zekred E. 2018. Association of Obesity with Rs1421085 and Rs9939609 Polymorphisms of FTO Gene with T2DM in Egyptian Females. *Int J Pharm Pharm Sci*, **10(9):** 73-78.

Ahlawat S, Sharma R, Maitra A, Roy M, and Tantia MS. 2014. Designing, optimization and validation of tetra-primer ARMS PCR protocol for genotyping mutations in caprine Fec genes. *Meta gene,* **2**: 439-49.

Almen MS, Rask-Andersen M, Jacobsson JA, Ameur A, Kalnina I, Moschonis G, Juhlin S, Bringeland N, Hedberg LA, Ignatovica V, Chrousos GP, Manios Y, Klovins J, Marcus C, Gyllensten U, Fredriksson R, and Schiöth HB. 2013. Determination of the obesity-associated gene variants within the entire *FTO* gene by ultra-deep targeted sequencing in obese and lean children. *Int J Obes*, **37(3)**: 424–431.

Attaoua R, Mkadem SA, Lautier C, Kaouache S, Renard E, Brun JF, Fedou C, Gris JC, Bringer J, and Grigorescu F. 2009. Association of the *FTO* gene with obesity and the metabolic syndrome is independent of the *IRS-2* gene in the female population of Southern France. *Diabetes Metab.*, **35(6):** 476-483.

Benyshek, D. 2007. The developmental origins of obesity and related health disorders - Prenatal and perinatal factors. *Coll Antropol*., **31(1):** 11-7.

Black RE, Victora CG, Walker SP, Bhutta ZA, Christian P, de Onis M, Ezzati M, Grantham-McGregor S, Katz J, Martorell R, Uauy R, and Maternal and Child Nutrition Study Group. 2013. Maternal and child undernutrition and overweight in lowincome and middle-income countries. *Lancet*, **382(9890):** 427e51.

Butler MG. 2016. Single gene and syndromic causes of obesity: Illustrative examples. *Prog Mol Biol Transl Sci*, **140**: 1-45.

Chearskul S, Kooptiwut S, Pummoung S, Vongsaiyat S, Churintaraphan M, Semprasert N, Onreabroi S, and Phattharayuttawat S. 2012. Obesity and appetite-related hormones. *J Med Assoc Thai*, **95(11):**1472-9.

Claussnitzer M, Dankel SN, Quon G, Meuleman W, Haugen C, Glunk V. Sousa, I, Beaudry, J, Puviindran, V, Abdennur, N, Liu, J, Svensson, P, Hsu, Y, J Drucker, D, Mellgren, G, Hui, C, Hauner, H, and Kellis, M. 2015. *FTO* obesity variant circuitry and adipocyte browning in humans. *N Engl J Med*, **373**:895–907.

Desai M, Beall M, and Ross MG. 2013. Developmental origins of obesity: programmed adipogenesis. *Curr Diab Rep*, **13(1):** 27–33.

Dina C, Meyre D, Gallina S, Durand E, Korner A, Jacobson P, Carlsson LM, Kiess W, Vatin V, Lecoeur C, Delplanque J, Vaillant E, Pattou F, Ruiz J, Weill J, Levy-Marchal C, Horber F, Potoczna N, Hercberg S, Le Stunff C, Bougnères P, Kovacs P, Marre M, Balkau B, Cauchi S, Chèvre JC, and Froguel P. 2007. Variation in *FTO* contributes to childhood obesity and severe adult obesity. *Nature Genet*. **39:** 724-726.

Feng Y, Wang F, Pan H, Qiu S, Lü J, Wu L, Wang J, and Lu C. 2014. Obesity-associated gene *FTO* rs9939609 polymorphism in relation to the risk of tuberculosis. *BMC Infect Dis.***14**: 592.

Freathy RM, Timpson NJ, Lawlor DA, Pouta A, Ben-Shlomo Y, Ruokonen A, Ebrahim S, Shields B, Zeggini E, Weedon MN, Lindgren CM, Lango H, Melzer D, Ferrucci L, Paolisso G, Neville MJ, Karpe F, Palmer CN, Morris AD, Elliott P, Jarvelin MR, Smith GD, McCarthy MI, Hattersley AT, and Frayling TM. 2008. Common variation in the *FTO* gene alters diabetes-related metabolic traits to the extent expected given its effect on BMI. *Diabetes*, **57(5):**1419-26.

Friedewald WT, Levy RI, and Fredrickson DS. 1972. Estimation of the concentration of low-density lipoprotein cholesterol in plasma, without use of the preparative ultracentrifuge. *Clin Chem.*, **18**:499-502.

Gerken T, Girard CA, Tung YC, Webby CJ, Saudek V, Hewitson KS, Yeo GS, McDonough MA, Cunliffe S, McNeill LA, Galvanovskis J, Rorsman P, Robins P, Prieur X, Coll AP, Ma M, Jovanovic Z, Farooqi IS, Sedgwick B, Barroso I, Lindahl T, Ponting CP, Ashcroft FM, O'Rahilly S, and Schofield CJ. 2007. The obesity-associated *FTO* gene encodes a 2-oxoglutarate-dependent nucleic acid demethylase. *Science*, **318(5855):**1469–1472.

Graffelman J and Weir BS. 2016. Testing for Hardy–Weinberg equilibrium at biallelic genetic markers on the X chromosome. *Heredity*, **116(6):** 558–568.

Hsiao TJ and Lin E. 2016. Association of a common rs9939609 variant in the fat mass and obesity-associated (*FTO*) gene with obesity and metabolic phenotypes in a Taiwanese population: a replication study. *J Genet*, **95(3):** 595-601.

Iraqi Ministry of Health (2016) "Annual Statistical Report 2016" https://moh.gov.iq/index.php. (March 38, 2018)

Janghorbani M, and Amini M. 2012. Normal fasting plasma glucose and risk of prediabetes and type 2 diabetes: the Isfahan Diabetes Prevention Study. *Rev Diabet Stud*, ***8*(4)**: 490-8.

Lakens D. 2013. Calculating and reporting effect sizes to facilitate cumulative science: a practical primer for t-tests and ANOVAs. *Front Psychol.*, **4**: 863.

Leddy MA, Power ML, and Schulkin J. 2008. The impact of maternal obesity on maternal and fetal health. *Rev Obstet Gynecol.*, **1(4):** 170–178.

Matthews DR, Hosker JP, Rudenski AS, Naylor BA, Treacher DF, and Turner RC. 1985. Homeostasis model assessment: insulin resistance and beta-cell function from fasting plasma glucose and insulin concentrations in man. *Diabetol.*, **28(7):** 412–9.

Meyre D, Delplanque J, Chèvre J, Lecoeur C, Lobbens S, Gallina S, Durand E, Vatin V, Degraeve F, Proença C, Gaget S, Körner A, Kovacs P, Kiess W, Tichet J, Marre M, Hartikainen AL, Horber F, Potoczna N, Hercberg S, Levy-Marchal C, Pattou F, Heude B, Tauber M, McCarthy MI, Blakemore AI, Montpetit A, Polychronakos C, Weill J, Coin LJ, Asher J, Elliott P, Järvelin MR, Visvikis-Siest S, Balkau B, Sladek R, Balding D, Walley A, Dina C, and Froguel P. 2009. Genome-wide association study for early-onset and morbid adult obesity identifies three new risk loci in European populations. *Nat Genet.*, **41(2)**: 157-159.

Mogre V, Nyaba R, and Aleyira S. 2014. Lifestyle risk factors of general and abdominal obesity in students of the school of medicine and health science of the university of development studies, tamale, Ghana. *ISRN Obes*. **2014**:508382.

Ng M, Fleming T, Robinson M, Thomson B, Graetz N, Margono C, Mullany EC, Biryukov S, Abbafati C, Abera SF, *et. al*.2013. Global, regional, and national prevalence of overweight and obesity in children and adults during 1980–2013: a systematic analysis for the Global Burden of Disease Study 2013. *Lancet*, **384**:766–81.

Ramadhanzaidan S, Abd Al Kareem F, and Alkhazrajy LA. 2011. Genetic Polymorphisms in the Fat Mass and Obesity-Associated Gene Confers Risk of Obesity in Iraqi Population *Am J Infect Dis.*, **7 (2):** 40-44.

Salanti G, Amountza G, Ntzani EE and Ioannidis JP. 2005. Hardy–Weinberg equilibrium in genetic association studies: an empirical evaluation of reporting, deviations, and power. *Eur J Human Genet*, **13(7):** 840-848.

Sanchez-Pulido L and Andrade-Navarro MA. 2007. The *FTO* (fat mass and obesity associated) gene codes for a novel member of the non-heme dioxygenase superfamily. *BMC Biochem*., ***8***: 23.

Sobalska-Kwapis M, Suchanecka A, Słomka M, Siewierska-Górska A, Kępka E, and Strapagie D. 2017. Genetic association of *FTO*/IRX region with obesity and overweight in the Polish population. *PLoS One*, **12(6):** e0180295.

Solak M, Erdogan MO, Yildiz SH, Ucok K, Yuksel S, Terzi ES, and Bestepe A. 2014. Association of obesity with rs1421085 and rs9939609 polymorphisms of *FTO* gene. *Mol Biol Rep*, **41(11)**:7381–7386.

Tanvig M, Wehberg S, Vinter C, Joergensen J, Ovesen P, Beck-Nielsen H, Jensen D, and Christesen H. 2013. Pregestational body mass index isrelated to neonatal abdominal circumference at birth—a Danish population-based study. *BJOG*, **120**:320–330.

Tanvig M. 2014. Offspring body size and metabolic profile - effects of lifestyle intervention in obese pregnant women. *Med J*.,**61(7):**B4893.

Turnpenny PD and Ellard S. 2016. **Emery's Elements of Medical Genetics**, 15th edition. Elsevier Health Sciences, Netherlands. chapter 7.

Ugwuja E, Ogbonna N, Nwibo A, and Onimawo I. 2013. Overweight and Obesity, Lipid Profile and Atherogenic Indices among Civil Servants in Abakaliki, South Eastern Nigeria. *Ann Med Health Sci Res*, **3(1):** 13–18.

Wittke-Thompson JK, Pluzhnikov A, and Cox NJ. 2005. Rational inferences about departures from Hardy-Weinberg equilibrium. *Am J Hum Genet,* **76(6):**967–986.

World Health Organization. (2018). "**WHO Obesity and overweight Fact sheet".** WHO, Geneva, Switzerland, http://www.who.int/mediacentre/factsheets/fs311/en/. (Feb. 22, 2018)

Wrzosek M, Zakrzewska A, Ruczko L, Jabłonowska-Lietz B, and Nowicka G. 2016. Association between rs9930506 polymorphism of the fat mass & obesity-associated (*FTO*) gene & onset of obesity in Polish adults. *Indian J Med Res*, **143(3):** 281–287.

Yang Q, Xiao T, Guo J, and Su Z. 2017. Complex Relationship between Obesity and the Fat Mass and Obesity Locus. *Int J Biol Sci*, **13(5):**615-629.

JJBS

Volume 13, Number 1,March 2020
ISSN 1995-6673
Pages 35 - 40

Jordan Journal of Biological Sciences

High Ability of Cellulose Degradation by Constructed *E. coli* Recombinant Strains

Mohamed S. Abdel-Salam[1,*] , Wafaa K. Hegazy[1], Azhar A. Hussain[2], Hoda H. Abo-Ghalia[2] and Safa S. Hafez[2]

[1]*Microbial Genetics Department, National Research Centre, 33 EL Bohouth St. – Dokki- Giza- P.O. 12622;* [2]*Botany Department, Faculty of Women for Arts, Science and Education, Ain Shams University, Egypt.*

Received April 1, 2019; Revised April 29, 2019; Accepted May 6, 2019

ABSTRACT

Endo-β-1, 4 glucanase gene (*eglS*) from local isolate *Bacillus subtilis* BTN7A was isolated, sequenced and cloned by using PCR technique. *EglS*-primers were designed. Optimization of both PCR program and mixture content was identified. The *eglS* sequence was submitted into the GenBank. The gene expressed efficiently in *E.coli* DH5α. The recombinant *E.coli* harboring recombinant vector pGEM® –T Easy /eglS produced much higher enzyme yields than its parental strain which has non-detectable cellulase activity. The new construct also had about 78%-98% higher activity than *B. subtilis* BTN7A donor strain. For enhancing recombinant enzyme expression, different optimum parameters (temperature, inoculum level, incubation time, and carbon source of the growth media) were investigated. Maximum enzyme production of the recombinant strain was 37.9 U/ml obtained after 24h grown on the growth media, supplemented with CMC as a sole source of carbon at 37°C. The data demonstrated that the presence of endo-β-1, 4 glucanase (EGL) with endo-β-1, 3-1, 4 glucanase; (BGL) showed a highly synergistic effect in hydrolyzing cellulose. The specific activities were increased up to 60.6 U/ml when mixed culture of both recombinant *E. coli* harboring *eglS* gene and *E. coli* harboring *bgls* gene, inoculated in CMC medium. The constructed strain can be used for biodegradation of cellulosic wastes as an essential step for their conversion to economic valuable products.

Keywords: *Bacillus subtilis*; Endo-β-1,4 glucanase; Endo-β-1, 3-1, 4 glucanase; Cellulase; Gene cloning; PCR

1. Introduction

Cellulose is the most abundant polymer in the biosphere and most preeminent waste on earth (Moo-Young *et al.,* 1987). This polymer is built up from units of glucose attached by β-1, 4 linkages. This agriculture waste is considered as a huge renewable bioresource (Jarvis, 2003 and Zhang &Lynd 2004), where it has a high potential to be used as an inexpensive feedstock for bioconversion to important products such as acetone and ethanol.

The biological conversion of lignocellulosic wastes requires the use of cellulolytic and hemicellulolytic enzymes (Jourdier *et al.,* 2012). Degradation of cellulose occurred by glycosyl hydrolase enzymes families (Bayer *et al.*, 1998). Cellobiohydrolase, endoglucanase (Carboxy-methyl-celllulase), and β-glucosidases are three types of enzymes required for cellulosic hydrolysis (Bhat, 2000). Cellulases depolymerize cellulose as environmental friendly process (Karmakar and Ray, 2011 and Kuhad *et al.*, 2011).

A variety of *Bacillus* species produce cellulases, including strains of *B. cereus* (Thayer and David 1978) *Bacillus subtilis*, (Hussain *et al.,* 2017), *B. licheniformis* (Dhillon *et al.,* 1985), *Bacillus* sp. KSM-330 (Ozaki and Ito, 1991), *Bacillus thuringiensis* strains (Lin *et al*., 2012) and alkaliphilic *Bacillus* (Horikoshi, 1997). Bacterial cellulase complexes act as synergic multi enzyme systems. However; most of these bacteria produce mainly endoglucanases (Wood, 1985). By contrast, there are reports of certain *Bacillus* endoglucanases (CMCase) that have shown detectable activity on microcrystalline cellulose (Kim, 1995).

In addition, application of cellulases commercially has different obstacles including their high prices and the poor knowledge of their interactive actions and their mechanisms (Juturu and Wu 2014).

Open-air agriculture-waste-burning is the most remarkable source of pollution. For many decades, different places in Egypt including Cairo suffered from a serious environmental problem of air pollution mostly because of burning rice husks. This behavior is responsible for extremely increasing air pollution over the limits set by World Health Organization.

The objective of this study was to clone endo-β-1, 4 glucanase (*eglS*) gene from *B. subtilis* subsp. *subtilis* BTN7A and optimize its expression under control of different growth conditions, aiming to develop a recombinant strain with a high ability of cellulose degradation, where the end product of the hydrolysis may be identified as a cheap source of essential material for second generation of ethanol production and other important economical products. The ultimate aim of this

* Corresponding author e-mail: sass-one@hotmail.com.

research was to reduce pollution in our country through biodegradation of cellulosic wastes and converting them into useful materials.

2. Materials and Methods

2.1. Bacterial strains

Bacillus subtilis subsp. *subtilis* BTN7A is a highly cellulolytic indigenous strain isolated from Egypt (Hussain *et al.,* 2017); it was used as a source of endo-β-1, 4 glucanase (*eglS*) gene. *E. coli* DH5α was used as a recipient in transformation. Plasmid pGEM®-T Easy Vector (Promega Co., Madison, USA) was used for gene cloning. T-*Bgls*-1 is a r ecombinant *E. coli* strain harbouring endo-β-1, 3-1, 4 glucanase (*bgls*) gene from *B. subtilis* subsp. *subtilis* BTN7A (Hegazy *et al*., 2018).

2.2. Media

Luria-Bertani agar medium (LB) (Bertani 1952), and Bushnell- Haas medium (BHM) (Bushnell and Haas 1941) supplemented with carboxymethyl cellulose (CMC) or cellulose as a s ole carbon source, were used as bacterial growth media.

2.3. Bioinformatics

Different web-based tools, including The National Center for Biotechnology Information (NCBI), webcutter 2.0 software, primer design (Primer3), Plasmid Mapping (Dong *et al.,* 2004), and SnapGene®Viewer program, have been used throughout this study.

All molecular biology manipulations were performed according to standard protocols (Sambrook and Russell, 2001) and kits suppliers' instructions unless specified otherwise.

Agarose gel electrophoresis (1%) was used for DNA analysis. The obtained DNA bands were visualized using UV transilluminator, and then photographed for analysis.

Plasmid DNA was isolated using DNA-spin™ plasmid DNA purification Kit (INTRON BIOTECHNOLOGY).

2.4. Isolation of eglS gene

Primers to amplify *eglS* CDS and the flanking region were designed based on sequence in GeneBank database using Primer3. The eglS reverse primer was (AATGATGCGAAGGAGGAAAA) and eglS forward primer was (TTACTGATGTCCGCCAAAAA), and the expected *eglS* fragment was 1557 bp.

Total genomic DNA was extracted according to (Dashti *et al*., 2009) from *B. subtilis* BTN7A strain. PCR amplification of *eglS* gene was carried out using Go Taq® Flexi DNA Polymerase Kit (Promega Co., Madison, USA). It was done in a total volume of 50µL containing: 10 µL of 5x Green Go Taq® Flexi buffer, (2-8) µL of 25 mM of $MgCl_2$, 1 µL of 10mM dNTPs, 0.75 µL of forward *eglS* primer, 0.75 µL of reverse *eglS* primer, 1.5 µL of template DNA, 0.25 µL of Go Taq DNA polymerase (5 unites/ µL) and then volume was adjusted to 50 µL with water (nuclease free).

PCR amplification was performed in the thermal cycler programmed for one cycle at 95ºC for 5 minutes, then 30 cycles as follows: one minute at 95ºC for denaturation, one minute at 50ºC for annealing, 90 seconds at 72ºC for elongation then 5 minutes at 72ºC for final extension, and the reaction mixtures were held at 4ºC.

The PCR products were analyzed by 1% agarose gel electrophoresis. The DNA band containing *eglS* gene was purified from gel, and sent to Macrogen Co., Korea for sequencing**.**

2.5. Cloning of eglS gene

EglS gene was cloned with pGEM®-T Easy Vector. It was done as follows: Five µL of 2x Rapid Ligation Buffer, 1-3 µL PCR product, and the volume was adjusted to 8 µL with water (nuclease free). 1 µL pGEM®-T Easy Vector and 1 µ L T4 DNA Ligase were added, briefly mixed together by pipetting, and the tube was incubated overnight at 4ºC.

Five µL of ligated DNA were used to transform *E. coli* DH5α by heat-shock treatment and transformants were selected using ampicillin resistance and white/blue screening method (i.e., IPTG/X-gal).

2.6. Cellulase activity assay

Cellulase activity was measured in the supernatant or in the cell lysate using (3, 5-dinitrosalisylicacid) DNS which measures the amount of reducing sugar liberated from CMC or cellulose, according to (Miller, 1959).

Total protein concentration in the intracellular (pellets) and in extracellular (supernatant) was determined according to (Bradford 1976). Tested isolates were incubated for 24 h t hen centrifuged at 13,000 rpm for 10 min. One ml of Bradford reagent was added to 50µL supernatant for 10 min. The optical density was measured at 595 nm against blank using spectrophotometer (SHIMADZU UV-Vis spectrophotometer 1201).

Intracellular soluble protein was done as follows: 1.5mL from bacterial culture were harvested by centrifugation, the pellet was resuspended in 350µL Smart™ Bacterial Protein Extraction solution (INTRON BIOTECHNOLOGY) by vigorously vortexing for 1 min. Sample was centrifuged for 5 min at 13,000 rpm. The supernatant was used for intracellular protein determination using Bradford reagent as described above for extra-cellular protein determination.

Protein standard curve was generated using different concentrations of bovine serum albumin (BSA) ranging from 10 to 100 µg/mL distilled water.

Cellulase specific activity was calculated by dividing the end product concentration (µmol reducing sugars/ min) expressed as units by the total protein (mg) of the sample.

3. Results and Discussion

Interactive cooperation between cellulases enzymes is essential process for cellulose depolymerization to glucose. The current study focused on the development of a recombinant strain with a high ability of cellulose degradation; to this goal the two cellulases enzymes endo-β-1, 4 g lucanase (EGL) and endo-β-1, 3-1, 4 glucanase (BGL) were manipulated and expressed under the effect of different environmental factors. Synergistic effect of the two enzymes in hydrolyzing cellulose was studied.

3.1. Isolation of endo-β-1,4 glucanase (eglS) gene

The *eglS* coding sequence was amplified from *B. subtilis* BTN7A by PCR using the designed primers. A 1557 bp DNA band containing the *eglS* gene was successfully obtained after PCR amplification. Results

indicated that addition of 5 µL of 25mM $MgCl_2$ produced the highest *eglS* DNA concentration.

The obtained DNA band was purified using MEGAquick-spin™ Total Fragment DNA purification kit and sequenced by (Macrogen Co., Korea). The complete CDS sequence of *eglS* was deposited in GenBank (Accession number KM009052.1). The *eglS* –CDS (1500 bp) which encodes for 500 amino acids was shown in (Figure 1).

atgaaacggtcaatctcgatttttattacgtgtttattgattacgttattgacaatgggcggcatgctggcttcgccggcatcagcagcagggacaaaaaacgccagtagccaagaatggccagctt
agcataaaaggtacacagctcgttaaccgagacggtaaagcggtacagctgaaggggatcagttcacacggattgcaatggtatggagaatatgtcaataaagacagcttaaaatggctgagg
gacgattggggtatcaccgttttccgtgcagcgatgtatgcggcagatggcggttacattgacaacccgtccgtgaaaaataaagtaaaagaagcggttgaagcggcaaaagagcttgggatat
atgtcatcattgactggcatatcttaaatgacggtaatccaaaccaaaataaagagaaggcaaaagaattcttcaaggaaatgtcaagtctttacggtaacacgccaaacgtcatttatgaaatt
gcaaacgaaccaaacggtgatgtgaactggaagcgtgatattaaaccgtatgcggaagaagtgatttccgttatccgcaaaaatgatccagacaacatcatcattgtcggaaccggtacatgga
gccaggatgtgaatgatgcagccgatgaccagctaagagatgcaaacgttatgtacgcacttcatttttatgccggcacacacggccagtttttacgggataaagcaaactatgcactcagcaaa
ggagcgcctatttttgtgacagaatgggggacaagtgatgcttccggaaatggcggtgtattccttgatcaatcgcgggaatggctgaaatatctcgatagcaagaccattagctgggtgaactg
gaatctttctgataagcaggaatcatcctcagctttaaagccgggggcatctaaaacaggcggctggcagttgtcagatttatctgcttcaggaacattcgttagagaaaacattctcggcaccaa
agattcgacgaaggacattcctgaaacgccagcaaaagataaacccacacaggaaaacggtatttctgtacaatacagagcaggggatgggagtatgaacagcaaccaaatccgtccgcagc
ttcaaataaaaaataacggcaataccacggttgatttaaaagatgtcactgcccgttactggaataaagcgaaaaacaaaggccaaaactttgactgtgactacgcgcagattggatgcggcaa
tgtgacacacaagtttgtgacgttgcataaaccaaagcaaggtgcagatacctatctggaacttgggtttaaaaacggaacgctggcaccgggagcaagcacagggaatattcagctccgtctt
cacaatgatgactggagcaattatgcacaaagcggcgattattcctttttcaaatcaaatacgtttaaaacaacgaaaaaaatcacattatatgatcaaggaaaactgatttggggaacagaacc
aaatttag

A

MKRSISIFITCLLITLLTMGGMLASPASAAGTKTPVAKNGQLSIKGTQLVNRDGKAVQLKGISSHGLQWYGEYVNKDSLKW
LRDDWGITVFRAAMYAADGGYIDNPSVKNKVKEAVEAAKELGIYVIIDWHILNDGNPNQNKEKAKEFFKEMSSLYGNTPN
VIYEIANEPNGDVNWKRDIKPYAEEVISVIRKNDPDNIIIVGTGTWSQDVNDAADDQLRDANVMYALHFYAGTHGQFLRDK
ANYALSKGAPIFVTEWGTSDASGNGGVFLDQSREWLKYLDSKTISWVNWNLSDKQESSSALKPGASKTGGWQLSDLSASG
TFVRENILGTKDSTKDIPETPAKDKPTQENGISVQYRAGDGSMNSNQIRPQLQIKNNGNTTVDLKDVTARYWNKAKNKGQ
NFDCDYAQIGCGNVTHKFVTLHKPKQGADTYLELGFKNGTLAPGASTGNIQLRLHNDDWSNYAQSGDYSFFKSNTFKTTK
KITLYDQGKLIWGTEPN

B

Figure 1. *Bacillus subtilis* subsp. *subtilis* strain BTN7A endo-β-1,4 glucanase (*eglS*) gene, complete CDS (A) and its deduced amino acids sequence (B).

3.2. Cloning of eglS gene

A 1557 bp band of endo-β-1,4glucanase (*eglS*) gene obtained after PCR was purified and ligated with pGEM®-T Easy Cloning Vector using T4 DNA ligase. The recombinant plasmid was named EglS-nrc-1 (4573bp) (Figure 2). *E. coli* DH5α was used as heterologous new host for the recombinant plasmid (EglS-nrc-1) by transformation.

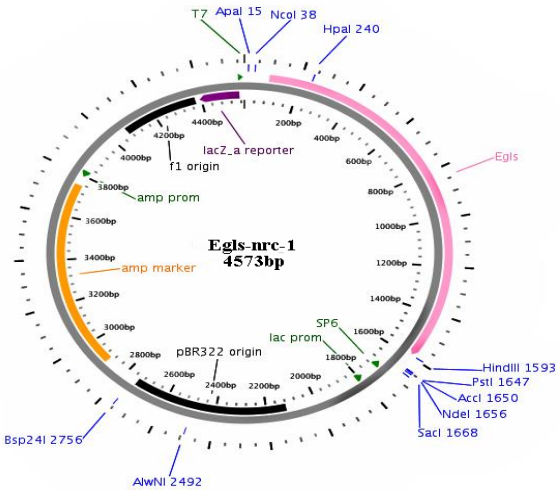

Figure 2. EglS-nrc-1 recombinant plasmid containing *B. subtilis* subsp. *subtilis* BTN7A *eglS* gene.

3.3. Detection of eglS gene in pGEM®-T Easy /eglS (EglS-nrc-1) plasmid

Blue/white colonies screening technique and ampicillin resistant were used to select *E. coli* DH5α EglS - transformants. To confirm the existence of *eglS* gene in *E. coli* transformants, nine ampicillin resistant and white colonies were randomly selected, named T-eglS1 to T-eglS9. They were grown in LB broth at 37°C for 24h and their plasmids were isolated. T he occurrences of *eglS* within these plasmids were tested using PCR amplification and the designed *eglS*-primers. All tested nine transformants showed one DNA band of 1557 bp corresponding to *eglS* gene (Figure 3).

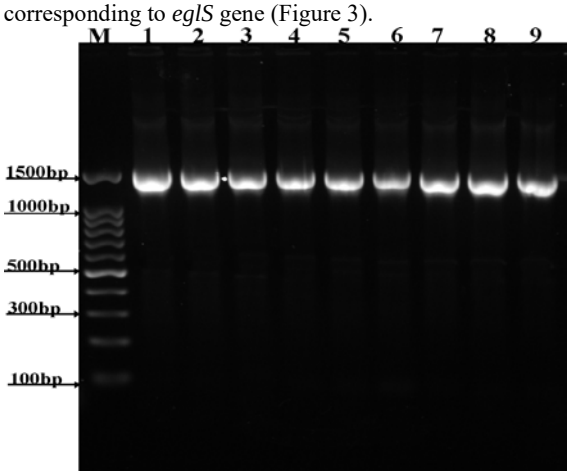

Figure 3. An agarose gel (1 %) electrophoresis of the amplification of *eglS* gene of nine *E. coli* DH5α (EglS-nrc-1) transformants. Lane M: 100bp DNA ladder, lane1: T-eglS1; lane2: T-eglS2; lane3: T-eglS3; lane4: T-eglS4; lane5: T-eglS5; lane6: T-eglS6; lane7: T-eglS7; lane8: T-eglS8 and lane9: T-eglS9 transformants.

3.4. Optimization of Carboxymethylcelllulase (CMCase) activity

3.4.1. Temperature effect

Cellulase activity of three stains; *E. coli* T-*eglS*1 (transformant), *B. subtilis* BTN7A (donor) and *E. coli* DH5α (recipient) were measured at 37°C and 55°C. Crude

enzyme preparations from bacterial cultures were used to degrade CMC, and reducing sugar was determined after 30 min of incubation with substrate at 37°C or 55°C.

The results presented in Figure 4 indicated that the two temperatures used; 37°C and 55°C were suitable for enzyme production; however, there was about 30.4% reduction in their activities at 55°C compared to their activities at 37°C. The effect of temperature was previously studied by many reports; some observed that the optimum temperature of *B. subtilis* -endoglucanase production ranged from 35 °C to 39 ° C (Deka *et.al,* 2013; Gautam and Sharma, 2014; Lee *et al.,* 2010), while Wei *et.al* (2015) concluded that it was 60 ° C. Chan and Au (1987) reported that it might be even up to 65 °C.

The present data (Figure 4) also revealed that *eglS* gene expressed successfully in *E. coli* DH5α, and the enzyme activity of the constructed strain *E. coli* DH5α (T-eglS1) was much higher than the enzyme activity of its parental strain which has low constitutive level of celulases activity (negligible value). Moreover the new construct T-eglS1 produced much higher enzyme yield than its donor strain *B. subtilis* BTN7A. It produced 27 U/ mg at 37°C which was about 78% more than *B. subtilis* BTN7A, and 20.88 U/ mg at 55°C which was about 98% more than *B. subtilis* BTN7A. Similar result on *blgs* production has been previously reported (Hegazy *et al*., 2018). The data obtained was also in agreement with Pandey *et al.,* (2014) who demonstrated that up to four times increase in cellulase production had been obtained by cloning *B. subtilis* IARI-SP-1-*eglS* gene in the expression vector pET-28a and over expressed in *E. coli* BL21 DE3.

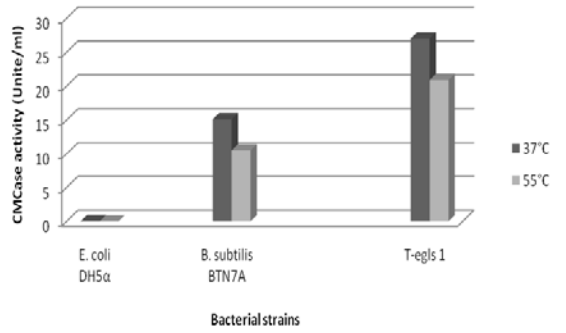

Figure 4 Effect of temperature on CMCase activity of *E. coli* DH5α, B.*subtilis* BTN7A (donor) and T-eglS-1(transformant)*

*The selected bacterial strains were inoculated into flasks containing 20 mL LB broth medium and incubated at 37°C for 24h under shaking (120 rpm). Enzyme activity was calculated at 37°Cor 55°C.

3.4.2. Inoculum size effect

Two different inoculum sizes (X and 2X) of *E. coli* TeglS-1 cultures were inoculated into three types of media; LB, BHM broth medium supplemented with CMC or cellulose as a sole carbon source. The three culture sets were incubated at 37 °C up to 3 days with shaking (120 rpm), and CMCase activity was determined daily. Data presented in Figure 5 indicated that the cellulolytic activity was increased by doubling the inoculum size. And the highest activity produced after 24 h of incubation in BHM medium supplemented with CMC.

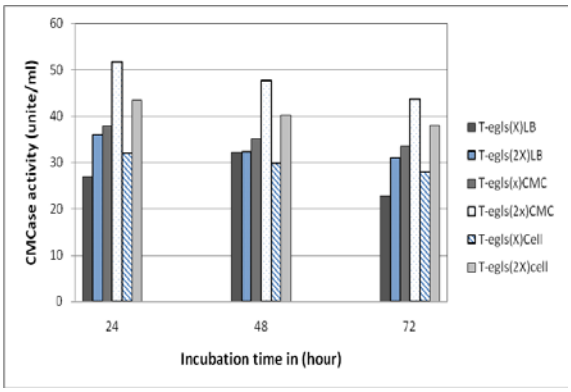

Figure 5 Effect of inoculum size, carbon source of the growth medium and incubation time on enzyme activity*

X = bacterial inoculum corresponding to OD_{620} = 0.01

2X = bacterial inoculum corresponding to OD_{620} = 0.02

* Bacterial cell were grown into complete LB medium and two minimal media of BHM amended with carboxymethyl cellulose (CMC) or cellulose powder as a sole carbon source at 37°C up to 3 days under shaking (120 rpm) and the enzyme activity of the culture supernatant was determined.

3.4.3. Synergising effect of co-culture of E. coli –eglS with E. coli – bgls and carbon source of the growth media

E. coli clone containing *eglS* gene designated as T-eglS and a mixture culture of *E. coli eglS*1 and *E. coli bgls*1 were grown into LB or BHM broth medium supplemented with CMC or cellulose as a sole carbon source, at 37 °C for 3 days shaking incubator, and then their enzymes activities in cell –free culture supernatant were daily measured.

Results presented in Figure 6 revealed that the highest cellulolytic activity was observed after 24 h and by increasing the incubation time the enzyme activity was decreased. It was also noticed that Carboxymethyl cellulose (CMC) was the best carbon source regulating both *eglS* and *bgls* expressions. This finding is in agreement with (Azadian *et al.,* 2017, Gautam and Sharma 2014, Hegazy *et al.,* 2018, Sadhu *et al.,* 2013 and Shaikh *et al.,* 2013) and with Sreena and Sebastian (2018) who found that CMC among the most important parameter had positive effect on cellulase production by *B. subtilis* MU.

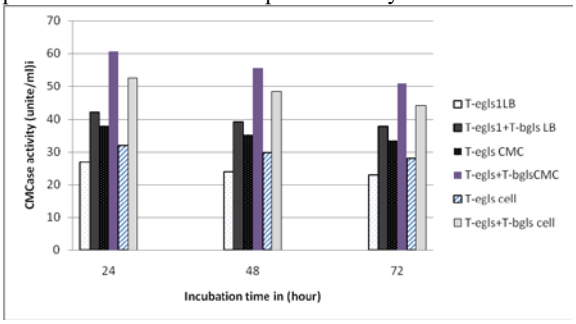

Figure 6. Synergizing effect of co-culture of *E.coli* –eglS with *E.coli* -bgls and carbon source of the growth media with incubation time*

* Bacterial cell were grown into LB or BHM broth medium supplemented with CMC or cellulose as a sole carbon source, at 37 °C for 3 days in shaking incubator, and then their enzymes activities in cell –free culture supernatant were daily measured.

By inoculating a mixture of both T-*eglS* and T-*bgls*, the cellulase activity reached the maximum value among all tested inoculation conditions. It reached up to 60.6 U/ mL at 24 h the occurrence of the two endoglucanase enzymes; *eglS* plus *bgls* suggesting synergic cellulolytic system in bacterial strain th at play a role in complete cellulose hydrolysis. The previous data indicated that endoglucanase expression in *E coli* showed a high potential for enhancement of the enzyme production.

4. Conclusions

A successful endo-β-1, 4 glucanase (*eglS*) gene cloning method was described using the PCR technique. The new constructed plasmid was transformed into *E. coli,* and *eglS* expression was studied in the new exogenous bacterial host. Optimum enzyme activity was identified including temperature, inoculum size, carbon source of the growth media and incubation time. CMC had positive regulation effect in *eglS* expression. The present study illustrates the synergistic cooperative interactions between both of the endo-β-1, 4 glucanase and the endo-β-1, 3-1, 4 glucanase enzymes on cellulose degradation. Further studies are planned to use the identified optimum conditions for biodegradation of cellulolytic-waste biomass. New cellulolytic microorganisms could be developed to gain such economical properties for cellulose degradation by introducing the two endoglucanase genes, *eglS* and *bgls*, into new bacterial hosts.

Acknowledgment

This work was supported by National Research Centre, Dokki, Giza, Egypt.

References

Azadian F, Badoei-dalfard A, Namaki-Shoushtari A, Karami Z and Hassan Shahian M. 2017. Production and characterization of an acido-thermophilic, organic solvent stable cellulase from *Bacillus sonorensis* HSC7 by conversion of lignocellulosic wastes. *JGEB*, **15**:187–196.

Bayer EA, Chanzy H, Lamed R. and Shoham Y. 1998. Cellulose, cellulases and cellulosomes. *Cur Opinion in Structural Biol.,* **8**:548-557.

Bertani G. 1952. Studies on Lysogenesis. I. The mode of phage liberation by lysogenic *Escherichia coli*. *J. Bacteriol.*, **62**:293-300.

Bhat MK 2000. Cellulases and related enzymes in biotechnology. *Biotechnol Advances*, **18**(5): 355–383.

Bradford MM 1976. Rapid and sensitive method for the quantitation of microgram quantities of protein utilizing the principle of protein-dye binding. *Anal. Biochem.*, **72**: 248–254.

Bushnell LD and Haas HF 1941. The utilization of certain hydrocarbons by microorganisms. *J. Bacteriol.*, **41**:653.

Chan KY and Au KS. 1987. Studies on cellulase production by a *Bacillus subtilis. Antonie Van Leeuwenhoek*, **53**(2):125-136.

Dashti AA, Jadaon MM, Abdulsamad AM and Dashti HM. 2009. Heat treatment of bacteria: a simple method of DNA extraction for molecular techniques. *Kuwait Med J*, **41**(2):117–122.

Deka D, Das SP, Sahoo N, Das D, Jawed M, Goyal D and Goyal A. 2013. Enhanced cellulase production from *Bacillus subtilis* by optimizing physical parameters for bioethanol production. *ISRN Biotechnol., doi.org/10.5402/2013/965310.*

Dhillon N, C hhibber S, and Saxena, M. 1985.A constitutive endoglucanase (CMCase) from *Bacillus licheniformis*-1, *Biotechnol Lett*., **7:(9),**695–697.

Dong X, Stothard P, Forsythe IJ and Wishart DS. 2004. PlasMapper: a w eb server for drawing and auto-annotating plasmid maps. *Nucleic Acids Res.*, **32:** (Web Server issue): W660-W664.

Gautam R and Sharma J. 2014. Optimization, Purification of Cellulase Produced From *Bacillus Subtilis* . Inaquosorum Under Solid State Fermentation And Its Potential Applications in Denim Industry. *IJSR*, **3**(6): 1759- 1763.

Hegazy WK, Abdel-Salam MS, Hussain AA, Abo-Ghalia HH and Hafez SS. 2018. Improvement of cellulose degradation by cloning of endo-β-1, 3-1, 4 glucanase (bgls) gene from *Bacillus subtilis* BTN7A strain. *JGEB*, **16** (2): 281-285.

Horikoshi, K 1997. Alkaline cellulases from alkaliphilic *Bacillus*: enzymatic properties, genetics, and application to detergents. *Extremophiles*, **1(2):** 61–66.

Hussain AA, Abdel-Salam MS, Abo-Ghalia HH, Hegazy WK and Hafez SS. 2017. Optimization and molecular identification of novel cellulose degrading bacteria isolated from Egyptian environment. *JGEB*, **15**: 77–85.

Jarvis, M 2003. Cellulose stacks up. *Nature*, **426**: 611–612.

Jourdier E, Ben C F, Poughon L, Larroche C and Monot F. 2012. Simple kinetic m odel of cellulose production by *Trichderma reesei* for productivity or yield maximization. *Chem Eng Transactions*, **27**: 313-318.

Juturu V and Wu JC. 2014. Microbial cellulases: Engineering, production and applications. *Renewable and Sustainable Energy Rev.,* **33**: 188–203.

Karmakar M, and Ray RR. 2011. Current trends in research and application of microbial cellulases. *Res J Microbiol.*, **6**: 41–53.

Kim CH, 1995.Characterization and substrate specificity of an endo-β-1,4-D-glucanase I (Avicelase I) from an extracellular multienzyme complex of *Bacillus circulans. Appl Environ Microbiol.,* **61(3):** 959–965.

Kuhad RC, Gupta R and Singh A. 2011. Microbial cellulases and their industrial applications. *Enzyme Res*. http://dx.doi.org/ 10.4061/2011/280696.

Lee BH, Kim BK, Lee YJ, Chung CH and Lee JW. 2010. Industrial scale of optimization for the production of carboxymethylcellulase from rice bran by a marine bacterium, *Bacillus subtilis* subsp. *subtilis* A-53. *Enzyme and Microbial Technol.*, **46**(1): 38–42.

Lin L, Kan X, Yan H and Wang D. 2012. C haracterization of extracellular cellulose-degrading enzymes from *Bacillus thuringiensis* strains. *Electron. J. Biotechnol*, **15** (3):1–7.

Miller GL. 1959. Use of Dinitrosalicylic acid reagent for determination of reducing sugar. *Anal. Chem.*, **31**:426-428.

Moo-Young M, Lamptey J, Glick B and Bungay H. 1987. **Biomass Conversion Technology,** Pergamon Press, Oxford.

Ozaki K and I to S, 1991.Purification and properties of an acid endo-1,4-β-glucanase from Bacillus sp. KSM-330. *J Gen Microbiol.*, **137 (1):** 41–48.

Pandey S, Kushwahb J, Tiwaria R, Kumarb R, Somvanshib VS, Naina L and Saxenaa AK. 2014. Cloning and expression of β-1,4-endoglucanase gene from *Bacillus subtilis* isolated from soil long term irrigated with effluents of paper and pulp mill. *Microbiol Res.*, **169**:693–698.

Sadhu S, Ghosh PK, De TK and Maiti TK. 2013. Optimization of cultural condition and synergistic effect of lactose with carboxymethyl cellulose on cellulase production by *Bacillus sp.*

isolated from fecal matter of elephant (*Elephad maximus*). *Adv Microbiol*, **3**:280–288.

Sambrook J and Russell DW, Editors. 2001. **Molecular Cloning: A Laboratory Manual.** N.Y: Cold Spring Harbor Laboratory Press.

Shaikh NM, Patel AA, Mehta SA and Patel ND. 2013. Isolation and screening of cellulolytic bacteria inhabiting different environment and optimization of cellulase production univers. *Environ Sci Technol*, **1**:39–49.

Sreena CP and Sebastian D. 2018. Augmented cellulase production by *Bacillus subtilis* strain MU S1 using different statistical experimental designs. *JGEB*, **16**: 9–16.

Thayer, D W and David, C A., 1978 "Growth of seeded cellulolytic enrichment cultures on mesquite wood, *Appl Environ Microbiol*., **36(2):** 291–296.

Wei KSC, Teoh TC, Koshy P, Salmah I and Zainudinb A., 2015. Cloning, expression and characterization of the endoglucanase gene from *Bacillus subtilis* UMC7 isolated from the gut of the indigenous termite Macrotermes malaccensis in *Escherichia coli*. *Electronic J Biotechnol*., **8**: 103–109.

Wood, T M., 1985.Properties of cellulolytic enzyme systems. *Biochemical Soc Transactions,* **13(2):** 407–410.

Zhang YHP and Lynd LR, 2004. Toward an aggregated understanding of enzymatic hydrolysis of cellulose: Noncomplex cellulase systems. *Biotechnol Bioeng.*, **88**(7): 797–824.

JJBS

Volume 13, Number 1,March 2020
ISSN 1995-6673
Pages 41 - 45

Jordan Journal of Biological Sciences

Sexual Ambiguity Diagnosis: Cytogenetics and Fluorescence *In Situ* Hybridization (FISH)

Amine Bessaad[1,*] , Yacef Sihem[1] and Belaid AiT AbdelKader[2]

[1] *Organism and Populations Biology Department, Natural Sciences and Life Faculty, Saad Dahleb Blida1 University;* [2] *Cytogenetic Laboratory, Centre Pierre et Marie Curie, Algeria*

Received April 2, 2019; Revised April 24, 2019; Accepted May 8, 2019

Abstract

The sexual differentiation depends on a succession of events that can be the seat of dysfunctions leading to sexual ambiguity. Sexual development disorders might be caused by genetic (chromosomal) or hormonal anomalies; hence, an accurate diagnosis is required. The purpose of this work is to show the impact of classical method and a molecular technic on sexual ambiguities diagnosis and their eventual complementarity in order to unveil the source of the anomalies. In order to fulfil this aim, we have studied three cases of patients with sexual ambiguities addressed in cytogenetic laboratory of Centre Pierre et Marie Curie, Algeria. Concerning the methodology used to diagnose the ambiguities, we started by the cytogenetic for highlighting any chromosomal aberrations. To refine the results, we used a molecular method restricted to the in situ hybridization by fluorescence (FISH). The results obtained indicate that the karyotype allows the analysis of number and macro structural anomalies that affect the chromosomes, but with a limited resolving power that requires using more precise technics, such as FISH, to highlight chromosomal micro reshuffling in the etiology of human sexual ambiguity. The findings indicate that the combination of classical cytogenetics and molecular diagnostics allows highlighting new genotype as the origin of sexual ambiguities at genic order with different complexity levels such as mosaicism.

Keywords: Sexual ambiguity, Pseudo hermaphroditism, Cytogenetic, Karyotype, FISH.

1. Introduction

The sexual differentiation and genital organs development of both internal and external ones, in addition to the differentiation of secondary sexual character, represent a series of complex events that lead to implement a functional reproductive apparel of a f ertile individual (Muczynski, 2011). Sexual differentiations anomalies correspond to congenital chromosomal atypia, gonadic or anatomic sexual development. Due to their several causes, the problem of sexual differentiation anomaly diagnosis will arise at birth with each new born having aspects of external genital organs that are not complying with the norm. These aspects range from posterior penile hypospadias to clitoral hypertrophy. Among these two extremities genital organs are frankly ambiguous (Alaoui Belghiti, 2011).

Human cytogenetic is a recent discipline dating from 1956 with an exact determination of human chromosomes number (Tijo and Levan, 1956). In 1970, the introduction of chromosomes banding technics has improved the resolution and the sensitivity of classic cytogenetic analysis, allowing both number and structure of chromosomes studies (Ferguson-Smith, 1976). Finally, in situ hybridization fluorescence appearance in 1986 and its rapid development provide today a whole range of tools permitting an accurate study and scrutiny of chromosomes and their structure.

Fortunately, these technics made the identification of many autosomal and gonosomal pathologies possible, like sexual ambiguities or sex determinism anomalies (SDA).

It is highly important to show the role of cytogenetic and FISH studies in the sex determinism pathology. This article will present three cases of sexual ambiguities collection from the cytogenetic service in “Centre Pierre et Marie Curie (CPMC) “

2. Patients and Methods

After a cl inical consultation for an anamnesis and conducting the therapy, taking pictures of patients then a blood sample were carried out.

A conic tube is used where the phytohemagglutinin is added in the middle of cell culture RPMI (Roswell Park Memorial Institute medium); it will serve both the cytogenetic and the FISH methods. The protocol of the shared part of both technics is demonstrated in figure 1.

Once the culture is conducted, we collect the blocked cells in the metaphase stage to move to both technics, the conventional cytogenetic then to the FISH if necessary.

* Corresponding author e-mail: a72bessaad@gmail.com.

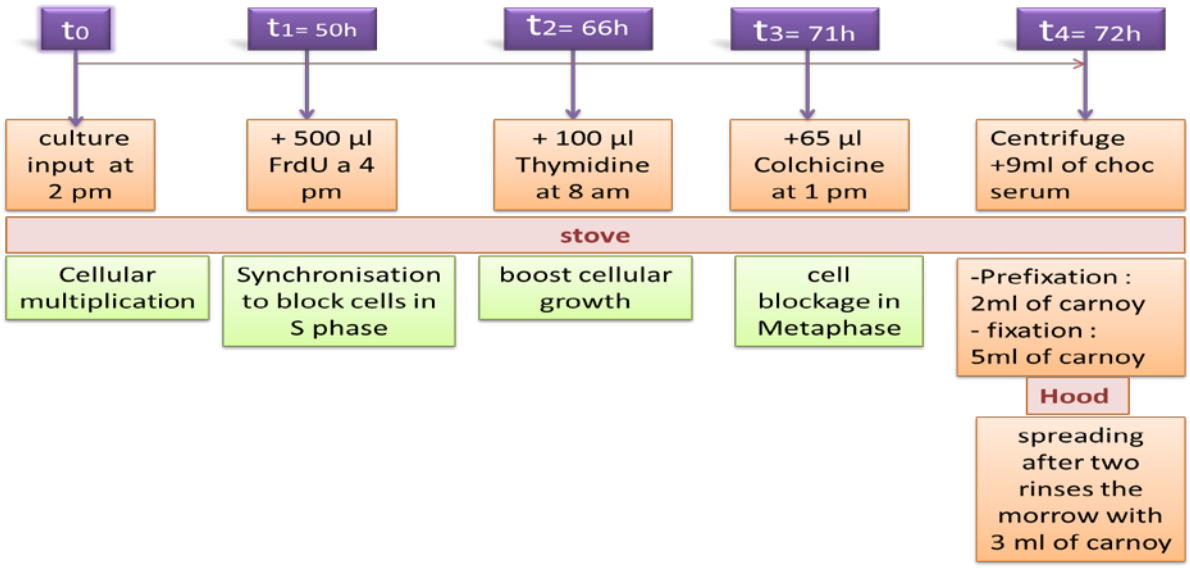

Figure 1. Illustration of the common part of karyotype and FISH with the different steps of lymphocytes culture**.**

2.1. Conventional cytogenetic (karyotype).

In this work, the R karyotype banding treatment is discussed. It is the thermal denaturation moderated at 87°C lasting 20 to 25 minutes in an ionic environment Earl PH 6.5 (Earl's balanced salt solution).

Chromosomes banding is observed with a fluorescence microscope (Zeiss MOTORISE) with a low magnification (10 x) in order to spot mitosis, then (100 x) by using immersion oil. The capture is done by image acquisition software (Meta System IKAROS) that allows the chromosomes classification (Figure 2).

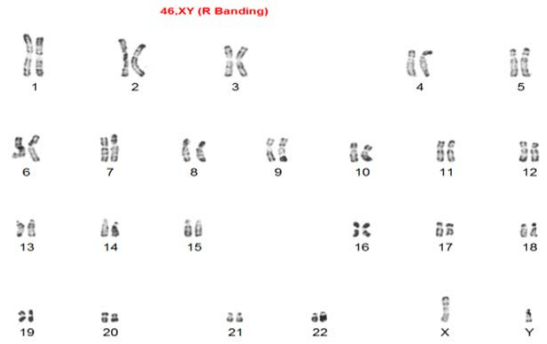

Figure 2. Normal karyotype in R bands (the Picture of cytogenetic laboratory, CPMC)

2.2. The FISH method

The in situ hybridization by fluorescence (FISH) technic consists of hybridizing a fluorescent molecular probe with a chromosomal target on a glass slide (Pinkel et al, 1988). We put 10 µl of probe on the sample. The sample and probe denaturation is made in the ThermoBrite to 75°C during 2 min the capture is done by an image acquisition softeware (Meta System ISIS).

3. Results

3.1. Patient A

3.1.1. Clinical

Patient A is from a 3rd degree consanguineous marriage. 10 years old (1m 36, 35kg) is a targeted case of sexual ambiguity therapy. The patient represents a male phenotype with ambiguous genital organs: Micro penis, absence of the left testicle, but the right testicle position is normal. Hormonal analysis report reveals that the rate of testosterones is low. Family antecedents: notion of ambiguity in a paternal female cousin

3.1.2. Cytogenetic and FISH results

The patient's standard Karyotype shows a presence of xx gonosomes (Figure 3). In order to determine precisely the cause of sexual ambiguity, we have realised a FISH to look for the major gene of testicular determinism carried by the short arm of y chromosome called sexual determining region of y chromosome (SRY). We have used a SRY YP 11.2 (Cytocell) probe coloured in red, a witness probe of the Y chromosome: DYZ1 (cyto cell) coloured in green and a witness probe DXZ1 (Cytocell) of X chromosome coloured in blue.

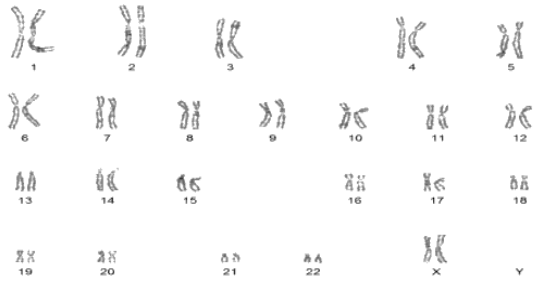

Figure 3. R bands Karyotype (46XX) of patient A.

The FISH result indicates that there is a presence of a blue signal corresponding to x chromosome and a red signal corresponding to SRY gene , the chromosomal formula of this patient is then (46, xx ish YP 11.2 (SRY)+) (Figure 4).

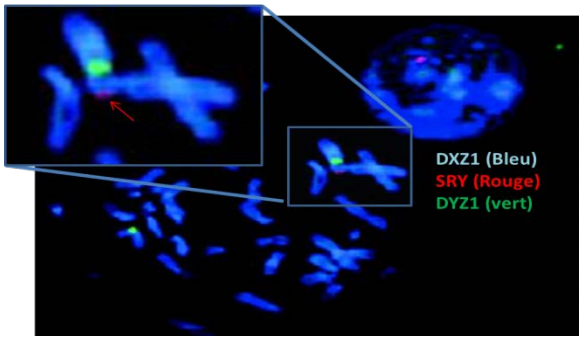

Figure 4. Bicolored FISH, centromere probe of X chromosome and red probe for the SRY gene

3.2. Patient B

3.2.1. Clinical

Patient b is from a 3rd degree consanguineous marriage, 28 y ears old (1m82, 70Kg). She presents ambiguous external genitalia with a gynecomastia of reduced volume and size with normal nipples. The pelvic abdominal ultrasound imaging indicates the presence of both ectopic testicles of low inguinal region. The hormonal analysis report shows high levels of Follicle stimulating hormone (FSH) and testosterone.

3.2.2. Cytogenetic and FISH results

The R Karyotype bands of the B patient reveal a normal male karyotype where there is no detection of Chromosomal aberration. Even though the results of karyotype confirm the suspected diagnosis, a FISH was used to look for the SRY gene.

The results of this FISH reveal three signals, a b lue signal (X) , a green signal (Y) and a red signal (SRY) that confirm the presence of this gene that is localised in YP 11.2. The chromosomal formula of this B patient is then (46xy ish YP11.2 (SRY+).

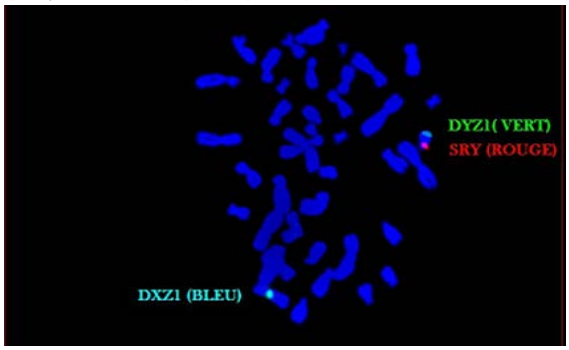

Figure 5. FISH results showing that the presence of red signal corresponds to the presence of the SRY gene.

3.3. Patient C

3.3.1. Clinical

The patient C is from a consanguineous marriage, 4 years old, presenting an advanced staturo-ponderal. He was addressed in cytogenetic laboratory due to sexual ambiguity suspicion linked to a congenital hyperplasia of the adrenal glands.

The genital exam reveals a w ell-developed penis according to the patient age which measures 8cm accompanied by hypospadias that signifies a hyper-pigmented scrotum of palpable empty testicles. The abdo-pelvic ultrasound imaging reveals the presence of female internal genital organs (left lateralised uterus).

3.3.2. Cytogenetic and FISH results

The standard karyotype of this patient reveals a mosaicism that constitutes three different cell populations : (66%) of mitosis studied presents a normal female karyotype 46 X X, (19%) presents a normal male karyotype 46 XY, and the third population (15%) presents an extra X chromosome so a 47 XXY karyotype (Figure 6). T o get more precise results, a F ISH was conducted to find the SRY gene. The results of this FISH are normal for the 46XX population, presence of two blue signals corresponding to X chromosomes with no presence of both signals red and green.

Concerning the 46 XY population, presence of a green signal corresponding to Y chromosome, a blue signal corresponding to X chromosome and the absence of the red signal allows deducing that there was no pr obe hybridization with the SRY gene.

Regarding the 47 XXY population, there is a presence of two blue signals corresponding to X chromosomes and a green signal corresponding to Y chromosome. The absence of the red signal reveals that this SRY gene have been deleted (Figure 7).

The chromosomal formula of this patient is:

(mos 46,XX [71] ish Yp11.2 (SRY-)/46,XY [20] ish Yp11.2 (SRY-)/ 47,XXY [16] ish Yp11.2 (SRY)).

(A)

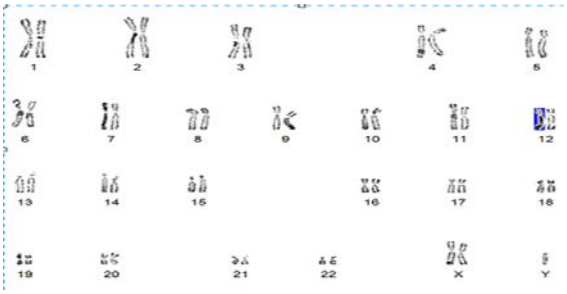

(B)

(C)

Figure 6. R karyotype bands reveals three cellular populations, (A) 46, XX, (B) 46, XY et (C) 47, XXY.

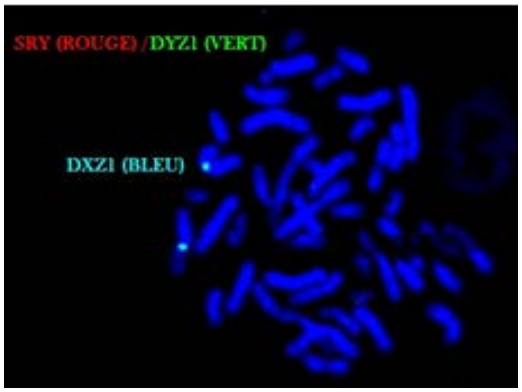

Figure 7. FISH: the red signal absence corresponds to the SRY gene absence.

This patient presenting with a male phenotype having three distinct cellular populations clarifies that this mosaicism has occurred in the post zygotic phase by a mitotic segregation anomaly where the population with an extra X chromosome drift, whereas the patient FISH reveals a normal result for the 46XX population (absence of the SRY gene) and also the SRY gene deletion in both populations 46, XY et 47, XXY.

4. Discussion

The patient A presents a male phenotype with 46XX karyotype; after looking for the SRY gene by the FISH, we highlighted a small segment of the short arm terminal part of Y chromosome on one of the two X chromosomes that seems as a consequence of a terminal exchange between DNA identical sequence of short arms X and Y chromosomes at the level of specific sites called PAR homologous regions (pseudo autosomal region) Xp-Yp (Jack, 2003); explained hereby a homologous genetic combination initiated precisely at the leptotene stage by double–strand breaks during meiosis (meiotic crossing over) that is the process in which the genetic material is exchanged between homologous chromosomes (Jack, 2003; Guichaoua *et al*, 2009). The presence of SRY is sufficient for the testicular determinism. Thus, it can be a male sex with two X chromosomes whenever one of X chromosomes carries the SRY gene, which explains the observed phenotype (Stephen, 2004).

The patient B presents with a male karyotype 46 XY associated with a female phenotype. The SRY gene implies its expression in this patient, which leads to the testicles development. For more precise analyses, the patient was addressed in the molecular biology laboratory.

Although this gonadic intersexual case is rarely encountered, the XY karyotype (positive SRY) is associated with a lateral hermaphroditism with one testicle. This anomaly form can be linked to a female phenotype. The origin of this anomaly can be related to mutation in sex determinism gene interacting with the SRY gene; for example, mutations and translocations in SOX 9 gene are sometimes responsible for sex reversion from male sex to female sex (Kuttenn et al, 2003). Autosomes deletions are also implied, such as 9p24 deletion leading to reversion or sexual ambiguity (Paget, 2001).

In the patient C, the gene deletion implies its non-expression in this patient, which explains part of the phenotype observed (absence of testicles and presence of uterus). Indeed, a conduction of the FISH is recommended on a large number of cellular populations to find out which of the population carries the SRY gene that will make the patient male phenotype explanation possible.

All genital organs' discovery is a traumatising event for both parents at their baby's birth and for the ambiguous people themselves. According to the ill formation type, functional consequences may prevent any sexual activity, harm the couple's life, and trouble fertility (Bazin, 2002).

In this study, the medical care consists of Chromosomal, endocrine and radiologic examinations. Thus, sexual ambiguity diagnosis is a very delicate process that necessitates an interdisciplinary collaboration (Gueniche *et al*, 2008).

The karyotype makes an overall vision of the genome possible, but there are limits due to the existence of cryptic reshuffle that cannot be highlighted by this technic. However, actually we have molecular cytogenetic technics such as the FISH CGH-array and other technics that have a large contribution like gathered information on the DNA-break point that are exactly localised where the indication can be guided to highlight the extra genital anomalies.

In addition to the molecular diagnostics mentioned above, currently DNA sequencing is widely used due to its accuracy and its resolution in structure and mutation of gene determination leading the ambiguity anomalies to occur.

During this work, it has been possible to combine different cytogenetic technics and appraise their the limits and disadvantages in order to use them as a response to a sexual ambiguity suspicion raised by a therapist, being frequent or rare in the population where these molecular processes are highly unavoidable.

Acknowledgement

We would like to express our sincere gratitude to Miss Amina Amzal, from Ali Lounici, Blida 2 university in Algeria, for English editing.

References

Alaoui Belghiti Youssef M. 2011. Prise en charge des anomalies de différenciation sexuelle. Thèse en médecine, Université sidi Mohamed ben Abdallah, Maroc: P 9.

Bazin A. 2002. Bases de cytogénétique préalables à la prise en charge des ambigüités sexuelles. Elsevier SAS. 15 : 97-9.

Ferguson-Smith MA. 1976. Meiosis in the human male. *In*: Pearson PL, Lewis KR, (Eds). **Chromosomes Today,** Volume 5. New York: John Wiley & Sons;. pp. 33–41.

Gueniche K, Jacquot M, Thibaud E, Polak P. 2008. L'identité sexuée en impasse. Neuropsychiatrie de l'enfance et de l'adolescence. 56 : 377-385.

Guichaoua M R, Geoffroy-Siraudin C, Tassistro V, Ghalamoun-Slaimi R, Perrin J, Metzler-Guillemain. 2009. Chromosomes sexuels et méiose. *Gynécologie Obstétrique & Fertilité,* **37**(11-12) : 895-900.

Jack J. 2003. **Génétique Moléculaire Humain : Les éléments de base de la génétique**. Edition de Boeck. 1ére édition : Page 66.

Kuttenn F, Acremont MF, Mowszowicz I. 2003. Endocrinologie-Nutrition : Anomalies de la différenciation sexuelle. Encycl. Méd. Chir. Editions Scientifiques et Médicales Elsevier SAS. Page 1.

Paget R. 2001. Etude cytogénétique et moléculaire d'un cas d'intersexualité chez le chien et le cheval. Thèse de doctorat en science vétérinaire. École nationale vétérinaire Toulouse, France : 67-79.

Pinkel D, Landegent J, Collins C, Fuscoe J, Segraves R, Lucas J, Gray J. 1988. Fluorescence in situ hybridization with human chromosome-specific libraries: Detection of trisomy 21 and translocations of chromosome 4. *Proc. Natl. Acad. Sc*i. **85** :9138-9142.

Rajon AM. 2008. Ce que nous apprennent les parents d'enfants porteurs d'ambiguïté génitale. Neuropsychiatrie de l'enfance et de l'adolescence. 56 : 370-3.

Stephen D. 2004. **Biologie : Génétique**. Edition de Boeck. 1 ère édition : Page 231.

Tijo, JH and Levan, A. 1956. The chromosome number of man. Hereditas, **42**: 1-6.

Vincent Muczynski. 2011. Polluants environnementaux et développement du testicule fœtale humain. Thèse de doctorat en biologie de la reproduction et du développement, Université PARIS-SUD 11 France.

JJBS

Volume 13, Number 1,March 2020
ISSN 1995-6673
Pages 47 - 54

Jordan Journal of Biological Sciences

Mixotrophic Cultivation of *Coccomyxa subellipsoidea* Microalga on Industrial Dairy Wastewater as an Innovative Method for Biodiesel Lipids Production

Hoda. H. Senousy[1*] and Sawsan Abd Ellatif [2]

[1] *Botany and Microbiology Department, Faculty of Science, Cairo University, Giza, 12613,*[2] *Bioprocess Development Department, Genetic Engineering and Biotechnology Research Institute (GEBRI), City for Scientific Research and Technology Applications, New Bourg El-Arab City, Universities and Research District, 21934 Alexandria, Egypt.*

Received March 24, 2019; Revised May 4, 2019; Accepted May 18, 2019

Abstract

Global demand for new energy resources is continuously raising as non-renewable fossil fuels cost and combustion rise over the years. Cultivation of *Coccomyxa subellipsoidea* HSSASE8 with accession No. KT277791.1 was cultivated on basal medium supplemented with different proportions (20, 40, 60, 80 or 100%) of sterile or unsterile wastewater in a bioreactor. The chemical component of dairy wastewater, biomass, lipid content, fatty acids profile, total nitrogen (TN) and total phosphorus removal (TP) were estimated. The maximum biomass production was at 60% dairy wastewater (DWW) dilutions (918.15±0.07 and 909.09±0.04 mg/L in unsterile and sterile conditions, respectively). The removal percentage of total N (310±132.9- 0.0 mg/L) and total P (279.5±56.2- mg/L) was at 100%. In addition, total organic carbon (TOC) ranged from 182.6-2.42 (94.58%) and 182.6-3.86 (83.47%) at 60% DWW dilution. The maximum lipid contents of the dry cell weight (DCW) were 75.16%±5.3 and 80.67±5.6 in sterile and unsterile conditions, respectively, while the fatty acids composition revealed that the highest yield of fatty acids (C16-C18) ranged between 68.54% and 72.54% (w/w) at unsterile condition compared with sterile condition (68.27- 71.34%).

Keywords: Microalgae; *C. subellipsoidea*, Mixotrophic, Photobioreactor; Biodiesel, Fatty acid profile

1. Introduction

Biodiesel is presently undergoing extensive attention owing to its excellent power as a bright, continuous and environmentally friendly energy source option compared to fossil fuels (Griffiths *et al*., 2012).The international concerns owing to exhausting petroleum reserves can be a reason for extending the sum of investigators on biodiesel production (Schenk *et al*., 1998). Successful algal biodiesel production mainly depends on picking the right species with vital properties, for instance, biomass and fatty acid productivity, respectively. Green microalgae in comparison to blue-green algae are found to be potential biodiesel feedstocks (Lei *et al*., 2012). The algae lipid content varies greatly according to different growth conditions which may vary to be within 1 to >50%. The eukaryotic algae have high levels of TAGs that is not common in cyanobacteria or other prokaryotes in general (Carolina *et al*., 2017).

The dairy industry is regarded as one of the dominant industries with strong commercial value in the horticultural district (Gavala *et al*., 1999). Meanwhile, dairy waste effluents represent one of the significant sources of water pollution.

That is the reason why there is a crucial need for the treatment of dairy wastewater (DWW) prior to consumption or disposal (Karadag *et al*., 2015; Rad and Lewis 2014). On the other hand, it has satisfactory minerals like N (14–830 mg/l), and P (9–280 mg/l) required for biological management, in addition to a high protein content, a high organic matter content, traces of heavy metals and easy biodegradability (Gavala *et al*., 1999 and Sarkar *et al.,* 2006). In recent years, many studies proved that microalgae have to reach a vigorous measure of biomass viewed as third generation feedstock for biofuels and animal forage (Rad and Lewis 2014).

The coupling of microalgae cultivation with DWW treatment and recycling is represented in our study as an effective strategy for microalgae-based biofuel production (Gao *et al.,* 2014 and Alvarez-Diaz *et al.,* 2015). Therefore, the aim of this work was to cultivate *C. subellipsoidea* HSSASE8 microalga in DWW which has nutrients required for microalgae proliferation in order to achieve both benefits of mineral discharge and biomass production for biodiesel generation. In addition, the total fatty acid methyl esters (FAME) was measured by gas chromatography (instead of the determination of raw lipids using solvent extraction) as a signal for determining the efficiency of this alga in biodiesel production.

* Corresponding author e-mail: hodasenousy1@hotmail.com; hodasenousy2@gmail.com.

2. Materials and Methods

2.1. Isolation and culture of microalgae

2.1.1. Samples collection

Coccomyxa subellipsoidea microalga was isolated from agricultural drainage water (Bahr hadus pump station No. 3 with Latitude/Longitude (31°02'07.0"N-31°44'35.1"E) in El-Daqhlia Governorate, Egypt) during summer of 2014 by the Department of Botany, Faculty of Science, Cairo University, Egypt and was registered in GenBank under the name of *C. subellipsoidea* HSSASE8 with Accession Number: (KT277791.1).

2.1.2. Media preparation

Sterilized and raw dairy wastewater was used for the preparation of modified Basal Bold medium containing(g/L) 0.25; $NaNO_3$, 1.25; $MgSO_4 \cdot 7H_2O$, 1.0; KH_2PO_4, 1.25; EDTA, 0.5; boric acid, 0.1142; $CaCl_2$, 0.111; $FeSO_4 \cdot 7H_2O$, 0.0498; $ZnSO_4 \cdot 7H_2O$, 0.0382; $CuSO_4 \cdot 5H_2O$, 0.0157; $MnCl_2 \cdot 4H_2O$, 0.0144; $Na_2MoO_4 \cdot 2H_2O$, 0.01192 and $CoNO_3 \cdot 6H_2O$, 0.0049 in 1 L distilled water and the pH of the medium was adjusted to 6.5 prior to autoclaving.

2.1.3. Characteristics of wastewaters

The DWW used in this research was collected from a local dairy transformation plant in Golden Pack Company, 6 October City, Egypt. It was immediately divided into two groups. The first one was the unsterile dairy wastewater which is primary effluent wastewater refined with a clean cloth to exclude large fragments and kept for a week to sit down any visible solid molecules. After that, the wastewater was centrifuged at 11,000 (g) for 15 min to eliminate microscopic particles. The second group was the sterile dairy wastewater which was refined using 0.2 µm nylon microfilters to get rid of the suspended solid particles and microbes, followed with autoclaving the supernatant.

2.1.4. Microalga growth

The microalgal seed culture was inoculated at 10% concentration (V/V) per100 mL of Bold Basal Medium (BBM) in a 250 mL Erlenmeyer flask (The American Public Health Association, 2012), and further incubated in a shaker under continuous illumination with white fluorescent light of 2000 lux intensity at 150 rpm and 28 °C for 14 days. The sterile algal culture was developed by streptomycin and penicillin antibiotics treatment (Sigma-Aldrich, USA) to remove commensal bacteria in the cultures and to verify the axenic status of microalgae (Droop, 1967). The microalgae suspension in BBM was adjusted using a spectrophotometer to 0.6± 0.05 optical density at 540 nm for further experiments.

2.2. Optimization of biomass and lipid accumulation

To evaluate the suitability of DWW as an enriching medium for microalgae growing under mixotrophic conditions, five different sets of experiments were conducted. Partial substitution of the BBM medium with sterile/non-sterile DWW was tested by supplementing 1L flasks with 500 m L working volumes by five various proportions 20% (A), 40% (B), 60% (C), 80% (D)or 100 (E) of (sterile/non-sterile DWW(v/v). Inoculate 10 % (20mL) of the *C. subellipsoidea* HSSASE8 microalga suspension (V inoculum/V BBM). The experiments were carried out at 25°C, pH (7.5), and 150 rpm with cool-white fluorescent light illumination at 2000 lux intensity The experiments were carried out in three replicates (n=3). Culture growth was estimated by measuring dry cell weight (DCW) and lipid productivity after 20 days.

For large scale production under controllable mixotrophic conditions, 100 ml of *C. subellipsoidea* HSSASE8 growing suspension in 7L bioreactor (BioFlo 110, New Brunswick Scientific, USA) containing 2L running volume of the experiments sets (A-E) of sterile/non-sterile dairy wastewater DWW (v/v)) as optimum concentrations showed high growth biomass and lipid content. The main structure consists of a vessel, a fundamental control unit for beginning and performing process criteria, and a function unit to regulate temperature (25°C), turbulence, and pumps for continuous sterile aeration (150 mL/min) for 20 days under illumination intensity (2000 lux). The experiments were conducted at Bioprocess Development dept., GEBRI, SRTA-City in three replicate. DCW and fatty acids were measured at the end of the culture period at the Central lap of SRTA-City.

2.3. Analytical methods

2.3.1. Microalgae growth

As mention before, the algal growth and nutrients consumed in the growing batches followed daily during the experimental period by taking a sample volume of 10mL from growth suspension. Centrifuged at 11,000 (g) for 15 min, the supernatants were diluted and investigated for BOD, COD, TN, and TP to measure the mineral consumption. Development of algal cells in BBM supplemented with various concentrations of DWW was checked by determining the optical density at 680 nm using UV/visible spectrophotometer (Optizen, Korea).

2.3.2. Biomass production and lipid content

The algal biomass was harvested after growth of algal for twenty days batch culture and the dry weight (g/L) of culture suspension sample was determined as described by Droop (1967), weighing a dried sample of the culture suspensions. About 10 mL growth cultures were filtered through pre-weighed filter papers (Whatman GF/C 1.2mm, 90mm in width). Then, they were dried overnight at 110 °C and evaluated again at cabinet temperature to determine dry biomass accumulation per liter of culture broth (g/L). The OD of the microalgal suspension was measured at 680nm using a spectrophotometer. When needed, the sample was diluted to present an absorbance between 0.1–1.0. The OD_{680} was then switched to a dry cell weight (DCW) applying a linear relationship between OD_{680} and DCW (g/L), (The American Public Health Association., 1998).

At the end of experiments (20 days), lipid content analyzed gravimetrically according to solvent-based extraction method (Bligh and Dyer, 1959; Araujo *et al.,* 2013). Briefly, 35 m L of microalgal culture were centrifuged at 3900 (g) and 4 °C for 20 m in. The supernatant was thrown and the algal cells were resuspended in 2.5 mL of distilled water. 1.25 mL of chloroform and 2.5 mL of methanol were added. The mixture was applied to a sonication procedure for 30 min with overnight shaking. Then, 1.25 mL of chloroform were added and the mixture was sonicated for 30 min with shaking for 2 h. 1.25 mL distilled water was added with

shaking for 1 h. the mixture was then centrifuged at 3900 (g) and 4 °C for 5 min. The lipid-chloroform layer (in the bottom) was genteelly pipetted and transferred in a new tube, resuspended in 5 mL of deionized water and vortexed for 30 s at room temperature. 2.5 mL of chloroform were added with shaking for 1 h. The mixture was centrifuged at 3900 (g) and 4 °C for 5 min. The lipid-chloroform layer was gently pipetted and transferred in a new tube, washed with 5 m L of NaCl solution (5 %) and vortexed. The mixture was centrifuged at 3900 (g) and 4 °C for 5 min. The chloroform layer was pipetted and transferred in a pre-weighed tube. Chloroform was dry in the oven at 105°C for 1h and total lipid weight was calculated.

2.3.3. Transesterification of lipid into Fatty acid methyl esters(FAME)

The algal lipid was transesterified into fatty acid methyl esters (FAME) where most extraction methods were based on rout of Bligh and Dryer in 1959 as reported by (Lewis *et al*, 2000). Each 10 mg of lipid was dissolved in 2 mL of hexane and 0.2 mL of freshly prepared methanolic KOH (2M) as a catalyst. The mixture was Vortexed for 2 to 5 min followed by brief centrifugation. The upper hexane layer was gathered for FAME analysis.

2.3.4. Fatty acids profiles

The algal cells utilized for fatty acid profiles analysis were collected by centrifugation at 5000 rpm and 4°C for 30 min, and the algal pellets were lyophilized by a freeze dryer. Lipid and fatty acid composition analysis was performed as described by Jean-Michel Girard (2014) with slight modification. Briefly, 15 to 20mg of freeze-dried algal biomass was dissolved in 5 m L of sulfuric acid/methanol (2:98, v/v). The mixture was warmed to reflux using Dien-Stark apparatus. After cooling, the reaction mixture was rinsed twice with saturated sodium hydrogen carbonate aqueous solution and evaporated over anhydrous sodium sulfate. The fatty acid methyl esters (FAMEs) gained as mentioned by Ichihara *et al.,* (1996) dissolving analysis by 5 column (30 m × 0.25 mm, film thickness 0.25 um) with helium as carrier gas at 1.33 mL/ min. The injection port held at 210°C, the detector temperature adapted to 230°C. The segregation ratio kept 1:10 and ionization voltage maintained at 70 eV. One µL specimen injected. The oven computed as follows: at 40 °C for 2 min and afterward raised to 210°C at 5°C/min at which the column retained for 5 min. The fatty acids were classified by matching the retention times with those of standard (Fatty acids -Sigma-Aldrich) and assessed by relating their peak area with that of the internal standard.

2.4. Statistical analysis

All the data obtained from the experiments replica was assessed by calculating the standard deviation of the means, and the Least Significant Difference (LSD) between the mean values was calculated at the 0.05 levels using SPSS V.16

3. Result

3.1. Characteristics of dairy wastewater

The components of the main effluent dairy wastewater used in this experiment were illustrated in Table 1. Mineral concentrations, Biological Oxygen Demand (BOD), Chemical Oxygen Demand (COD), Total Phosphorus (TP) and Total Nitrogen (TN) were calculated corresponding to the standard method as specified by The American Public Health Association (APHA, 2012). The diverse components including Na, K, Ca, Fe and Mn were tested by inductively coupled plasma-atomic emission spectrometry (ICP-MS, Agilent Technologies, Japan).

Table 1. Physico-chemical properties of the primary effluent dairy wastewater.

Parameters	Units	Dairy wastewater
Chemical oxygen demand	mg O_2/L	2453.6±361.2
Biochemical oxygen demand	mg O_2/L	1645.2±156.26
Total organic carbon	mg/L	182.65±13.2
Total suspended solids	mg/L	674±83.7
Total phosphate	mg/L	279.5±56.2
Total nitrogen	mg/L	310±132.9
pH		7.5±0.3
Na	mg/L	517±46.2
K	mg/L	5420±487.7
Ca	mg/L	1273±940.1
Fe	mg/L	31±6.4
Mn	mg/L	16.7±3.8

Data were shown by mean values ± standard deviation of three individual repetitions

3.2. Growth biomass evaluation

Significant lipid composition is one of the major benchmarks for the choice of microalgae strains as a sustainable source for the production of biofuel. The freshwater algae confirmed in the existing work were chosen not solely on the principle of a great lipid and fatty acid composition but further on excessive growth rates and significant cell density with little cost. Upon cultivation of microalga, the water samples were analyzed for physicochemical properties (Table 1).

The *C. subellipsoidea* HSSASE8 microalgae were grown in BBM media supplemented with five different dilutions (20% (A), 40% (B), 60% (C), 80% (D) and 100 (E)) of sterile or unsterile DWW under a mixotrophic condition at a s mall scale in shake flask experiment (Figure 1A) and at large scale in bioreactor batch experiments up to 10 days (Figure 1B).

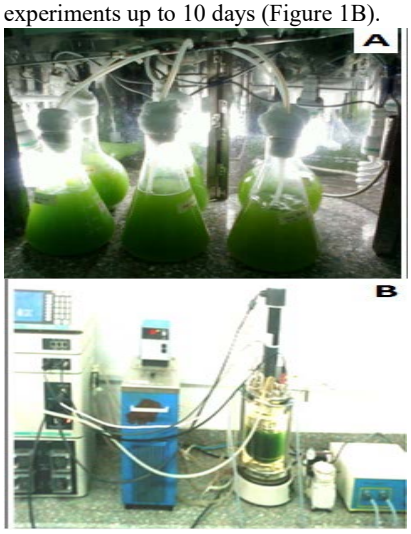

Figure 1. Growth optimization of C. subellipsoidea microalgae in BBM media supplemented with 20%, 40%, 60%, 80% and 100 of sterile/unsterile Dairy using shake flak methods(A) and bioreactor for large scale biomass production & lipid productivity (B).

All biomasses of sterile and unsterile batches showed a continual increase in biomasses with time (Figure 2). This increase in biomass reached the maximum after 8 days in

A, B, C and E treatments, while it reached the maximum after 7 days in D treatment and then slightly decreased in the next cultivation time (48h). The growth of *C. subellipsoidea* HSSASE8 microalga was greatly promoted by DWW treatment, and the most abundant biomass was achieved at 60% (918.15 mg/L and 776.09 mg/L for unsterile and sterile DWW dilutions, respectively). This was followed by biomasses in unsterile condition at 80% (573.01mg/L) and 100% (563.11mg/L) of DWW. On the other hand, the minimum biomasses were obtained at 20% (9.72mg/L) in sterile DWW dilutions.

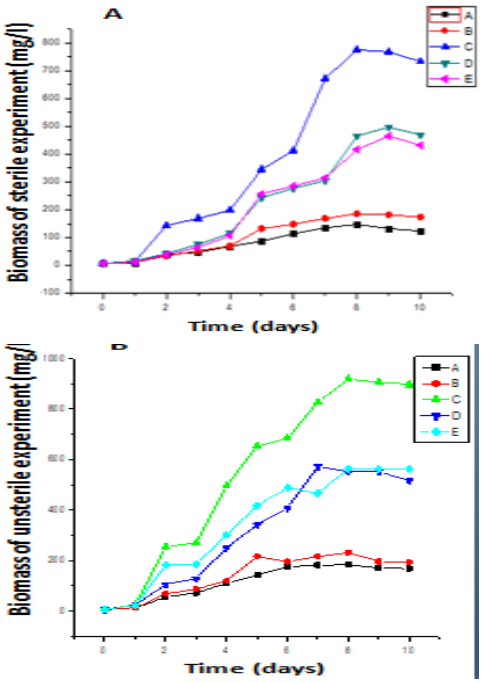

Figure 2. Growth biomass curve (DW) of *C. subellipsoidea* microalga in basal medium supplemented with different dilutions; 20% (A), 40% (B), 60% (C), 80% (D and 100 (E) of sterile DWW (A) and unsterile DWW (B) within 10 days.

3.3. Nutrients removal

In the present study, a primary parameter for monitoring DWW effluent quality (Table 1) indicated that the initial nutrients loads TN (310mg/l), TP (279.5mg/l), TOC (182.65 mg/l) of DWW effluent were beyond the minimal discharge values (TN 15–20 mg/l, TP 0.5–1.0 mg/l, TOC 20–30 mg/l) established by State Environmental Protection Administration of China (SEPAC). An overview of the elimination of macro and microelement showed a p articular decline in these elements in all concentrations of dairy wastewater. The usage of nutrient elements by *C. subellipsoidea* HSSASE8 microalga enhanced their production and decreased the nutrient accumulation in the dairy wastewater, aiding the purpose of the advanced wastewater management and biomass production. Therefore, the strength of *C. subellipsoidea* HSSASE8 to remove TN, TP and TOC was studied in bioreactor running under different dilutions of DWW up to 10 days in bioreactor batch culture, and the data are shown in Figures3. An efficient performance in reductions of TN, TP and TOC were signed by *C. subellipsoidea* HSSASE8 cells as a r eturn to DWW substrate feeding. Specifically, the measured consumption figures of TN ranged from 301 to 0.0mg/w (100%) (Figure 3A and B) was achieved in 60% DWW batches in the first 7thand 8thcultivation days of unsterile and sterile conditions, respectively. Moreover, the consumption rates of TP ranged from 279.5-0.0 mg/w (100%) (Figure 3C and D) were in 60% DWW batches in the 9thand 10thcultivation days of unsterile and sterile conditions respectively whereas the reduction values of TOC ranged from 182.6-2.42 mg/w (94.58%), and 182.6-3.86 mg/w (83.47%) (Figure 3E and F) was measured in 60% DWW batches in the 10thcultivation day in unsterile and sterile conditions, respectively. It is obvious that a maximum TN, TP, and TOC reduction by *C. subellipsoidea* HSSASE8 was recorded in 60% unsterile DWW culture media, which is higher than that at 60% sterile DWW culture batches. It was remarkable that *C. subellipsoidea* HSSASE8 growth slowed down when TN, TP, and TOC nutrients were no longer detected in DWW culture batch media, suggesting that the exhaustion of these nutrients may limit the growth of microalga.

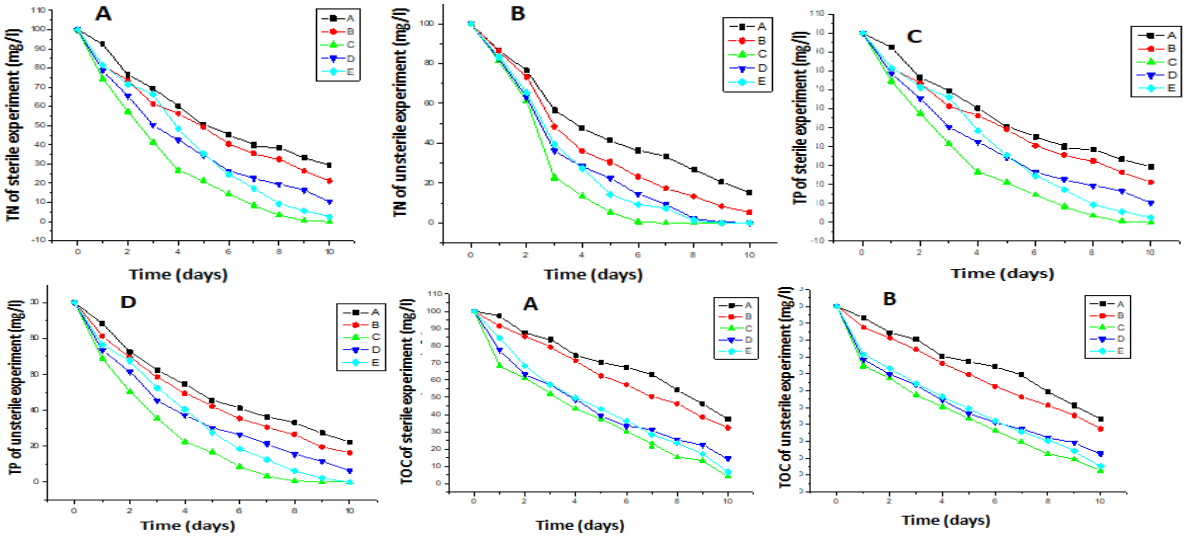

Figure 3. Nutrients removal of TN (A & B), TP (C & D) and TOC (E & F) versus time by C. subellipsoidea microalgae cultivated in basal medium supplemented with different dilutions; 20% (A), 40% (B), 60% (C), 80% (D and 100 (E) of sterile/unsterile Dairy WW.

C. subellipsoidea HSSASE8 fulfills the essential benchmarks for biodiesel production, essentially excessive lipid content and massive growth yield, adding another interest of usage of drain water and alleviate environmental deterioration. In a request to assess its cost-benefit an alternative competitive C-N source likes DWW of varied concentrations that was appeared as a good nutrient supplement and may be used for algal cultivation that agrees with that found by Ian Charles Woertz (2007).

.

3.4. The lipid content and fatty acid profile

The lipid contents and fatty acid profiles represent a potential indicator of biodiesel yield. Lipids substances biosynthetically related to fatty acids and their derivatives (Chisti, 2007). In the present study, the total lipid content of the *C. subellipsoidea* HSSASE8 microalgae after 10 days was determined. Results prove that the process of partial replacement to synthetic media with dairy wastewater decrease the comprehensive cost of biofuel production. The total lipid content of *C. subellipsoidea* HSSASE8 cultivated in sterile or unsterile DWW supplemented media was improved and directly proportional to the algal biomass concentration, ranged from 34.46to 80.67% (DCW) response to the cultivation in growth media supplemented with different dilutions (A-E) of sterile or unsterile DWW substrate. It was obvious in Figure 4 that the total lipid content varied significantly across the different medium treatment strategies. It was clear that the increase in the lipid content in unsterile treatments was higher than that in sterile treatments. The highest lipid contents (39.66% and 47.62% for sterile and unsterile substrate, respectively) were achieved by incorporation of 60% of DWW. However, the minimal lipid contents (24.3 and 27.30% for sterile and unsterile substrate, respectively) were recorded at 20% of DWW.

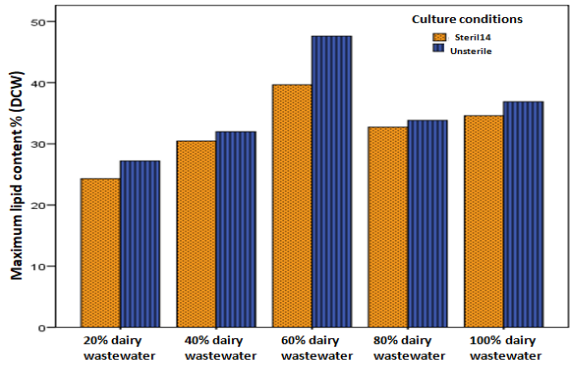

Figure 4. Maximum lipid content in dry biomass produced by *C. subellipsoidea* cultivated in basal medium supplemented with different concentration; 20% (A), 40% (B), 60% (C), and 80 % (D and 100 (E) of sterile/unsterile Dairy WW.

4. Discussion

It is noteworthy that the growth characteristics of *C. subellipsoidea* HSSASE8 as successful, promising commercial microalgae strain in DWW supplemented media under bioreactor patch condition that allows rapid biomass production with high lipid content. The algal growth stimulated and increased as the DWW dilutions (20%, 40%, 80% and 100%, v/v) increased either in sterile or unsterile experiments. Overall, the unsterile treatments exhibited a s ignificant increase in biomass production as compared with sterilized DWW. The growth of *C. subellipsoidea* HSSASE8 microalga was greatly promoted by DWW. The increase of DWW concentration in cultivation media enhanced the lipid content accumulation (Chisti, 2007 and Ian Charles Woertz, 2009) with the tested microalgae grown in DWW and a possible feedstock for biodiesel where they reported that the total lipid content of the algae ranged from 8% to 29% of algal dry mass. A group (Kothari *et al.,* 2013) at California Polytechnic State University worked on algae grown on dairy and municipal wastewater for simultaneous nutrient discharge and lipid production for biofuel feedstock. The research pointed out that the lipid productivity reached 2.8 $g/m^2/d$ and lipid content varied from 4.9%-29% corresponding to 11,000 L/ha/yr (1,200 gallons/acre/year). The relative lipid content on the 10^{th} day (1.6 g) and 15^{th} day (1.2 g) of the batch experiment was noticed to be richer than that reached in BG-11 growth medium on the 10^{th} day (1.27 g) and 15^{th} day (1.0 g).

Results of a previous study (Mahendraperumal *et al*., 2014) indicated clearly a significant reduction in the content of phosphorus (44.36mg/l), ammonias nitrogen (20.73 mg/l) and total organic carbon (3701 mg/l) as compared to raw wastewater. Our results agree with the results showed by Jimenez-Perez *et al*. (2004) in that great TN uptake reached by *S. intermedius* and *Nannochloris sp.*

The increment in overall lipid content under nitrogen limitation can be accepted because the enzymes involved in lipid synthesis are less responsive to a reduction in cellular soluble protein matter than those involved in carbohydrate synthesis (Ian Charles Woertz *et al.,* 2009). They were well declared that, under N-deficient conditions, algal cells often have an excess of carbon metabolites and smaller NP uptake rates of *Chlorella kessleri* developed in artificial wastewater that showed efficiency removal of N and P under high illumination. Distinctly, Nitrogen diminished to 136.5 from 168.1 mg NO_3-N/l in 3 days, while the effectiveness of removed phosphate was hardly 8 - 20% of the original compositions (Lee and Lee, 2001). Nitrogen is an effective macro component of microalgae ranging from 1 t o 10% of the growing biomass, and still a key element for improving the lipid content in algal cells (Miao and Wu, 2007). Phosphorus is essential for growth and alternative processes, dealing with energy delivery and biosynthesis of DNA (Ebrahimian *et al*., 2014). The chief process for TN and TP removal is assumed to be biomass uptake. This utilization of nutrients from wastewater demonstrates the potential cost savings when compared to the purchase of fertilizers. The massive uptake of minerals by biomass points out that the biomass junk left behind after oil extraction will have the power as a crop manure.

The microalga cellular content of *C. subellipsoidea* HSSASE8 was significantly increased when inoculated in growth medium with different proportions 20, 40, 60, 80, and 100% of sterile/unsterile DWW within 10 cultivation days. Our results clearly show the increase in total fatty acids in an unsterile treat as twice as in sterile treats. Moreover, our results show the increase in total polysaturated fatty acids in unsterile treatments as twice as in sterile conditions and all detected fatty acids including carbon chain length, branching of the chain, and degree of

unsaturation acids as revealed by GC analyses, The fatty acid composition summarized in the (Table 2 and Figure 5) showed that the highest yield of unsaturated fatty acids (C16-C18) ranged from (68.54-72.54% w/w) at unsterile substrates as compared with (68.27- 71.34%) in sterile conditions. Fatty acid profiles characterized with particular of the high-proportioned palmitic acid (C16:0), behenic acid (C22:0), linolenic acid (C18:3) and linoleic acid (C18:2) were the dominant fatty acids occurring in the accumulated lipids in *C. subellipsoidea* HSSASE8 during growth on sterile and unsterile DWW growth media. In addition in the unsterile conditions, linoleic acid and linolenic polyunsaturated fatty acid (PUFA) was significantly enhanced up to 1.5- 2 folds at the 60% DWW concentration as compared with 20% unsterile experiment. Some earlier review lumped all polyunsaturated fatty acids together as essential fatty acids. Essential fatty acids play an important role in the life and death of cardiac cells (Kaur *et al*., 2014).

The ratio of saturated FA was commonly two folds greater than that of unsaturated one during production on DWW growth medium. This is a suitable fatty acid profile for biodiesel production, since biodiesel gained from saturated oils have a further oxidative stability and fewer NOx emissions. Overall, that the relative fatty acids accumulated in the *C. subellipsoidea* HSSASE8 cells grown in unsterile DWW batches were significantly higher than those grown in sterile DWW treatments may be attributed to the indigenous wastewater bacteria that exhibit a potential role in degradation *of* organic compounds enhancing the growth and biomass productivity rate of *C. subellipsoidea* HSSASE8 cells as compared with sterile condition. Meanwhile, nitrogen limited growth often enhances algal lipid metabolism (Fields *et al*., 2014 and Griffits *et al*., 2012) and the existence of bacteria in algal cultures can improve NH_4-N removal from wastewaters. While algae efficiently pick up NH_4-N, bacteria take part in NH_4-N removal through nitrification (Wang, 2015). The fatty acids recommended as feedstock for high-quality biodiesel were characterized with C16–C18 long-chain groups, as well as a cer tain degree of unsaturation. As summarized in Table 2, *C. subellipsoidea* HSSASE8 cells grown in unsterile and sterile DWW produced a high proportion of C16-C18 fatty acids (68.54-72.54% w/w). Our results provide a foundation for improving the yield of lipid-based biodiesel production from cultivation of *C. subellipsoidea* HSSASE8 on D WW in the future, in addition to a nutrients removal result in wastewater treatment.

Table 1. Composition of fatty acids (%, w/w) in *C. subellipsoidea* grown on basal medium supplemented with different dilutions of sterile/unsterile DWW.

Fatty acid profile	Growth media condition	Dairy wastewater proportions				
		20% (A)	40% (B)	60% (C)	80% (D)	100%(E)
		Fatty acid composition (%, w/w)				
Lauric acid (C12:0)	Sterile	1.70±8.83	2.38±0.03	2.73±0.03	3.71±0.03	3.5±0.02
	Unsterile	1.77±0.09	3.41±0.02	3.14±1.15	3.82±0.03	3.63±0.04
Myristic acid (C14:0)	Sterile	1.1±0.02	1.27±0.03	2.83±0.04	1.58±0.03	1.55±0.04
	Unsterile	1.19±0.04	1.33±0.03	2.09±0.05	1.62±0.03	1.64±0.04
Palmitic acid (C16:0)	Sterile	5.4±0.35	8.77±0.05	16.87±0.08	9.53±0.12	12.42±0.08
	Unsterile	5.72±0.02	8.91±0.04	18.46±0.04	10.4±0.03	13.49±0.1
hexadecatrienoic acid (C16:3)	Sterile	0.73±0.02	1.23±0.15	2.2±0.05	1.79±0.03	1.66±0.01
	Unsterile	0.82±0.04	1.24±0.04	3.45±0.03	1.92±0.02	1.74±0.02
Stearic acid (C18:0)	Sterile	3.95±0.07	5.3±0.06	7.69±0.06	6.69±0.03	6.82±0.03
	Unsterile	4.33±0.04	5.60±0.03	9.15±0.06	6.92±0.03	7.22±0.04
Oleic acid (C18:1)	Sterile	2.28±0.06	2.86±0.06	4.94±0.09	3.2±0.07	3.44±0.07
	Unsterile	2.42±0.04	3.15±0.04	5.31±0.03	3.37±0.03	3.6±0.03
Linoleic acid (C18:2)	Sterile	5.28±0.05	5.92±0.08	8.57±0.15	6.27±0.14	6.14±0.06
	Unsterile	5.47±0.05	6.20±0.03	8.71±0.04	6.50±0.02	6.41±0.05
Linolenic acid (C18:3)	Sterile	5.96±0.08	8.43±0.04	12.99±0.11	8.63±0.07	9.67±0.03
	Unsterile	6.23±0.11	8.63±0.03	13.43±0.04	9.75±0.05	10.47±0.06
Arachidic acid (C20:0)	Sterile	0.42±0.03	0.71±0.03	2.1±0.04	1.58±0.02	1.52±0.03
	Unsterile	0.69±0.02	0.84±0.02	2.31±0.03	1.75±0.03	1.65±0.03
Behenic acid (C22:0)	Sterile	7.64±0.03	8.2±0.06	14.24±0.09	9.60±0.03	12.09±0.13
	Unsterile	7.82±0.04	9.44±0.02	14.61±0.07	10.2±0.03	12.49±0.02

Data were shown by mean values ± standard deviation of three individual repetitions.

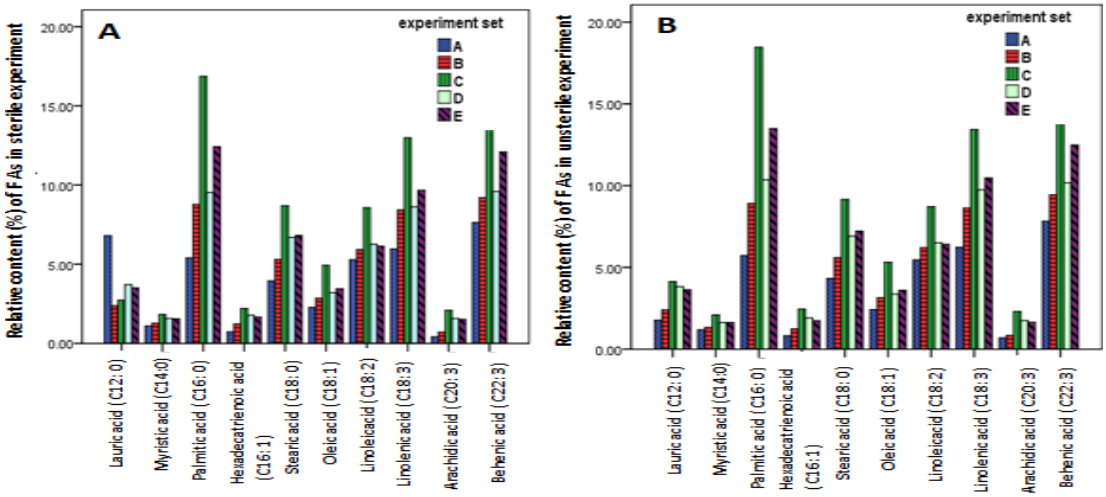

Figure 5. Fatty acid profile of lipids produced by C. subellipsoidea cultivated in basal medium supplemented with different concentration; 20% (A), 40% (B), 60% (C), 80% (D and 100 (E) of sterile/unsterile Dairy WW.

5. Conclusion

The study suggests that *Coccomyxa subellipsoidea* HSSASE8 cells, in particular, may show adequate growth in components of dairy wastewater, such as cheese whey, as the limiting nitrogen source, resulting in cost-effectual and feasible alternative commercial mediums for biomass production, without requiring expensive carbon sources in cultivation medium. In addition, the close elimination of TN, TP, and (94.58%) of TOC by C. subellipsoidea HSSASE8 with the support of DWW operation offers a reasonable solution of waste control. The gas chromatography evaluation proved that the FA analysis is advantageous when concluding the fitness of algal lipids for applications as biodiesel or nutritional demands. *Coccomyxa subellipsoidea* HSSASE8 oils have a high ratio of 16 -18 carbon chained fatty acids as reasonable biodiesel candidates (Lin and Lin, 2012). Moreover, in this study, a significant build- up in neutral lipid composition and conversion of fatty acid distribution with a powerful improvement in the magnitude of essential polyunsaturated fatty acids were obtained. Future research should concentrate on bi oengineering of *Coccomyxa subellipsoidea* HSSASE8 for high lipid accumulation because it would be one of the highly promising ways to meet the energy demand using microalgae as a feedstock for third generation biofuel.

Acknowledgments

We would like to thank Professor Dr. Usama Beshay, Professor of Microbiology, bioprocess dept., City of scientific research and technology application for his guidance while using most instruments. Also, we would like to thank Professor Soha Elsayed Mostafa in Environment Research Institute, Agricultural Research Centre for her support. And I also like to thank Dr. Elsayed Shabaan Abd Elrazik in arid land cultivation and research institute, SRTA-City for his advice while working on this study.

Conflict of Interest

The authors declare that they have no conflicts of interest.

References

Alvarez-Diaz PD, Ruiz J, Arbib Z, Barragan J, Garrido-Perez MC and Perales JA. 2015. Wastewater treatment and biodiesel production by *Scenedesmus obliquus* in a two-stage cultivation process. *Bioresour Technol.*,**181**:90–6.

Araujo GS, Matos LJBL, Fernandes JO, Cartaxo SJM, Gonçalves LRB, Fernandes FAN and Farias WRL. 2013. Extraction of lipids from microalgae by ultrasound application: prospection of the optimal extraction method. *Ultrason Sonochem.*,**20**:95–8.

Bischoff HW and Bold HC. Phycological Studies IV. 1963. Some Soil Algae from Enchanted Rock and Related Algal Species, *University of Texas Publication,* No. 6318: 1–95.

Bligh E and Dyer W. 1959. A rapid method for total lipid extraction and purification. *CAN J Biochem Phys.*,**37**: 911-917.

Chisti Y. 2007. Biodiesel from microalgae. *Biotechnol Adv.*,**25**:294–306.

Carolina B, María BP, Gisela RF, Natalia S, Silvia EM and María VB. 2017. BMC Genomics.,**18 (1)**: 1-23.

Droop MR. 1967. A procedure for routine purification of algal cultures with antibiotics. *Br Phycol Bull.*, 3:295-297.

Ebrahimian A, Kariminia HR and Vosoughi M. 2014. Lipid production in mixotrophic cultivation of *Chlorella vulgaris* in a mixture of primary and secondary municipal wastewater. *Renew Energy.*,**71**:502–508.

Fields MW, Hise A, Lohman EJ, Bell T, Gardner RD, Carredor L, Moll K, Peyton BM, Characklis GW and Gerlach R. 2014. Sources and resources: importance of nutrients, resource allocation, and ecology in microalgal cultivation for lipid accumulation. *Appl Microbial Biotechnol.*,**98**: 4805–4816.

Gao F, Yang ZH, Li C, Wang YJ, Jin WH and Deng YB. 2014. Concentrated microalgae cultivation in treated sewage by membrane photobioreactor operated in batch flow mode. *Bioresour Technol.*,**167**:441–6.

Gavala N, Kopsinis H, Skiadas IV, Stamatelatou K, and Lyberatos G. 1999. Treatment of dairy wastewater using an up-flow anaerobic sludge blanket reactor. *J Agric Eng Res.*,**73**: 59–63.

Griffiths MJ, Hille RP and Harrison STL. 2012. Lipid productivity, settling potential and fatty acid profile of 11 microalgal species grown under nitrogen replete and limited conditions. *J Appl Phycol.*,**24**: 989–1001.

Ian Charles Woertz. 2007. Lipid productivity of algae grown on dairy wastewater as a possible feedstock for biodiesel.MSc dissertation, California Polytechnic University, San Luis Obispo, USA**.**1-87.

Ian Charles Woertz A, Feffer T, Lundquist and Nelson Y. 2009. Algae grown on dairy and municipal wastewater for simultaneous nutrient removal and lipid production for biofuel feedstock. *J Environ Eng.*,**135**: 1115–1122.

Ichihara K, Shibahara A, Yamamoto K and Nakayama T. 1996. An improved method for rapid analysis of the fatty acids of glycerolipids. *Lipids*,**31(5)**:535-9.

Jean-MichelG,Mhammed B H,Jonathan G, Nathalie F,Michèle H, *et al.* 2014. Mixotrophic cultivation of green microalgae *Scenedesmus obliquus* on cheese whey permeate for biodiesel production, *Algal Res.*,**5**: 241–248.

Jimenez-Perez MV, Sanches-Castillo P, Romera O, Fernandez-Moreno D, and Perez-Martinez C. 2004. Growth and nutrient removal in free and immobilized planktonic green algae isolated from pig manure. *Enz MicrobTech.*,**34**: 392-398.

Karadag D, Köroğlu OE, Ozkaya B and Cakmakci M. 2015. A review on anaerobic biofilm reactors for the treatment of dairy industry wastewater. *Process Biochem.*,**50**:262-271.

Kaur N, Chugh V and Gupta AK. 2014. Essential fatty acids as functional components of foods- a review. *J Food Sci Technol.*,**51(10)**:2289–2303.

Kothari R, Prasad R, Kumar V and Singh DP, 2013. Production of biodiesel from microalgae *Chlamydomonas polypyrenoideum* grown on dairy industry wastewater. *Bioresour Technol.,***144**: 499-503.

Lee K and Lee CG. 2001. Effect of light/dark cycles on waste-water treatments by microalgae. *Biotechnol BioprocEng.,***6**: 194-199.

Lei A, Chen H, Shen G, Hu Z, Chen L and Wang J. 2012. Expression of fatty acid synthesis genes and fatty acid accumulation in *Haematococcus pluvialis* under different stressors. *Biotechnol Biofuels*,**5**:18.

Lewis TPD, Nichols, *et al.,* 2000. Evaluation of extraction methods for recovery of fatty acids from lipid producing microheterotrophs*. J Microbiol Meth.*,**43(2)**: 107-116.

Lin CY and Lin YW. 2012. Fuel characteristics of biodiesel produced from a high-acid oilFrom soybean soapstock by supercritical-methanol transesterification. *Energies.,* **5**: 2370-2380.

Mahendraperumal G, Deval S and Ekta S. 2014. B iomass and lipid accumulation of microalgae grown on dairy wastewater as a possible feedstock for biodiesel production. *Int J SciRes.*,**3 (12)**: 909- 913.

Miao X and Wu Q. 2007. Biodiesel production from heterotrophic microalgal oil. *Bioresour Technol.*,**97**:841–846.

Rad SJ and Lewis MJ. 2014. Water utilization, energy utilization and waste water man-agreement in the dairy industry: *A review Int J Dairy Technol.*,**67**:1-20.

Sarkar B, Chakrabarti PP, Vijaykumar A and Kale V. 2006. Wastewater treatment in dairy industries – possibility of reuse. *Desalination*,**195**:141-52.

Schenk PM, Thomas-Hall SR, Stephens E, Marx UC, Mussgnug JH, Tredici MR and Zittelli GC. 1998. Efficiency of sunlight utilization: tubular versus flat photobioreactors. *Biotechnol. Bioeng.*,**57**: 187–197.

The American Public Health Association. 1998. Methods for biomass production. In: Standard methods for the examination of water and wastewater. *Baltimor*e, MD. USA.

The American Public Health Association. 2012. Standard methods for the examination of water and wastewater. 2nd ed. Washington DC.

Wang M, Yang H, Ergas SJ and Steen P. 2012. A novel shortcut nitrogen removal process using an algal bacterial consortium in a photo-sequencing batch reactor (PSBR). *Water Res.*,**87**: 38–48.

JJBS

Volume 13, Number 1,March 2020
ISSN 1995-6673
Pages 55 - 58

Jordan Journal of Biological Sciences

Determination of the Pigment Content and Antioxidant Activity of the Marine Microalga *Tetraselmis suecica*

Sri Sedjati*, Delianis Pringgenies and Muhamad Fajri

Department of Marine Science, Diponegoro University, Jl. Prof. Soedarto SH, Semarang, 50251, Indonesia

Received April 8, 2019; Revised May 18, 2019; Accepted May 24, 2019

Abstract

Marine microalgae or phytoplankton are marine microorganisms that act as producers. In addition to their important role in the sea, microalgae also have potential application in medicine and can be a good source of food. This study aims to determine the content of chlorophyll a and chlorophyll b pigments, carotenoids as well as antioxidant activity in samples of *Tetraselmis suecica* marine microalga using the DPPH (1, 1-diphenyl-2-picrylhydrazyl) method. The research samples were obtained from the Natural Feed Laboratory of the Brackish Water Aquaculture Center (BBPBAP), Jepara. The study included the following stages: sample preparation, sample extraction, and measurements of pigment content and antioxidant activity using DPPH method. The results showed that acetone extract of marine microalga *Tetraselmis suecica* contained 1.688 mg/g of chlorophyll a, 0.713 mg/g of chlorophyll b, and 5.380 µg/g of carotenoid, as well as an IC_{50} value of 37.320 ppm. It was concluded that the antioxidant activity of *the Tetraselmis suecica* was very strong, i.e. the IC_{50} value found was less than 50 ppm.

Keywords: Pigments, Antioxidants, *Tetraselmis suecica*, DPPH

1. Introduction

Bioactive compounds are found in the body of animals and plants. This compound has various important roles in the human body as an antioxidant, antibacterial, anti-inflammatory and anticancer agent. Various studies on bioactive compounds have been carried out for human health (Lordan *et al*., 2011; Cikos *et al*., 2018).

Antioxidants are defined as compounds that can inhibit and prevent lipid oxidation processes by preventing the formation of free radical reactions (peroxides) (Kikuzaki *et al*., 2002). Antioxidants can inhibit and prevent the oxidation process. They are very beneficial for health and play an important role in maintaining the quality of food products. Antioxidant benefits for health can be seen from its contribution in preventing cancer and tumors, vasoconstriction, and premature aging. The presence of antioxidants in food products prevents the oxidation process that can cause damage, such as rancidity, color and aroma changes, and other physical damage (Firdiyani, 2015).

Today, the most commonly used antioxidants are synthetic antioxidants, such as butylated hydroxyanisol (BHA), butylated hydroxytoluene (BHT), tertbutyl-hydroquinone (TBHQ) dan propyl gallate (PG). Various studies on B HA and BHT found that prolonged use of these synthetic compounds can cause tumors in animals. The use of this type of antioxidant can be very dangerous, so it is necessary to find a source of natural antioxidants that are relatively safer. Natural antioxidants can be found in land and sea. These antioxidants are naturally occurring in many plants and animals and can be developed as potential alternatives for synthetic antioxidants (Vadlapudi *et al*., 2012).

Microalgae shows promising potential to produce various important biochemical compounds for food, medical treatment, research, and other uses. Also, there are still many important chemical compounds that need to be studied in microalgae. This marine species has the potential to become a natural resource of compounds that can be used as food ingredients and improve the nutrition of food consumed by humans and animals. Previous research has been carried out on algal biomass as a source of protein and systematically uses it for active components and drugs (Raja *et al*., 2008).

A study by Maligan *et al*. (2015) found that acetone extract from *Tetraselmis* sp. contains 21.73 mg / g of total chlorophyll, and antioxidant activity of 21.04 ppm; another study by Abdilah *et al.* (2014) found that the total chlorophyll content and antioxidant of acetone extract of the same species of microalgae were 10.603 mg/g and 27.59 ppm respectively.

Green microalgae is rich in chlorophyll and carotenoids. The pigment is part of the compound that acts as a neutralizing free radicals. Based on these facts, the study aims to determine and measure pigment and antioxidant compounds in *Tetraselmis suecica*.

* Corresponding author e-mail: sedjati69@gmail.com.

2. Materials and Methods

2.1. Sample preparation

Tetraselmis suecica microalga was obtained by culture from the Jepara Brackish Water Research Center. The samples were centrifuged for 10 minutes at a speed of 3000 rpm and then separated from sea water. Then, they were dehydrated at room temperature for 24 hours.

2.2. Assesment of carotenoid and chlorophyll content

0.1 gram of dry sample was extracted with 10 mL of 80% acetone. The filtrate obtained were placed in cuvettes. The content of chlorophyll and carotenoids were measured by a spectrophotometer, at 480 nm, 645 nm, and 663 nm of wavelengths. The absorbance value, carotenoid content, and chlorophyll content were analyzed using the method used in Dere (1998) and Harborne (1984).

2.3. Assesment of antioxidant activity with DPPH method

Crude extract was extracted using technical acetone solvents, with a ratio of 1: 5 to samples and solvents. Maceration was carried out for 24 hours. The results of maceration were filtered using filter paper to separate the filtrate and residue. Extraction with acetone solvent was carried out to obtain a crude extract of microalga, which would be used in the antioxidant test using DPPH. The filtrate from the extraction with acetone solvent was then concentrated using 40°C evaporator rotatory equipment to obtain a crude extract of the sample.

DPPH 0.1 mM solution was made by dissolving DPPH crystals in 100 mL of 95% methanol solvent. Extract samples were grouped into 4 concentration series of 0, 25, 50, 100 and 200 ppm. 4 mL of extract samples from each concentration were added with 1 ml DPPH, incubated for 30 minutes in a dark room. A blank solution was made by dissolving 1 mL of DPPH solution in 4 mL of methanol solution. The absorbance rate is measured at a wavelength of 517 nm using Shimadzu UV1800 spectrophotometer. The measurement of each sample was repeated three times (Badrinath *et al*., 2010).

2.4. Assesment of inhibition concentration (IC50)

Inhibition concentration (IC_{50}) is calculated by the linear regression equation obtained from the correlation between extract concentration and inhibition percentage. The linear regression equation obtained is y = bx + a, whereas x is Inhibition Concentration 50% (IC_{50}). By entering y = 50 into the simple linear regression equation, the value of x can be obtained (Badrinath *et al*., 2010).

3. Results

3.1. Assesment of chlorophyll and carotenoid contents in Tetraselmis suecica

The test results of the chlorophyll and carotenoid pigments in *Tetraselmis suecica* showed that the chlorophyll a content was higher (1.688 mg / g ± 0.266) than the chlorophyll b content (0.713 mg / g ± 0.335). The carotenoid content appeared to be of the highest percentage (5.38 µg / g ± 0.042) compared to that of chlorophyll a and chlorophyll b, as seen in the spectra pattern and absorbance value (Figure 1) and the results of measurement of pigment contents (Table 1).

Table 1. Assesmentof chlorophyll and carotenoid pigments content of *Tetraselmissuecica* acetone extract (n = 3 replications)

No.	Pigment	Content
1.	Chlorophyll a	1.688 mg/g ± 0.266
2.	Chlorophyll b	0.713 mg/g ± 0.335
3.	Carotenoid	5.38 µg/g ± 0.042

Assesment of spectral pattern and absorbance value of *Tetraselmis suecica* extract with acetone solvent showed that it peaked at the approximation of 400 - 450 nm, with lower peaks at absorbance 584.5 nm, 617.5 nm and 662.5 nm.

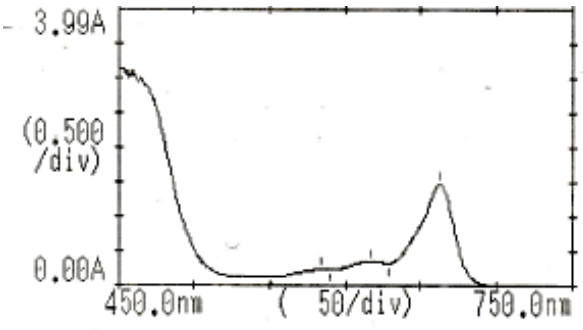

Figure 1. Spectral pattern of chlorophyll and carotenoids of *Tetraselmis suecica* acetone extract

3.2. Extraction yield

By filtering 3 liters of *Tetraselmis suecica* culture, 30 grams of dry biomass was obtained, which was then extracted with 300mL of acetone solvent. This process resulted in 1.9 grams (6.33%) of extract. The resulting extract was in the form of deep green paste.

3.3. Antioxidant activity test

The antioxidant activity of *Tetraselmis suecica* extract was determined based on the percentage of inhibition and DPPH value used. Data obtained from the results of antioxidant activity test was analyzed using a linear regression test. The result of the analysis was a linear regression equation used to calculate the IC_{50} value obtained. The results of the calculation of the percentage of inhibition and inhibition of the concentration of IC_{50} extract of *Tetraselmis suecica* were IC_{50} 38.26 ppm, as seen in Table 2 and Figure 2.

Table 2. Inhibition percentage and IC_{50} of *Tetraselmis suecia* acetone extract.

Concentration (ppm)	Mean of Inhibition Percentage	IC_{50} (ppm)
0	0	
25	62.771	
50	76.046	38.26
100	83.405	
200	88.745	

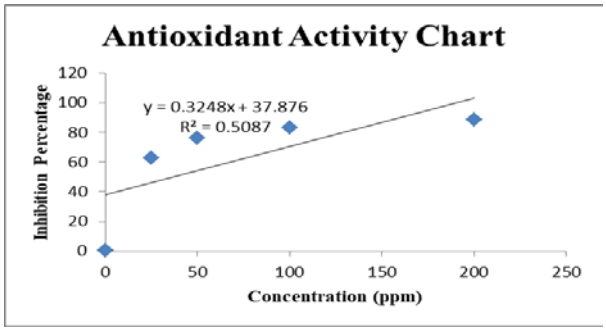

Figure 2. Regression test result chart.

4. Discussions

4.1. Assesment of chlorophyll and carotenoids

Measurement of pigment content in this study produced chlorophyll a value of 1.6885 mg/g and chlorophyll b value of 0.7139 mg/g. Previous research conducted by Ginting (2018) measured the values of chlorophyll a and chlorophyll b at 48 µg/mL and 40.88 µg/mL respectively, and Sani *et al*. (2014) measured of total chlorophyll between 3.65-19.20 mg/g. According to Harborne (1984), the spectral characteristics of chlorophyll pigments show major peak around 400 nm, a number of small peaks at 500 - 600 nm and other major peaks between 630 - 688 nm.

Chlorophyll measurement is one of the initial tests in determining antioxidant activity. Chlorophyll is a compound with free electrons structure from nitrogen atoms. The principle of free radicals is compounds that lack electrons. To complement the lack of electrons, free radicals will take electrons from human cells, which can eventually trigger cancer. Chlorophyll acts as an antioxidant by donating free electrons to free radicals, which stabilize the free radical structure (Firdiyani, 2015). Chlorophyll is an important antioxidant in food. The results of the research of Hsu *et al*. (2013) proved that chlorophyll and its derivatives (pheophytins) can prevent DNA damage with the same mechanism of antioxidant action against radical DPPH. Chlorophyll have the role of increased antioxidant activity.

This puts carotenoids as the prominent antioxidant agents in plants. By calculating the absorbance value of *Tetraselmis suecica* extract, a carotenoid value of 5.38 µg / g was obtained. Previous studies conducted on *Tetraselmis chuii* measured its carotenoid value at 6.70 µg / mL (Ginting, 2018). Carotenoids neutralize free radicals in three ways, namely electron transfer, hydrogen abstraction and the addition of radical species (Martinez *et al*., 2010). The process produces a carotenoid molecule that is radical, after which the electrons will be relocated so that it is spread throughout the carotenoid structure. This way, radical compounds can be stabilized in a short time by releasing heat (Dimara and Yenusi, 2011).

4.2. Antioxidant activity test

Antioxidants are compounds that can delay, inhibit and prevent molecular oxidation by preventing the formation of free radicals (Rohman, 2016). One test of antioxidant activity in a sample is by using a measurement of sample solution concentration which can reduce DPPH activity by 50% or IC_{50}. The IC_{50} value is derived from linear regression equation for the correlation of extract concentration to the value of DPPH inhibition. DPPH is a free radical that can react to compounds that can donate hydrogen atoms, which can be useful for testing the antioxidant activity of certain components in extracts. IC_{50} denotes the concentration needed by the sample to reduce DPPH by 50%, the smaller the IC_{50} value the higher the value of its antioxidant activity (Badrinath *et al*., 2010).

Antioxidant compounds will react with DPPH free radicals through the mechanism of donating hydrogen atoms and causing DPPH color to shift from purple to pale yellow, which has been measured with a wavelength of 517 nm (Rohman, 2016). The Lambert-Beer law states that the higher the extract concentration, the higher the absorbance value is. The parameter used to show antioxidant activity is the value of inhibitory concentration (IC_{50}). Inhibitory concentration is the concentration of an antioxidant which causes DPPH to lose 50% of its radical character (Molyneux, 2004).

Based on t he IC_{50} calculation results in this study, *Tetraselmis suecica* extract has a value of 37.32 ppm. This finding proved that the antioxidants in *Tetraselmis suecica* are strong antioxidants, since the value of the measured IC_{50} was under 50 ppm (Molyneux, 2004). Several studies proved that certain types of microalga produce natural antioxidant content. A study by Ridlo *et al*. (2017) found that chlorophyll and carotenoid contents had positive correlation with antioxidant activity. This finding affirmed a previous study by Pramesti (2013) which stated that the structure of chlorophyll has an important role in antioxidant activity. Chlorophyll is able to capture radical compounds with the presence of a main structure in the form of tetrapyrrole and conjugated polyene. Ferruzzi *et al*. (2002) complement this finding by stating that the structure of the porphyrin ring and magnesium, well known in chlorophyll, also play an important role in inhibiting free radicals. The explanation by Dutta *et al*. (2011), Young and Lowe (2018) stated that carotenoids are pigments that act as antioxidants. The compound can counteract the oxygen singlet (singlet oxygen quenching) via conjugation C = C bond in the carbon chain of the polyene. Carotenoid pigments can also scavenge peroxyl radical, transformed into carotenoids peroxide radical and easily broken down, so it is not harmful to live cells.

5. Conclusion

Based on the results of the study, it was concluded that the extract of *Tetraselmis suecica* showed the potential as a source of strong natural antioxidants. Its acetone extract had pigment content 1.689 mg/g of chlorophyll a, 0.714 mg/g of chlorophyll b, and 5.38 µg/g of carotenoids, but IC_{50} value 37.32 ppm, which meant significant antioxidant activity. The antioxidant activity of *the Tetraselmis suecica* extract was very strong, i.e. the IC_{50} value found was less than 50 ppm.

References

Abdillah F, Raya I and Ahmad A. 2014.Antioxidant activity and toxicity of C o(II) chlorophyll derivative extract . *Journal of Chemistry FMIPA Universitas Hasanudin*, **18(3)**: 1-10.

Badarinath AV, Rao KM, Chetty CMS, Ramkanth S, Rajan TVS and Gnanaprakash K. 2010. A review on in-vitro antioxidant

methods : comparisons, correlations and considerations. *Inter Jl Pharma Technol Res.*, **2(2)**: 1276-1285.

Cikos AM, Jokic S, Subaric D and Jerkovic I. 2018. Overview on the application of modern methods for the extraction of bioactive compounds from marine macroalgae. *Mar. Drugs*, **16(10)**: 348-368.

Dere S, Gunes T and Sivaci R. 1998. Spectrophotometric determination of chlorophyll-a, b, and total carotenoid content of some algae species using different solvent. *J of Botany*, **22**:13-17.

Dimara L and Yenusi TNB. 2011. Antibacterial and antioxidant activity of chlorophyll pigments extracts of seaweed *Caulerpa racemosa* (Forsskal) J.Agardh. *Papua J Biol*., **3(2)**: 53-58.

Dutta D, C haudhuri UR and Chakraborty R. 2011. Structure, health benefits, antioxidant property and processing and storage of carotenoids. *African J Food, Agricul, Nutrition and Develop.*, **4(13)**:1510–20.

Ferruzzi MG, Bohm V, Courtney PD and Schwartz SJ. 2002. Antioxidant and antimutagenic activity of dietary chlorophyll derivatives determined by radical scavenging and bacterial reverse mutagenesis assays. *J Food Sci*., **67(7)**:2589- 2595.

Firdiyanti F, Agustini TW and Ma'ruf WF. 2015. Extraction of bioactive compounds as natural antioxidants from fresh spirulina platensis using diffrent solvents. *JPHPI*., **18(1)**: 28-37.

Ginting NK, Sedjati S, Supriyantini E and Ridlo A. 2018. Effect of lighting on pigment content *Tetraselmis chuii* as a source of natural antioxidants. *Bulletin Oceanografi Marina*, **7(2)**: 91-97.

Harborne JB. 1984**. Phytochemical Methods: A Guide to Modern Techniques of Plant Analysis**. second ed. Chapman and Hall, London.

Hsu C, Chao P, Hu S and Yang C. 2013. The antioxidant and free radical scavenging activities of chlorophyll and pheophytins. *Food and Nutrition Sci.*, **4**:1–8.

Kikuzaki H, Hisamoto M, Hirose K, Akiyama K and Taniguchi H. 2002. Antioxidant properties of ferulic acid and its related compounds. *J Agricul Food Chem.*, **50(7)**: 2161-2168.

Lordan S, Ross SP and Stanton C. 2011. Marine bioactives as functional food ingredients: potential to reduce the incidence of chronic diseases. *Mar. Drugs*, **9:** 1056-1100

Maligan JM, Marditia AP, and Putri WDR. 2015. Analysis of marine microalgae *Tetraselmis chuii* extract bioactive compounds as a ntural antioxidants source. *Rekapangan J*., **9(2)**: 1-10.

Martinez A, Vargas R and Galano A. 2010. Theoretical study on the chemical fate of adducts formed through free radical addition reactions to carotenoids. *Theor Chem Acc.*, **127**: 595–603.

Molyneux P. 2004. The use of the stable free radical diphenylpicrylhydrazyl (dpph) for estimating antioxidant activity. *Songklanakarin J Sci. Technol*., **26(2)**: 211-219.

Pramesti R. 2013. Antioxidant activity of s eaweed extract Caulerpa serrulata used D PPH (1,1 difenil 2 pikrilhidrazil) method. *Bulletin Oseanografi Marina*, **2(2)**: 7-15.

Raja R, Hermaiswarva S, Kumar NA, Sridhar S and Rengasamy R. 2008. A perspective on the biotechnological potential of microalgae. *Crit Revi Microbiol*., **34 (2)**: 77–88.

Ridlo A., Pramesti R., Koesoemadji, Supriyantini E dan Soenardjo N. 2017. Antioxidant activity of mangrove leaves extracts Rhizopora mucronata. *Bulletin Oseanografi Marina*, **6(2)**: 110-116.

Rohman A. 2016. **Lipid: Chemical Physics Properties and Its Analysis**. Pustaka Pelajar, Yogyakarta.

Sani RN, Nisa FC, Andriani RD and Maligan JM. 2014. Analysis of yield and phytochemical screening ethanol extracts of marine microalga *Tetraselmis* sp. *J Food and Agroindustries*, **2(2)**: 121-126.

Vadlapudi V, Kaladhar DSVGK, Paul MJ, Kumar SVNS and Behara M. 2012. Antioxidant activities of marine algae: a review. *Inter J Recent Sci Res.*, **3(7)**: 574-580.

Young A and Lowe G. 2018. Carotenoids-Antioxidant Properties. *Antioxidants,***7 (2)**: 28-31.

JJBS

Jordan Journal of Biological Sciences

Volume 13, Number 1,March 2020
ISSN 1995-6673
Pages 59 - 67

Studies on five *Silene* L. Taxa in Saint Catherine Protectorate, South Sinai, Egypt

Sami H. Rabei [1*], Reham M. Nada[1] and Ibrahim EL Gamal[2]

[1] Department of Botany and microbiology, Faculty of Science, Damietta University, New Damietta, Post Box 34517, Damietta; [2] Saint Catherine Protectorate, Nature Conservation Sector (NCS), Egyptian Environmental Affairs Agency (EEAA), Egypt

Received April 7, 2019; Revised May 19, 2019; Accepted May 24, 2019

Abstract

This work aims to document morphological and anatomical features of *Silene* L. taxa in Saint Catherine protectorate as well as their distribution. Five *Silene* taxa are investigated representing 17% of all Egyptian *Silene*; three of these taxa are endemic. Investigated taxa grow in 5 microhabitats (slope, gorges terraces, farsh (basin) and wadis) either alone or associated with other species. The total populations of three *Silene* taxa (*S. odontopetala* Fenzl subsp. *congesta* Boiss, *S. leucophylla* Boiss, and *S. oreosinaica* Chowdhuri; the latter two are endemics) were represented by a low number of individuals (60−140) and are threatened by abiotic and biotic risks which may lead to their extinction.

Keywords: Anatomy, Endemic, Morphological characters, *Silene***,** Sinai.

1. Introduction

Saint Catherine Protectorate (SKP) extends over virtually the entire mountain massif of southern Sinai, with an area of about 4350 km². and lies between 33° 55′ to 34° 30′E and 28° 30′ to 28° 35′N (Moustafa and Klopatek 1995). The diversity of both land-forms and geologic structures of Saint Catherine protectorate leads to the differentiation of a number of microhabitats, each of which has its peculiar environmental conditions and unique flora which is rich in medicinal, rare and endemic plants. Six landforms (microhabitats) types can be recognized viz. wadis, terraces, slopes, gorges, farsh (basin) and caves (Khedr 2007). Environmental conditions and human impact such as over collection, over grazing, and feral donkeys have a significant influence on diversity and distribution of the threatened endemic and medicinal plants (Abd El-Wahab *et al.* 2004; Assi 2007 ; Omar *et al* 2015).

Caryophyllaceae includes about 100 genera (3000 species) distributed mainly in the Mediterranean and Irano-Turanean areas (Hernández-Ledesma *et al*. 2015). According to (Bittrich 1993), three subfamilies were recognized: -Viz.: Alsinoideae –Burnett., Caryophylloideae. Arn. and Paronychioideae -A.St.Hil.ex Fenzl Caryophylloideae was classified by Bittrich (l.c.) into three tribes, i.e. Caryophylleae, Drypideae and Sileneae.

The genus *Silene* comprises about 700 species (Boshra and Farhad 2014) distributed mainly in north temperate regions and especially in the Mediterranean and West Asia and also found in Tropical and South Africa (Abdul Ghafoor 1978); the Mediterranean region hosts the majority of the *Silene* taxa (Oxelman *et al*. 1997).

In the flora of Egypt *Silene* is represented by 29 taxa including 2 subspecies, and 11 varieties (Boulos, 1999 ; 2009) distributed all over the country especially in Sinai which hosts 19 taxa, among them seven taxa hosts in Saint Catherine protectorate (about 25% of the Egyptian *Silene* spp.) viz. *S. arabica* Boiss. *S. linearis* Decne. *S. odontopetala* Fenzl subsp. *congesta* Boiss., *S. villosa* Forssk ., *S. leucophylla* Boiss., *S. schimperiana* Boiss. and *S. oreosinaica* Chowdhuri. The last three are endemic (Radford 2011; Ghaly 2015).

The aims of the present study are: (1) to provide detailed morphological characters of five studied taxa based on field observation, (2) to provide an account about twelve anatomical characteristics of the studied taxa, and (3) to give ecological notes about *Silene* taxa from Saint Catherine protectorate

2. Material and Methods

2.1. Data collection (morphological and ecological data)

Eighty-five quadrates (5 × 5 m) were surveyed in the period from October-2015−August-2016. Morphological characters were studied and the parameter measured from freshly collected specimens; 20 plants per taxa were examined as well as herbarium specimen kept in Cairo University "CAI" and Saint Catherine protectorate "SKPH" herbaria. The morphological terminology follows Stearn (1973). Microhabitats, number of individuals, taxa frequency, density, cover and abundance were also annotated. The threats were determined depending on filed observation; we recorded any sign that may be a threat to the target species in each quadrate (Table 1). Identification and distribution in Egypt is based on Täckholm (1974) and

* Corresponding author e-mail: samirabei@du.edu.eg.

Boulos (1999). Nomenclature, accepted name as well as synonyms, were verified using International Plant Names Index (IPNI) http://www.ipni.org/ipni/plantnamesearch page.do .

Herbarium specimens were deposited in the Department of Botany and microbiology, Faculty of Science, Herbarium, Damietta University as well as in the herbarium of Saint Catherine Protectorate (SKPH). The distribution maps were prepared using ArcGIS ver. 10.2. and Cluster analysis using past software version 3.11. https://folk.uio.no/ohammer/past/Past.

2.2. Anatomy

The sections were taken from a fresh leaf and third internode and prepared according to Johansen (1940). Staining was carried out using the safranin and fast green according to Sass (1958). The samples were examined and photographed by using XSZ-N107 research microscope fitted with premiere MA88-900 digital camera.

3. Results and Discussion

3.1. Systematic treatment

Key of investigated taxa

1 Flowers solitary .. ……*S. schimperiana*

1 Flowers not as above……2

2a Calyx oblong-cylindrical, Petals purple to whitish violet. Basel leaves ovate to spathaulate, 0.6−3 × 0.1−0.8 cm. arranged in rosette shape, olive color; *S. leucophylla*

2b Calyx tubular, Petals white, leaves linear 1 -2 x 0.1-0.2cm…… *S. linearis*

2c Calyx sub sessile, campanulate; nerved with violet nerve, Inflorescence dichasium cyme, congest, (Capitate), Petals pale violet (pink). Basel leaves oblanceolate 1-4.6 x 0.3 - 0.8 cm ……*S. odontopetala* subsp. *Congesta*

2d Calyx tubular, nerved with yellow nerve, hairy. Petals white with very pale pink edges. Basal leaves lanceeolate, 0.4- 4.5cm. x0.1 - 0.9cm arranged in rosette shape;

……*S.oreosinaica*

Silene schimperiana Boiss. Diagn. Pl. Orient. ser. 1, 1:31 (1942); Boiss., Fl. Orient. 1:641 (1867); Dinsmore in Post & Dinsmore, Fl. Syria ed. 2, 1:187 (1932); Täckh., Stud. F1. Egypt ed. 1:390 (1956); Hassib & Montasir, Man. Fl. Egypt 1:94 (1957); Täckh., Stud. Fl. Egypt ed. 2: 86 (1974); Hosny *et al*, Taecholomia, 14:13 (1992); Boulos, Fl. Egypt 1:62 (1999); Hosny in El Hadidy, Fl. Aegyptiaca, 1(2):129 (2000); Boulos, Fl. Egypt checklist: 36 (2009).

Type: In rupibus Jugi Sinaitici Arabiae loco Bostan dicto; *Schimper* 422.

Perennial, with woody structure at the base, up to 120 cm. long. Stem cylindrical with swollen nodes, glabrous, internode 2-6 cm. long. Basal leaves linear to spathulate 1.4-8.x0.2 0.5cm. with acute apex, entire margin, symmetrical base, petiolate, blue green in color, arranged in rosette shape. Cauline leaves linear to spathulate, opposite decussate, with acute apex, entire margin, symmetrical base. Flowers solitary. Calyx oblong-cylindrical 2-2.7 cm. long, 10 nerved, glabrous, 5 united sepals. calyx teeth, triangular with acute apex 2 – 3 mm. long, calyx facing sun nerved by violet color (field observation). Petals five white in the upper side and yellowish in the back side, sometimes with violet nerves, 3.5 - 5.2 cm. long (with claw length 1.5 - 2.7 cm and limp 2 -2.7 cm.). Fruit oblong capsule 2.8 cm in length. (Figure 3E, 4 E and table 1).

Flowering and fruiting times: Flowering time March – May; fruiting time July−August.

Habitat: Slope, terraces, gorges, and farsh.

Distribution in Egypt: Rare, endemic, confined to southern Sinai.

Representative specimens: South Sinai, July 1943, Hassib *et al*. s.n. (CAI); South Sinai, Step-way to Gebel Musa; 11 May 1956; Täckholm s.n. (CAI); South Sinai, Wadi Talaa, 8. Oct.1983, Hadidi *et al*. s.n. (CAI); South Sinai, SKP, Wadi Gebal region, Al shaq, 9-April-2004, Fayed *et al*, s.n (SKPH); South Sinai, SKP, El Geragenia ,22-Dec-2015, El Gamal, s.n., (Demitta university, faculty of Science herbarium); South Sinai, SKP., Gabal El Dair, 21-5-2016, El Gamal, s.n., (SKPH).

Silene leucophylla Boiss., Diagn. P1. Orient. 1.1:29 (1842); Boiss., Fl. Orient., 1:634 (1867); Täckh., Stud. Fl. Egypt, ed. 1:390 (1956); Hassib & Montasir, Man. Fl. Egypt 1:94 (1957); Täckh., Stud. Fl. Egypt ed. 2:85 (1974). Hosny *et al*., Taecholomia, 14: 11 (1992); Boulos, Fl. Egypt, 1:61 (1999); Hosny in El Hadidy, Fl. Aegyptiaca 1, 1(2): 130 (2000); Boulos, Fl. Egypt checklist: 36 (2009).

Type: SINAI: *In rupibus et praeruptis umbrosis montis St. Catharinae*, 28 May et 6 June, 1835, *Schimper* 297, 351 (HBG holotype).

Perennial, with woody structure at the base up to 30 cm long. Stem, erect, hairy, cylindrical, internode length 2−5 cm. Basal leaves ovate to spathaulate, rarely orbicular 0.6−3 × 0.1−0.8 cm arranged in rosette shape; petiolate, petiole 0.4−3 cm. long, olive color, with acute apex and entire margins. Cauline leaves ovate to spathaulate 0.3−1.2 × 0.1−0.5 cm. opposite decussate, petiolate, with acute apex and entire margins. Inflorescence cymose; with 3-9 flowers, pedicelled; Pedicel length 0.4−0.7 cm. calyx oblong-cylindrical, 1.2-1.9 x 0.1-0.3cm., 10 nerved, hairy, calyx teeth triangular *c*.3mm.long. Petals 5 purple to whitish violet to violet, 2.8−5.5 cm long (with claw length 0.5−0.7 cm and limb 2−2.3 cm. long). Fruit oblong ovoid capsule 1.9 cm. long (Figure 3A, 4A and table 1).

Flowering and fruiting times: Flowering time March−April, fruiting- time July−September.

Habitat: Slopes, terraces and gorges (rocky crevices).

Distribution in Egypt: Rare, endemic confined to Saint Catherine protectorate (South Sinai).

Representative specimens: : On the step-way to Gebel Musa, 11 May 1956, Täckholm s.n. (CAI); Wadi Gebal region, Al Shaq, 13-May-2004, Fayed *et al*. s.n. (SKP H);Shaq Mousa, 22-May-2016, El Gamal, s.n. (SKPH & Damiatta University Herbarium); El Geragenia, 22-December-2015, El Gamal, s.n. (SKPH); El Gabal El Ahmar, 26-May-2016 El Gamal, s.n. (CAI & SKPH).

Silene linearis Decne. Fl. Sinaica, ser. 3, 2:376 (1835); Boiss., Fl. Orient., 1:602 (1867); Aschers, & Schweinf., Fl. Egypte 2:47 (1887); Sickenb., Mem. Inst., Egypt. 4, 2:185 (1901); Muschl., Man., Fl. Egypt 1:339 (1912); Ramis, Best.-Tabel l. Fl.

Aegypt.: 76 (1929); Täckh., Stud.Fl. Egypt, ed. 1:392 (1956); Hassib & Montasir, Man. Fl.Egypt. 1:95 (1957); Täckh., Stud. Fl. Egypt ed.2:86 (1974); Hosny *et al*., Taecholomia, 14:19 (1992); Boulos, Fl. Egypt 1:64 (1999); Hosny in El-Hadidy Fl. Aegyptiaca,1(2): 122 (2000); Boulos, Fl. Egypt checklist :37 (2009).

Type: Le desert du Sinai; Bové 178 (P, holotype).

=*Silene arenosa* K. Koch, in Linnaea 23, 6:712 (1851).

Annual or Short perennial herb, erect, up to 90 cm long. Stem, glabrous, cylindrical, branching from the base, internodes 1.8-5cm.long. Basal leaf linear 1 -2 x 0.1-0.2cm., with acute apex, entire margin, sessile, symmetrical base and hairy. Cauline leaves linear (0.5-1.2. x 0.1cm), opposite decussate with acute apex, entire margin, sessile and hairy. Inflorescence cymes. Calyx tubular, 10 nerved; 1-2cm.long, with short triangle to linear teeth. Petals five, white in color, 1-1.5 cm. long (with claw 0.4 -0.6 cm. long and limb 0.6-0.9 cm. long. Fruit cylindrical capsule. (Figure 3 B, 4 B and table 1).

Flower ing and fruiting times: Flowering time March - May, fruiting time July−August.

Habitat: Slope, gorges and terrace.

Distribution in Egypt: Eastern desert, Red coastal strip, Sinai.

Representative specimens Sinai : El Raha plain, 13.May.1956, Hadidi, s.n. (CAI) ; Wadi Feiran, 21Aug.1982,Hadidi *et al*., s.n. (CAI); Wadi El Ghadir,, 4.Feb.1961, Täckholm *et al*., s.n. (CAI); South Sinaï ,Wadi Thamman, 9-April-2004, Fayed *et al*., s.n (SKPH); Wadi Al–Arbaa'en SKP, 2-May-2004, Shaltout *et al*., s.n (SKPH); Wadi Ferian, SKP, 7-May-2004 Shaltout *et al*., s.n. (SKPH). South Sinai Wadi El Fara`a, 6-May-2004, Shaltout *et al*., s.n. (SKPH); South Sinai, Gabal El Dair, 4-Feb-2016 El -Gamal s.n. (SKPH).

Silene odontopetala Fenzl subsp. *congesta* Boiss.

Silene odontopetala Fenzl var. *congesta* Boiss. Fl. Orient. 1:626 (1867); Täckh., Stud. Fl. Egypt ed., 1:389(1956); Hassib & Montasir, Man. F1. Egypt, 1:93 (1957); Täckh., Stud. Fl. Egypt ed. 2:85 (1974); Hosny *et al*,Taecholomia, 14:13 (1992) ; Boulos, Fl. Egypt 1:61 (1999); Hosny in El Hadidy, Fl. Aegyptiaca, 1(2):131 (2000); Boulos, Fl. Egypt Checklist :36 (2009).

Type: In -monte Sinaico St Catherinae; *Schimper* 296 (G, –holotype)

syn. S.-sinaica Boiss., Diagn. p1. Orient. ser. 1,1:25 (1843);

Perennial, with woody structure at the base, 20-25 cm .long. Stem hairy, erect or ascending, internode 2 - 6 cm. long. Basal leaves oblanceolate 1-4.6 x 0.3 - 0.8 cm. with acute apex, entire margin, symmetrical base, petiolate. Cauline leaves oblanceolate 0.5-1.2. x 0.2 - x 0.4cm opposite decussate, acute, entire, symmetrical. Inflorescence dichasium cyme, congest, (capitate). Calyx sub sessile, campanulate *C.*0.9 cm. long, broad, hairy, pedicel 0.2 - 0.5 cm. long, 10 nerved. Bract ovate, 0.4 - 0.8 cm. long usually with medial violet nerve, Petals five white or pink *c.*1.3 cm. long (with claw length 0.4 -0.5 cm. long and limp 0.9 cm. long). Fruit ovate capsule0.4 - 0.8 cm. long. (Figure 3 C, 4 C and table 1).

Flowering and fruiting times: Flowering time March - May, fruiting time July−September

Habitat: Slops, (Rocky crevices).

Distribution in Egypt: Rare, confined to southern Sinai.

Representative specimens: South Sinai, Abo Mahsour, 23-May-2016, El Gamal, s.n. (Damietta university herbarium & SKPH). South Sinai: AboMahsour, South Sinai: El Gabal el Ahmar, 26-May-2016, El Gamal,s.n. (CAI, SKPH)

Silene oreosinaica Chowdhuri .Not. Roy. But. Gard. Edinb. 22:269 (1957); Hosny *et al*., Taecholomia, 14:15 (1992); Boulos, Fl. Egypt 1:62 (1999); Hosny in El Hadidy Fl. Aegyptiaca, 1(2):131 (2000); Boulos, Fl. Egypt checklist :36 (2009); Rabei *et al* (2016) Scientific Journal for Damietta Faculty of Science 6 (1) 2016.

Type: Sinai, in Rupium fissuris montis St. Catharinae; *Schimper* 352 (1835); (K, holotype).

Perennial, with woody structure at the base up to 25 cm. long. Stem, hairy, cylindrical; internode up to 5 cm. long. Basal leaves lanceeolate, 0.4- 4.5. x0.1 - 0.9 cm. arranged in rosette shape with acute apex, entire margins, symmetrical base and sessile. Cauline leaves lanceeolate, smaller than basal leaves 0.4-2.5 x0.1 - 0. 2 cm, opposite decussate with acute apex, entire margin, symmetrical base and sessile, Inflorescence racemes, pedicle; Pedicel length 0.5 cm. long. Calyx tubular 0.8 -1.2 cm. long, 10 nerved with yellow nerve, hairy. Bract lanceolate. Petals 5 white in color with very pale pink edges 1.1- 1.9 cm. long (claw 0.4 -0.6 cm. long and limp 0.7-1.2 cm. long). Petals that exposed to the sun are converted to rose color (field observation). Fruit ovoid cylindrical Capsule, 0.8 -1.2 cm. long. (Figure 3D,4 D and table 1).

Flowering and fruiting times: Flowering time during spring months usually March – May; rarely during December and January fruiting time July−October.

Habitat: Slops, (Rocky crevices).

Distribution in Egypt: Rare, endemic confined to Saint Catherine protectorate(southern Sinai).

Representative specimens: South Sinai: wadi Feiran, 21.Aug. 1982, Hadidi *et al*. s. n. (CAI); South Sinai: Gebel Catherine, Ein Shinar, 9.Oct. 1983, Hosny s.n. (CAI); South Sinai: SKP, Shaq Mousa ,7-Jan-2016 El Gamal, s.n. (SKPH); South Sinai: SKP ,Shaq Mousa, 25-March-2016, El Gamal, s.n. (CAI & SKPH); South Sinai: SKP ,Om Mesla, 22-May-2016, El Gamal,s.n. (SKPH); South Sinai: SKP, Om Mesla ,20-Jun-2016, El Gamal, s.n. (Damietta university faculty of Science herbarium).

3.2. Anatomical characters (Figures 5A−E and table 3)

The transverse section of the stem revealed that it is circular, solid stem, in all studied taxa; the epidermis consisting of single layer of rectangular-oval cells in *S. leucophylla*, *S. linearis*, *S. oreosinaica* while consisting of single layer of rectangular cells in both *S. odontopetala* subsp. *Congesta* and *S.schimperiana* . Anisocytic and Diacytic stomata are present in *S. odontopetala* and *S.schimperiana* respectively. Druses are consecrated in both cortex and pith for all studied species except *S. oreosinaica* observed in cortex only, raphides observed only in *S. schimperiana*.

The transverse section of the lamina and epidermal surfaces revealed that leaves of the studied taxa were dorsiventral; thick walled parenchyma is present in all

taxa except in *S. schimperiana;* only *S. linearis* displays leaves with sclerenchyma patches. Druses are present in all studied taxa. Raphides were present in *S. leucophylla*, and *S. odontopetala* subsp. *congesta* and absent in the other taxa. Oil globules were present only in *S. schimperiana*. Stomata type is anisocytic in *S. leucophylla, S. odontopetala* subsp. *congesta* and *S. oreosinaica*, while it is diacytic in two species viz. *S. linearis* and *S. schimperiana*. Our present results are in agreement with Metcalfe and Chalk (1950) who reported that in general, the stomata are diacytic, i.e. Caryophyllacous type, but with some exceptions where stomata are anisocytic and calcium oxalate crystals are commonly found in *Diathus* and *Silene.*

Cluster analysis of the anatomical characters of five *Silene* taxa identified two main clades: the first one included *S. odontopetalia* and *S. oerosinica* with sub clade included *S. leucophylla* and the second one included *S. lineares* and *S. schimperina.* (Figure 6). Stomata type; stem epidermis, raphides, oil globules are significant characters to separate studied taxa from each other.

3.3. Ecological notes

According to Khedr (2007), six microhabitats can be recognized in Saint Catherine protectorate: wadi bed, Terraces, slopes, gorges, Farsh and caves. Investigated *Silene* taxa are distributed in five out of these six habitats, i.e. slope, gorge, terraces, farsh (Basin) and wadis. *S. schimperiana* is recorded in five microhabitats with high number of individuals, and density. The average frequency in three microhabitats are slope, gorges terraces was 34.12% and 47.06% for *S. linearis S.* and *S. leucophylla* respectively, density 0.07 for both species, while the covering was 1.40/2.65 and abundance 3.50/5.17 respectively for *S. leucophylla*, and *S. linearis*, while *S. odontopetala* and *S. oreosinaica* were recorded only in the slope microhabitat with frequency 15.29/12.94% respectively, density of 0.03 for both taxa, cover of 0.47/0.71 respectively and abundance of 4.62/5.73 respectively.

In eco-geographical terms, *Silene oreosinaica* is restricted in two sites, *S. odontopetala* subsp. *congesta* is recorded in three sites, while *S. schimperiana, S. leucophylla* and *S. linearis* are widely distributed in Saint Catherine protectorate Figure 2 A-D and table 3).

The studied taxa grow either alone or associated with other species. The most common associates are *Chiliadenus montanus* (Vahl) Brullo, *Stachys aegyptiaca* Pers. *Centaurea scoparia* Sieber ex Spreng., *Seriphidium herba-alba* (Asso) Soják *Scrophularia libanotica* Boiss., and *Galium sinaicum* (Delile ex Decne) Boiss.

The population size of the studied *Silene* species is critically for *S. odontopetala* subsp. *congesta*, *S. leucophylla*, and *S. oreosinaica* (the last two are endemic) with total number of individuals in all studied area ranging between 60 and 140.

S. odontopetala subsp.congesta and *S. oreosinaica* are restricted to high altitude localities (2055−2313m a.s.l.), while *S. leucophylla* and S. *linearis* recorded at 1770−2226 m a.s.l., and *S. schimperiana* at 1328−2318 m a.s.l.

The threat of genetic erosion of *Silene* is a result of abiotic effect such as scarcity of water, or biotic factors like the effect of overgrazing by domestic and wild animals, especially flowering parts overgrazing. Therefore, it could lead to the extinction of the endemic species from Egypt; the result obtained is in agreement with previous studies like Assi (2007), Omar *et al* (2015; 2017) and Ghaly (2015).

Figure 1. Showing SKP microhabitats A= wadi B= Terraces, C=Slope, D=George, E= Farsh (basin) and F= cave

Table 1. Morphological characters of *Silene* species

Character	*S. leucophyla*	*S. lineares*	*S. odontopetalia*	*S. oerosinica*	*S. schimperina*
longevity perennial	1	1	1	1	1
Height up to (cm.)	30	70	25	25	140
Stem ascending	0	0	1	1	0
Stem erect	1	1	1	1	1
Lanceolate basal leaves (B.L)	0	0	0	1	0
Linear(B.L)	0	1	0	0	1
Oblanceolate (B.L)	0	0	1	0	0
Ovate (B.L)	1	0	0	0	0
Spatulate (B.L).	1	0	0	0	1
Orbicular (B.L)	1	0	0	0	0
Basal leaf length (cm.)	3	2	4.6	4.5	8
Basal leaf width (cm.)	0.8	0.2	0.8	0.9	0.5
Lanceolate Cauline leaves (C.L)	0	0	0	1	0
Linear (C.L)	0	1	0	0	1
Oblanceolate (C.L)	0	0	1	0	0
Ovate (C.L)	1	0	0	0	0
Spatulate (C.L).	1	0	0	0	1
white petal	0	0	1	1	1
pink petal	0	0	1	1	0
violet petal	1	0	0	0	0
yellowish petal	0	1	0	0	0
leaf blade (entire)	1	1	1	1	1
Capsule: length (cm.)	1.9	2	0.4	1	2.8
Solitary flowers	0	0	0	0	1
cymes Inflorescence	1	1	1	0	0
racemes Inflorescence	0	0	0	1	0
Ave. diameter (cm)	11.3	15	10	12	25
Leaf length (cm)	0.4 – 2	1-2	1-4.6	1 -4.5	1.4-8
Leaf width(cm)	0.1 - 0.6	0.1-0.2	0.3-0.8	0.3-0.9	0.3-0.5
petiole length(cm)	0.4 -3	0	0	0	0
#flowers/ inflorescence	3-9	4	5 flowers in capitate	6	Solitary

Table 2. Anatomical characters of five *Silene* taxa.

Character	*S. leucophyla*	*S. lineares*	*S. odontopetalia*	*S. oerosinica*	*S. schimperina*
Stem shape	1	1	1	1	1
cortex (thick walled)	0	1	1	1	0
no. vascular bands	10	14	13	8	7
Druses in cortex	1	1	1	1	1
Druses in pith	1	1	1	0	1
Raphides in stem	0	0	0	0	1
Stomata in stem	0	0	1	0	1
leaf thick walled	1	1	1	1	0
Sclerenchyma patches	0	1	0	0	0
Leaf druses	1	0	0	0	0
Raphides in leaf	1	0	0	0	0
Prismatic crystals	1	0	0	0	0
Rounded mid rib	1	1	0	0	1
Semi-rounded mid rib	0	0	1	1	0
Anisocytic stomata	1	0	1	1	0
Diacytic stomata	0	1	0	0	1

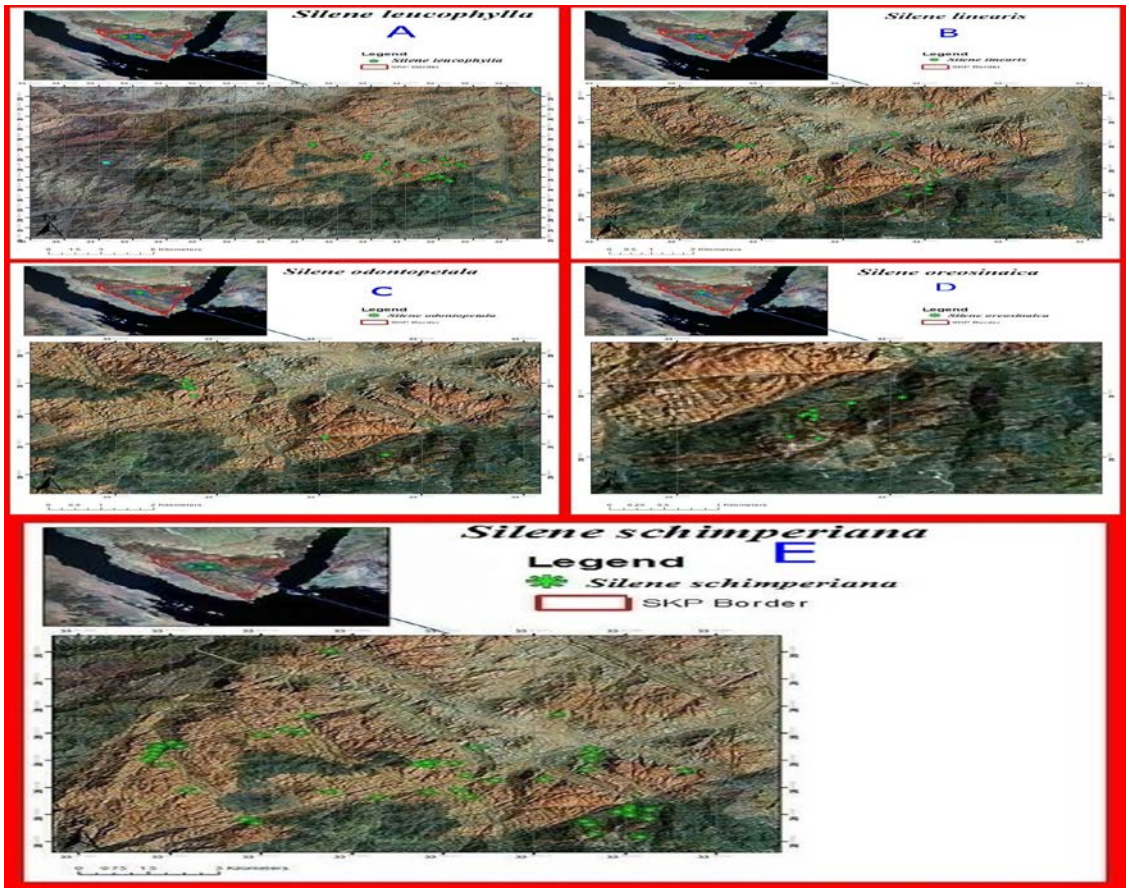

Figure 2. *Silene* distribution maps, A= *S. leucophylla*, B= *S. linearis*, C= *S. odontopetala*, D= *S. oreosinaica* and E= *S. schimperiana*

Table 3. Ecological notes of *Silene* taxa

	Silene taxa				
Parameter	*S.leucophylla*	*S. linearis*	*S. odontopetala*	*S. oreosinaica*	*S. schimperiana*
Frequency (%)	47.06	34.12	15.29	12.94	69.41
Abundance	3.50	5.17	4.62	5.73	12.00
Density	0.07	0.07	0.03	0.03	0.33
Cover %	1.40	2.65	0.47	0.71	34.74
Microhabitat	Slope, gorges terraces. in all aspect except flat	Slope, gorges, terraces in all aspect except flat	Slop in north aspect	Slop in north aspect	Slope, terraces, gorges, farsh, wadi. in all aspect
Elevation (m a.s.l)	1770 - 2226	1772 - 2170	2106 -2313	2055 - 2310	1328 - 2318
Global Distribution	Endemic to SKP	Egypt, Palestine, Saudi Arabia	Egypt and Iran	Endemic to SKP	Endemic to SKP
SKP Distribution	El faraa, Shq mousa, Abu gifa, El Zawateen, El mealq, Abu Groose,. El Fara'a, Abu Walee, El Qalab, El Talaa ,El Gragenia ,Wadi Telah ,Farsh Shobie, Farsh el Safsafa, Earsh elia, Gabel katerina ,El gabal el Amher, Wadi el Shak and El Mathar	Wadi El arbeen, El faraa ,Shq mousa, Abu mahshoue ,Ab uo groose ,Gabal El Dair, El Gabal el Amher ,Wadi el Shak Shreg ,El Mathar, El Meserdy and El Galat El Azrak	Restricted in 3 sites farsh abu mhasour region, el Gabal el Ahmer and Om Meslla region.	Recorded in two sites shak mousa (maeen shinera) and Om Meslla in Gabal Katerina region.	Wadi El arbeen ,El faraa ,Shq mousa, Abu Gifa, El Zawateen, El Mealq, Abu Mahshoue ,W. El Fara'a ,El Qalab, El Talaa El Gragenia, Rehibe nada, Shq telaha, Gabel katerina ,El Gabal El Amher ,Shreg ,El Shikh Awad ,Wadi El Shak,El meserdy El Galat El Azrak
Associated species	Mostly solitary or associated with one or more of *Pterocephalus sanctus. Diplotaxis harra. Chiliadenus montanus, Galium*	*Chiliadenus montanus, Stachys aegyptiaca, Centaurea scoparia, Seriphidium herba-alba,*	Mostly solitary or associated with *Scrophularia libanotica and /or Galium sinaicum*	Mostly solitary or associated with *Scrophularia libanotica, and Tanacetum sinaicum.*	*Achillea fragrantissima. Alkana orientalis. Anarrhinum pubescens, Bufonia multiceps, Chiliadenus montanus, Cotoneaster orbicularis Crataegus sinaica, Deverra triradiata,*

	sinaicum Arenaria deflexa, Polygala sinaica, Phagnalon nitidum. Stachys aegyptiaca, Tanacetum sinaicum.	*Arenaria deflexa. Gypsophila capillaris, Nepeta eptemcrenata, Silene schimperiana, Teucrium leucocladum Phlomis aurea.*	*Echinops glaberrimus, Fagonia Arabica, Ficus palmate, Matthiola longipetala, Papaver decaisnei, Plantago sinaica, Pterocephalus sanctus, Seriphidium herba-album, Stachys aegyptiaca, Nepeta septemcrenata, Tanacetum sinaicum, Phlomis aurea, Origanum syriacum, Kickxia acerbiana, Teucrium polium, Thymus decussatus, Gypsophila capillaris, Silene.linearis, Verbascum sinaiticum*
Threats	The threat of genetic Silene is a result of abiotic effect such as scarcity of water, or biotic one like effect of grazing by domestic and wild animal.		

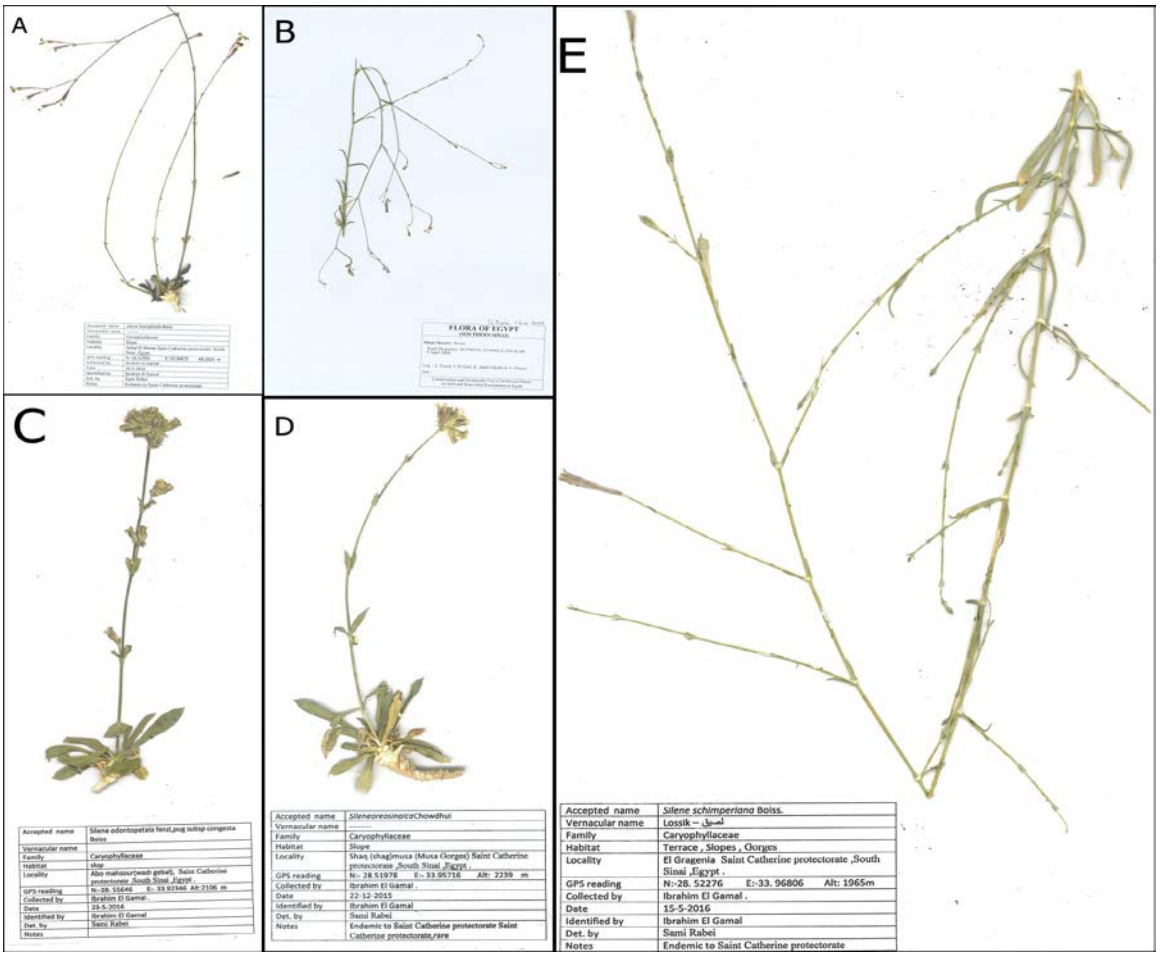

Figure 3. *Silene* herbarium specimen, A= *S. leucophylla*, B= *S. linearis*, C= *S. odontopetala*, D= *S. oreosinaica* and E= *S. schimperiana*

Figure 4. Photos of A= S. leucophylla. B= S. linearis, C= S. odontopetala, D= S. oreosinaica and E= S. schimperiana

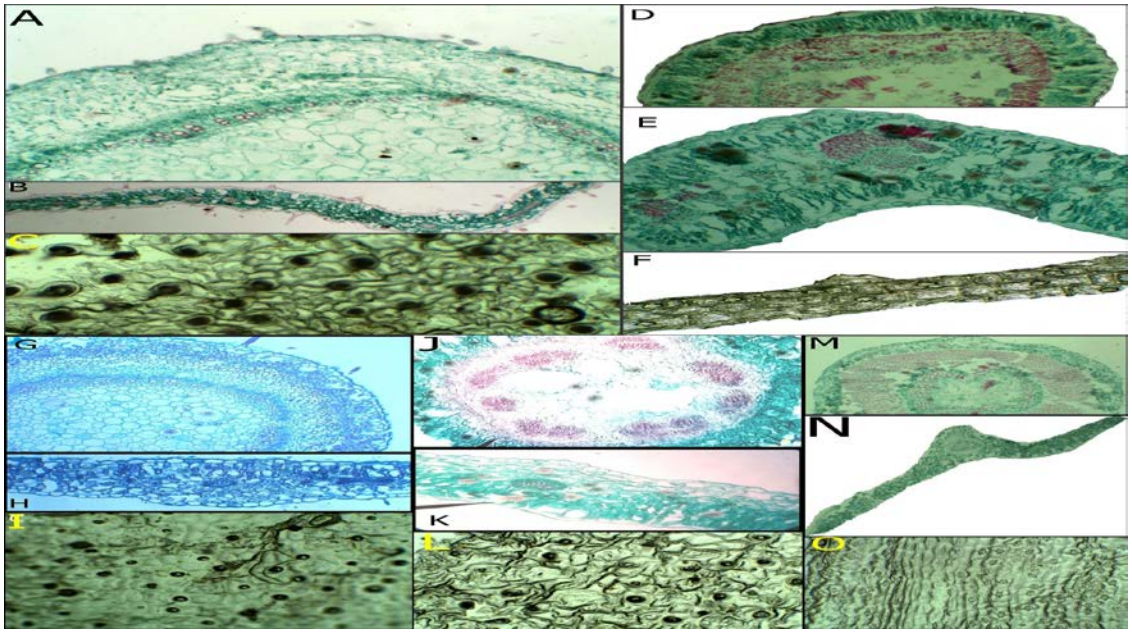

Figure 5. A, B and C showing *S. leucophylla* stem, leaf T.S and epidermal cells. D,E and F showing *S. linearis* stem ,leaf T.S and epidermal cells, G, H and I showing *S. odontopetala subsp. congesta* stem ,leaf T.S and epidermal cells, J,K and L showing *S. oreosinaica* stem ,leaf T.S and epidermal cells M,N and O showing *S. Schimperiana* stem, leaf T.S and epidermal cells

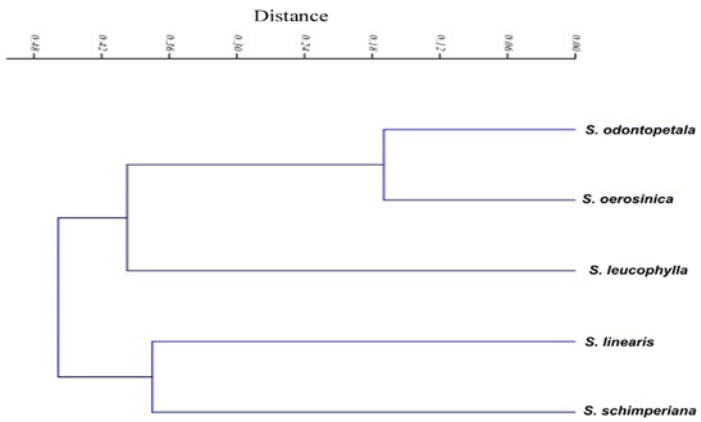

Figure 6. Dendogram showing the relationship among *Silene* taxa

4. Conclusion

Field observations revealed that *Silene* populations of the investigated taxa have restricted population, no new seedling, and low seed fitting. Additional reasons include scarcity of water, overgrazing (especially flowering parts) by domestic and wild animals as well as over collection for scientific research.

Therefore, these factors could cause the extinction of the endemic species from Egypt. A scientific program aiming at controlling the continuous destruction of *Silene* taxa in Saint Catherine Protectorate by in-situ conservation (restoration and rehabilitation program) and ex-situ conservation (seed preservation in seed bank, more control on plant collection for different purposes e.g. collection for scientific purposes and as green fodder) of these taxa is urgently needed.

References

Abd El-Wahab R, Zaghloul M and Mosustafa A. 2004. Conservation of medicinal plants in Saint Katherine protectorate, South Sinai, Egypt. Evaluation of ecological status and human impact. Proceeding of First Inter Conference on Strategy of Egyptian Herbaria, Giza, Egypt.

Abdul Ghafoor,. 1978. **Caryophyllaceae,** 59. In: Jafri SMH and El-Gadi A (Eds), ***Flora of Libya.*** Al Fateh University, Tripoli.

Assi R. 2007 .Medicinal plants Threat Analysis and Threat Reduction Assessment Report. Conservation and Sustainable Use of Medicinal Plants in Arid and Semi-arid Eco-systems Project, Egypt, Final Report (GEF and UNDP) (Project No: 12347/12348) 62p.

Bittrich V. 1993. **Caryophyllaceae Juss**. *In*: Kubitzki K., Rohwer, J. and Bittrich, V. (eds.), **The Families and Genera of Vascular Plants**, Magnoliid, Hamamelid and Caryophyllid Families, vol. 2. Springer Verlag, Berlin, pp. 223.

Boshra A, Farhad A. 2014. Chemical composition of volatile oil from *Silene avromana* .Boiss. and Haussk http://www.bio.uaic.ro/publicatii/anale_vegetala/anale_veg_index.html ISSN: 1223-6578, E-ISSN: 2247-271

Boulos L .2009. **Flora of Egypt Checklist,** Revised Annotated Edition. Al-Hadara Publishing, Cairo.

Boulos L .1999. **Flora of Egypt.** vol 1**.** Al-Hadara Publishing, Cairo.

Ghaly O. 2015 .Taxonomical and Molecular Characterization of Endemic Species at Saint Katherine Protectorate- Sinai- Egypt. PhD dissertation. Mansoura University.

Hernández-Ledesma P, Berendsohn W G, Borsch T, von Mering S, Akhani H, Arias S, Castañeda-Noa I, Eggli U, Eriksson R, Flores-Olvera H, Fuentes-Bazán S, Kadereit G, Klak C, Korotkova N, Nyffeler R, Ocampo G, Ochoterena H, Oxelman B, Rabeler R K, Sanchez A, Schlumpberger B O, Uotila P. 2015. A taxonomic backbone for the global synthesis of species diversity in the angiosperm order Caryophyllales. *Willdenowia* **45:** 281–383**.**

Johansen D A .1940. **Plant Microtechnique**. McGraw-Hill Book co., New York.

Khedr A. 2007. Assessment, classification, and analysis of microhabitats supporting globally significant plant species of Saint Katherine's Protectorate: In: Conservation and Sustainable Use of Medicinal Plants in Arid and Semi-arid Eco-systems Project, Egypt, Final Report (GEF and UNDP) (Project No: 12347/12348). Unpublished report 37p.

Metcalfe C R and Chalk L. 1950. **Anatomy of the Dicotyledons**. Oxford at the Clarendon Press. UK. **1.** 147-152.

Moustafa A and Klopatek J .1995. Vegetation and landforms of the Saint Katherine area, Southern Sinai, Egypt. *J. Arid Environ*. **30,** 385–395**.**

Omar K. 2017. Community based conservation of threatened plants *Silene schimperiana* and *Polygala sinaica* in South Sinai, Egypt. *www.Rufford.org*

Omar, K., Mohammed, A.A., Nagi, A., Elgamal, I., Elmarakby, A., Shalouf, A., Elasayed, A., Mehana, S. (2015): Conservation Challenges inside Protected Areas of Egypt - Part II – St. Katherine Protectorate: Conservation Status Assessment of some threatened plant species. Report to Nature Conservation Sector, Ministry of Environment - Strengthening Protected Area Financing.

Oxelman B, Liden M, Berglund D. 1997. Chloroplast rps16 intron phylogeny of the tribe Sileneae (Caryophyllaceae) *Plant Syst Evol***., 206**:393-394

Radford E A, Catullo G, Montmollin B.de. (Eds.). 2011. **Important Plant Areas of the South and East Mediterranean Region:** priority sites for conservation. IUCN, Switzerland Malaga, Spain: IUCN. **VIII** + **108** p. Spain.

Sass J. E. 1958. **Botanical Microtechnique**. 3nd Ed. The Iowa state college press, Ames. s

Stearn W T. 1973. **Botanical Latin**. Newton Abbott: David and Charles.

Täckholm, V. 1974 .**Students' Flora of Egypt** (2nd Ed.). Cairo University.

JJBS

Volume 13, Number 1,June 2020
ISSN 1995-6673
Pages 69 - 76

Jordan Journal of Biological Sciences

Antibacterial and Antibiofilm activities of Malaysian *Trigona* honey against *Pseudomonas aeruginosa* ATCC 10145 and *Streptococcus pyogenes* ATCC 19615

Mohammad A. Al-kafaween, Abu Bakar M. Hilmi*, Norzawani Jaffar, Hamid A. N. Al-Jamal, Mohd K. Zahri and Fatima I. Jibril

Faculty of Health Sciences, Universiti Sultan Zainal Abidin, Terengganu, Malaysia.

Received May 10, 2019; Revised May 20, 2019; Accepted May 28, 2019

Abstract

This study aimed to investigate the antibacterial and antibiofilm activities of *Trigona* honey against *Pseudomonas aeruginosa* and *Streptococcus pyogenes*. The antimicrobial and anti-biofilm activities were examined by agar well diffusion assays, minimum inhibitory concentration (MIC), minimum bactericidal concentration (MBC), time-kill curve, biofilm formation in 96-well plates and scanning electron microscope (SEM). Larger zones of inhibition were recorded from the agar well diffusion method. *Trigona* honey samples showed clear zones of inhibitions against *P. aeruginosa* and *S. pyogenes*, 25.2±0.6mm and 26.7±1.0mm respectively. *Trigona* honey possessed the lowest MIC value against *P. aeruginosa* and *S. pyogenes* was 20% (w/v) and MBC was 25% (w/v). In addition, MIC_{50} was between 10%-12.5% (w/v) and MIC_{90} was between 20%-25% (w/v) concentration of honey for both bacteria. In time-kill curve, *Trigona* honey inhibited *P. aeruginosa* and *S. pyogenes* in a 3 $\log_{10}$ at 18 hours, and total viable counts (TVCs) were killed after 24 hours at honey concentration of 25%. In biofilm degradation assay, *Trigona* honey degraded 70% of *P. aeruginosa* and 68% of *S. pyogenes* biofilm. Also in biofilm inhibition assay, *Trigona* honey inhibited 91% of *P. aeruginosa* and 89% of *Streptococcus pyogenes* biofilms. SEM images of *P. aeruginosa* and *S. pyogenes* showed that *Trigona* honey changed shape, size of cells, destroyed cell wall integrity and lysed the cells in both bacteria. Scanning electron microscope images for biofilm of *P. aeruginosa* and *S. pyogenes* showed that *Trigona* honey decreased cell density, and cells appeared curved of *P. aeruginosa* and rough, holes and crevices of *S. pyogenes*. In sum, *Trigona* honey disrupted and damaged biofilm formation. This study demonstrated that *Trigona* honey has high antibacterial and antibiofilm activities against both bacteria *in vitro* and showed the efficacy of honey against biofilm in different degrees of potential effect. The study supports previous finding that *Trigona* honey can be used as an alternative medicine for various bacterial infections.

Keywords: *P. aeruginosa*, *S. pyogenes*, Antibacterial, Antibiofilm, *Trigona* honey, Scanning electron microscope (SEM).

1. Introduction

Antibiotics have been extensively used to prevent bacteria in modern medical treatments. The efficiency of antibiotics is highly significant; however, it leads to the emergence of antibiotic-resistant for some bacteria (Badet and Quero, 2011; Nassar *et al.,* 2011). Resistant bacteria are not easily eliminated because of evolvement in adaption model and surviving pattern against antibiotics (Lee *et al.*, 2011). Survival of bacteria in a patient could lead to persistent infection by forming bacterial biofilm. Biofilm is a type of self-produced extracellular matrix which is embedded by the bacteria to provide a protective environment for them to grow (Al-Saadi *et al.,* 2016; Jaffar *et al.,* 2016). The biofilm supplies nutrient to the bacteria and protects them from eradication by the drugs (Costerton *et al.*, 1999; Doern *et al.*, 2009).

Antimicrobial agents are important in reducing the global burden of infectious diseases. However, as resistant pathogens develop and spread, the effectiveness of the antibiotics is diminished (Levy and Marshall, 2004; Mandal *et al.,* 2009). An alternative antimicrobial agent is urgently needed, and these circumstances have led to a re-evaluation of the therapeutic use of ancient remedies such as plants and honeys (Fatima *et al.*, 2018.; 2019). The use of traditional medicine to treat infection has been practiced since the existence of mankind and is one of the oldest traditional medicine which is important for the treatment of human ailments (Boorn *et al.,* 2010). Many researchers have reported the antibacterial activity of honey with broad-spectrum activity after being tested against pathogenic bacteria, oral bacteria as well as food spoilage bacteria (Boorn *et al.,* 2010; Lusby *et al*., 2005; Mundo *et al* ., 2004; Roberts *et al.*, 2012). In most ancient cultures, honey has been used for both nutritional and medical purposes. Currently, an alternative medicine using bee based products as a treatment for human diseases, known as apitherapy, is being practiced (Alandejani *et al.*, 2009; Ng *et al.*, 2017; Shahjahan and Halim, 2007).

Stingless bees are found in tropical and subtropical regions including central and south America, Africa, Asia,

* Corresponding author e-mail: mhilmiab@unisza.edu.my, mohammadalkafaween25@yahoo.com.

and northern Australia (Guerrini *et al.*, 2009; Shahjahan and Halim, 2007). *Trigona* bee which is known as 'Kelulut' is a commercial stingless bee species abundantly found in Malaysia. This bee produces Kelulut honey, a multi floral honey which is stored in cluster of small resin dome of their nests. Kelulut honey has been reported to have excellent antibacterial properties and is useful medically and therapeutically (Fabíola *et al.*, 2014; Fabíola *et al.*, 2016; Shahjahan and Halim, 2007). Honey from stingless bees has a distinct taste and aroma, is more fluid in texture, and has low crystallization. Stingless bee honey has variable and broad-spectrum activities against many different kinds of wound and enteric bacteria (Anthimidou and Mossialos, 2013; Ramalivhana *et al.*, 2014).The removal of exudate after wounds dressing with honey was increasing healing process in inflamed wounds (Ahmed *et al.*, 2003). Honey is hygroscopic, which enables dehydrating bacteria by decreasing the moisture of the environment. Its high sugar content and low pH level might prevent the growth of microbes (Eswaran *et al.*, 2015; Nishio *et al.,* 2016). An injured intestinal mucosa may be healed by using honey because it stimulates the growth of new tissues and works as an anti-inflammatory agent (Kek *et al.*, 2014). This study was carried out to investigate the antibacterial and antibiofilm activities of *Trigona* honey against *P. aeruginosa* and *S. pyogenes*.

2. Materials and Methods

2.1. Culture bacteria

Two strains of *Pseudomonas aeruginosa* (ATCC 10145) and *Streptococcus pyogenes* (ATCC 19615) were used for this study. Working bacterial culture was prepared by picking up 2-4 morphologically identical colonies from stock culture and then was suspended in 10 mL of sterile Mueller Hinton Broth (MHB) in sterilized universal bottles. The inoculum was incubated at 37°C for 24 hours before proceed to the subsequent assay (Shehu *et al*., 2016; Zainol *et al*., 2013).

2.2. Honey samples

Fresh *Trigona* honey samples were obtained from a bee farm located in Kelantan a state in East Coast of Peninsula Malaysia. Honey samples were stored in the dark at room temperature.

2.3. Agar well diffusion assay

Sterile distilled water was used to dilute *Trigona* honey to achieve 75%, 50%, 25%, and 10% (w/v) concentration of honey. A few single colony of *P. aeruginosa* and *S. pyogenes* were aseptically picked from the fresh culture plate using sterile cotton swab and then were suspended into 10 mL of saline solution. The inoculum density was adjusted to 0.5 McFarland (Hudzicki, 2009; Zainol *et al*., 2013). A sterile cotton swab was then dipped into the bacterial suspension and was rotated onto the tube with firm pressure to remove excess fluid. The swab was streaked over the entire surface of plate for three times and each time the plate was rotated approximately 90º to ensure even distribution of bacterial suspension onto the Mueller-Hinton agar surface. A sterile 9 mm cork borer (Fisher Scientific, UK) was used to create six wells of agar plate. The wells of agar plate were labelled and were added with 170 µ L of the five different honey concentration; 100%, 75%, 50%, 25%, and 10% (w/v). The well with distilled water was used as a n egative control. The agar plates were then incubated at 37ºC for 24 ho urs. Digital venire calliper (mutiarasaintifik, Malaysia) was used to measure the zones of inhibition. The assay was carried out in triplicate for each of the test organism.

2.4. Minimum inhibitory concentration (MIC) assay

To determine the MIC of *Trigona* honey, a broth micro dilution method was used. A few single colonies of *P. aeruginosa* and *S. pyogenes* isolates were aseptically picked from the fresh culture plate by using a sterile loop and then were suspended into 10 mL of MHB and incubated for 24 hours at 37°C. The inoculum density was diluted with MHB to achieve to 0.5 McFarland at 600 nm by using a spectrophotometer (Genesys 20, Thermo Scientific) (Hudzicki, 2009; Zainol *et al.,* 2013). The honey samples were freshly prepared for MIC. A bacterial suspension was inoculated together with nine different concentrations of honey (50%, 25%, 20%, 12.5%, 10%, 6.3%, 5%, 3.1% and 1.6%). After that, 200 µl of each concentration of honey with inoculum was added to wells. Column number 10 w as filled with 200 µl of honey as a corresponding negative control, column number 11 w as filled with 200 µL of inoculum as a bacterial growth control, and finally, column number 12 was filled with 200 µl of broth as a sterility control. The plates were incubated at 37°C for 24 hours. After 24 hours, visual inspection was done. Bacteria growths were assessed by turbidity in the wells and were compared to the positive and negative controls. Absorbance was measured by using the microtiter plate reader (Tecan Infinite 200 PRO, Austria) at 570 nm. The MIC_{50} and MIC_{90} was determined by using the following formula (Bouacha *et al*., 2018; Lye, 2015; Zainol *et al*., 2013):

$$\% \text{ Inhibition} = 1 - \frac{\text{OD of the test well} - \text{OD of corresponding negative control}}{\text{OD of bacterial growth control} - \text{OD of sterility control}} \times 100$$

2.5. Minimum Bactericidal Concentration (MBC) Assay

The MBC was determined after obtaining the MIC results. After 96-well plate was incubated overnight, the well without turbidity was selected for MBC assay. A sterile wire loop was gently and aseptically dipped into the selected wells (once at a time to ensure sterility before getting dipped into another well to avoid possible contamination) and then sub-cultured on fresh nutrient agar plate. The plates was labelled and incubated at 37ºC for 24 hours. Plate free of any bacterial growth was recorded as the MBC value (Zainol *et al.,* 2013).

2.6. Determination of the time-kill curve

Bactericidal or bacteriostatic of *P. aeruginosa* and *S. pyogenes* was determined by the time-kill curve. Firstly, 0.5 g of honey samples were mixed with 1.5 mL of inoculum and then were adjusted to 10^4 CFU/mL to achieve 25% concentration of *Trigona* honey. Inoculum without honey was used as a positive control. Broth without bacteria was used as a negative control. All inoculums were incubated at 37°C. Inoculums were collected at different time points, serially diluted in broth, plated on nutrient agar and cultured for 24 hours at 37°C to determine the total CFUs in each tube (Bonapace *et al.,* 2000; Boorn *et al.*, 2010; Bouacha *et al.*, 2018). Mean of Log_{10} CFU/mL against time were plotted for each

inoculum. The Log Reduction (LR) was calculated for each inoculum by subtracting the Log_{10} CFU at zero time and the Log_{10} CFU at 24 hours of incubation. The experiments were performed in triplicate at three different time (Bouacha *et al.*, 2018; Mandal and Mandal, 2011).

2.7. Scanning Electron Microscopy (SEM)

The effects of *Trigona* honey on the morphology of *P. aeruginosa* and *S. pyogenes* was examined by SEM (JEOL 6360LA, Japan). Firstly one tube containing 0.4 g of honey was mixed with 1.6 ml of inoculum and then was adjusted to 0.5 McFarland to reach 20% (w/v) concentration of *Trigona* honey. The second tube was filled with 1 mL of inoculum and was used as a control. Subsequently, the tubes were incubated at 37˚C for 24 hours. All samples were then centrifuged at 3500 rpm for 5 minutes. Pellets were collected and were fixed overnight with 2.5% (v/v) glutaraldehyde in 0.01 M phosphate buffer solution (PBS). The samples were washed three times with 0.01 PBS for 10 minutes followed by deionized water for 10 minutes. All samples were dehydrated with ascending concentrations of ethanol for 10 minutes as following; 25% (v/v), 50% (v/v), 75% (v/v), 95% (v/v) and 100% (v/v). After dehydration, the samples were transferred to the carbon tape on copper stage and were graduated to obtain an even and thin layer of sample. The samples were coated with platinum for 1 minute before were placed onto the copper stage holder and were viewed by the SEM (Ng *et al*., 2017). In addition to planktonic stage, the effects of *Trigona* honey of *P. aeruginosa* and *S. pyogenes* biofilms were also examined by SEM.

2.8. Biofilm degradation assay

The different series concentration of honey samples were prepared as follows;100%, 90%, 80, 70, 60%, 50%, 40%, 30%, 20% and 10% (w/v).To form *P. aeruginosa* and *S. pyogenes* biofilms, 200 µL inoculums were pipetted into 96-well plate. The well with inoculum only was used as a positive control, the well with broth only was used as a sterility control and the well with honey only was used as a corresponding negative control. The plates were initially incubated at 37°C for 72 hours. Subsequently, the 200 µL of planktonic cells were carefully removed before being replaced with 200 µL of honey at different concentration as mentioned above for overnight incubation. The wells were washed by using sterile distilled water for three times, and then were stained with 200 µL of 0.1% (w/v) crystal violet for 10 minutes before washing with PBS for three times (Jaffar *et al*., 2016). The plates were kept at room temperature for air dried and were reconstituted with 200 µL of 95% ethanol. Finally, the degradation of biofilms was measured by using micro plate reader (Tecan Infinite 200 PRO, Austria) at the wavelength of 570 nm. The experiments were performed in triplicate (Cooper *et al*., 2014; Cooper *et al*., 2011).

2.9. Biofilm inhibition assay

Inoculums with nine different concentrations of 90%, 80%, 70%, 60%, 50%, 40%, 30%, 20% and 10% were prepared and then 200µL of each inoculums were pipetted into a 96-well plate. The well with inoculum only (100% concentration) was used as a positive control, the well with broth only was used as a sterility control and the wells with honey only was used as a corresponding negative control. The plate was incubated at 37°C for 72 hours. After incubation, the inoculums were removed and the remaining biofilm was washed three times with sterile distilled water. The biofilm was then stained with 200 µL of 0.1% (w/v) crystal violet for 10 min before washing with PBS for three times. The plate was then kept at room temperature. The dried stained biofilm was reconstituted with 200 µL of 95% ethanol and was incubated for 5 min. The inhibition of biofilm was measured by micro plate reader at the wavelength of 570 nm. The experiments were performed in triplicate (Cooper *et al*., 2014; Jaffar *et al*., 2016; AL-Kafaween *et al*., 2019 a, b).

2.10. Degradation and inhibition biofilm analysis

The degradation and the inhibition of biofilm were calculated as following (Cooper *et al*., 2014; Cooper *et al*., 2011; Low, 2013; Lu *et al*., 2014; Ng *et al*., 2014).

$$\text{Biofilm (\%)} = \frac{\text{OD (positive control)} - \text{OD (treatment)}}{\text{OD (positive control)}} \times 100\%$$

3. Results

3.1. Agar well diffusion assay

Agar well-diffusion assay shows the zone of inhibition for *P. aeruginosa* and *S. pyogenes* after being treated with *Trigona* honey. *Trigona* honey exhibits a great inhibition zone on *P. aeruginosa* and *S. pyogenes* cultures. The MIC of *Trigona* honey against *P. aeruginosa* and *S. pyogenes* was 20% as shown in Figure 1. MIC_{50} was between 10%-12.5% concentration of honey and MIC_{90} was between 20%-25% for *P. aeruginosa* and *S. pyogenes* as shown in Figure 2.

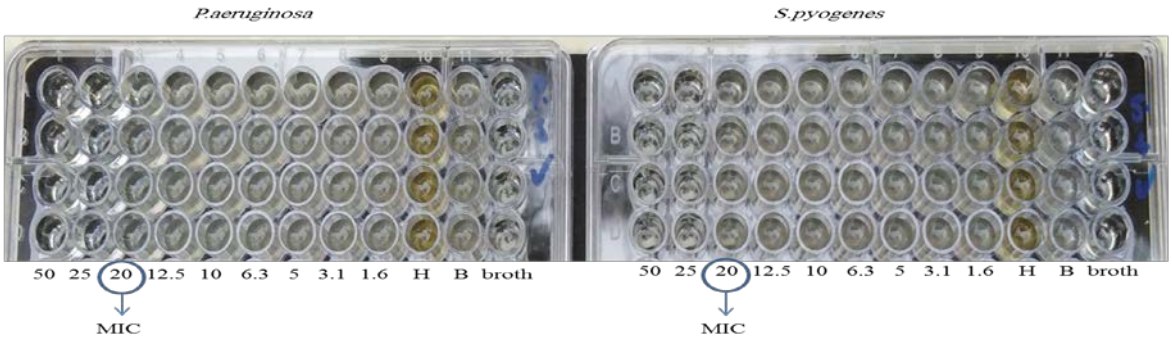

Figure 1. MIC of *Trigona* honey against *P. aeruginosa and S. pyogenes.* H: *Trigona* honey. B: Bacteria (inoculum)

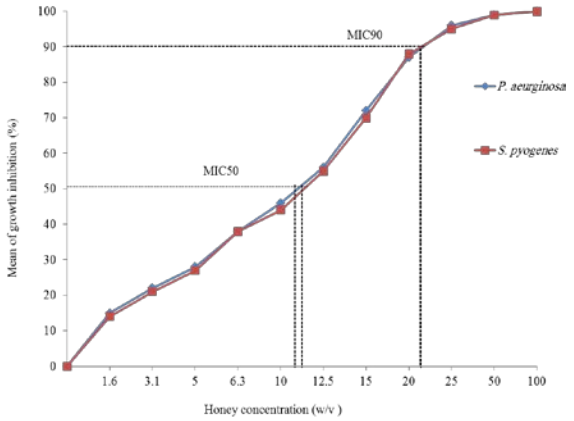

Figure 2. The percentage of bacterial growth inhibition by *Trigona* honey.

3.2. Minimum Bactericidal Concentration (MBC)

The minimum bactericidal concentration (MBC) was determined as the lowest concentration of honey that enables abolishing bacterial growth. The MBC of *Trigona* honey against *P. aeruginosa* and *S. pyogenes* was 25% (Appendix 1-4)

3.3. Time-Kill Curve for P. aeruginosa and S. pyogenes

The time-kill curve clearly shows the increased number of *P. aeruginosa* and *S. pyogenes* cultures as shown in Figure 3 a nd 4. However, after getting treated with *Trigona* honey, *P. aeruginosa* and *S. pyogenes* demonstrate 1 $\log_{10}$ reduction in total viable counts (TVCs) at 6 hour s. At 12 hours *P. aeruginosa* and *S. pyogenes*were decreased 2 $\log_{10}$ reduction in TVCs and at 18 hours they decreased 3 $\log_{10}$ reduction. *P. aeruginosa* and *S. pyogenes* were killed after 24 hour s and were decreased 4 $\log_{10}$ reduction.

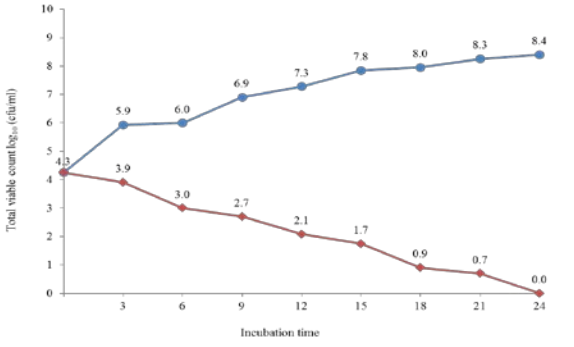

Figure 3. Time-kill curve of *P. aeruginosa*. TVCs of *P. aeruginosa* in the absence (blue) and presence of *Trigona* honey (red).

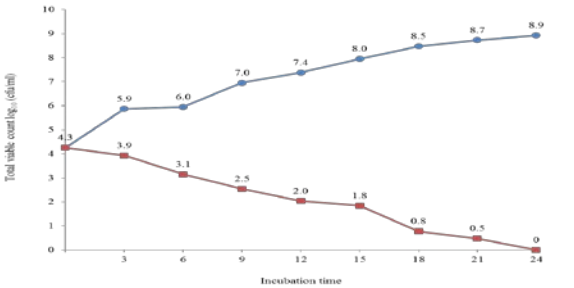

Figure 4. Time-kill curve of *S. pyogenes*. TVCs of *S. pyogenes*in the absence (blue) and presence of *Trigona* honey (red).

3.4. SEM for P. aeruginosa and S. pyogenes

SEM micrographs of *P. aeruginosa* demonstrate the rod shaped with regular structure and normal size as shown in Figure 5 (A). After being treated with honey, there were changes in shape and size of the cells and the cell wall was destroyed. Deformation and lysis of cells were also observed in Figure 5 (B). *P. aeruginosa* biofilm shows hundreds of bacterial cells are connected by a substantial amount of extracellular matrix producing stringy morphology and covering most of the area as shown in Figure 5 (C). The images of biofilm obtained by SEM provided convincing evidence of loss and disruption on viability and integrity of biofilm after being triggered by *Trigona* honey. The biofilm was noticeably shorter, the cell density was decreased, composed of layers of rod shaped cells, appeared in curved and distorted as shown in Figure 5 (D). SEM micrographs of *S. pyogenes* demonstrate the regular cocci with chain structure were observed in Figure 5 (E). After adding the *Trigona* honey, the cells were enlarged than normal size and closed each other as shown in Figure 5 (F). The morphological changes, such as abnormal shape and cell division, incomplete separation of cocci, ruptured and swelling cell were observed in Figure 5 (F). *S. pyogenes* biofilm shows numerous cells and diverse thickness connected to each other by extracellular matrix as shown in Figure 5 (G). Microscopic *S. pyogenes* biofilm with honey shows uneven shape of bacteria, and also the cell surfaces appear in rough, with holes and crevices. The structure of cells was damaged as shown in Figure 5 (H).

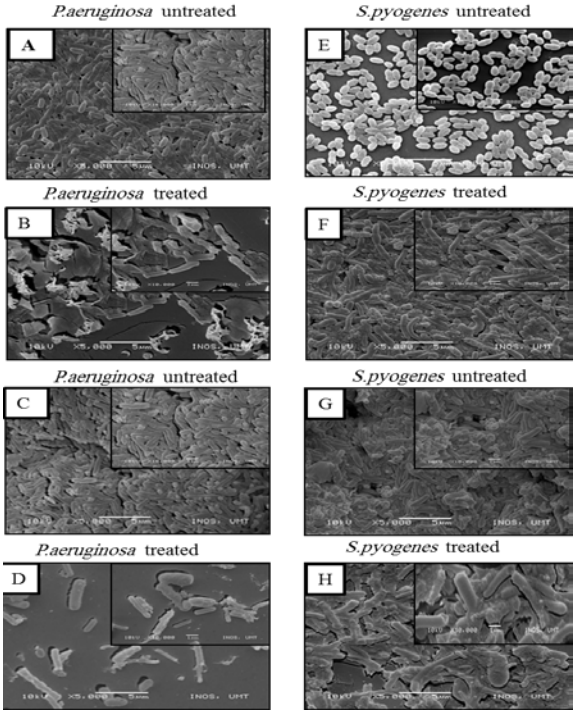

Figure 5. SEM of *P. aeruginosa* at planktonic stage (A) and after adding with *Trigona* honey (B).*P. aeruginosa* biofilm (C) and after honey treatment (D). SEM of *S. pyogenes* at planktonic stage (E) and after adding with *Trigona* honey (F). *S. pyogenes* biofilm (G) and after honey treatment (H).Viewed at 5000x and 10000x magnification. Scale bar 5µm.

3.5. Biofilm degradation assay

Trigona honey samples were able to reduce the biofilms mass of *P. aeruginosa* and *S. pyogenes*. Different concentrations of *Trigona* honey samples cause's different effects on biofilm degradation. *Trigona* honey was able to reduce 70%, 61%, 54%, 45%, 40%, 38%, 29%, 24%, 12% and 8 % biofilm mass of *P. aeruginosa* after being treated with 100%, 90%, 80%, 70%, 60%, 50%, 40%, 30%, 20% and 10% (w/v) of honey concentration respectively. Similarly, *Trigona* honey was able to reduce 68%, 60%, 52%, 40%, 36%, 32%, 26%, 25%, 13% and 9 % biofilm mass of *S. pyogenes* at honey concentration of 100%, 90%, 80%, 70%, 60%, 50%, 40%, 30%, 20%, and 10 % (w/v) respectively.

3.6. Biofilm inhibition assay

Trigona honey samples at different concentrations are able to inhibit biofilms formation of *P. aeruginosa* and *S. pyogenes* at different levels. All of honey concentrations show the inhibition effect on bi ofilm formation. *Trigona* honey inhibits 91%, 84%, 78%, 72%, 49%, 27%, 26%, 13% and 9% of *P. aeruginosa* biofilm at honey concentration of 90%, 80%, 70%, 60%, 50%, 40%, 30%, 20% and 10% (w/v) respectively. Similarly, *Trigona* honey inhibits 89%, 81%, 73%, 68%, 45%, 23%, 19%, 11% and 7% of *S. pyogenes* biofilm at honey concentration of 90%, 80%, 70%, 60%, 50%, 40%, 30%, 20% and 10 % (w/v) respectively.

4. Discussion

Antibacterial activities of honey have been broadly discussed among researchers worldwide. It is postulated to be close on several factors such as osmolarity, pH and other major constituents such as phenolic acids and flavonoids (Fatima *et al*., 2018; 2019; Zainol *et al*., 2013). Limitations of some antibacterial assay such as agar well-diffusion test were discovered including the insensitivity in detecting low level of antimicrobial activity, variation in the experimental conditions and permeability of non-polar components. Agar well-diffusion test may not be the most appropriate method to evaluate the antibacterial activity of honey (Balouiri *et al*., 2016).

Micro-broth dilution was performed to determine the MIC for antibacterial activities of honey toward all the tested bacteria. MIC is the lowest concentration of honey solution required to inhibit 99% of bacterial growth. MBC is defined as the lowest concentration of honey required to kill at least 99% of the tested bacterial strains (Zainol *et al*., 2013). MIC and MBC values are 20% and 25% (w/v), respectively, for both bacteria. Previous studies by (Abbas, 2014; Bouacha *et al*., 2018; Shenoy *et al*., 2012; Zainol *et al*., 2013) demonstrated that MIC for *Kelulut* honey, *Algerian* honey, *Manuka* honey *and Egyptian clover* honey against *P. aeruginosa* was at 20% concentration and MBC was at 25% concentration. Other studies showed that MIC for *Manuka* honey against *S. pyogenes* was at 20% concentration and MBC was at 25% concentration (Maddocks *et al*., 2012; Mandal and Mandal, 2011). Also a study by (Roberts *et al*., 2012) reported that MIC for *Manuka* honey against *P. aeruginosa* was at 12% concentration and MBC was at 16% concentration.

The time kill curve is used to determine the bactericidal or bacteriostatic activity of antimicrobials. It is analyzed by plotting $\log_{10}$ CFU/mL versus time. Total cell count is defined as the total number of both dead and living cells in the sample, whereas total viable count (TVC) is defined as the number of living cells (Singleton, 2004). To maintain and minimize the impact of time-kill variables, several factors should be considered when performing time-kill studies. These variations affect the results and their interpretation. Firstly, the initial or starting inoculum of 10^4 to 10^7 CFU/mL should be applied. Secondly, the samples should be incubated at 37°C. Thirdly, the assay should be continued up to 24 hours (Klepser *et al*., 1998). In this study, all these conditions were applied in the time-kill assays. The $\log_{10}$ CFU/mL for *P. aeruginosa* and *S. pyogenes* treated with *Trigona* honey was noticed at 12 hours which is almost half of *P. aeruginosa* and *S. pyogenes* were killed ($\log_{10}$ CFU/mL=2.1) and ($\log_{10}$ CFU /mL=2.0) respectively. Similarly, at 24 hours almost 100% of *P. aeruginosa* and *S. pyogenes* were killed ($\log_{10}$ CFU/mL=0) and ($\log_{10}$ CFU/mL=0) respectively.

SEM is an essential tool to observe the structural and physical changes that occur to cells after adding certain agents. In this study, SEM was used to determine membrane integrity, morphological changes of cells and evidence of cell division before and after exposure to honey. The mechanism of antimicrobial effects of honey is not yet fully understood. The effects of honey on bacteria could be complicated because of the complexity of honey compound. Nevertheless, observation of the bacterial structures and morphological variation presents valuable knowledge of complete understanding of antimicrobial and antibiofilm actions of *Trigona* honey on both bacteria.

Cell destruction and lysis were observed in *P. aeruginosa* and *S. pyogenes*, which affected the structure of the cell wall. In this study, MIC 20% was used for SEM because it is the lowest concentration that enables inhibiting planktonic and biofilm. A similar study has reported that *Manuka* honey at concentration of 20% affected the structure and viability of *P. aeruginosa* and distorted the cells (Henriques *et al*., 2011). Another study using *Manuka* honey showed that concentration of 10% honey affected the structure of *Staphylococcus aureus* (Henriques *et al*., 2010). Studies by (Nishio *et al*., 2016; Zakaria, 2015) showed that Stingless bees honey and Sider omani honey have disrupted the cell wall and inhibited cell division of *P. aeruginosa*, *S. pyogenes* and *Staphylococcus aureus.*

The four major biological activities of honey are acidity, non-hydrogen peroxide activity, high osmotic effect, and the presence of phytochemical components which is beneficial in controlling bacterial colonization and additionally disruption of biofilms (Al-Waili *et al*., 2011; Zainol *et al*., 2013). High osmotic effect of honey due to the high contents of sugar in honey also plays a role in reducing biofilm mass (Fatima *et al*., 2018). Besides high osmotic effect of *Trigona* honey, acidity of honey is assumed to be a r ole in reducing biofilm mass as well. Acidity of *Trigona* honey, which is within the range of pH 3.2 to 4.5, creates an unfavourable environment for bacterial growth whereas their optimum pH for growth is about pH 7.2 to 7.4 (Fatima *et al*., 2018).

5. Conclusion

The study revealed antibacterial and antibiofilm activities of *Trigona* honey against *P. aeruginosa* and *S. pyogenes*. Ag ar well diffusion, MIC, MBC, time-kill curve, biofilm degradation and biofilm inhibition proved that *Trigona* honey has a high antibacterial and antibiofilm activities against both bacteria. Moreover, SEM images showed that *P. aeruginosa* and *S. pyogenes* of planktonic and biofilm were lysed and disrupted after being treated with concentration 20% (w/v). Our finding suggests the consumption of 100% concentration of *Trigona* honey will degrade 70% of *P. aeruginosa* and 68% *S. pyogenes* biofilms. Also, consumption of 100% concentration of *Trigona* honey will inhibit 91% of *P. aeruginosa* and 89% *S. pyogenes* biofilms. Therefore, the Malaysian Trigona honey shows promising potential as an antibacterial agent.

Acknowledgments

This work was supported by internal research grant (Uni SZA/2017/DPU/37 R0018R341). Authors thank staff laboratory members of the Faculty of Health, Uni SZA.

References

Fatima IJ, Mohd Hilmi AB, Salwani I and Lavaniya M. 2018. Physicochemical characteristics of malaysian stingless bee honey from trigona species. *Inter Med J Malaysia,* **17**:187-191.

Abbas, HA. 2014. Comparative antibacterial and antibiofilm activities of manuka honey and Egyptian clover honey. *Asian J Appl Sci.,* **2 (2)**: 110–115.

Ahmed A KJ, Hoekstra, M J, Hage, J J, Karim, R B and Krizek, TJ. 2003. Honey-medicated dressing: transformation of an ancient remedy into modern therapy. *Annals Plastic Surgery,* **50**: 143-148.

AL-Kafaween MA, Khan RS, Hilmi ABM and Ariff TM.2019a.Characterization of biofilm formation by *Escherichia coli*: An *in vitro* study. *J App Biol Biotech*, 7:17-19.

AL-Kafaween MA, Khan RS, Hilmi ABM and Bouacha M.2019b. Effect of growth media and optical density on biofilm formation by *Staphylococcus epidermidis*. *EC Microbiol*., **15**: 277-282.

Al-Saadi MAK, Abdul-Lateef, L A and Kareem, MA. 2016. Detection of biofilm formation and effect of vinegar on biofilm of *Streptococcus pyogenes* isolated from patients with tonsillitis. *Inter J PharmTech Reas,* **9**:9.

Al-Waili N, Salom, K and Al-Ghamdi, AA. 2011. Honey for wound healing, ulcers, and burns; data supporting its use in clinical practice. *The Sci World J.,* **11**:766-787.

Alandejani T, Marsan J, Ferris W, Slinger R and Chan F. 2009. Effectiveness of honey on *Staphylococcus aureus* and *Pseudomonas aeruginosa* biofilms. *Otolaryngology-Head and Neck Surg.,* **141**: 114-118.

Anthimidou E and Mossialos, D. 2013. Antibacterial activity of Greek and Cypriot honeys against *Staphylococcus aureus* and *Pseudomonas aeruginosa* in comparison to manuka honey. *J Med Food,* **16**: 42-47.

Badet C and Quero F.2011. The *in vitro* effect of manuka honeys on growth and adherence of oral bacteria. *Anaerobe,* **17**: 19-22.

Balouiri M, Sadiki M and Ibnsouda, S K. 2016. Methods for *in vitro* evaluating antimicrobial activity: A review. *J Pharm Analysis,* **6**: 71-79.

Biluca FC, Della B, Fabiana, de Oliveira, Gabriela P, Pereira, L M, Gonzaga, LV, Costa, A C O and Fett, R. 2014. 5-HMF and carbohydrates content in stingless bee honey by CE before and after thermal treatment. *Food Chem,* **159**: 244-249.

Biluca F C, Braghini F, Gonzaga L V, Costa A C O and Fett, R. 2016. Physicochemical profiles, minerals and bioactive compounds of stingless bee honey (Meliponinae). *J Food Composition and Analysis,* **50**: 61-69.

Bonapace, CR, White, RL, Friedrich, LV, and Bosso, JA.2000. Evaluation of antibiotic synergy against *Acinetobacter baumannii*: a comparison with Etest, time-kill, and checkerboard methods. *Diagnostic Microbiol Infect Dis.,* **38**: 43-50.

Boorn KL, Khor, Y-Y, Sweetman, E, Tan, F, Heard, TA, and Hammer, KA. 2010. Antimicrobial activity of honey from the stingless bee Trigona carbonaria determined by agar diffusion, agar dilution, broth microdilution and time-kill methodology. *J Appl Microbiol.,* **108**: 1534-1543.

Bouacha, Mabrouka, Ayed, Hayette, and Grara, Nedjoud. 2018. Honey bee as alternative medicine to treat eleven multidrug-resistant bacteria causing urinary tract infection during pregnancy. *Scientia Pharmaceutica,* **86**: 14.

Cooper, Rose, Jenkins, L, and Hooper, S. 2014. Inhibition of biofilms of *Pseudomonas aeruginosa* by Medihoney *in vitro*.*J Wound Care,* **23**: 93-104.

Cooper, Rose, Jenkins, Leighton, and Rowlands, Richard.2011. Inhibition of biofilms through the use of manuka honey. *Wounds UK,* 7: 24-32.

Costerton, J William, Stewart, Philip S, and Greenberg, E Peter. 1999. Bacterial biofilms: a common cause of persistent infections. *Science,* **284**: 1318-1322.

Doern, Christopher D, Roberts, Amity L, Hong, Wenzhou, Nelson, Jessica, Lukomski, Slawomir, Swords, William E, and Reid, Sean D. 2009. Biofilm formation by group A Streptococcus: a role for the streptococcal regulator of virulence (Srv) and streptococcal cysteine protease (SpeB). *Microbiol.,* **155**: 46-52.

Eswaran, Vaishali K Varsha Uma, Priya, V, & Bhargava, HR.2015. A Comparative Study of the Biochemical, Antioxidative and Anti-microbial Activity of Apis and Trigona Honey Collected from Different Geographical Areas of India. *World Applied Sciences Journal,* 33: 160-167.

Guerrini, A, Bruni, R, Maietti, S, Poli, F, Rossi, D, Paganetto, G, Sacchetti, G.2009. Ecuadorian stingless bee (Meliponinae) honey: A chemical and functional profile of an ancient health product. *Food Chemistry,* 114: 1413-1420.

Henriques, AF, Jenkins, RE, Burton, NF, & Cooper, RA.2010. The intracellular effects of manuka honey on Staphylococcus aureus. *European journal of clinical microbiology & infectious diseases,* 29: 45.

Henriques, AF, Jenkins, RE, Burton, NF, & Cooper, RA. 2011. The effect of manuka honey on the structure of Pseudomonas aeruginosa. *European journal of clinical microbiology & infectious diseases,* 30: 167-171.

Hudzicki, Jan. (2009). Kirby-Bauer disk diffusion susceptibility test protocol.

Jaffar N, Miyazaki T and Maeda T.2016. Biofilm formation of periodontal pathogens on hydroxyapatite surfaces: Implications for periodontium damage. *Journal of Biomedical Materials Research Part A,* **104**: 2873-2880.

Fatima I J, , Hilmi A B M and Manivannan L. 2019. Isolation and characterization of polyphenols in natural honey for the treatment of human diseases. *Bulletin of the National Res Centre,* **43**: 4.

Kek S P, Chin N L, Yusof Y A, Tan S W and Chua L S. 2014. Total phenolic contents and colour intensity of Malaysian honeys from the Apis spp. and Trigona spp. bees. *Agriculture and Agricultural Science Procedia,* **2**: 150-155.

Klepser M E, Ernst EJ, Lewis R E, Ernst M E and Pfaller M A. 1998. Influence of test conditions on antifungal time-kill curve results: proposal for standardized methods. *Antimicrob Agents chemother.,* **42**:1207-1212.

Lee, Jin-Hyung, Park, Joo-Hyeon, Kim, Jung-Ae, Neupane, Ganesh Prasad, Cho, Moo Hwan, Lee, Chang-Soo, & Lee, Jintae.2011. Low concentrations of honey reduce biofilm formation, quorum sensing, and virulence in Escherichia coli O157: H7. *Biofouling,* 27: 1095-1104.

Levy, Stuart B, & Marshall, Bonnie. 2004. Antibacterial resistance worldwide: causes, challenges and responses. *Nature medicine,* 10: 122.

Low, Ka Lok.2013. Inhibitory effect on Staphylococcus Aureus Biofilm through the use of honey. *UTAR*.

Lu, Jing, Turnbull, Lynne, Burke, Catherine M, Liu, Michael, Carter, Dee A, Schlothauer, Ralf C, Harry, Elizabeth J. 2014. Manuka-type honeys can eradicate biofilms produced by Staphylococcus aureus strains with different biofilm-forming abilities. *PeerJ,* 2: 326.

Lusby, Patricia E, Coombes, Alexandra L, & Wilkinson, Jenny M. 2005. Bactericidal activity of different honeys against pathogenic bacteria. *Archives of medical research,* 36: 464-467.

Lye, Ping Ying.2015.Interactive effect of trigona honey and ampicillin on Staphylococcus aureus isolates of infected wound. *UTAR*.

Maddocks, Sarah E, Lopez, Marta Salinas, Rowlands, Richard S, & Cooper, Rose A. 2012. Manuka honey inhibits the development of Streptococcus pyogenes biofilms and causes reduced expression of two fibronectin binding proteins. *Microbiology,* 158: 781-790.

Mandal, Manisha Deb, & Mandal, Shyamapada.2011. Honey: its medicinal property and antibacterial activity. *Asian Pacific Journal of Tropical Biomedicine,* 1: 154.

Mandal S, Pal NK, Chowdhury I H and Debmandal M. 2009. Antibacterial activity of ciprofloxacin and trimethoprim, alone and in combination, against *Vibrio cholerae* O 1 Biotype El Tor serotype Ogawa isolates. *Polish J Microbiol.,* **58**: 57-60.

Mundo, Melissa A, Padilla-Zakour, Olga I, & Worobo, Randy W.2004. Growth inhibition of foodborne pathogens and food spoilage organisms by select raw honeys. *Intern J Food Microbiol.,* **97**: 1-8.

Nassar, Hani M, Li, Mingyun, & Gregory, Richard L.2011. Effect of honey on Streptococcus mutans growth and biofilm formation. *Applied and environmental microbiology*,78: 5538-5511.

Ng, Wen-Jie, Lim, Kit-Yin, Chong, Ju-Yee, & Low, Ka-Lok.2014. In vitro screening of honey against Enterococcus spp. biofilm. *Journal of Medical and Bioengineering,* 3:1.

Ng, Wen Jie, Chan, Yek Jia, Lau, Zhi Khoon, Lye, Ping Ying, & Ee, Kah Yaw.2017. Antioxidant properties and inhibitory effects of trigona honey against *staphylococcus aureus* planktonic and biofilm cultures. *Intern J,* **12**: 28-33.

Nishio, EK, Ribeiro, JM, Oliveira, AG, Andrade, CGTJ, Proni, EA, Kobayashi, RKT, & Nakazato, G.2016. Antibacterial synergic effect of honey from two stingless bees: *Scaptotrigona bipunctata* Lepeletier, 1836, and *S.postica* Latreille, 1807. *Scientific Reports,* **6**: 21641.

Ramalivhana, JN, Obi, CL, Samie, A, Iweriebor, BC, Uaboi-Egbenni, P, Idiaghe, JE, & Momba, MNB. 2014. Antibacterial activity of honey and medicinal plant extracts against Gram negative microorganisms. *African J Biotechnol.,* **13**:4.

Roberts, Aled EL, Maddocks, Sarah E, & Cooper, Rose A.2012. Manuka honey is bactericidal against *Pseudomonas aeruginosa* and results in differential expression of oprF and algD. *Microbiol,* **158**: 3005-3013.

Shahjahan, M, & Halim, Nurul A Bt A.2007. Antimicrobial Properties of'Kelulut'(Trigona Spp) Honey. *Malaysian Journal of Medical Sciences,* 14:1.

Shehu, Aminu, Ismail, Salwani, Rohin, Mohd Adzim Khalili, Harun, Azian, Aziz, Aniza Abd, & Haque, Mainul. 2016. Antifungal Properties of Malaysian Tualang Honey and Stingless Bee Propolis against Candida albicans and Cryptococcus neoformans.

Shenoy, Vishnu Prasad, Ballal, Mamatha, Shivananda, PG, & Bairy, Indira. 2012. Honey as an antimicrobial agent against Pseudomonas aeruginosa isolated from infected wounds. *Journal of global infectious diseases,* 4: 102.

Singleton, Paul.2004. *Bacteria in biology, biotechnology and medicine*: John Wiley and Sons, 2: 570.

Zainol, Mohd Izwan, Yusoff, Kamaruddin Mohd, & Yusof, Mohd Yasim Mohd. 2013. Antibacterial activity of selected Malaysian honey. *BMC Complementary and Alternative Medicine,* 13: 129.

Zakaria, Azza S.2015. Mechanism of antibacterial action of honey on pathogenic wound bacterial strains: A proteomic analysis. *Int Res J Pharm,* 6: 778-788.

Appendix

Appendix 1: MBC determination for *Trigona* honey against *P.aeruginosa*

Appendix 2: MBC determination for *Trigona* honey against *S.pyogenes*

Appendix 3: Log reduction (LR) for *P.aeruginosa* after 24 hours exposure to 25% of *Trigona* honey.

Time (hours)	Log_{10}CFU/ ml(A)	Log_{10}CFU/ ml+ honey(B)	LR=log_{10}(A) -log_{10}(B)	*P*- value
0	4.3	4.3	0	Initial
3	5.9	3.9	2	0.041
6	6.0	3.1	2.9	0.018
9	7.0	2.5	4.5	0.011
12	7.4	2.0	5.4	0.019
15	8.0	1.8	6.2	0.014
18	8.5	0.8	7.7	0.008
21	8.7	0.5	8.2	0.003
24	8.9	0	8.9	0.002

Appendix 4: Log reduction (LR) for *S.pyogenes* after 24 hours exposure to 25% of *Trigona* honey.

Time (hours)	Log_{10}CFU/ ml (A)	Log_{10}CFU/ ml+ honey(B)	LR=log_{10}(A) - log_{10}(B)	*P*- value
0	4.3	4.3	0	Initial
3	5.9	3.9	2	0.041
6	6.0	3.0	3	0.023
9	6.9	2.7	4.2	0.035
12	7.3	2.1	5.2	0.024
15	7.8	1.7	6.1	0.006
18	8.0	0.9	7.1	0.001
21	8.3	0.7	7.6	0.003
24	8.4	0	8.4	0.004

JJBS

Volume 13, Number 1,March 2020
ISSN 1995-6673
Pages 77 - 83

Jordan Journal of Biological Sciences

Estimation of Grape Seed Oil Alleviative Role on Cadmium Toxicity in Male Mice

Osama H.Elhamalawy[1] and Aida I. El makawy[2*]

[1]Department of Environment and Bio-Agriculture, Faculty of Agriculture, Al-Azhar University, Cairo; [2]Department of Cell Biology, National Research Center, 33 El Bohouth Street, Dokki- Giza-Egypt-P.O.12622.

Received April 14 , 2019; Revised May 18, 2019; Accepted May 28, 2019

Abstract

Cadmium (Cd) is a non-degradable environmental pollutant, and has the ability to collect in the body organs causing humans and animals health risks. The present study was conducted to estimate the protective role of grape seed oil (GSO) against cadmium chloride ($CdCl_2$) induced toxicity in male mice. Phenolics content and antioxidant capacity of GSO were measured. Male mice had gavages of $CdCl_2$ at a dose of (7.48 mg/kg body weight (b. w.) once a day for 30 successive days, whereas they were orally administered GSO at 1 mL/kg b. w. once a day for 30 successive days either pre or plus $CdCl_2$. After the treatment, liver enzymes, sperm characteristics and organs weights were investigated. Genotoxicity was evaluated using comet assay and micronucleus test. Results revealed that $CdCl_2$ induced elevation in ALT and AST, significantly increased the relative weights of liver, decreased the testes weight, sperm count and declined motility and elevated DNA damage in tested cells compared to control group. In contrast, administration of GSO at two regimens restored the organs' weights to the normal range, ameliorated liver enzymes, improved the sperm physical characteristics and alleviated DNA damage compared to $CdCl_2$ treated mice. Furthermore, GSO pre-administration was the best regimen in the attenuation of the toxic effects of $CdCl_2$. It can be concluded that GSO may possess a protective role against the toxicity of $CdCl_2$ male mice.

Keywords: Grape seed oil, Cadmium chloride, Organs weights, Liver enzymes, Sperm physical characters, Genotoxicity.

1. Introduction

Heavy metals are a paradigm of pollutants. They are stable high-density metals present in the environment because they are one of the components of earth's crust (Tchounwou *et al.,* 2012). The heavy metals quantity in the air, water, soil and tissues of living organisms has increased because of the human activities that caused their increase in the environment (Gana and Toba, 2015). Heavy metals are toxic, but the dose, degree of exposure and the chemical form of these metals lead to differences in the extent of their toxicity (Tchounwou *et al.*, 2012).

Cadmium (Cd) is a major industrial and environmental pollutant that is principally produced from smelting, mining, electroplating, battery industrialized, paints and plastics. The wide route of exposure to Cd mostly results from smoking, air pollution and Cd contaminated foods and water utilization (Honda *et al.,* 2010). It is accumulated in the liver, kidney and testis, so it is considered as one of the common poisonous heavy metals. Cd causes a broad range of negative health hazards including hepatotoxicity (Kisok, 2012). Wang *et al.* (2017) reported that cadmium is an endocrine disruptor known to apply toxic effects on the testes, with indicated sperm dysfunction during both chronic and acute cadmium exposure. In addition, Cd is known as human carcinogen that attacks DNA directly and disturbs DNA repair mechanism (Murugavel and Pari, 2010). It is confirmed that Cd induces oxidative stress through the creation of free radicals that may damage protein, lipid, enzymes and DNA (Naskar *et al.,* 2010).

Antioxidants provide potent free radicals scavengers and thwart the incidence of disease (Islam *et al.,* 2011). In recent times, using natural foodstuffs for diseases handling has been broadly suggested due to their protective effects (Soliman *et al.,* 2013; 2015). Such findings suggest that it is necessary to identify alternative drugs for protection against toxicity and the treatment of human diseases. Grape (*Vitis vinifera*) is one of the world's major fruit crops, and grape seed extract is a multifarious matrix with approximately 40% fiber, 16% oil, 11% proteins, and 7% phenols such as tannins and mineral (Shi *et al.,* 2003). The grape seed oil (GSO) has a lot of uses for food additive, cosmetics, controlling diseases and wound healing (Shivananda *et al.,* 2011). Many researchers have mentioned plentiful health benefits of GSO, where it is considered as a potent antioxidant for its polyphenols, flavonoids, unsaturated fatty acids and vitamin E contents (Hassanein and Abedel-Razek, 2009; Kikalishvili *et al.,* 2011; Hasseeb *et al.,* 2013). Grape seed extracts (GSE)

* Corresponding author e-mail: aelmakawy@yahoo.com.

possess antimutagenic and anticarcinogenic properties by inhibiting enzymes of free radicals productions (Maier *et al.*, 2009). Moreover, the exploitation of GSE may be helpful in withdrawing the side effects of chemotherapeutic agents (Aysun *et al.*, 2008). In addition, it is recognized that the GSO could supply protection against free radicals induced oxidative stress and cellular damage caused after exposure to heavy metals (Shinagawa *et al.*, 2015).

Consequently, the aim of this study was to estimate the potential protective role of grape seed oil against the toxicity induced by cadmium in liver and testis of mice. The study was carried out by monitoring DNA damage by micronucleus test and comet assay in male mice, by examining liver function (enzymes), sperm analysis, and by determining the body weight of animals.

2. Materials and Methods

2.1. Chemicals

Cadmium chloride ($CdCl_2$) was purchased from Sigma-Aldrich Company (St. Louis, MO, USA). Grape seed commercial oil (GSO) was purchased from EL Captin Company (Al Obour City, Cairo, Egypt). The aspartate aminotransferase (AST) and alanine aminotransferase (ALT) kits were purchased from Biodiagnostic Co., Egypt. All other chemicals were of analytical grade and purchased from standard commercial suppliers.

2.2. Animals and treatments

Male Swiss albino mice weighing 24±5 g (10-12 week old) were purchased from the Theodor Bilharz Research Institute, Giza, Egypt. Animals were housed in polypropylene cages (43cm× 30cm × 15cm, five mice per cage) with stainless steel covers in the Animal House of Environment and Bio-agriculture Department, Faculty of Agriculture, Al-Azhar University. Animals were kept under controlled temperature (23±4 °C), 50–55% relative humidity and photoperiod of 12 h light:12 h dark cycle. Throughout the experimental period, animals were maintained on standard mice pellet food (Salaam Feed Factory, El marg, Cairo) and tap water *ad libitum.* The mice were allowed to adapt to their surrounding environment for 2 weeks prior to start the experiments. All animals received human care in compliance with the guidelines of the Animal Care and Use Committee of the National Institutes of Health (NIH publication 86-23 revised 1985).

After acclimation, the animals were randomly divided into five groups (n = 10) according to approximately equal mean body weight (b.w.) and administered orally for 30 successive days with $CdCl_2$ (1/25 LD_{50}, 7.48 mg/kg b.w.) according to Yang *et al.* (2012a) and/or GSO (1mL/kg b.w.) according to Mokhtari *et al*. (2011). Experimental groups were as follows: Control group: animals were orally administered with saline. GSO group: animals were orally administered with GSO at dose of (1mL/kg b.w.). $CdCl_2$ group: animals were orally administered with $CdCl_2$ at dose of (1/25 LD_{50}). GSO pre-$CdCl_2$ group: animals were orally administered with 1 mL/kg b.w. GSO then with $CdCl_2$ (1/25 LD_{50}). GSO plus $CdCl_2$ group: animals were orally administered with 1 mL/kg b.w. GSO plus $CdCl_2$ (1/25 LD_{50}).

2.3. Grape seed oil total phenolic content

Total phenolic content (TPC) was determined using the Folin–Ciocalteau's reagent according to the method reported by Lin and Tang (2007) at 760 nm with a spectrophotometer (UV-1601; Shimadzu, Tokyo, Japan), and the quantification was done on the basis of the standard curve of gallic acid concentration ranging between 10 to 80 mg/mL (r^2= 0.99).

2.4. Measurement of antioxidant activity of grape seed oil

The ability of GSO at 50, 100 and 200µL to scavenge 2.9 mL of 1, 1-diphenyl 1-2-picrylhydrazyl (DPPH) free radical was estimated by the method of Singh *et al.* (2002).

2.5. . Relative organs weights

At the termination of the experiments, internal organs such as liver and testes were dissected out, trimmed of excess fat and weighted. The organs weight was presented as relative organ weight as follows:

$$\text{Relative organ weight} = \frac{\text{Organ weight (g)}}{\text{Final body weight (g)}} \times 100$$

2.6. Liver function investigation

Aspartate aminotransferase (AST) and alanine aminotransferase (ALT) liver enzymes activities were measured in serum by the method of Reitman and Frankel (1957).

2.7. Sperm collection and analysis

The epididymides from each mouse were removed and sperm was collected as quickly as possible after dissection. Epididymides was excised and minced in 1 mL of phosphate buffered saline (pH 7.2) to obtain sperm suspension; the sperms were filtered afterwards through a nylon mesh. The sperm count was assessed from right cauda epididymides while sperm motility was analyzed from the left one. Sperm count was performed according to Narayana *et al.* (2002) using a Neubauer hemocytometric chamber. Sperm motility was assessed by counting the motile sperms. Approximately 10 µL of sperm suspension was layered onto a warmed microscope slide. In each semen sample, at least 10 microscopic fields were examined with at least 100 sperm/field counted. The percentage of motile sperm was determined as described by Kvist and Bjorndahl (2002).

2.8. Bone marrow micronucleus assay

Bone marrow sampling, preparations of slide and scoring of micronucleated polychromatic erythrocytes (MNPCE) were done as described by Hayes *et al.* (2009). In brief, bone marrow was gently flushed out in fetal calf serum, centrifuged at 1000 rpm for 5 min and the medium was decanted. Pellet obtained was dispersed in 0.25 mL fetal calf serum, smeared on clean slides, fixed in 70% methanol, air dried and stained with May-Grunwald/ Giemsa protocol. Minimum of 2000 polychromatic erythrocytes/mouse were scored from treated or control group.

2.9. Single cell gel Electrophoresis in liver and testes

Single cell gel Electrophoresis (comet assay) was performed in liver and testes cells according to Bandyopadhyay *et al.* (2008). Briefly, 50 µL of cell suspension was mixed with 100 µL of 1 % low melting point (LMP) agarose and added to fully frosted slides

coated with 80 µL of 1 % normal melting point (NMP) agarose. The cells were then incubated in a lysis solution (2.5 mol L^{-1} NaCl, 100 mmol L^{-1} EDTA, 10 mmol L^{-1} Tris-HCL, 1 % Triton X-100, pH 10) at 4 °C for at least 2 h, at which the slides were placed into an alkaline solution (300 mmol L^{-1} NaOH, 1 mmol L^{-1} EDTA, pH 13) at 4 °C for 20 min so as to allow DNA unwinding, and electrophoresed at 25 V (300 mA) for 20 min. Finally, the slides were neutralized in 400 mmol/L Tris buffer (pH 7.5) for 15 min and stained with ethidium bromide (5 µg mL^{-1}). Images of 50 randomly selected nuclei per experimental group were captured using a fluorescence microscope (Eclipse 800, Nikon, Tokyo, Japan) and analyzed with image analysis software (Comet Assay IV, Perceptive Instruments, Suffolk, UK). Scored parameters included tail length, DNA percentage in tail and olive tail moment (OTM). Tail length is the maximum distance that the damaged DNA migrates from the center of the cell nucleus. DNA percentage in tail is the DNA content that migrates from the nucleus into the comet tail. OTM is the product of the tail length and percentage DNA, which gives a more integrated measurement of overall DNA damage in the cell.

2.10. Statistical analyses

Statistical analyses were performed with SPSS 16 software. Experimental data was analyzed using one-way analysis of variance (ANOVA) followed by Duncan's post hoc test for multiple comparisons between pairs. All values were expressed as mean ± S.D. and differences were considered as significant when ($P \leq 0.05$).

3. Results

3.1. Oil analysis

GSO was found to have high level of phenolic content (42.17±0.55 mg gallic acid /100g oil) and antioxidant activity (84.35±0.35) as show in Table 1. In addition, antioxidant activity analysis of GSO revealed that its scavenging activity was raised gradually with increasing the concentration as shown in Figure 1.

Table 1. Phenolic content and antioxidant activity in grape seed oil.

Character	M ± SD
Phenolic content (mg gallic acid /100g oil)	42.17±0.55
Antioxidant activity %	84.35±0.35

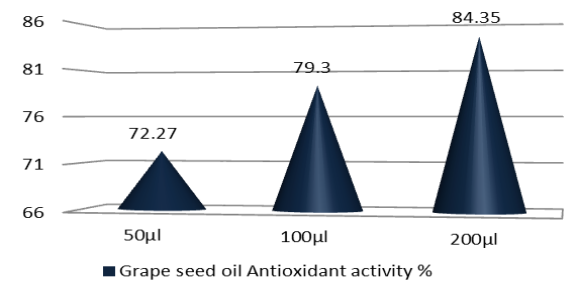

Figure 1. Grape seed oil antioxidant activity.

3.2. Relative organs weights

According to data presented in Table 2, there was no significant difference between both liver and testes relative weights of control and GSO treated groups. Oral administration of $CdCl_2$ to male mice for 30 successive days significantly increased ($P \leq 0.05$) the relative weights of liver (4.18±0.05) and decreased the testes weight (0.65±0.03) as compared to control (3.39±0.06 and 0.83±0.03), respectively. On the other hand, GSO administration either pre or plus $CdCl_2$ induced a significant decrease ($P \leq 0.05$) in the relative weights of liver (3.39±0.04 and 3.33±0.07, respectively) and increase in testes (0.77±0.02 and 0.74±0.02, respectively) compared with $CdCl_2$ treated mice.

Table 2. Relative organs weights of treated male mice with cadmium chloride ($CdCl_2$) and / or grape seed oil (GSO) for 30 consecutive days.

Treatments	Relative organs weights (g)	
	Liver	Testes
Control	3.39±0.06^{bc}	0.83±0.03^{a}
GSO (1 mL/kg b.wt)	3.46±0.03^{b}	0.86±0.02^{a}
$CdCl_2$ (1/25 LD_{50})	4.18±0.05^{a}	0.65±0.03^{c}
GSO pre-$CdCl_2$	3.39±0.04^{bc}	0.77±0.02^{b}
GSO plus $CdCl_2$	3.33±0.07^{b}	0.74±0.02^{b}

Data are expressed as means ± SD. Mean values in the same column within each parameter bearing the same superscript do not differ significantly ($P \leq 0.05$).

3.3. Liver function

The mean values of serum liver enzymes in $CdCl_2$ and/or GSO treated male mice are illustrated in Table 3. A significant increase ($P \leq 0.05$) in the mean values of ALT (43.50±3.31) and AST (46.25±4.11) was observed following the treatment with $CdCl_2$ for 30 successive days compared with control (24.50±1.29 and 31.00±1.83), respectively. In contrast, oral administration of GSO either pre or plus $CdCl_2$ produced a significant decrease ($P \leq 0.05$) in serum content of ALT (30.75±2.06 and 34.25±3.30, respectively) and AST (34.25±2.50 and 38.25±3.59, respectively) than that of $CdCl_2$ treated male mice.

Table 3. Serum liver enzymes of cadmium chloride ($CdCl_2$) and / or grape seed oil (GSO) treated male mice.

Treatments	ALT (U/L)	AST (U/L)
Control	24.50±1.29^{c}	31.00±1.83^{c}
GSO (1 mL/kg bw)	23.50±1.73^{c}	29.75±2.22^{c}
$CdCl_2$ (1/25 LD_{50})	43.50±3.31^{a}	46.25±4.11^{a}
GSO pre-$CdCl_2$	30.75±2.06^{b}	34.25±2.50^{bc}
GSO plus $CdCl_2$	34.25±3.30^{b}	38.25±3.59^{b}

Data is expressed as means ± SD. Mean values in the same column within eachparameter bearing the same superscript do ot differ significantly ($P \leq 0.05$).

3.4. Sperm analysis

As shown in Figure 2, treatment with $CdCl_2$ for 30 successive days caused a significant decline ($P \leq 0.05$) in the mean values of sperm count (284.20±29.51) and motility (54.00±5.09) compared with control

(465.40±22.41 and 85.00±3.53), respectively. By contrast, supplementation of GSO to male mice either before or with $CdCl_2$ significantly improved ($P \leq 0.05$) the decrease of sperm count (447.20±22.70 and 400.60±28.02, respectively) and motility (82.00±2.55 and 76.25±2.44, respectively) compared with $CdCl_2$ treated mice.

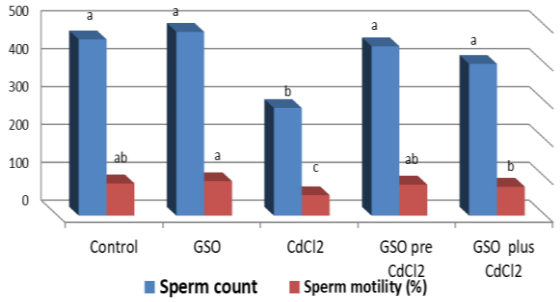

Figure 2. Sperm count and motility in cadmium chloride ($CdCl_2$) and/or grape seed oil (GSO) treated mice for 30 consecutive days. Data is expressed as means ± SD. Mean values in the same column within each parameter bearing the same superscript do not differ significantly ($P \leq 0.05$).

3.5. Effect of CdCl2 and/or GSO on micronuclei number and PCEs/NCEs percentage in bone marrow

Results in Table 4 showed that there were no statistically significant differences in the numbers of MN in the control and GSO-treated groups. While, $CdCl_2$ significantly increased ($P \leq 0.05$) the frequency of MNPCEs (40.67±6.76) as compared to control (5.33±1.33). On the other side, administration of GSO either pre or plus $CdCl_2$ decreased significantly ($P \leq 0.05$) the frequencies of MNPCEs (16.67±2.90 and 26.00±2.00) than in $CdCl_2$ group (40.67+6.76). Concerning to the PCEs/NCEs percentage, data analysis revealed that $CdCl_2$ caused marked toxicity in bone marrow cells, where it is significantly decreased ($P \leq 0.05$) the percentage of PCEs/NCEs. Along with that, GSO ameliorated the toxicity of $CdCl_2$ by increasing the PCEs/NCEs percentage.

Table 4. Frequencies of PCEs, NCEs, MN and PCEs/NCEs percentage in bone marrow cells of cadmium chloride ($CdCl_2$) and/or grape seed oil (GSO) treated mice.

Treatments	PCEs /2000Cell	NCEs /2000Cell	MNPCEs /2000Cell	PCEs/NCEs %
Control	1440.67±32.44^{b}	559.33±32.44^{c}	5.33±1.33^{c}	0.025+0.002^{b}
GSO (1 mL/kg b.w.)	1544.00±16.77^{a}	456.00±16.77^{d}	4.00±1.15^{c}	0.033+0.001^{a}
$CdCl_2$ (1/25 LD_{50})	1181.33±32.91^{d}	818.67±32.91^{a}	40.67±6.76^{a}	0.014+0.001^{d}
GSO pre-$CdCl_2$	1384.67±27.55^{bc}	615.33±27.55^{bc}	16.67±2.90^{b}	0.022+0.002^{bc}
GSO plus $CdCl_2$	1311.33±28.48^{c}	688.67±28.48^{b}	26.00±2.00^{b}	0.018+0.001^{cd}

Data is expressed as means ± SD. Mean values in the same column within each parameter bearing the same superscript do not differ significantly ($P \leq 0.05$). * PCEs: Polychromatic erythrocytes NCEs: Normochromatic erythrocytes MN: Micronuclei.

3.6. Effect of CdCl2 and/or GSO on tailed cells, tail length, tail DNA % and olive tail moment in liver and testes

The mean values of tailed, intact cells, tail length, tail DNA % and olive tail moment in $CdCl_2$ and/or GSO treated liver and testes are presented in Tables 5 and 6. There were no significant differences in all tested parameters between control and GSO treated animals in both organs cells. The values of tailed cell percentage, tail length, DNA percentage in tail and olive tail moment in liver cells of male mice treated with $CdCl_2$ were significantly increased ($P \leq 0.05$) compared to those of control. However, supplementation of GSO to male mice either pre or plus $CdCl_2$ caused a significant alleviation ($P \leq 0.05$) in the values of above-mentioned parameters than in $CdCl_2$ treated animals values. In addition, $CdCl_2$ caused a significant rise ($P \leq 0.05$) in all values of testes cells compared to control. By contrast, administration of GSO plus $CdCl_2$ with both patterns repressed significantly ($P \leq 0.05$) the increase in the all previously mentioned parameters rate as compared to those caused by $CdCl_2$.

Table 5. The mean values of intact, tailed cells, tail length, tail DNA % and olive tail moment in cadmium chloride ($CdCl_2$) and/or grape seed oil (GSO) treated liver**.**

Treatments	Intact cells (%)	Tailed cells (%)	Tail length (µm)	Tail DNA (%)	Olive tail moment (µm)
Control	86.17±0.38^{ab}	13.83±0.38^{cd}	9.04±0.57^{d}	13.04±0.37^{d}	1.18±0.07^{d}
GSO (1 mL/kg b.w.)	87.30±0.79^{a}	12.70±0.79^{d}	8.44±0.46^{d}	12.22±0.73^{d}	1.03±0.04^{d}
$CdCl_2$ (1/25 LD_{50})	70.33±3.26^{d}	29.67±3.26^{a}	19.56±0.58^{a}	21.78±0.41^{a}	4.26±0.09^{a}
GSO pre-$CdCl_2$	83.40±1.44^{bc}	16.60±1.44^{bc}	11.40±0.77^{c}	14.53±0.55^{c}	1.66±0.14^{c}
GSO plus $CdCl_2$	80.73±1.86^{c}	19.27±1.86^{b}	13.40±0.61^{b}	16.16±0.31^{b}	2.16±0.10^{b}

Data is expressed as means ± SD. Mean values in the same column within each parameter bearing the same superscript do not differ significantly ($P \leq 0.05$).

Table 6. Effect of cadmium chloride ($CdCl_2$) and/or grape seed oil (GSO) on Tailed cells, Tail length, Tail DNA % and Olive tail moment in testes.

Treatments	Intact cells(%)	Tailed cells (%)	Tail length (µm)	Tail DNA (%)	Olive tail moment (µm)
Control	87.23±0.65[a]	12.77±0.65[d]	7.54±0.58[cd]	10.61±0.62[d]	0.79±0.02[d]
GSO	87.70±0.36[a]	12.30±0.36[d]	6.91±0.59[d]	10.49±0.48[d]	0.72±0.05[d]
CdCl2	67.76±1.35[d]	32.24±1.35[a]	14.90±0.89[a]	18.40±0.65[a]	2.74±0.19[a]
GSO pre-$CdCl_2$	82.43±1.02[b]	17.57±1.02[c]	8.61±0.54[c]	12.15±0.51[c]	1.04±0.03[c]
GSO plus $CdCl_2$	77.86±2.04[c]	22.14±2.04[b]	9.87±0.48[b]	14.45±0.53[b]	1.43±0.11[b]

Data is expressed as means ± SD. Mean values in the same column within each parameter bearing the same superscript do not differ significantly ($P \leq 0.05$).

4. Discussion

Grape seed products are nutraceutical agents generally utilized as health dietary supplements. The concern about GSO as a functional food has increased because of its high content of phenolic compounds, vitamin E, unsaturated fatty acids (UFAs) and phytosterols (Karaman *et al.*, 2015). This was in line with the result of oil analysis, which confirmed that GSO possess a high antioxidant capacity due to high content of gallic acid, catechin, proanthocyanidins, procyanidins and epicatechin.

Cadmium intoxicated mice showed clear increase in liver weight, may be because the hypertrophy was induced in the liver because of cadmium toxicity. This result is consistent with a previous report indicating that $CdCl_2$ toxicity leads to increasing the weight of liver in rats (Bashir *et al.*, 2014). Otherwise, cadmium produced loss in testis weight. This was consistent with the Elgawish and Ghanem (2014) study; they indicated that the reproductive organs weight was decreased in rats exposed to $CdCl_2$ as compared to the control. The decline in testes and epididymis weight may be ascribed to the inhibition of spermatogenesis, decreased elongated spermatids and steroidogenic enzyme activity (Takahashi and Oishi, 2003). Salem and Salem, (2016) observed that cadmium induced liver weight elevations and testes weights reduction. Conversely, GSO restored the organs weight to the normal range. Our results match with Bashir *et al.* (2014); they found that cadmium decreased water and food intake followed with retardation in growth rate and increase in liver weight. Authors interpreted that Cd accumulation causes disturbances in the body and liver weight of rats due to tissue damage and reduction in their functions. All these alterations induced by Cd intoxication were significantly restored to near normal levels upon pre-administration of GSE. In our study, marked hepatic damage was observed because of the significant elevation of the serum hepatic enzymes (ALT, AST) in the $CdCl_2$ group. These characteristic features of $CdCl_2$-induced liver toxicity are comparable to those formerly reported by other investigators (Obioha *et al.*, 2009; Renugadevi and Prabu, 2010; Shati, 2011; Salem and Salem, 2016). The elevation in liver enzymes activities in $CdCl_2$ intoxicated animals had been attributed to cellular leakage in the organ and loss of functional integrity of membrane architecture of hepatocytes (Salem and Salem, 2016). On the other hand, the disturbance in the levels of the hepatic enzymes in $CdCl_2$ intoxicated mice was ameliorated by both pre- and co-administration with the GSO, as there was a significant decrease in the levels of these enzymes in mice treated with GSO pre/plus $CdCl_2$. This was in agreement with Dogan and Celik (2012) as they indicated that the grape seed extract (GSE) efficiently protected the rats against alcohol-induced hepatotoxicity, as evidenced by AST, ALT enzyme levels reduction. In addition, Abdul-Hamid *et al.* (2018) found that GSE administration with amiodarone revealed obvious improvement for liver enzyme activity compared to amiodarone-treated animals. Bishayee *et al*. (2010) suggested that polyphenol existing in grape seed could reduce hepatic enzymes through the antioxidant actions.

Our findings clarified that $CdCl_2$ administration caused significant decrease in sperm count and motility. These findings were in consent with those of earlier studies by Oliveira *et al.* (2009) and Kaur and Sharma (2015) who observed significant reduction in sperm physical characters in $CdCl_2$ exposed mice. Acharya *et al.* (2008) clarified that reactive oxtgen species (ROS) generated by cadmium can cause spermatozoa lipid peroxidation and deleterious effects on cell membrane phosphatides, inducing sperm DNA oxidation and consequently sperm abnormalities and decline in alive sperm count. The GSO caused amelioration of physical properties of semen in mice. This was in agreement with Al-Shahari and El-kott (2019); they demonstrated a defensive impact of grape seeds extract against the poisoning of monosodium glutamate, whereas Yildirim *et al.* (2011) indicated that the GSE affects sperm movement sperms number, and motility (%), with less immotile and abnormal sperm morphology when contrasted with control. Also, Al-Saeed (2016) reported that GSO caused sperm count elevation in the diazinon treated rats. This could be due to the capability of GSO to either interfere with the spermatogenic processes in the seminiferous tubules, epididymal functions of testosterone on hypothalamic release factor and anterior pituitary secretion of gonadotropins that may lead to activation of spermatogenesis.

Our data showed that $CdCl_2$ induced DNA damage measured by MN and comet assays in liver and testes cells which is considered as indicator of its genotoxicity. Likewise, Abd-El-Moneim *et al.* (2017); El-Habit and Abdel Moneim (2014) reported significant elevations in micronuclei number in murine bone marrow cells exposed to $CdCl_2$. Moreover, Mahrous *et al.* (2015) discovered highly significant frequencies of micronuclei in Nile tilapia fish treated with $CdCl_2$. Also, the results of DNA damage measured by comet assay were in consent with several studies, like Karimi *et al.* (2012) who observed significant alterations in DNA in mice kidney cells

exposed to $CdCl_2$ as compared with control mice. Abd-El-Moneim *et al.* (2017) indicated that the rates of DNA damage in liver cells of $CdCl_2$ contaminated diet fed mice were significantly increased, with significant elevation in comet parameters including (tailed cells %, tail length, tail DNA % and tail moment). In addition, Skipper *et al.* (2016) found significant elevation of DNA damage measured by comet assay in liver carcinoma cells of humans treated with $CdCl_2$. Many studies revealed that $CdCl_2$ oral administration in drinking water of rats enhanced oxidative stress and subsequently the excess of ROS, which may induce DNA damage. Literature data pointed that cadmium induced DNA damage, thus leading to the creation of single and double strand breaks (Yang *et al.*, 2012b; Virk *et al.*, 2013; De Souza Predes *et al.*, 2014). Administration of GSO before or during the treatment with $CdCl_2$ ameliorates the genotoxicity induced by $CdCl_2$ in both tested organs. These results were in agreement with study of Cavusoglu *et al.* (2014), which confirmed that oral gavages with grape seed extract significantly ameliorated the indices of hepatotoxicity, nephrotoxicity, lipid peroxidation, and genotoxicity induced by benzene. They showed a significant reduction in the frequency of MNs when compared with the group treated with benzene alone.

5. Conclusion

Grape seed oil is wealthy in phenolics, fatty acids and vitamins, with economic value to pharmaceutical and food industry. It has useful properties for health, such as anti-inflammatory, cardioprotective, antimicrobial, and anti-cancer activities, and may interact with cellular and molecular pathways. GSO showed marked alleviative role against $CdCl_2$ hepatotoxicity and genotoxicity in male mice. These activities could be attributed to high content of phenolics and antioxidant activity which is reflected in renewed liver enzymes, semen character and reduction of DNA damage almost to normal range. Therefore, the GSO may be efficient to diminish the heavy metals health risk.

References

Abd-El-Moneim MO, Abd El-Kader AH, Abd El-Rahim HA, Radwan AH, Fadel M and Farag MI. 2017. Modulatory role of *Saccharomyces cerevisiae* against cadmium-induced genotoxicity in mice. *J Arab Soc Med Res*., **12:** 27-38.

Abdou MH and Wahb MM. 2016. Neuroprotection of grape seed extract and pyridoxine against triton-induced neurotoxicity. *Oxid Med Cell Longev*., **5:** 1-8.

Abdul-Hamid M, Galaly RS, Mahmoud H and Mostafa F. 2018. The protective effect of grape seed and *Ginkgo biloba* against hepatotoxicity induced by the antidysrhythmic drug ‘‘amiodarone” in male albino rats. *J Basic Appl Sci*., **7:** 223–230.

Acharya UR, Mishra M, Patro J and Panda MK. 2008. Effect of vitamins C and E on spermatogenesis in mice exposed to cadmium. *Reprod Toxicol*., **25:** 84–88.

Al- Attar SM. 2017. Antimutagenic effect of grape seed extracted oil on diazinon induced genotoxicity in albino mice. *Iraqi J Cancer Med Genet*., **10(1):** 56-62.

AL-Saeed HM. 2016. Effect of grape seed oil on alterations of hematological parameters and semen fluid quality induced by diazinon in male rats. *Indo – Asian J Multidisciplinary Res* (IAJMR), **2(6):** 843–855.

Al-Shahari AE and El-kott FA. 2019. Potential effect of grape seeds extract against monosodium glutamate induced infertility in rats. *Int J Pharmacol*., **15:** 287-294.

Aysun C, Leylagul K, Ismail K, Sibel H, Recep S, Ahmet O, Okan O and Osman S. 2008. The effect of grape seed extract on radiation- induced oxidative stress in the rat liver. *Turk J Gatroenterol*., **19(2):** 92-98.

Bandyopadhyay A, Ghoshal S and Mukherjee A. 2008. Genotoxicity testing of low-calorie sweeteners: aspartame, acesulfame-K, and saccharin. *Drug Chem Toxicol.*, **31(4):** 447-57.

Bashir N, Manoharan V and Prabu MS. 2014. Protective role of grape seed proanthocyanidins against cadmium induced hepatic dysfunction in rats. *Toxicol Res*., **3:** 131–141.

Bishayee A, Darvesh SA, PolitisT, and McGory R. 2010. Resveratrol and liver disease: from bench to bedside and community. *Liver Int*., **30(8):** 1103–1114.

Cavusoglu K, Yalcin E, Yapar K, Gur B and Cicek F. 2014. The protective role of grape seed extract against chronic toxicity of benzene in Swiss albino mice. *Cumhuriyet Univ Facul Sci J*., **35(1):** 1-11.

De Souza Predes F, da Silva Diamante AM, Foglio AM, Camargo AC and Aoyama H. 2014. Hepatoprotective effect of *Arctium lappa* root extract on cadmium toxicity in adult Wistar rats. *Biol Trace Element Res*., **160:** 250-257.

Dogan A and Celik I. 2012. Hepatoprotective and antioxidant activities of grape seeds against ethanol-induced oxidative stress in rats. *Br J Nutr*., **107(1):** 45-51.

Elgawish RAR and Ghanem ME. 2014. Effect of long term cadmium chloride exposure on testicular function in male albino rats. *Am J Anim Vet Sci*., **9:** 182-188.

El-Habit OH and Abdel Moneim AE. 2014. Testing the genotoxicity, cytotoxicity and oxidative stress of cadmium and nickel and their additive effect in male mice. *Biol Trace Elem Res*., **159:** 364–372.

Gana AJ and Toba AP. 2015. Environmental pollution and sustainability. *J Res Environ Sci Toxicol.*, **4(1):** 1-9.

Hassanein M M and Abedel-Razek AG. 2009. Chromatographic quantitation of some bioactive minor components in oils of wheat germ and grape seeds produced as by-products. *J Oleo Sci.*, **58:** 227–233.

Hasseeb MM, Al-Hizab FA and Hamouda MA. 2013. Impacts of grape seed oil supplementation against the acrylamide induced lesions in male genital organs of rats. *Pak Vet J*., **33:** 282–286.

Hayes J, Doherty AT, Adkins DJ, Oldman K and O'Donovan MR. 2009. The rat bone marrow micronucleus test-study design and statistical power. *Mutagenesis* **24 (5):** 419-24.

Honda R, Swaddiwudhipong W, Nishijo M, Mahasakpan P, Teeyakasem W and Ruangyuttikarn W. 2010. Cadmium induced renal dysfunction among residents of rice farming area downstream from a zinc-mineralized belt in Thailand. *Toxicol Lett.*, **198:** 26-32.

Islam MR, Shahnaj MP, Raihan MO, Hasan SMR and Islam ME. 2011. *In vitro* and *in vivo* antioxidant potential of ethanolic extract of *Syzigium jambos* (L) bark**.** *Int J Res Ayurveda Pharm*., **2:** 810-815.

Karaman S, Karasu S and Tornuk F. 2015. Recovery potential of cold press byproducts obtained from the edible oil industry: physicochemical, bioactive, and antimicrobial properties. *J Agric Food Chem.*, **63(8):** 2305–2313.

Karimi MM, Sani MJ, Mahmudabadi AZ, Sani AJ and Khatibi SR. 2012. Effect of acute toxicity of cadmium in mice kidney cells. *Iran J Toxicol*., **6:** 691–698.

Kaur S and Sharma S. 2015. Evaluation of toxic effect of cadmium on sperm count, sperm motility and sperm abnormality in albino mice. *Int J Adv Res*., **3:** 335–343.

Kikalishvili B, Zurabashvili D, Nikolaishvili M, Zurabashvili Z and Giorgobiani I. 2011. The most biological important constances of Rkatsiteli grape oil and its effect as a 5% and 10% food-additive. *Georgian Med News*., **195:** 85–87

Kisok K. 2012. Blood cadmium concentration and lipid profile in Korean adults. *Environ Res*., **112:** 225–229.

Kvist U and Björndahl L. 2002**. Manual on Basic Semen Analysis**. ESHRE Monographs. Oxford, United Kingdom: Oxford University Press.

Lin J and Tang C. 2007. Determination of total phenolic and flavonoid contents in selected fruits and vegetables, as well as their stimulatory effects on mouse splenocyte proliferatio. *Food Chem.***, 101(1):** 140-147.

Mahrous KF, Hassan AM, Radwan HA and Mahmoud MA. 2015. Inhibition of cadmium induced genotoxicity and histopathological changes in Nile tilapia fish by Egyptian and Tunisian montmorillonite clay. *Ecotoxicol Environ Saf*., **119**: 140–147.

Maier T, Schieber A, Kammerer D and Carle R. 2009. Residues of grape (*Vitis vinifera* L.) seed oil production as a valuable source of phenolic antioxidants. *Food Chem*., **112:** 551-559.

Miltonprabu N, Basher V and Manoharan E. 2016. Hepatoprotective effect of grape seed proanthocyanidins on cadmium-induced hepatic injury in rats: possible involvement of mitochondrial dysfunction, inflammation and apoptosis. *J Toxicol Rep*., **3:** 63-70.

Mokhtari M, sarkaki A, Sharifi E and Basiryan E. 2011. Antinociceptive effects of grape seed oil with use of formalin test in male rats. Inter Conference on Food Engineering and Biotechnol (**ICFEB)**, 48-53.

Murugavel P and Pari L. 2010. Effect of dially tetrasulfide on cadmium induced oxidative damage in the liver of rats. *Hum Exp Toxicol*., **26:** 527–534.

Narayana K, D'Souza UJA and Rao KPS. 2002. Ribavirin induced sperm shapeabnormalities in Wistar rats. *Mutat Res*., **513:** 193–196.

Naskar S, Islam A, Mazumder UK, Saha P, Haldar PK and Gupta M. 2010. *In vitro* and *in vivo* antioxidant potential of hydro-methanolic extract of *Phoenix dactylifera* fruits. *J Sci Res*., **2:** 144-157.

Obioha UE, Suru SM, Ola-Mudathir KF and Faremi TY. 2009. Hepatoprotective potentials of onion and garlic extracts on cadmium-induced oxidative damage in rats. *Biol Trace Elem Res*., **129:** 143-156.

Oliveira H, Spanò M, Santos C and Pereira M. 2009. Adverse effects of cadmium exposure on mouse sperm. *Reprod Toxicol*., **28:** 550–555.

Reitman A and Frankel S. 1957. A colorimetric method for the determination of serum glutamic oxalacetic and glutamic pyruvic transaminases. *Am J Clin Path*., **28:** 56.

Renugadevi J and Prabu SM. 2010. Cadmium-induced hepatotoxicity in rats and the protective effect of naringenin. *Exp Toxicol Pathol*., **62:** 171-181.

Salem NA and Salem EA. 2016. Hepatorenal and testicular protective effects of lycopene against cadmium induced toxicity in male rats. *J Nephrol Ther*., **6:** 265.

Shati AA. 2011. Effects of *Origanum majorana* L. on cadmium induced hepatotoxicity and nephrotoxicity in albino rats. *Saudi Med J*., **32(8):** 797-805.

Shi J, Yu J, Pohorly JE and Kakuda Y. 2003. Polyphenolics in grape seeds-biochemistry and functionality. *J Med Food*., **6(4):** 291-9.

Shinagawa FB, De Santana FC, Torres LRO and Mancini-Filho J. 2015. Grape seed oil: a potential functional food. *Food Sci Technol Campinas*., **35:** 399-406.

Shivananda NB, Dan Ramdath D, Marshall JR, Isitor G, Xue S and Shi J. 2011. Wound healing properties of the oils of *Vitis vinifera* and *Vaccinium macrocarpon*. *Phytother Res***., 25:** 1201–1208.

Singh RP, Murthy KN and Jayaprakasha GK. 2002. Studies on the antioxidant activity of pomegranate *(Punica granatum)* peel and seed extracts using *in vitro* models. *J Agric Food Chem***., 50:** 81-86.

Skipper A, Sims JN, Yedjou CG and Tchounwou PB. 2016. Cadmium chloride induces DNA damage and apoptosis of human liver carcinoma cells via oxidative stress. *Int J Environ Res Public Health*, **13:**1–10.

Soliman MM, Attia HF, Hussein MM, Hassan ME and Ismail TA. 2013. Protective effect of N-acetylcystiene against titanium dioxide nanoparticles modulated immune responses in male albino rats. *Am J Immunol*., **9:** 148-158.

Soliman MM, Baiomy AA and Yassin MH. 2015. Molecular and histopathological study on the ameliorative effects of curcumin against lead acetate-induced hepatotoxicity and nephrototoxicity in Wistar rats. *Biol Trace Elem Res*., **167:** 91-102.

Takahashi O and Oishi S. 2003. Testicular toxicity of dietarily or parenterally administered bisphenol A in rats and mice. *Food Chem Toxicol*., **41:** 1035-1044.

Tchounwou PB, Yedjou CG, Patlolla AK and Sutton DJ. 2012. Heavy metal toxicity and the environment. *Molecular, Clin Environ Toxicol.*, **3:** 133-164.

Virk P, Elobeid M, Hamad S, Korany Z and Al-Amin M. 2013. Ameliorative effects of *Emblica officinalis* and *Rosmarinus officinalis* on cadmium-induced oxidative stress in Wistar rats. *J Med Plants Res*., **7:** 805-818.

Wang H, Chang M, Peng T, Yang Y, Li N, Luo T, Cheng Y, Zhou M, Zeng X and Zheng L. 2017. Exposure to cadmium impairs sperm functions by reducing catsper in mice. *Cell Physiol Biochem.*, **42:** 44-54.

Yang XF, Ge YM, Jiang JQ, Xu ZY, Cui YH and Wang ZL. 2012a. Acute toxic effect of cadmium chloride in mice. *Chin J Vet Sci*., **32:** 467-471.

Yang XF, Ge YM, Zhang HT, Ning HM, Jiang JQ, Qi YH and Wang ZL. 2012b.Damaging effects of water-borne cadmium chloride on DNA of lung cells of immature mice. *Genet Mol Res*., **11:** 4323-4329.

Yildirim NC, Kandemir MF and Benzer F. 2011. Beneficial effects of grape seed extract against Cisplatin-induced testicular damage in rabbits. *Digest J Nanomat Biostruct.*, **6:** 155-159.

JJBS

Volume 13, Number 1,March 2020
ISSN 1995-6673
Pages 85 - 91

Jordan Journal of Biological Sciences

Process Optimization of Waste Corn Oil Hydrolysis Using Extracellular Lipase of *Tritirachium oryzae* W5H in Oil-Aqueous Biphasic System

Muhamad O. Al-limoun*

Department of Biological Sciences, Faculty of Science, Mutah University, Mutah, Karak, 61710 Jordan

Received April 4 , 2019; Revised May 29, 2019; Accepted June 1, 2019

Abstract

Increasing demands for efficient management of waste cooking oil were currently brought up to prevent sewer system blockage, reducing wastewater treatment cost and to overcome many environmental associated drawbacks. Among the several suggested approaches, ecofriendly bioconversion and biodegradation of waste oil using microbes and their enzymes were proposed and preferred. Therefore, in the current project, process optimization of domestically collected waste corn oil hydrolysis was performed by investigating the most relevant operational parameters. Maximum degree of hydrolysis of 96.8% with enzyme stability of 92% residual activity was achieved at the optimized operational parameters of pH 5.0, 33^{o}C, 300 rpm mixing speed in the presence of 4.6 g oil and 368.2 enzyme unit per g oil in 1:5 volume ratio biphasic reaction mixture. The reusability of the biocatalyst in further hydrolysis experiments under the previously described optimum conditions showed reduced results of approximately 62% hydrolysis after 12 hr reaction time due to enzyme instability. Previous studies regarding extracellular lipase production by the species *Tritirachium oryzae* W5H were not available in the literature, which makes this report the first reporting extracellular lipase production and application in waste oil hydrolysis. The recent results supported the employment of the extracellular lipase from the indigenous fungi *Tritirachium oryzae* W5H for the bioremediation of used cooking oil.

Keywords: *Tritirachium oryzae* W5H, Indigenous fungi, Extracellular lipase, Waste corn oil hydrolysis.

1. Introduction

Edible and non-edible vegetable oils are natural hydrocarbons of plant origin used tremendously in human life for cooking, as basic ingredients in processed foods and personal care products, in soaps and detergents manufacturing, and in many other commercial products. Despite of their importance in human life, the bulk emission of waste cooking oil originated from both domestic and industrial human activities has become a major concern of municipalities worldwide (Husain *et al*., 2014). Many serious environmental issues arise due to the impetuous and irresponsible practice of direct discharge of waste cooking oil into the sewer system, which causes the blockage of sewer pipes and finally leads to an increase of wastewater treatment cost (Lopes *et al*., 2019). Therefore, pretreatment, recycling, down cycling and valorization of waste cooking oil are important as to prevent sewer blockage and to reduce their environmental impacts (He *et al*., 2017; Husain *et al*., 2014). Furthermore, the International Fat, Oil and Grease (FOG) management programs has stressed considering waste oil as valuable and renewable resources rather than simply a waste (Wallace *et al*., 2017).

From the environmental point of view, the management of used oil through biotechnological processes is generally more preferable compared to the physical and chemical approaches. This ecofriendly bioconversion and bioremediation of waste cooking oil using the intracellular and extracellular activities of microorganisms or their enzymatic systems have been reported. For instance, high quality biodiesel and derived fuel were produced through enzymatic activities using food grease trap and low-quality oils feedstocks under milled conditions by immobilized lipases from *Candida antarctica*, *Thermomyces lanuginosa* and *Mucor miehei* (Pinotti *et al*., 2018; Chang *et al*., 2018; Vescovi *et al*., 2016). Furthermore, the microbial bioconversion of waste cooking oils supplemented to the growth media of *Yarrowia lipolytica* W29, *Aspergillus* and *Penicillium* strains enhanced lipase enzyme and lipid-rich biomasses production (Lopes *et al*., 2019; Papanikolaou *et al*., 2011). The bioconversion of residual soybean oil and palm oil-based waste cooking oil into the close analog of plastics, polyhydroxyalkanoates (PHAs), by *Cupriavidus necator* strains was also reported (Nascimento *et al*., 2018; Kamilah *et al*., 2018). Other valuable biomaterials such as rhamnolipid, biosurfactant, biolubricants, carotene and methane were also obtained through the microbial bioconversion of other waste cooking oils (Ozdal *et al*., 2017; Chowdhury *et al*., 2013; Nanou *et al*., 2017; Liu *et al*., 2018).

However, lipolytic hydrolysis of waste cooking oil is the main principle reaction in all aforementioned microbial and enzymatic bioprocesses. Lipases (EC 3.1.1.3) are

* Corresponding author e-mail: moallimoun@mutah.edu.jo.

biocatalysts that catalyze the hydrolysis of triacylglycerols into free fatty acids and glycerol (Preczeski *et al*., 2018). Subsequently, the free fatty acids and glycerol were utilized either by microbial or in enzymatic production of lubricants, biodiesel, lactic acid, ethanol and biosurfactants (Dobson *et al.*, 2012; Nicol *et al*., 2012; Chowdhury *et al*., 2016; Vescovi *et al*., 2016; Xu *et al*., 2016; Yuwa-amornpitak and Chookietwatana, 2018). Similar to other bioprocesses, successful lipolytic hydrolysis of waste cooking oil is influenced by biocatalyst availability and other operational parameters such as temperature, pH, aqueous phase to oil phase ratio, oil loading and mixing speed (Jamie *et al*., 2017). Therefore, in the current project, process optimization of waste corn oil hydrolysis was investigated using the extracellular lipase produced by the indigenous fungal strain *Tritirachium oryzae* W5H.

2. Materials and Methods

2.1. Fungal strain and enzyme production

The investigated lipolytic fungus strain, *Tritirachium oryzae* W5H, was recovered from contaminated indigenous soil samples obtained from olive oil mills in Al-Karak province, south of Jordan. The fungal strain was identified using internal transcribed spacer (ITS) sequencing (GENWIZ, USA). The ITS gene sequence was registered in NCBI database and MK028996 accession number was obtained. Extracellular lipase enzyme by *Tritirachium oryzae* W5H was produced under the optimized conditions of 0.5% (w/v) glycerol, 1.0% (w/v) peptone, 0.6% (w/v) olive oil and 0.5% (w/v) NaCl. The sterilized media (pH 6.0) were inoculated with 1.0 mL of 1.63 $x10^6$ spore suspension and incubated at 35°C with 150 rpm agitation speed (Incu-Shaker 10L, Benchmark, Germany) for 96 hr (unpublished results).

2.2. Process optimization of waste corn oil hydrolysis in oil-aqueous biphasic system

The optimization of bioprocess parameters of waste corn oil hydrolysis was performed using one parameter per time approach. The studied operational parameters include aqueous phase pH (4-6), reaction temperature (33-37^{o}C), mixing speed (100-400 rpm), waste corn oil amount (9.2, 6.9 and 4.6 g), hydrophobic organic solvents (cyclohexane, n-hexane and isooctane), oil to aqueous phase volume ratio (1:7.5, 1:5.0 and 1:2.5 v:v) and amount of enzyme loading (184.1, 276.1, and 368.2 enzyme unit per g oil). In addition, aqueous phase recovery percentage and biocatalysts reusability were also determined. The hydrolysis reaction of waste corn oil was conducted in oil-aqueous biphasic system. The waste corn oil was domestically-collected after two to three times frying activities.

The initial experiment of the biphasic system composed of 20 mL of crude enzyme filtrate (184.1 EU/g oil), citrate buffer solution (pH 5.0), distilled water (DW) and 9.2 g of waste corn oil incubated at 35^{o}C with 200 rpm mixing speed. In all experiments, the final concentration of citrate buffer in the aqueous phase and the oil to aqueous phase volume ratio were maintained as 50 mM and 1:5, respectively unless otherwise stated. All experiments were conducted as 12 hr time profile in 100 mL conical flask using multi-position magnetic stirrer (Super-Nuova Multi-Place, Thermo Scientific, USA) under controlled temperature (Incu-Shaker 10L, Benchmark, Germany). Sample aliquots were withdrawn every 2 hr of the reaction time and analyzed for degree of hydrolysis and lipase stability.

Hydrolysis degree (%) of waste corn oil was measured using the titration method of the reaction mixture against 0.2 M KOH solution. Residual activity of lipase enzyme through the course of the reaction was evaluated and compared to the original activity at zero time. The composition of the blank experiment was formulated and incubated as the test experiment with the exception that the crude enzyme filtrate was replaced with thermally deactivated enzyme filtrate (DeAngelis *et al*., 2007).

2.3. Enzyme recovery and reusability

The aqueous phase containing the applied crude enzyme in the biphasic reaction mixture was separated from the oil phase using separation funnel. The recovery percentage of the separated aqueous phase was calculated from the ratio between the recovered volume and the original volume applied multiplied by 100%. The possible reusability of the recovered biocatalysts was measured by applying the recovered aqueous solution in the second hydrolysis experiment. The obtained degrees of hydrolysis from the second run were expressed as time profile and compared with the results of the degrees of hydrolysis of the initial experiment.

2.4. Enzyme stability

Enzyme stability throughout the course of the reaction was assessed by measuring the remaining enzyme activity for every 2 hr. Enzyme stability was expressed as residual activity (%) calculated from the ratio between the enzyme activity obtained throughout the course of the reaction and the original activity at zero time multiplied by 100%. Lipase activity was determined using copper soap colorimetry method as described by Kwon and Rhee (1986). The intensity absorbance of the recovered green color of isooctane phase containing the liberated free fatty acids-copper complex was measured at 715 nm (SPUV-19, SCO TECH, Germany) and compared to oleic acid as standard curve. One unit (U) of lipase enzyme activity was defined as: the amount of lipase enzyme that releases 1.0 µmol of free fatty acid per min under specific assay conditions.

2.5. Degree of waste corn oil hydrolysis

Hydrolysis degree of waste corn oil was obtained through titration of 2.0 mL sample aliquots of the hydrolysis reaction mixture by 0.2 M potassium hydroxide using digital titration system (Digitrate, Jencons, UK). To each sample, 15 mL of diethyl ether-ethanol mixture (1:1 v:v) containing phenolphthalein as pH indicator was added. Acid value (AV) was calculated using the following equation:

$$AV = \frac{56.1\ X\ CKOH\ X\ Vtitra}{m}$$

where CKOH is the concentration of KOH (M), Vtitra is the amount of titration (mL) and m is the amount of oil sample (g). Hydrolysis degree (X%) was calculated using the following equation:

$$X\% = \left(\frac{AV}{SV}\right) X\ 100\%$$

The saponification value of 92.3 ± 0.52 for waste corn oil was determined experimentally according to the AOAC Official Method 920.160 (1989).

2.6. Statistical analysis

Results were expressed as the mean value of three independent determinations. Standard deviations for each of the experimental results were indicated by error bars in the figures and were calculated using Microsoft Excel software (2010). Student *t* test was performed using SPSS version 16.0.1. Significant differences from the experiment with the highest degree of hydrolysis were designated in figures as $*$ ($p \leq 0.05$).

3. Results

3.1. Extracellular lipase production by Tritirachium oryzae W5H

Extracellular lipase production by *T. oryzae* W5H was carried out using the optimized enzyme production medium. Maximum lipase production of 84.7 ± 0.63 U/mL was obtained under the improved production conditions and medium composition. The extracellular crude enzyme filtrate used in the subsequent waste corn oil hydrolysis experiments was obtained through filtration.

3.2. Process optimization of waste corn oil hydrolysis in biphasic oil-aqueous system

3.2.1. Effect of pH

The influence of the aqueous phase pH on the extracellular lipase catalytic activity and stability was illustrated in Figure 1. It was observed that the highest hydrolysis percentage of 42.5% of waste corn oil occurred at the most stable pH of 5.0 suggesting the hydrolytic activity relatively depending on the enzyme stability. A slight deviation from the optimum pH by 1.0 unit led to significant reduction in oil hydrolysis noted as 35.8 and 37.2% at pH 4.0 and 6.0, respectively.

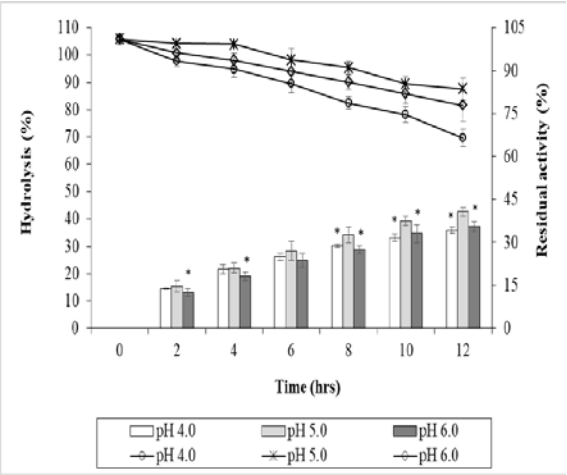

Figure 1. Effect of aqueous phase pH on lipase enzyme activity in waste corn oil hydrolysis. Columns represent the oil hydrolysis results while lines represent enzyme stability results.

3.2.2. Effect of temperature

As demonstrated in Figure 2, comparable degrees of hydrolysis with non-significant differences of 42.7 and 43.1% were obtained when the hydrolysis experiments were conducted at 33 and 35°C, respectively. Meanwhile, at elevated temperature of 37°C, less enzyme activity together with lesser enzyme stability were detected. The results clearly indicated the direct impact of operating temperature on enzyme stability and hence enzyme activity in oil hydrolysis. Although a higher degree of hydrolysis was obtained at 35°C, the following experiments were conducted at 33°C taking into consideration the highest enzyme stability of 91.7% residual activity which is 10% higher compared to the enzyme stability at 35°C.

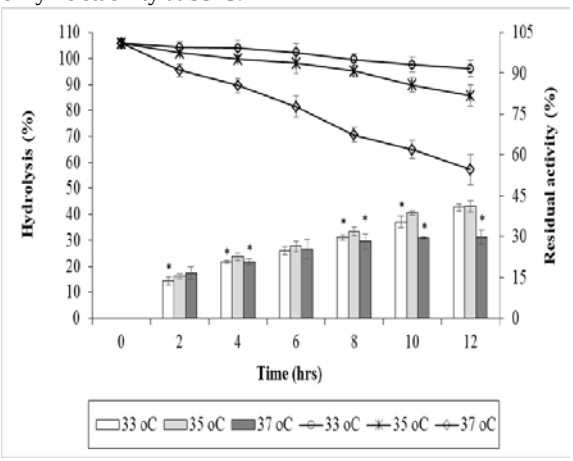

Figure 2. Effect of incubation temperature on extracellular lipase activity in waste corn oil hydrolysis. Columns represent the oil hydrolysis results while lines represent enzyme stability results.

3.2.3. Effect of mixing speed

An investigation into the impacts of 100, 200, 300 and 400 rpm mixing speeds of the reaction mixture was conducted in order to determine their effects on waste corn oil hydrolysis process (Figure 3). The results clearly indicated that a maximum degree of hydrolysis of 48.3% was obtained at 300 rpm mixing speed. At lower or higher rotation speeds, significantly less corn oil hydrolysis was obtained. However, enzyme stability was not affected by the mechanical shearing as comparable residual activities were obtained throughout all the investigated mixing speeds.

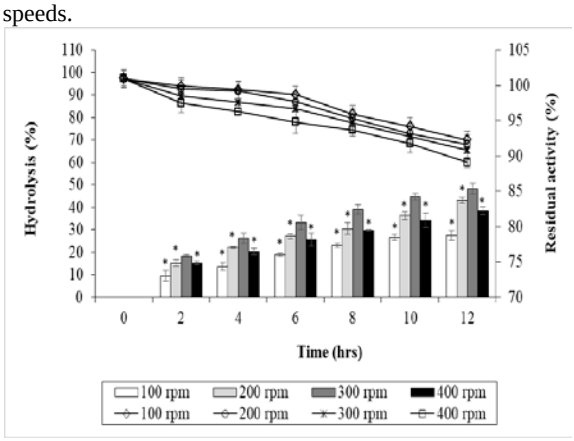

Figure 3. Effect of mixing speed (rpm) on extracellular lipase activity in waste corn oil hydrolysis. Columns represent the oil hydrolysis results while lines represent enzyme stability results.

3.2.4. Effect of waste corn oil amount

In this experiment, the effect of waste corn oil amount on degree of hydrolysis was evaluated. From the results

presented in Figure 4, the waste corn oil amounts 9.2, 6.9 and 4.6 g showed significantly linear improvements in the degree of oil hydrolysis when the substrate concentration was lowered. Maximum degree of hydrolysis was obtained when 4.6 g waste corn oil was applied into the reaction mixture with 72.8 hydrolysis percentage recorded after 12 hr. Obviously, enzyme stability was not a critical determinant in this experiment as similar stability results with more than 91% residual activities were attained throughout the 12 hr reaction time.

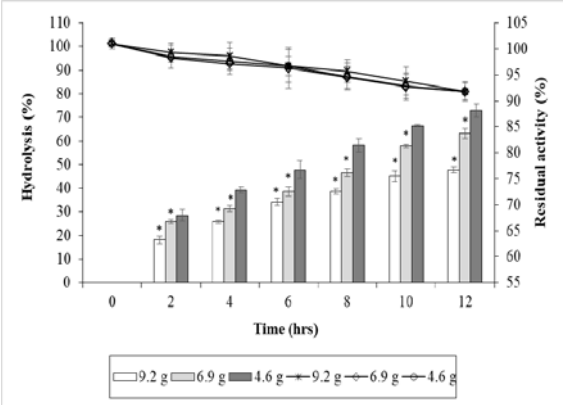

Figure 4. Effect of waste corn amount on extracellular lipase activity in waste corn oil hydrolysis. Columns represent the oil hydrolysis results while lines represent enzyme stability results.

3.2.5. Effect of organic solvents

Hydrophobic organic solvents of cyclohexane, n-hexane and isooctane were tested for their effect on the hydrolysis of waste corn oil by the crude lipase of *T. oryzae* W5H (Figure 5). All the tested water immiscible organic solvents have negative effects on the enzyme stability and therefore result in significantly lower waste corn oil hydrolysis percentage as compared with the control. Cyclohexane showed the lowest enzyme stability and hydrolysis results followed by n-hexane and finally isooctane. Therefore, the following experiments were conducted without the addition of any organic solvents to the oil phase.

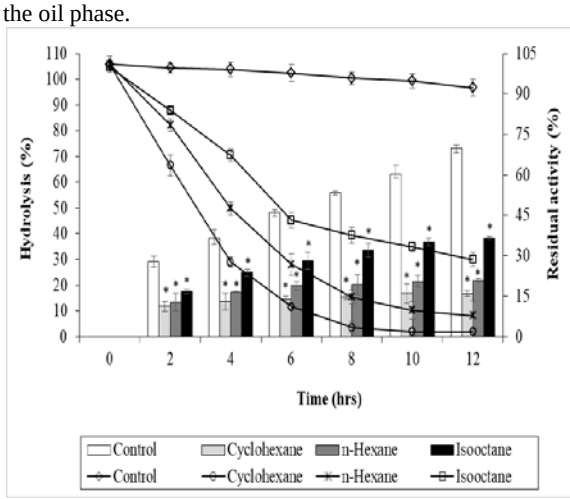

Figure 5. Effect of immiscible organic solvents on extracellular lipase activity in waste corn oil hydrolysis. Columns represent the oil hydrolysis results while lines represent enzyme stability results.

3.2.6. Effect of oil to aqueous phase volume ratio

The time profiles in Figure 6 illustrated the influence of the varied volume ratios between the two phases of the reaction mixture on waste corn oil hydrolysis degree. The maximum degree of hydrolysis of 72.9% was recorded when the volume ratio of the two phases was maintained as 1:5 (v:v). On the other hand, a significant reduction in oil degree of hydrolysis results was observed at lower and higher investigated volume ratios with the lowest recorded as 37.2% when the volume ratio was adjusted to 1:2.5 (v:v). It was also noted that the residual enzyme activity remains constant between 89-91% throughout the entire time profile, suggesting the negligible effect of the studied parameter on enzyme stability.

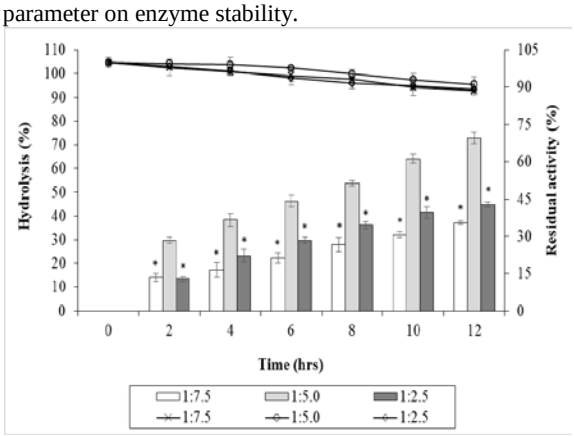

Figure 6. Effect of oil to aqueous phase volume ratios on extracellular lipase activity in waste corn oil hydrolysis. Columns represent the oil hydrolysis results while lines represent enzyme stability results.

3.2.7. Effect of enzyme loading on waste corn oil hydrolysis

As depicted in Figure 7, the increment in enzyme loading per gram oil showed a significant improvement in oil degree of hydrolysis. The maximum degree of hydrolysis of 96.8% was achieved when the highest enzyme loading of 368.2 EU per g oil was applied, indicating the importance of biocatalyst availability in oil hydrolysis applications. The accumulative effect of various parameters on waste corn oil hydrolysis showed a significant improvement in the degree of hydrolysis from 42.5% to 96.8% after optimization. The results of the enzyme stability analysis showed that 90-92% residual activity could be maintained by applying the optimized operational parameters, which is preferable in such kinds of enzymatic applications.

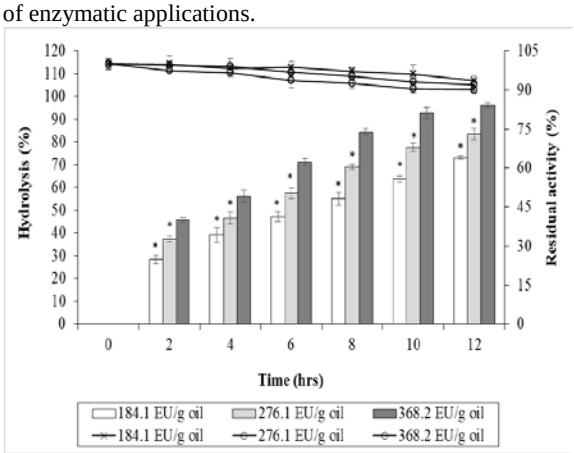

Figure 7. Effect of enzyme loading on extracellular lipase activity in waste corn oil hydrolysis. Columns represent the oil hydrolysis results while lines represent enzyme stability results.

3.3. Recovery and reusability

A total of 20.3 mL aqueous phase representing 80.1% of the original aqueous phase applied in the first run was recovered. The recovered volume of the aqueous phase was topped up to 25 mL using used aqueous phase collected from other flasks. The results in Figure 8 showed that when the recovered biocatalysts were used in second hydrolysis experiment, the enzyme gave significantly much lower hydrolysis results compared to the fresh biocatalysts. Such reduced results can be explained through the enzyme stability analysis as the enzyme gradually lost most of its activity throughout the course of the reaction reaching 23.1% residual activity after 12 hrs reaction time. Meanwhile, throughout the first 12 hrs in the first run the enzyme maintained 92.1% of its original activity.

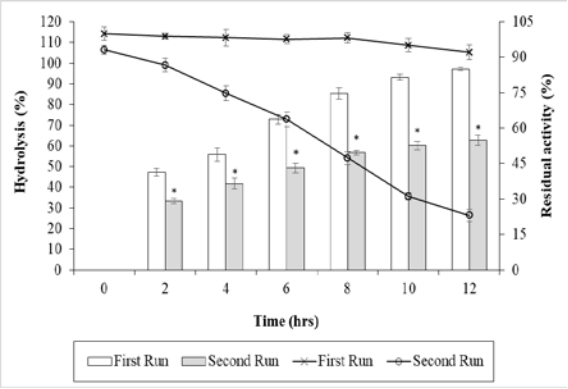

Figure 8. Enzyme reusability in waste corn oil hydrolysis. Columns represent the oil hydrolysis results while lines represent enzyme stability results.

4. Discussion

From the environmental point of view, enzyme mediated oil biodegradation processes are more preferable than other conventional methods (Goswami *et al*., 2013). The involvement of microorganisms and their associated lipolytic enzymes in the bioremediation of lipidic contaminated wastewater represent a promising opportunity in wastewater treatment (Hu *et al*., 2018). Higher waste oil hydrolysis can be achieved under improved process parameters that support higher enzyme activity and maintain its stability at longer reaction times (Kanmani *et al*., 2015; Goswami *et al*., 2009). Therefore, in the current study the effects of several operational parameters on waste corn oil hydrolysis by *T. oryzae* W5H extracellular lipase were evaluated.

When investigated, the pH of the aqueous phase showed a direct influence on the enzyme catalytic activity and stability. pH 5.0 was observed as the optimum pH when the enzyme was most active and stable. The lower activity and stability results observed at other investigated pH values were most probably due to the influence of pH on the ionization state of the enzyme causing progressive reduction in the enzyme activity and stability (Goswami *et al*., 2009). The enhanced degree of hydrolysis of waste oil observed at 33 and 35^{o}C can be accredited to the preferable catalytic activity and substrate solubility at the aforementioned temperatures (Goswami and Basu, 2012). At an elevated temperature of 37^{o}C, the reduction in hydrolysis rate and enzyme stability might be due to the effect of temperature on the ionization state of catalytically important amino acids in the active site and the state of the reaction emulsion interface (Gupta *et al*., 2012; Maidina *et al*., 2008).

The linear enhancement in waste corn oil hydrolysis with the increment of mixing speed that peaked at 300 rpm can be explained by the continuous formation of smaller oil droplets that leads to interfacial contact enhancement between the enzyme and substrate (Jamie *et al*., 2017). Lower enzyme activity obtained at higher mixing speed of 400 rpm was most properly due to the desorption of the enzyme from the interface (Al-Zuhair *et al*., 2008) rather than the deactivation of the enzyme by the mechanical shear stress (Raspe *et al*., 2013), which was proven by the enzyme stability results. The highest degradation rate at lower substrate concentration (4.6 g oil) was expected due to the presence of proportional substrate molecules to access the active sites of the available enzymes at the interface (Cavalcanti-Oliveira *et al*., 2011). On the other hand, the depleted hydrolysis results at higher substrate concentrations can be explained by the saturation of the active sites with the excess substrate molecules and not enzyme intolerance toward higher substrate concentrations as indicated by enzyme stability findings (Serri *et al*., 2008).

Although they are not preferable additives (Jamie *et al*., 2017), hydrophobic organic solvents are routinely included in oil hydrolysis processes to promote the reaction by reducing substrate viscosity by forming finer oil droplets with better interfacial area (Raspe *et al*., 2013). However, this was not the case in the current work as the addition of the three hydrophobic organic solvents resulted in less degrees of oil hydrolysis compared to the control reaction due to the interfacial tension destabilizing the molecular forces of the enzyme (Kumar *et al*., 2016; Al-limoun *et al*., 2015). The order of the catalytic performance and the stability of the enzyme in presence of organic solvents were in correlation with the partitioning coefficient (log p) of the tested solvents with the highest stability, and hence activity, obtained in the presence of the most hydrophobic solvent, isooctane (Priyanka *et al*., 2019; Al-limoun *et al*., 2019).

As the hydrolysis action of the lipase enzyme occurs at the interface of the emulsion, the increase in the aqueous phase volume up to 1:5 (v/v) ratio improved waste corn oil degradation due to the increase in the interfacial area and substrate availability at the interface. Meanwhile, excess amount of aqueous phase reduced enzyme activity due to the competition of water molecules with the substrate for the active site of the enzyme (Nguyen *et al*., 2018). The elevated improvement in the degree of hydrolysis with the increase in enzyme concentration can be accredited to the accumulative adsorption of enzyme molecules monolayer at the interface of the reaction-reaching saturation point (Jamie *et al*., 2017; Santos *et al*., 2015). Finally, the unfortunate reusability results of the biocatalyst in relation to the initial run can be explained by the instability of the enzyme in prolonged repetitive application.

5. Conclusion

The influences of the reaction parameters on waste corn oil hydrolysis by *T. oryzae* W5H extracellular crude lipase were explored using stepwise evaluation approach. The

stepwise improvement of waste corn oil hydrolysis resulted in 96-97% hydrolysis with residual activity of 92.1%. Unfortunately, the reuse of the recovered enzyme in second hydrolysis experiment resulted in much less hydrolysis percentage due to the instability of the enzyme in longer operation time. The current results indicated the potential use of the extracellular lipase enzyme produced by *T. oryzae* W5H in the bioremediation of used cooking oil under either a natural or an experimental environment.

Acknowledgment

This study was funded by the Deanship of Scientific Research, Mu'tah University-Jordan (grant No. 120/14/ 321).

References

Allimoun MO, Ananzeh MR and Khleifat KM. 2015. Screening selection and optimization of extracellular methanol and ethanol tolerant lipase from *Acinetobacter* sp. K5b4. *Int J Biosci.*, **6**: 44-56.

Al-Limoun MO, Khleifat KM, Alsharafa KY, Qaralleh HN and Alrawashdeh SA. 2019. Purification and characterization of a mesophilic organic solvent tolerant lipase produced by *Acinetobacter* sp. K5b4. *Biocatal Biotransform.*, **37**: 139-151.

Al-Zuhair S, Ramachandran KB and Hasan M. 2008. Effect of enzyme molecules covering of oil–water interfacial area on the kinetic of oil hydrolysis. *Chem Eng J.*, **139**: 540-548.

American Oil Chemists' Society. 1989. AOCS Official Method 920.160. **Saponification Value. Sampling and Analysis of Commercial Fats and Oils**. Champaign, Illinois:

Cavalcanti-Oliveira EDA, Silva PRD, Ramos AP, Aranda DAG and Freire DMG. 2011. Study of soybean oil hydrolysis catalyzed by *Thermomyces lanuginosus* lipase and its application to biodiesel production via hydroesterification. *Enzyme Res.*, 2011, Article ID 618692, 8 pages.

Chang FC, Tsai MJ and Ko CH. 2018. Agricultural waste derived fuel from oil meal and waste cooking oil. *Environ Sci Pollut Res Int.* , **25**: 5223-5230.

Chowdhury A, Mitra D and Biswas D. 2013. Biolubricant synthesis from waste cooking oil via enzymatic hydrolysis followed by chemical esterification. *J Chem Technol Biotechnol.*, **88**: 139-144.

Chowdhury A, Sarkar D and Mitra D. 2016. Esterification of free fatty acids derived from waste cooking oil with octanol: Process optimization and kinetic modeling. *Chem Eng Technol.*, **39**: 730-740.

DeAngelis YM, Saunders CW, Johnstone KR, Reeder NL, Coleman CG, Kaczvinsky Jr JR, ... and Keough TW. 2007. Isolation and expression of a *Malassezia globosa* lipase gene, LIP1. *J Investig Dermatol*, **127**: 2138-2146.

Dobson R, Gray V and Rumbold K. 2012. Microbial utilization of crude glycerol for the production of value-added products. *J Ind Microbiol Biotechnol.*, **39**: 217-226.

Goswami D, Basu JK and De S. 2009. Optimization of process variables in castor oil hydrolysis by *Candida rugosa* lipase with buffer as dispersion medium. *Biotechnol Bioprocess Eng.*, **14**: 220-224.

Goswami D, Basu JK and De S. 2013. Lipase applications in oil hydrolysis with a case study on castor oil: a review. *Crit Rev Biotechnol.*, **33**: 81-96.

Goswami D, De S and Basu JK. 2012. Effects of process variables and additives on mustard oil hydrolysis by porcine pancreas lipase. *Braz J Chem Eng*, **29**: 449-460

Gupta S, Ingole P, Singh K and Bhattacharya A. 2012. Comparative study of the hydrolysis of different oils by lipase-immobilized membranes. *J Appl Polym Sci*, **124**: 17-26.

He X, de los Reyes III FL and Ducoste JJ. 2017. A critical review of fat, oil, and grease (FOG) in sewer collection systems: Challenges and control. *Crit Rev Environ Sci Technol*, **47**: 1191-1217.

Hu J, Cai W, Wang C, Du X, Lin J and Cai J. 2018. Purification and characterization of alkaline lipase production by *Pseudomonas aeruginosa* HFE733 and application for biodegradation in food wastewater treatment. *Biotechnol Biotechnol Equip*, **32**: 583-590.

Husain IA, Alkhatib MAF, Jammi MS, Mirghani ME, Zainudin ZB and Hoda A. 2014. Problems, control, and treatment of fat, oil, and grease (FOG): a review. *J Oleo Sci*, **63**: 747-752.

Jamie A, Alshami AS, Maliabari ZO and Ateih MA. 2017. Development and validation of a kinetic model for enzymatic hydrolysis using *Candida rugosa* lipase. *J Bioprocess Biotech*, **7**: 297.

Kamilah H, Al-Gheethi A, Yang TA and Sudesh K. 2018. The use of palm oil-based waste cooking oil to enhance the production of Polyhydroxybutyrate [P (3HB)] by *Cupriavidus necator* H16 strain. *Arab J Sci Eng*, **43**: 3453-3463.

Kanmani P, Kumaresan K and Aravind J. 2015. Utilization of coconut oil mill waste as a substrate for optimized lipase production, oil biodegradation and enzyme purification studies in *Staphylococcus pasteuri*. *Electron J Biotechnol*, **18**: 20-28.

Kumar A, Dhar K, Kanwar SS and Arora PK. 2016. Lipase catalysis in organic solvents: advantages and applications. *Biol Proced Online*, **18**: 2.

Kwon DY and Rhee JS. 1986. A simple and rapid colorimetric method for determination of free fatty acids for lipase assay. *J Am Oil Chem Soc.*, **63**: 89-92.

Liu P, Ji J, Wu Q, Ren J, Wu G, Yu Z, Xiong J, Tian F, Zafar Y and Li X. 2018. *Klebsiella pneumoniae* sp. LZU10 degrades oil in food waste and enhances methane production from co-digestion of food waste and straw. *Int Biodeter Biodegrad.*., **126**: 28-36.

Lopes M, Miranda SM, Alves JM, Pereira AS and Belo I. 2019. Waste cooking oils as feedstock for lipase and lipid-rich biomass production. *Eur J Lipid Sci Technol.*, **121**: 1800188.

Maidina AB, Belova AB, Levashov AV and Klyachko NL. 2008. Choice of temperature for safflower oil hydrolysis catalyzed by *Candida rugosa* lipase. *Moscow Univ Chem Bull.*, **63**: 108-110.

Nanou K, Roukas T, Papadakis E and Kotzekidou P. 2017. Carotene production from waste cooking oil by *Blakeslea trispora* in a bubble column reactor: The role of oxidative stress. *Eng Life Sci.***, 17**:775-780.

Nascimento LL, Neves Nunes JM, Rodrigues PR and Druzian JI. 2018. Bioconversion of residual soybean oil into polyhydroxyalkanoates. *J Appl Polym Sci.*, **135**: 46255.

Nguyen TAV, Le TD, Phan HN and Tran LB. 2018. Hydrolysis activity of virgin coconut oil using lipase from different sources. *Scientifica*, **2018:** Article ID 9120942, 6 pages.

Nicol RW, Marchand K and Lubitz WD. 2012. Bioconversion of crude glycerol by fungi. *Appl Microbiol Biotechnol.*, **93**: 1865-1875.

Ozdal M, Gurkok S and Ozdal OG. 2017. Optimization of rhamnolipid production by *Pseudomonas aeruginosa* OG1 using waste frying oil and chicken feather peptone. *Biotech.*, **7**: 117.

Papanikolaou S, Dimou A, Fakas S, Diamantopoulou P, Philippoussis A, Galiotou-Panayotou M and Aggelis G. 2011. Biotechnological conversion of waste cooking olive oil into lipid-rich biomass using *Aspergillus* and *Penicillium* strains. *J Appl Microbiol.*, **110**: 1138-1150.

Pinotti LM, Benevides LC, Lira TS, de Oliveira JP and Cassini ST. 2018. Biodiesel production from oily residues containing high free fatty acids. *Waste Biomass Valori*, **9**: 293-299.

Preczeski KP, Kamanski AB, Scapini T, Camargo AF, Modkoski TA, Rossetto V, ... and Treichel H. 2018. Efficient and low-cost alternative of lipase concentration aiming at the application in the treatment of waste cooking oils. *Bioprocess Biosyst Eng.*, **41**: 851-857.

Priyanka P, Kinsella G, Henehan GT and Ryan BJ. 2019. Isolation, purification and characterization of a novel solvent stable lipase from *Pseudomonas reinekei*. *Protein Expr Purif*, **153**: 121-130.

Raspe DT, Cardozo Filho L and da Silva C. 2013. Effect of additives and process variables on enzymatic hydrolysis of macauba kernel oil (*Acrocomia aculeata*). *Int J Chem Eng.*, **2013**: ,Article ID438270,8pages.

Santos LD, Coutinho JA and Ventura SP. 2015. From water-in-oil to oil-in-water emulsions to optimize the production of fatty acids using ionic liquids in micellar systems. *Biotechnol Prog.*, **31**: 1473-1480.

Serri NA, Kamarudin AH and Rahaman A. 2008. Preliminary studies for production of fatty acids from hydrolysis of cooking palm oil using *C. rugosa* lipase. *J Phys Sci.*, **19**: 79-88.

Vescovi V, Rojas MJ, Baraldo Jr A, Botta DC, Santana FAM, Costa JP, … and Tardioli PW. 2016. Lipase-catalyzed production of biodiesel by hydrolysis of waste cooking oil followed by esterification of free fatty acids. *J Am Oil Chem Soc.*, **93**: 1615-1624.

Wallace T, Gibbons D, O'Dwyer M and Curran TP. 2017. International evolution of fat, oil and grease (FOG) waste management–a review. *J Environ Manage.*, **187**: 424-435.

Xu MH, Kuan IC, Deng FY, Lee SL, Kao WC and Yu CY. 2016. Immobilization of lipase from *Candida rugosa* and its application for the synthesis of biodiesel in a two-step process. *Asia-Pac J Chem Eng.*, **11**: 910-917.

Yuwa-amornpitak T and Chookietwatana K. 2018. Bioconversion of waste cooking oil glycerol from cabbage extract to lactic acid by *Rhizopus microsporus*. *Braz J Microbiol.*, **49**: 178-184.

JJBS

Volume 13, Number 1,March 2020
ISSN 1995-6673
Pages 93 - 100

Jordan Journal of Biological Sciences

Molecular and Biochemical Changes of Indole-3-Acetic Acid in the Expanding Leaves of Barley (*Hordeum vulgare* L.) under Salinity Stress

Amal M. Harb[1*], Khaldoun J. AL-Hadid[2] and Ahmad S. Sharab[2]

[1]*Department of Biological Sciences, Faculty of Science, Yarmouk University;* [2]*Department of Biological Sciences, Faculty of Science, The University of Jordan, Jordan*

Received April 28, 2019; Revised May 30, 2019; Accepted June 1, 2019

Abstract

Indole-3-acetic acid (IAA) is a major natural auxin that plays a crucial role in many developmental and physiological processes in plants and in plants' tolerance to abiotic stress such as salinity. Salinity is a major abiotic stress that threatens many important crops such as barley. In this study, IAA biosynthesis genes of the YUC family and the IAA transport genes of the PIN family were identified in barley. Eight YUC genes (*HvYUCs*) and 8 PIN genes (*HvPINs*) were identified in barley. Phylogenetic analysis revealed that the majority of YUC and PIN genes were evolutionarily related to their orthologues in arabidopsis and rice. Conserved domain analysis revealed the presence of domains characteristic of these gene families. The results of IAA quantification showed a rapid decrease in IAA concentration upon exposure to salinity (at day 1 of salinity stress). After this rapid decrease, IAA concentration increased to normal levels compared with the control plants (at day 2, 4, and 8 of salinity stress). The transcription profile analysis of *HvYUCs* and *HvPINs* genes revealed differential changes in gene transcription level at different time points of salinity stress. This suggests a key role of IAA in barley as a physiological response to salinity stress.

Keywords:Abiotic stress, Auxin, Genes, HvYUCs, HvPINs.

1. Introduction

Salinity is a major abiotic stress that threatens the growth and reproduction of different crop plants. In fact, salinity stress results in great losses in the yield of many important crops. Moreover, a high percentage of land worldwide cannot be cultivated due to high salinity while a high percentage of the world population is undernourished. According to the Food and Agriculture Organization (FAO) (2018), about one out of every nine people is undernourished. Therefore, good efforts are needed to increase crop production to meet the increasing demand for food by the world's population.

Salinity stress affects the growth of plants in two phases. During the first phase, it causes osmotic stress that reduces water absorption by plants and eventually leads to growth retardation. Growth retardation is a consequence of the inhibition of photosynthesis. Photosynthesis is inhibited due to low CO_2 concentration, which results from stomatal closure under water deficit in the first phase of salinity stress (Sudhakar *et al*., 2001; Abogadallah 2010; Marti *et al.*, 2011). In the second phase, salt ions accumulate in plant tissues, resulting in salt toxicity (Munns and Tester 2008).

Plants are complex biological systems and they can respond to salinity stress through a wide variety of molecular, biochemical, physiological, and morphological changes. The response of plants to salinity stress depends on the genotype, species, and developmental stage. Many strategies have been developed by plants to minimize the negative effects of salinity stress (Prasch and Sonnewald 2015). Under stress conditions, plants reallocate energy and nutrients toward defense responses to save their reproductive capacity. Changes in the allocation of energy and nutrients under stress conditions are mediated by complex signaling networks. Moreover, this redirection of resources by the stressed plants has many consequences, including early flowering and a reduction in the accumulation of biomass (Munns and Gilliham 2015; Prasch and Sonnewald 2015).

Barley (*Hordeum vulgare*) is the fourth largest crop worldwide and is cultivated in relatively dry areas (Distelfed *et al.,* 2014; Hiei *et al.,* 2014). Unlike wheat (*Triticum aestivum*), barley is used mainly as animal feed. The barley genome is diploid (2n=2x=14), with a size of about 5.1 Gb (Bennett and Leitch 2012). Under environmental stresses, barley exhibits more stress tolerance than wheat; however, barley yield is estimated to decrease under future stress conditions such as increased salinity (Ingvordsen *et al.,* 2015).

Plant hormones were shown to play an important role in the adaptation of plants to different abiotic stresses through several responses (Peleg and Blumwald 2011; Bielach *et al.,* 2017). Indeed, a deep understanding of the role played by plant hormones and their interactions under

* Corresponding author e-mail: aharb@yu.edu.jo.

abiotic stress might pave the way for the targeted genetic engineering of stress-tolerant crops (Wani *et al.,* 2016). Many previous studies have shown the important role of plant hormones in response to salinity stress (Javid *et al.,* 2011; Kaya *et al.,* 2009; Ryu and Cho 2015).

As a major plant hormone, auxin is a key regulator of plant growth and development, and many other biological processes (Vanneste and Friml 2009; Balzan *et al.,* 2014). Auxin homeostasis in plants is regulated by the *de novo* biosynthesis, transport, conjugation/deconjugation, and inactivation (Korasick *et al.,* 2013). Indole-3-acetic acid (IAA) is the most common auxin in plants (Korasick *et al.,* 2013). In poplar plants (*Populus euphratica and Populus x canescens*), free IAA was decreased in the xylem of salinity treated plants for 48 h (Junghans *et al.,* 2006). The level of phytohormones, including IAA, was also decreased in creeping bentgrass (*Agrostis stolonifera*) plants under salinity (Krishnan and Merewitz 2015). A decrease in IAA levels under salinity stress was also shown in rice (*Oryza sativa*) and tomato (*Solanum lycopersicum*) (Nilsen and Orcutt 1996; Dunlap and Binzel 1996, respectively). Long-term exposure (10, 15, and 22 days) of tomato plants to 100 mM NaCl resulted in a highly significant decrease of IAA level with treatment time (Ghanem *et al.,* 2008). In maize (*Zea mays*), a salinity-tolerant genotype maintained the level of IAA in its root under salinity, whereas the level of Indole Butyric acid (IBA) was increased in its leaves (Zörb *et al.,* 2013). An increase in IAA level was shown in wild species of common bean (*Phaseolus vulgaris*), whereas a decrease in its level was shown in the cultivated species (Yurekli *et al.,* 2004).

There are two biosynthetic pathways for IAA: tryptophan-dependent and tryptophan-independent (Woodward and Bartel 2005). Based on numerous recent studies, the tryptophan-independent pathway is not a major pathway for auxin biosynthesis in plants (Kasahara 2016). The tryptophan-dependent pathway was shown to occur via different pathways: the indole-3-acetamide (IAM) pathway; the indole-3-pyruvic acid (IPA) pathway; the tryptamine (TAM) pathway; and the indole-3-acetaldoxmide (IAOX) pathway (Mano and Nemoto 2012). From an evolutionary point of view, it was suggested that either IAM and/or IPA is the major auxin biosynthetic pathway in plants (Mano and Nemoto 2012). Moreover, many biochemical and genetic studies have demonstrated the critical role of the IPA biosynthetic pathway in auxin biosynthesis in many plant species such as maize, rice, *Arabidopsis thaliana*, and *Marchantia polymorpha* (Kasahara 2016). Indeed, this pathway is the first completely identified biosynthesis pathway of auxin, and it is shown to be conserved in land plants (Mashiguchi *et al.,* 2011; Kasahara 2016). The two main gene families in the IPA pathway are TAA1/TAR (aminotransferases) and the YUC (flavin monooxygenases) gene families (Zhao 2012). The YUC genes catalyze the rate-limiting step in auxin biosynthesis (Zhao 2012). Orthologs of the *TAA1/TAR* genes and of *YUC* genes are widely distributed in vascular and nonvascular plants (Kasahara 2016).

A major aspect of auxin biology is its differential distribution, which is achieved by polar auxin transport (Balzan *et al.,* 2014). The polar transport of auxin is crucial for normal development and in response to external environmental changes. Four types of auxin transporters were identified in plants: the PIN-FORMED (PIN) exporters, the ATP-binding cassette (ABC)-B/multi-drug resistance/P-glycoprotein (ABCB/MDR/PGP) subfamily of ABC transporters, the AUXIN1/LIKE-AUX1 (AUX/LAX) importers, and the newly described PIN-LIKES (PILS) proteins (Balzan *et al.,* 2014). Auxin transport was mostly studied in Arabidopsis and in monocot models such as rice, maize, *Sorghum bicolor*, and *Brachypodium distachyon* (Balzan *et al.,* 2014). In a latest review, short- as well as long-distance auxin transport was shown to be critical for different physiological responses of plants under different environmental conditions (Korver *et al.,* 2018).

The objective of this study was to investigate the contribution of IAA in the response of barley plants to salinity stress. To fulfill this objective, changes in IAA concentration at the biochemical and molecular levels in barley plants under salinity stress were monitored. Changes in the level of IAA in the expanding leaf of barley plants under salinity stress were recorded in a time course. Moreover, a time course of the transcription profile of selected IAA biosynthesis and transport genes in the expanding barley leaves was tested under salinity stress.

2. Materials and Methods

2.1. Identification of auxin biosynthesis and transport genes in barley

For the identification of barley orthologous genes, gene sequences for auxin biosynthesis (YUC genes) and transport (PIN genes) of *Arabidopsis thaliana* were retrieved from TAIR (https://www.arabidopsis.org/). These sequences were then blasted against the rice genome (Rice Genome Annotation Project (http://rice.plantbiology.msu.edu/index.shtml). Rice YUC and PIN genes were then blasted against the barley genome IPK (http://webblast.ipk-gatersleben.de/barley_ibsc/). High score hits were chosen for the alignment analysis and construction of a phylogenetic tree. The putative protein sequences for barley (HvYUC) and the (HvPIN) gene family were aligned using ClustalW and then a phylogenetic tree was constructed using the Neighbor-Joining method and the bootstrap analysis, with 1,000 replicates in the MEGA software version X (*Kumar et al.,* 2018). The conserved motifs in *HvYUC* and *HvPIN* genes were derived using the NCBI conserved domain search (https://www.ncbi.nlm.gov/Structure/cdd/wrpsb.cgi). The gene structure for all HvYUCs and HvPINs were retrieved from Ensembl Plants (https://plants.ensembl.org/Hordeum_vulgare). The protein transmembrane topology of *HvPIN* genes was predicted by using the TMHHM Server v2.0 (Krogh *et al.,* 2001).

2.2. Primer design for barley YUC and PIN genes

Gene sequences of HvYUCs and HvPINs were used to design primers using Primer3 (http://primer3.ut.ee/) (Table 1).

Table.1 Primer sequences and PCR product size of auxin biosynthesis and transport genes of barley.

Target gene	Forward primer 5' ------ 3'	Reverse primer 5' --------- 3'	Product size (bp)
HvYUC2	AGTGAGGGCA AGAGAGTCCA	CTATGCAGTTGGA GCGTTCA	240
HvYUC3	GGAAGCGACTT CTTCAGTGG	GGGTACCAGCTGT GTTGGTT	210
HvYUC6	GCGCTAGCAAA GATCAGGTC	GTGAAGCCGACG GAGTAGAG	247
HvYUC7	TCGTTGGATCT GGAAACTCC	GGTCATTGGACCC ATTTTTG	244
HvPIN4	GCTTCAACCAG TCCGACTTC	GCTCCTTGTTCGA GTTGGAG	243
HvPIN2	GAGGACCTCCA CATGTTCGT	CTGTTCCCGAAGC TGAAGTC	176
HvPIN7	GACCCGTTCCA GGTCAACTA	CGAGTTGGTGAGT GTGGAGA	168
HvPIN8	GTATCCCGTTG CTGAAAGGA	CTGGCCCTCATGG TATGTCT	215
SALM	GGGAGATTGGC TCTGGAAAT	GCCTCTTGGGTGT GGTTTAG	110

2.3. Plant growth and salinity stress

Barley (*Hordeum vulgare* cv Morex) grains were surface sterilized by 70% ethanol for 1 min, then 1% sodium hypochlorite for 10 min followed by 3 times (each for 5 min) rinse with sterile water. The grains were then germinated on two sheets of moist filter paper in glass dishes in the darkness for 2 days at 22˚C. Afterwards, 120 germinated grains were transferred to perlite rooting medium in 64-well trays. There were 4 trays: 2 for the control and 2 for the salinity stress. Seedlings were kept to grow for 5 days under conditions of 22/20˚C day/night, 70% humidity, 16/8 light/dark at 100 µmol/m^2/s. During growth, barley seedlings were supplemented by half-strength Hoagland's solution (Hoagland No. 2 basal salt mixture, Sigma-Aldrich, USA). At day 7 of germination (5 days after transfer to pots), a group of plants (60 plants in 2 trays) were exposed to salinity stress of 100 mM as the final NaCl concentration. This final NaCl concentration was given in 25 mM increments each day from day 7 of germination until day 11. A volume of 1 L of NaCl solution and half-strength Hoagland's solution was added to the bottom of each tray. Another group (60 plants in 2 trays) is the control group that was given half-strength Hoagland's solution. Afterwards, the expanding leaves were harvested at days 1, 2, 4, and 8 after their exposure to the final salt concentration (100 mM NaCl). Leaf samples were snap frozen in liquid nitrogen and kept at −80˚C for IAA analysis and RNA isolation. Five expanding leaves from five randomly chosen plants were pooled in one biological replicate and three biological replicates were sampled for each treatment (control and salinity stress).

2.4. RNA isolation

Total RNA was isolated using Quick-RNA^{TM}Plant Miniprep-Zymo following the manufacturer's instructions (Zymo Research Corporation, USA). RNA was detected quantitatively using Epoch Microplate Spectrophotometer (BIOTEK, USA). RNA was purified from DNA contamination using RQ1 RNase-Free DNase (Promega, USA). 1.0 µg of total RNA was used to synthesize the complementary DNA strand (cDNA) using GoScript^{TM} Reverse Transcription System (Promega, USA).

2.5. Semi-quantitative PCR

Specific primers of HvYUCs and HvPINs were used to test the expression of these genes. The following PCR mixture of a total volume of 20 µL was prepared:10 µL of 2x PCR master mix (i-MAX II, iNtRON Biotechnology, Korea), 1 µL cDNA (0.2 µg), 1 µL gene-specific forward primer (10 pmol μL^{-1}), 1 µL gene-specific reverse primer (10 pmol μL^{-1}), and free-nuclease water. The genes were amplified in 35 cycles according to the following PCR program: initial denaturation at 95˚C for 2 min, denaturation at 95˚C for 30 s, annealing at 58˚C for 30 s, extension at 72˚C for 30 s, and final extension at 72˚C for 5 min. S-adenosyl-L-methionine-dependent methyl-transferase superfamily (*SALM*) was used as a reference gene (Hua *et al*. 2015). The PCR products were visualized on agarose (2%) gel that was run for 1 hour at 100 V.

2.6. Determination of free IAA concentration

About 500 mg of barley leaf tissue was taken from each biological sample for the quantification of free IAA. Three biological samples from the control and the salinity stress groups were quantified. Free IAA was quantified using the Plant Indole 3 Acetic Acid (IAA) ELISA kit according to the manufacturer's instructions (Sunlong, China). Free IAA concentration was expressed in ng/g fresh weight.

2.7. Statistical analysis

The concentration of free IAA in the different barley samples was analyzed using Student's *t*-test. A difference in means less than 0.05 was considered significant.

3. Results

3.1. Identification of YUC and PIN genes in barley

A BLAST search of the 11 YUC genes and 8 PIN genes of *Arabidopsis* was executed in the rice genome database. In this search, the highest hit score revealed 6 *OsYUC* and 5 *OsPIN* genes. The sequences of *OsYUCs* and *OsPINs* were blasted against the barley genome IPK database. Eight (8) *HvYUC* genes and 8 *HvPIN* genes were identified and named *HvYUC1–HvYUC8* and *HvPIN1–HvPIN8*, respectively (Table 2). Two homologs, which were named *HvYUC3* and *HvYUC4*, were identified for *OsYUC3*. Moreover, *OsYUC4* showed two homologs, which were named *HvYUC5* and *HvYUC6* in the barley genome. One homolog that was named *HvYUC1*, *HvYUC2*, *HvYUC7* and *HvYUC8*, was identified in barley for each *OsYUC1*, *2*, *5*, and *6*, respectively. Three homologs were found for *OsPIN1* and were named *HvPIN1*, *2*, and *3*. Two homologs were found for *OsPIN3* and were named *HvPIN5* and *HvPIN6*. For *HvPIN2*, *4*, and 5, one homolog each was found and named *HvPIN4*, *HvPIN7*, and *HvPIN8*, respectively.

Table 2. Auxin biosynthesis (YUCs) and transport genes (PINs) in barley and in the two model plants, *Arabidopsis* and rice.

Gene abbreviation	Barley gene ID	*Arabidopsis* orthology locus	Rice
HvYUC1	HORVU3Hr1G057950	*AtYUC1*	*OsYUC1*
		AT4G32540	LOC_Os01g45760
HvYUC2	HORVU3Hr1G069580	*AtYUC2*	*OsYUC2*
		AT4G13260	LOC_Os01g53200
HvYUC3	HORVU5Hr1G125560	*AtYUC3*	*OsYUC3*
		AT1G04610	LOC_Os07g25540
HvYUC4	HORVU5Hr1G050630	*AtYUC3*	*OsYUC3*
		AT1G04610	LOC_Os07g25540
HvYUC5	HORVU2Hr1G116980	*AtYUC5*	*OsYUC4*
		AT5G43890	LOC_Os04g03980
HvYUC6	HORVU2Hr1G001820	*AtYUC5*	*OsYUC4*
		AT5G43890	LOC_Os04g03980
HvYUC7	HORVU1Hr1G022530	*AtYUC10*	*OsYUC5*
		AT1G48910	LOC_Os11g10140
HvYUC8	HORVU7Hr1G017620	*AtYUC11*	*OsYUC6*
		AT1G21430	LOC_Os12g08780
HvPIN1	HORVU7Hr1G038700	*AtPIN1*	*OsPIN1*
		AT1G73590	LOC_Os06g12610
HvPIN2	HORVU6Hr1G076110	*AtPIN1*	*OsPIN1*
		AT1G73590	LOC_Os06g12610
HvPIN3	HORVU4Hr1G026690	*AtPIN1*	*OsPIN1*
		AT1G73590	LOC_Os06g12610
PHvPIN4	HORVU7Hr1G110470	*AtPIN2*	*OsPIN2*
		AT5G57090	LOC_Os06g44970
HvPIN5	HORVU1Hr1G091030	*AtPIN3*	*OsPIN3*
		AT1G70940	LOC_Os01g45550
HvPIN6	HORVU3Hr1G057630	*AtPIN3*	*OsPIN3*
		AT1G70940	LOC_Os01g45550
HvPIN7	HORVU3Hr1G094000	*AtPIN5*	*OsPIN4*
		AT5G16530	LOC_Os01g69070
HvPIN8	HORVU3Hr1G067670	*AtPIN8*	*OsPIN5*
		AT5G15100	LOC_Os01g51780

Phylogenetic analysis using the full-length protein sequences of AtYUCs, OsYUCs, and HvYUCs showed that all the YUCs can be divided into three clades [Figure 1A (green lines)]. The first one is the largest clade, which includes 7 HvYUCs, 5 OsYUCs, and 9 AtYUCs. This clade includes HvYUC1, 3, 4, 5, 6, 7, and 8, OsYUC1, 3, 4, 5, and 6, and AtYUC1, 3, 4, 5, 7, 8, 9, 10, and 11. Clade II includes AtYUC2, OsYUC2, and HvYUC2, and Clade III has only AtYUC6. The phylogenetic tree of HvYUCs showed that these genes can be divided into three clades [Figure 1B (green line)]. HvYUC1, 3, 4, 5, and 6 are included in Clade I. Clade II includes HvYUC2 and Clade III includes HvYU7 and HvYUC8. Analysis of conserved domains revealed that all HvYUC genes have CzcO (predicted flavoprotein CzcO associated with the cation diffusion facilitator CzcD) (accession number domain COG2072) (Supplementary data file S1).

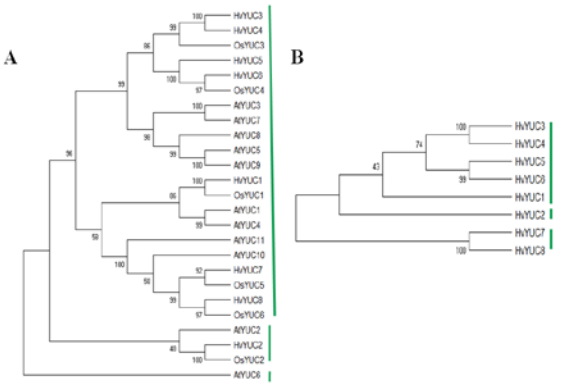

Figure 1. Phylogenetic analysis of YUC family genes. A. Phylogenetic tree of YUC genes in Arabidopsis (11 AtYUC genes), rice (6 OsYUC), and barley (8 HvYUC). B. Phylogenetic tree of YUC genes in barley. The unrooted trees were constructed by MEGAX software using the Neighbor-joining (NJ) method.

Phylogenetic analysis using the full-length protein sequences of AtPINs, OsPINs, and HvPINs showed that all the PIN genes can be divided into three clades [Figure 2A (green lines)]. The largest clade is clade I, which includes HvPIN4, 5, 7, and 8, OsPIN2, 4, and 5, and AtPIN2, 3, 4, 5, 6, 7, and 8. Clade II includes HvPIN1, 2, and 3, OsPIN1, and AtPIN1. HvPIN6 and OsPIN3 are included in clade III. The phylogenetic tree of HvPINs showed that these genes could be divided into two clades [Figure 2B (green lines)]. Clade I includes HvPIN1, 2, 3, 4, and 6 and clade II includes HvPIN5, 7, and 8.

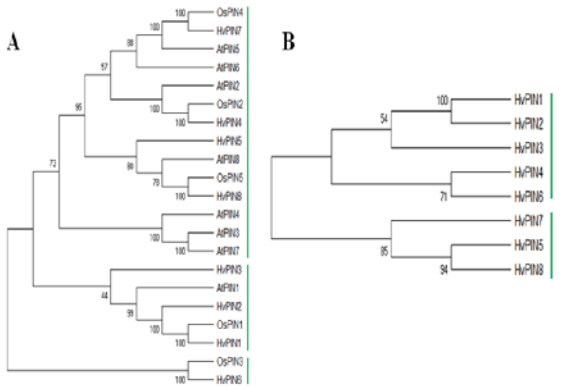

Figure 2. Phylogenetic analysis of PIN family genes. A. Phylogenetic tree of PIN genes in Arabidopsis (8 AtPINs), rice (5 OsPINs), and barley (8 HvPINs). B. Phylogenetic tree of PIN genes in barley. The unrooted trees were constructed by MEGAX software using the Neighbor-joining (NJ) method.

Gene structures of HvYUC and HvPIN genes showed differences in the number of exons and introns and the direction of transcription for each gene (Figures 3 and 4, respectively). Analysis of conserved domains revealed that all HvPIN genes have the membrane transport domain (accession number pfam03547), which is characteristic of auxin efflux carrier proteins (Supplementary data Table S1). Similar to other plant PINs, all HvPIN proteins except HvPIN6 and HvPIN7 have two hydrophobic segments located at the N- and C- termini and linked by a central hydrophilic loop (Figure 5 and Supplementary file S1). All HvPIN proteins possess 8 or 9 transmembrane helices except for HvPIN6 and HvPIN7, which have 0 and 5 transmembrane helices, respectively.

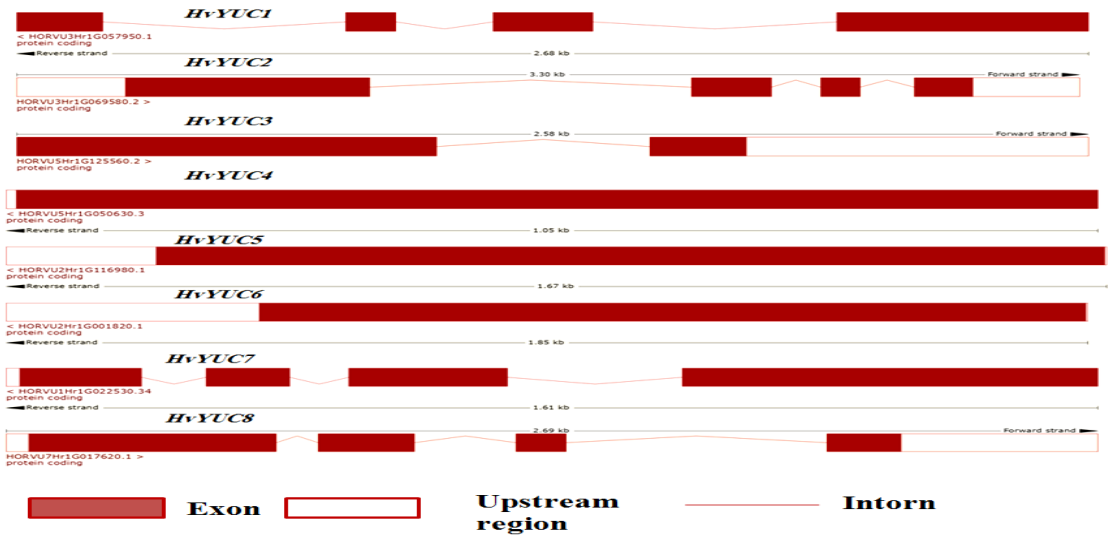

Figure 3. Gene structure of HvYUC genes

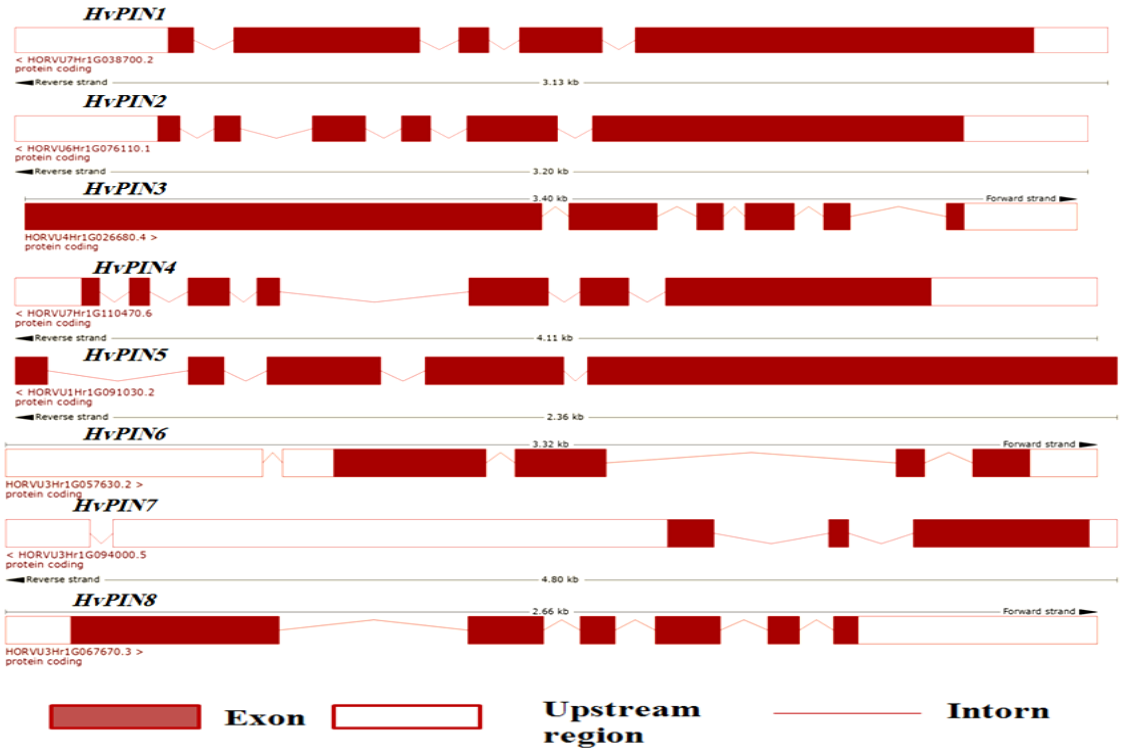

Figure 4. Gene structure of HvPIN genes

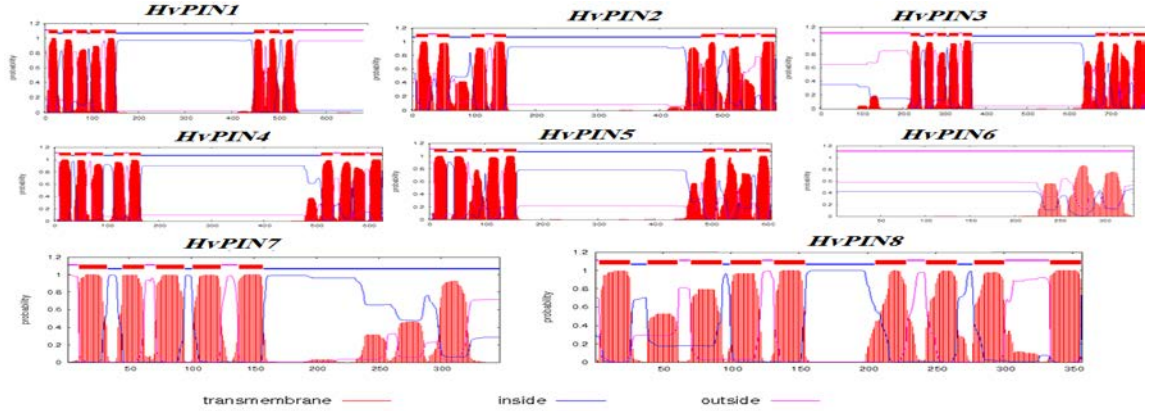

Figure 5. Transmembrane topology analysis of barley HvPIN proteins. The protein transmembrane topology was predicted by using the TMHHM Server v2.0 (Krogh et al. 2001). Red peaks represent the predicted transmembrane helices.

3.2. Rapid decrease in the concentration of free IAA in response to salinity stress

The concentration of free IAA was determined by immunological ELISA assay at different time points of salinity stress (1, 2, 4, and 8 days). After one day of salinity stress, the concentration of free IAA was significantly decreased ($P < 0.01$) (Figure 6). Free IAA concentration in barley plants under salinity stress was decreased by 25% of its concentration under control growth conditions (57 ng g^{-1} FW and 76.5 ng g^{-1} FW, respectively). After 2, 4, and 8 days of salinity treatment barley plants showed no difference in the concentration of free IAA compared with the control plants. Moreover, barley plants under control conditions did not show any significant change in the level of free IAA at different time points of their growth.

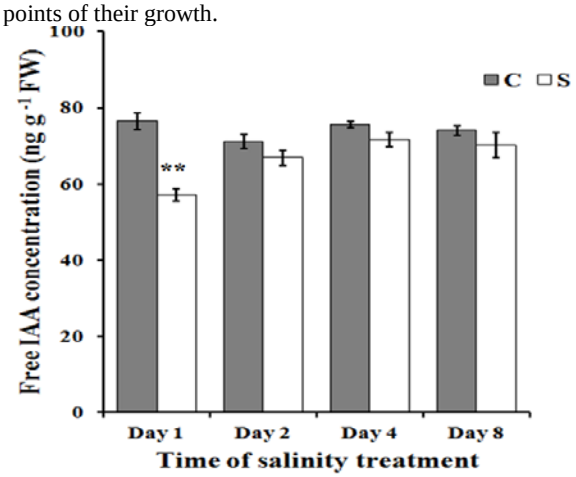

Figure 6. Concentration of free IAA in the expanding leaves of salinity-treated barley plants (S) and the control plants (C). Bars represent standard errors of the means. * $P< 0.05$, ** $P< 0.01$, and *** $P< 0.001$. Values are the means of three biological replicates.

3.3. differential transcription expression profile of HvYUC and HvPIN genes in barley plants under salinity stress

HvYUC genes showed differential transcription profiles in barley plants under salinity stress (Figure 7A). The transcription of *HvYUC2* and *HvYUC4* was not affected by salinity stress. The transcription expression of *HvYUC6* was down-regulated after 8 days of salinity stress but did not change after 1, 2, and 4 days of salinity stress. The transcription of *HvYUC7* was down-regulated after 1 day of salinity stress but did not change after 2, 4, and 8 days of salinity stress. Moreover, the transcription of *HvYUC2, 4, 6,* and *7* in the control barley plants did not change after different growth times (1, 2, 4, and 8 days).

The transcription of the majority of the tested PIN genes was not affected by salinity stress (Figure 7B). The transcription of *HvPIN4* was significantly up-regulated after 1 and 2 days of salinity stress. The transcription of *HvPIN2*, *HvPIN7* and *HvPIN8* was not altered in barley plants after different time points of salinity stress. Moreover, the transcription of *HvPIN4, 7* and *8* in the control barley plants was not altered after different growth times (1, 2, 4 and 8 days).

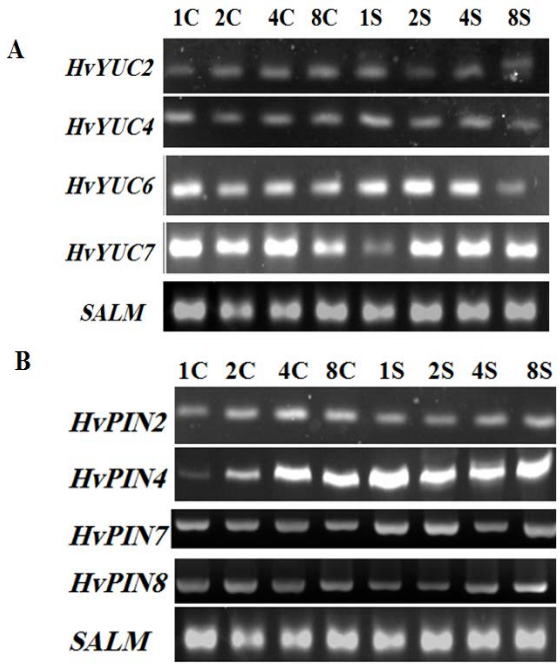

Figure 7. Transcription profile of HvYUC genes (A) and HvPIN genes (B) under control (C) and salinity stress (S) conditions after 1, 2, 4 and 8 days of salinity stress

4. Discussion

In this study, free IAA was quantified in barley seedlings under 100 mM salinity stress conditions compared with the control conditions, where no salinity stress was applied. A rapid decease in IAA concentration was observed in barley seedlings after 1 day of applying salinity stress. In other reports, the level of endogenous IAA was shown to be differentially altered in response to different abiotic stresses (Sharma *et al.*, 2015). In fact, salinity stress resulted in a significant decrease in IAA concentration in different plant species such as rice, tomato, poplar, and creeping bentgrass (Nilsen and Orcutt 1996; Dunlap and Binzel 1996; Junghans *et al.*, 2006; Krishnan and Merewitz 2015). The rapid decrease in IAA concentration in the expanding barley leaves under salinity stress shown here might be the cause of growth inhibition at this phase of salinity stress. Indeed, salinity stress was shown to stimulate a quiescent state in the early phase of its progression (Julkowska and Testerink 2015).

The rate-limiting step of IAA biosynthesis is the conversion of (indole-3-pyruvic acid) IPA into IAA: this step is catalyzed by members of the YUC gene family (Mashiguchi *et al.*, 2011; Zhao 2014). YUC genes are widely conserved in many plant species such as maize, rice, Arabidopsis, and Marchantia (Kasahara 2016). In this study, 6 *OsYUC* and 8 *HvYUC* genes were identified. Most of the *HvYUC* gene family members were phylogenetically related and clustered in one clade. This was the case in rice (Yamamoto *et al.*, 2007). Moreover, all eight proteins of the *HvYUC* genes contain the conserved domain CzcO (predicted flavoprotein CzcO associated with the cation diffusion facilitator CzcD). This match was shown for YUC genes in various plants species (Yamamoto *et al.*, 2007; Zheng *et al.*, 2016; Wang *et al.*, 2017). In the

present study, the transcription profile of *HvYUC* genes in the expanding barley leaves under salinity stress showed a significant down-regulation of *HvYUC7* after 1 day of salinity stress. Indeed, a significant reduction in the concentration of the free IAA was also shown after 1 day of salinity stress. This might suggest a critical role of *HvYUC7* in the biosynthesis of IAA in barley plants in response to salinity stress.

Auxin transport is crucial for the normal functioning of auxin under different environmental conditions (Forestan and Varotto 2012; Korver *et al.,* 2018). Members of the PIN gene family have a rate-limiting function as auxin efflux carriers. Moreover, they are crucial players in the maintenance of a steady-state of auxin levels, which is important for optimum and harmonized growth and developmental responses (Petrásek *et al.,* 2006; Křeček *et al.,* 2009). In the present study, auxin transport members of the PIN gene family were identified in barley. Eight different *HvPIN* genes were identified. Most *HvPIN* genes were shown to have the membrane transport domain, which is characteristic of auxin efflux carrier proteins (Křeček *et al.,* 2009; Zhou and Luo 2018). Low salinity stress inhibited the transcription of *AtPIN2* (Zhao *et al*., 2011). In Arabidopsis, salinity stress down-regulated the expression of PIN genes in the root tissues. This resulted in the inhibition of root meristem growth (Liu *et al.,* 2015). In soybean (*Glyine max*) plants, *GmPIN* genes responded differentially to the different abiotic stresses (Wang *et al.,* 2015). The results of quantitative PCR revealed that the number of down-regulated *GmPIN* genes under salinity stress was larger than that of the up-regulated genes. In watermelon (*Citrullus lanatus*), the transcription of PIN genes was differentially altered in response to different abiotic stresses (Yu *et al.,* 2017). The transcription of *ClPIN2* and *ClPIN10* was significantly down-regulated in the shoot tissue after 24 hours of salinity stress. In the root tissue, the transcription of *ClPIN2* and *ClPIN10* was not changed, but the transcription of the other *ClPIN* genes was up-regulated. Moreover, differential regulation of PIN genes was shown in cotton (*Gossypium hirsutum*) plants in response to drought and salinity stress and in leaf and root (He *et al.,* 2017). In the present study, the transcription of *HvPIN4* was up-regulated in the expanding barley leaves after 1 and 2 days of salinity stress. At 4 and 8 days of salinity stress the expression of this gene was high and the same in the two treatment groups. This increase in the expression of *HvPIN4* in the control group might be related to the progress in plant's development. Meaning, at these stages of development *HvPIN4* is switched on. The transcription profile of the other *HvPIN* genes was not altered in response to salinity stress. This indicates a regulatory role of *HvPIN4* in the expanding leaves of barley under salinity stress.

The regulation of auxin homeostasis is a complex process that requires the action of many gene families for biosynthesis, conjugation/deconjugation, transport and signaling. The maintenance of auxin homoeostasis is crucial for normal plant development, patterning, and growth. Plants under osmotic stress from drought or salinity show a significant decrease in auxin, and this results in growth inhibition as an acclimation strategy (Naser and Shani 2016). Therefore, dissection of the molecular and biochemical bases of auxin action in plants under salinity stress will help in the optimum utilization of this important growth regulator for the development of salinity-tolerant plants.

Acknowledgements

The authors are grateful to professor Ayed Allabdalla (Department of Horticulture, Faculty of Agriculture, Jordan University) for providing the barley grains genotype Morex.

Authors' contributions

AH and KA designed the study; AS conducted lab experiments; AH analyzed the data; AH wrote the manuscript, and KA and AH reviewed the manuscript.

Conflict of interest

Authors declare no conflict of interest.

References

Abogadallah G, Serag M and Quick W. 2010. Fine and coarse regulation of reactive oxygen species in the salt tolerant mutants of barnyard grass and their wild-type parents under salt stress. *Physiol Plant.,* **138**: 60-73.

Balzan S, Johal G and Carraro N. 2014. The role of auxin transporters in monocots development. *Front. Plant Sci.,* **5**: 393-404.

Bennett MD and Leitch, IJ. 2012. Plant DNA *C*-values database (release 6.0, Dec. 2012) http://www.kew.org/cvalues/.

Bielach A, Hrtyan M and Tognetti V. 2017. Plants under stress: Involvement of auxin and cytokinin. *Int J Mol Sci*., **18**: 1427-1450.

Distelfed A, Avni R and Fischer AM. 2014. Senescence, nutrient remobilization, and yield in wheat and barley. *J Exp Bot.,* **65**: 3783-3798.

Dunlap JR and Binzel ML. 1996. NaCl reduces indole-3-acetic acid levels in the roots of tomato plants independent of stress induced abscisic acid. *Plant Physiol.,* **112**: 379-384.

Forestan C and Varotto S. 2012. The role of PIN auxin efflux carriers in polar auxin transport and accumulation and their effect on shaping maize development. *Mol Plant,* **5**: 787-798.

Ghanem M, Albacete A, Martínez-Andújar C, et al. 2008. Hormonal changes during salinity-induced leaf senescence in tomato (*Solanum lycopersicum* L.). *J Exp Bot.,* **59**: 3039-3050.

He P, Zhao P, Wang L, et al. 2017. The PIN gene family in cotton (*Gossypium hirsutum*): genome-wide identification and gene expression analyses during root development and abiotic stress responses. *BMC Genomics,* **18**: 507-517.

Hiei Y, Ishida Y and Komari T. 2014. Progress of cereal transformation technology mediated by *Agrobacterium tumefaciens*. *Front Plant Sci*., **5**: 628-638.

Hua W, Zhu J, Shang Y, et al. 2015. Identification of suitable reference genes for barley gene expression under abiotic stresses and hormonal treatments. *Plant Mol Biol Report,* **33**: 1002-1012.

Ingvordsen C, Backes G, Lyngkjær M, et al. 2015. Significant decrease in yield under future climate conditions: Stability and production of 138 spring barley accessions. E*ur J Agron.,* **63**: 105-113.

Javid M, Sorooshzadeh A, Sanavy S and Allahdad I . 2011. The role of phytohormones in alleviating salt stress in crop plants. *Aust J Crop Sc.,* **5**: 726-734.

Julkowska M and Testerink C. 2015. Tuning plant signaling and growth to survive salt. *Trends Plant Sci*., **20**: 586-594.

Junghans U, Polle A, Düchting P, et al. 2006. Adaptation to high salinity in poplar involves changes in xylem anatomy and auxin physiology. *Plant Cell Environ.,* **29**: 1519-1531.

Kasahara H. 2016. Current aspects of auxin biosynthesis in plants. *Biosci Biotechnol Biochem.,* **80**: 34-42.

Kaya C, Tuna AL and Yokaş I. 2009. The role of plant hormones in plants under salinity stress. *In*: Ashraf M, Ozturk M, Athar H (Eds) **Salinity and Water Stress**. Tasks for vegetation sciences. Vol. 44. Springer,Dordrecht, pp 45-50.

Korasick D, Enders T and Strader L. 2013. Auxin biosynthesis and storage forms. *J Exp Bot.,* **64**: 2541-2555.

Korver R, Koevoets I and Testerink C. 2018. Out of shape during stress: A key role for auxin. *Trends Plant Sci.*, **2**: 783-793.

Kramer EM and Ackelsberg EM. 2015. Auxin metabolism rates and implications for plant development. *Front Plant Sci.*, **6**: 150-158.

Křeček P, Skůpa P, Naramoto S, et al. 2009. The PIN-FORMED (PIN) protein family of auxin transporters. *Genome Biol.,* **10**:249-259.

Krishnan S and Merewitz E. 2015. Phytohormone responses and cell viability during salinity stress in two creeping bentgrass cultivars differing in salt tolerance. *Am Soc Hortic Sci.,* **140**: 346-355.

Krogh A, Larsson B, von Heijne G and Sonnhammer EL. 2001. Predicting transmembrane protein topology with a hidden Markov model: application to complete genomes. *J Mol Biol.,* **305**: 567-580.

Kumar S, Stecher G, Li M, Knyaz C and Tamura K. 2018. MEGA X: Molecular Evolutionary Genetics Analysis across computing platforms. *Mol Biol Evol*., **35**: 1547-1549.

Liu W, Li RJ, Han TT, et al. 2015. Salt stress reduces root meristem size by nitric oxide-mediated modulation of auxin accumulation and signaling in Arabidopsis. *Plant Physiol.,***168**: 343-356.

Ludwig-Müller J. 2011. Auxin conjugates: their role for plant development and in the evolution of land plants. *J Exp Bot.,* **62**: 1757-1773.

Mano Y and Nemoto K. 2012. The pathway of auxin biosynthesis in plants. *J Exp Bot.,* **63**: 2853-2872.

Marti M, Florez-Sarasa I, Camejo D, et al. 2011. Response of mitochondrial thioredoxin PsTrxo1, antioxidant enzymes, and respiration to salinity in pea (*Pisum sativum* L.) leaves. *J Exp Bot*., **62**: 3863–3874.

Mashiguchi K, Tanaka K, Sakai T, et al. 2011. The main auxin biosynthesis pathway in Arabidopsis. *PNAS*, **45**: 18512-18517.

Munns R and Gilliham M. 2015. Salinity tolerance of crops – what is the cost? *New Phytol*., **208**: 668-673.

Munns R and Tester M. 2008. Mechanisms of salinity tolerance. *Annu Rev Plant Biol*., **59**: 651-681.

Naser V and Shani E. 2016. Auxin response under osmotic stress. *Plant Mol Biol.,* **91**: 661-672.

Nilsen E and Orcutt DM. 1996. **The Physiology of Plants under stress - Abiotic Factors**. Wiley, New York.

Peleg Z and Blumwald E. 2011. Hormone balance and abiotic stress tolerance in crop plants. *Curr Opin Plant Biol*., **14**: 290-295.

Petrásek J, Mravec J, Bouchard R, et al. 2006. PIN proteins perform a rate-limiting function in cellular auxin efflux. *Science.* **312**: 858-560.

Prasch CM and Sonnewald U. 2015. Signaling events in plants: Stress factors in combination change the picture. *Environ Exp Bot.,* **114**:4-14.

Ryu H and Cho YG. 2015. Plant hormone,s in salt stress tolerance. *J Plant Biol.,* **58**: 147-155.

Sharma E, Sharma R and Borah P. 2015. Emerging roles of auxin in abiotic stress responses. *In*: Pandey GK (Ed) **Elucidation of Abiotic Stress Signaling in Plants**. Springer, New York, pp 299-328.

Sudhakar C, Lakshmi A and Giridarakumar S. 2001. Changes in the antioxidant enzyme efficacy in two high yielding genotypes of mulberry (*Morus alba* L.) under NaCl salinity. *Plant Sci*., **161**: 613–619.

Vanneste S and Friml J. 2009. Auxin: a trigger for change in plant development. *Cell,* **136**: 1005-1056.

Wang W, Gu L, Ye S, et al. 2017. Genome-wide analysis and transcriptomic profiling of the auxin biosynthesis, transport and signaling family genes in moso bamboo (*Phyllostachys heterocycla*). *BMC Genomics,* **18**: 870-885.

Wang Y, Chai C, Valliyodan B, Maupin C, Annen B and Nguyen H T. 2015. Genome-wide analysis and expression profiling of the PIN auxin transporter gene family in soybean (*Glycine max*). *BMC Genomics*, **16**: 951-963.

Wani S, Kumar V, Shriram V and Sahd S. 2016. Phytohormones and their metabolic engineering for abiotic stress tolerance in crop plants. *Crop J*., **4**: 162-176.

Woodward AW and Bartel B. 2005. Auxin: regulation, action, and interaction. *Ann Bot.,* **95**: 707-735.

Yamamoto Y, Kamiya N, Morinaka Y, Matsuoka M and Sazuka T. 2007. Auxin biosynthesis by the YUCCA genes in rice. *Plant Physiol.,* **143**: 1362-1371.

Yu C, Dong W, Zhan Y, Huang Z, Li Z, Kim S and Zhang C. 2017. Genome-wide identification and expression analysis of ClLAX, ClPIN and ClABCB genes families in *Citrullus lanatus* under various abiotic stresses and grafting. *BMC Genetics*, **18**: 33-47.

Yurekli F, Porgali B and Turkan I. 2004. Variations in abscisic acid, indole-3-acetic acid, gibberellic acid and zeatin concentrations in two bean species subjected to salt stress. *Acta Biol Cracov Bot.,* **46**: 201-212.

Zhao Y. 2012. Biosynthesis: A simple two-step pathway converts tryptophan to indole-3-acetic acid in plants. *Mol Plant,* **5**: 334-338.

Zhao Y. 2014. **Auxin biosynthesis**. The Arabidopsis book. American Society of Plant Biologists. e0173. doi: 10.1199/tab.0173.

Zhao Y, Wang T and Zhang W, Li X. 2011. SOS3 mediates lateral root development under low salt stress through regulation of auxin redistribution and maxima in Arabidopsis. *New Phytol.,***189**: 1122-1134.

Zheng L, Zhang L, Duan K, et al. 2016. YUCCA type auxin biosynthesis genes encoding flavin monooxygenases in melon: Genome-wide identification and developmental expression analysis. *S Afr J Bot.,* **102**: 142-152.

Zhou JJ and Luo J. 2018. The PIN-FORMED auxin efflux carriers in plants. *Int J Mol Sci.,* **9**: 2759-2779.

Zörb C, Geilfus CM, Mühling KH and Ludwig-Müller J .2013. The influence of salt stress on ABA and auxin concentrations in two maize cultivars differing in salt resistance. *J Plant Physiol.,* **170**: 220-224.

JJBS

Jordan Journal of Biological Sciences

Volume 13, Number 1,March 2020
ISSN 1995-6673
Pages 101 - 105

Pitavastatin Enhances Doxorubicin-induced Apoptosis in MCF7 Breast Cancer Cells

Saeb H. Aliwaini*, Tarek A. El-Bashiti and Khalid M. Mortaja

Department of Biology and Biotechnology, Faculty of Science, Islamic University of Gaza, Palestine

Received May 16, 2019; Revised June 7, 2019; Accepted June 17, 2019

Abstract

Breast cancer is the most common malignancy in women worldwide. While doxorubicin is part of the standard therapy for metastatic breast cancer, it has limited success. Pitavastatin has been shown to enhance the anti-cancer activity of certain therapeutics. The current study, therefore, explored the anti-cancer activity of the combined treatment of doxorubicin and pitavastatin in MCF7 breast cancer cells. Cell proliferation and viability assays demonstrated that combined doxorubicin and pitavastatin treatment resulted in synergistic cytotoxicity and cell death. Western blotting analysis showed that pitavastatin treatment resulted in increasing levels of p53 and the cell cycle regulator p21 in both doxorubicin treated and untreated cells. Furthermore, we demonstrated that apoptosis induced by the combined treatment occurs through the intrinsic pathway as evident from the activation of caspase 9, caspase 7 and the reduction of BCL-2 level. This study provides novel evidence to suggest that combined treatment of doxorubicin and pitavastatin may be effectively combined to treat breast cancer with the potential to minimize the side effects associated with high doses of doxorubicin.

Keywords: Apoptosis; Chemotherapy; Doxorubicin, MCF7; Pitavastatin, Synergism

1. Introduction

Breast cancer is the most common type of cancer worldwide, and it is estimated that one out of eight women will develop breast cancer in their lifetime (Cheng *et al*., 1998). In spite of the fact that most of the patients are diagnosed in early and curable stages, metastatic breast cancer occurs in one third of patients affecting bone, liver and lung, and ultimately leading to death (Malki *et al*., 2009). The natural anthracycline antibiotic doxorubicin is considered the most active single therapy available for metastatic breast cancer. Doxorubicin induces death of cancer cells by different mechanisms such as topoisomerase II-α (TOP2A) inhibition (Barni & Mandala, 2005). Although breast cancer is one of the chemo-sensitive tumours, its response to doxorubicin treatment ranges from 28% to 43% only (Taylor *et al*., 1991; AbuHammad & Zihlif, 2013). Doxorubicin resistance leads to an unsuccessful outcome in nearly 50% of treated patients, making resistance a major cause of treatment failure.

Statins are widely prescribed drugs used for the inhibition of the mevalonate pathway which is responsible for cholesterol synthesis in human cells (Gopalan *et al*., 2013; Warita *et al*., 2014). In addition, statins have a wide range of anticancer activities in different cancers (Al-Qatati and Aliwaini, 2017; Gopalan *et al*., 2013; Lee *et al*., 2012; Tu *et al*., 2011). For example, simvastatin was shown to induce cell cycle arrest through activation of Chk1 kinase and inhibition of Cdc25A, cyclin A and CDK2 in multiple myeloma cells (Tu *et al*., 2011). Simvastatin induced cell cycle arrest was accompanied by intrinsic apoptosis as demonstrated by diminished Bcl-2 protein levels, increased cytosolic cytochrome c and active caspase 9 and caspase 3 levels. Recent studies have shown that erivastatin, pitavastatin and fluvastatin are potent anti-proliferative drugs in glioblastoma cells (Lee *et al*., 2012; McFarland *et al*., 2014). Other studies showed the ability of fluvastatin to reduce tumour growth in high-grade, stage 0/1 breast cancer patients (Garwood *et al*., 2010). Pitavastatin has been shown to exert potent cytotoxic effects on glioblastoma growth in vivo (Lee *et al*., 2012). The mechanism of action of pitavastatin includes up regulation of the cell cycle regulator p21 and inhibition of NF-κB, which resulted in cell cycle arrest and apoptosis (Fujino *et al*., 2006; Wang J, e*t al*., 2006). Interestingly, autophagic cell death was also shown to be induced by pitavastatin (Tsuboi *et al*., 2009). Finally, our recent findings showed that pitavastatin and dacarbazine synergistically inhibit melanoma cell survival by inducing cell cycle arrest, apoptosis and autophagy (Al-Qatati and Aliwaini, 2017). Whether pitavastatin has the ability to enhance doxorubicin anticancer activity is mostly unknown.

The present study therefore aimed to explore the effect of combined pitavastatin and doxorubicin treatment in breast cancer cells. The presented data shows that pitavastatin enhances doxorubicin induced cytotoxicity in MCF7 cells and further demonstrates that this occurs through induction of intrinsic apoptosis.

* Corresponding author e-mail: Saib.iwini@gmail.com; siwini@iugaza.edu.ps.

2. Materials and Methods

2.1. Cell culture and treatments

The human breast cancer cells MCF7 were obtained from Prof. Rana Abu-Dahab, The University of Jordan. They were maintained in Dulbecco's Modified Eagle Medium (DMEM) supplemented with 10% fetal bovine serum (FBS) in a humidified 5% CO_2 balanced air incubator at 37°C. Pitavastatin (Santa Cruz Biotechnology, Santa Cruz, CA, USA) and doxorubicin (Sigma-Aldrich, St Louis, MO, USA) were dissolved in dimethyl sulfoxide (DMSO) and water, respectively, to give stock concentration of 5 mM which were stored for no more than 5 days. Control cells were treated with equivalent concentrations of DMSO (vehicle).

2.2. Cytotoxicity assays

Breast cancer cells were seeded in 96-well plates at 8×10^3 cells per well and allowed to settle for 48 hours. Cells were treated individually with 0-5.0µM of pitavastatin, or 0.0- 0.5µM doxorubicin or vehicle for 48 hours (Al-Qatati and Aliwaini, 2017). Cytotoxicity was assessed using the 3-(4,5-dimethylthiazol-2-yl)-2,5-diphenyltetrazolium bromide (MTT) assay (Aliwaini *et al*., 2013) as per manufacturer's instructions (Roche Diagnostics, Mannheim, Germany). Briefly, 10 µL of MTT solution were added to each well and cells were incubated at 37°C for 4 hours, followed by addition of 100 µL solubilization buffer (10% sodium dodecyl sulfate /SDS) in 0.01M hydrochloric acid (HCl) and incubation for 16 hours at 37°C. Absorbance at 585 nm was determined for each well and the mean cell viability was calculated as a percentage of the mean cell survival of the vehicle control.

2.3. Viability assay

The trypan blue exclusion method was used to determine the total cell number and the proportion of live and dead cells. Briefly, MCF-7 cells were grown on 6-well plates at a density of 6×10^4 cells/well. After 24 hours, the cells were treated with different concentrations either of doxorubicin or pitavastatin for 48 hours. To determine whether the combined treatment of pitavastatin and doxorubicin may have a greater anti- cancer effect on MCF7 cells than doxorubicin alone, breast cancer cells were treated with 1 µM pitavastatin for 1 hour followed by treatment with increasing concentrations (0.05-0.5µM) of doxorubicin for 48 hours. After the 48 hours, cells were trypsinized, centrifuged, resuspended in 0.5 ml of the medium, mixed thoroughly with 50 µl of 0.4% Trypan blue (w/v), at room temperature for 5 min. The cells were then counted using a hemocytometer. Each experiment was repeated three times with triplicate samples in each. Statistically, the percentage of cell death was calculated by counting at least 300 cells per sample in several randomly selected fields using the formula of percentage of cell death = number of dead cells/number of total cells × 100.

2.4. Western blotting

To test whether pitavastatin induces cell cycle arrest and apoptosis, breast cancer cells were treated with vehicle, pitavastatin (1.0µM), doxorubicin (0.3µM) or pitavastatin- doxorubicin (1.0 and 0.3 µM, respectively) and western blotting with an antibody to p53 and p21, PARP cleavage, caspase 7, caspase 9, BCL-2 was performed. Cells were harvested and protein prepared as described previously (Aliwaini *et al*., 2013). Primary antibodies used were: anti-PARP1/2 (sc-7150), anti-p53 (sc-126), anti-p21 (sc- 756), anti-caspase 7 (sc-56063) and anti-caspase 9 sc-56076 (Santa Cruz Biotechnology, Santa Cruz, CA, USA), anti-β-actin (Sigma, St. Louis, MO, USA), anti-BCL-2 (sc-509). After primary antibody incubation, membranes were incubated with HRP-conjugated secondary antibodies at appropriate ratio (1:5000) (BioRad) and antibody-reactive proteins were visualized using the electrochemiluminescence reaction (ECL) detection system (Thermo Scientific, Hudson, NH, USA).

2.5. Statistical analysis

Results presented are the means ± SEM (the standard error of the means) of three independent experiments. Statistical analysis of data was performed using the 2-sample *t*-test (Excel, Microsoft, Redmond, WA, USA) or two-way ANOVA (Graph Pad Prism, La Jolla, CA, USA) and $p<0.05$ was considered statistically significant.

3. Results

3.1. Pitavastatin enhances doxorubicin induced death of breast cancer cells

The anti-proliferative effect of pitavastatin on breast cancer cell line was determined by MTT assay. MCF7 cells were treated using different concentrations (0.0µM–5.0µM) of pitavastatin. The results showed that pitavastatin exerts a pronounced anti-proliferative effect on MCF7 cells with an IC50 value of (3.38µM) (Figure 1a). While low concentrations of pitavastatin (0.5µM) and (1.0µM) show little cytotoxic effect on MCF7 cells, 5µM induces a very strong cytotoxic effect.

To confirm the inhibitory action of doxorubicin on MCF7 cells, the cells were treated with the drug at concentrations of 0.0µM–5.0µM and the proliferative activity was determined by MTT assay. The results show that both high and low concentrations of doxorubicin have cytotoxic effect on MCF7 cells with IC50 of (0.29µM). Low concentration of doxorubicin (0.25µM) killed 30 % of MCF7 cells, while high concentration (0.5µM) killed 60 % of MCF7 cells (Figure 1b). Figure 1b demonstrates that the combined treatment resulted in enhanced cytotoxic activity compared with doxorubicin treatment alone. While doxorubicin treatment induced 50% inhibition at 0.29µM, pre-treatment of cells with 1µM pitavastatin for 1 hour resulted in ~80% cell death at 0.3µM doxorubicin concentration.

To test the ability of pitavastatin to increase the percentage of cell death induced by doxorubicin, breast cancer cells were treated with 1µM pitavastatin for 1 hour followed by treatment with doxorubicin of for 48 hours. Figure 1c demonstrates that while doxorubicin treatment induced about 40% cell death, combined treatment resulted in about 70% cell death. These results demonstrate that combined pitavastatin and doxorubicin treatment cause a synergistic cytotoxic effect in breast cancer cells.

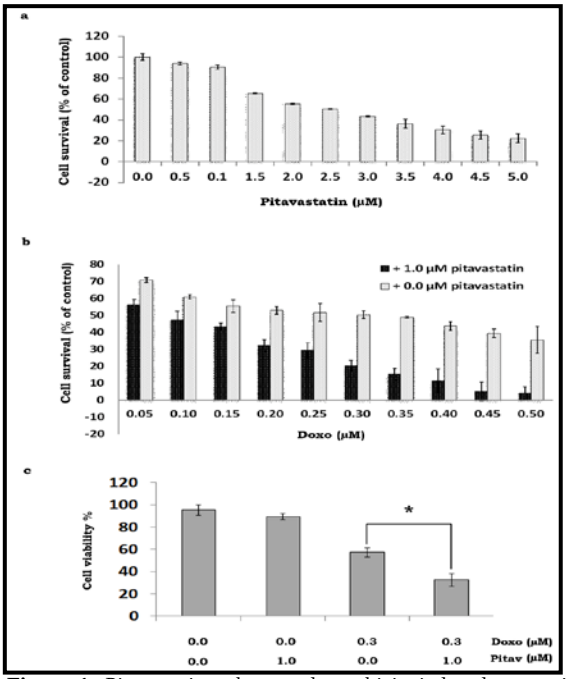

Figure 1. Pitavastatin enhances doxorubicin induced cytotoxic effect in breast cancer cells**.** Cell survival (MTT assay) of breast cancer cells (MCF7 cells) treated with increasing concentrations of pitavastatin (0.0µM - 5.0µM) or vehicle for 48h (a). MCF7 cells were treated with 1.0 µM pitavastatin for 1 hour and increasing concentrations (0.05-0.5µM) of doxorubicin (b). MCF7 cells treated with single treatment (vehicle, pitavastatin or doxorubicin) or combined treatment of 1.0 µM pitavastatin and 0.3µM doxorubicin (c). Results are presented as the mean percentage ± standard error of the mean of untreated cells and represent the pooled results of at least three experiments performed in quadruplicate.

3.2. Pitavastatin activates cell cycle regulators p53 and p21 levels in MCF7:

Figure 2 shows that p53 and its downstream target p21 increased in response to pitavastatin treatment. More importantly, while doxorubicin treatment also induced slight increase in both proteins, the combined treatment significantly increased both p53 and p21 levels.

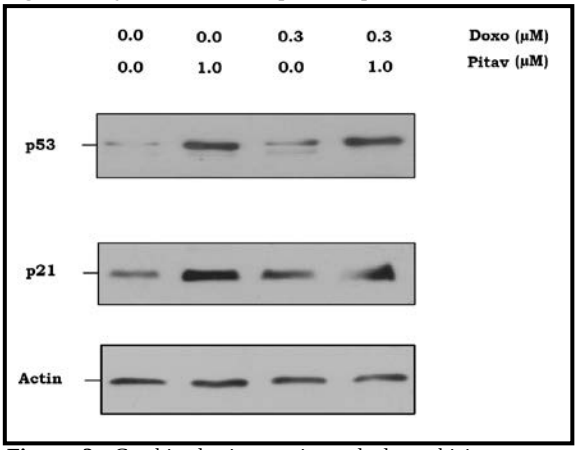

Figure 2. Combined pitavastatin and doxorubicin treatment activates cell cycle regulators. Breast cancer cells were treated with 1.0 µM pitavastatin (Pitav), 0.3µM doxorubicin (Doxo), pitavastatin- doxorubicin (1.0 and 0.3µM, respectively) or vehicle. Protein extracts were analyzed by SDS-PAGE (8-15%) and western blotting was performed by using antibodies against p53 and p21. Actin was detected as a loading control.

3.3. Pitavastatin increases apoptosis induced in MCF7 by Doxorubicin:

Total protein was extracted and resolved by SDS-PAGE and analyzed by western blot for cleaved PARP1. Figure 3 shows that combined treatment of pitavastatin-doxorubicin induced high level of PARP cleavage. However, single treatment of doxorubicin (0.3µM) or pitavastatin (1.0µM) induced very low levels of PARP cleavage. Figure 3 further shows that pitavastatin, doxorubicin and the combined (pitavastatin-doxorubicin) treatments decreased the anti-apoptotic protein BCL-2 and increased the apoptotic proteins (active caspase 9 and active caspase 7).

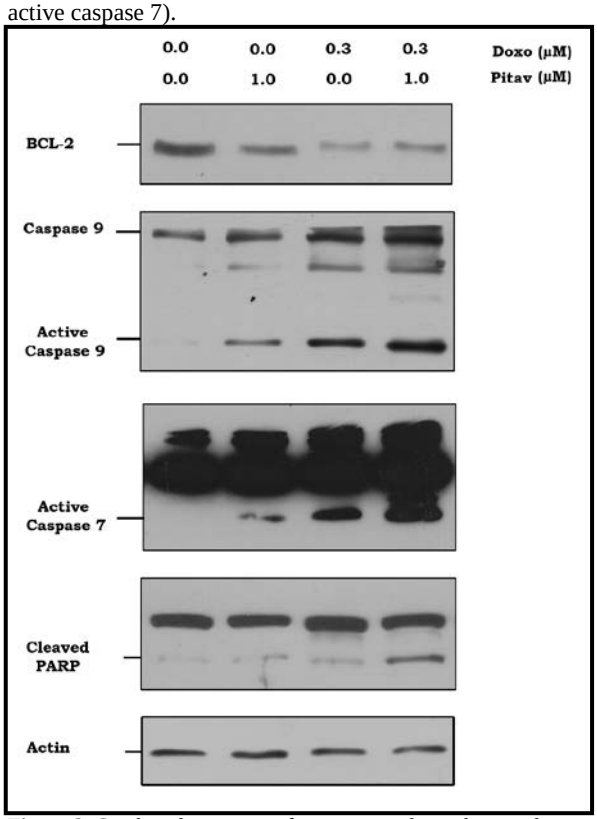

Figure 3. Combined treatment of pitavastatin-doxorubicin induces intrinsic apoptosis in breast cancer cells. MCF7 cells were treated with either vehicle, 1.0µM pitavastatin, 0.3µM doxorubicin or pitavastatin- doxorubicin (1.0 and 0.3µM, respectively). Protein extracts were analyzed by SDS-PAGE (8 and 15%) and western blotting using antibody to BCL-2, caspase 9, caspase 7 and cleaved PARP. Actin was detected as a loading control.

4. Discussion

Breast cancer continues to be the leading cause of cancer deaths among women, and its treatment is constantly evolving as new technologies, drugs, and strategies are discovered (Westbrook and Stearns, 2013). The choice of therapy depends on the molecular profile and the stage of breast cancer (Massarweh and Schiff, 2006). Doxorubicin is one of the most active therapeutics for metastatic breast cancer which inhibits tumor growth by inducing cell cycle arrest and apoptosis (Barni and Mandala, 2005). In spite of its strong anti-cancer activity, doxorubicin can treat less than 43% of metastatic breast cancer patients (Taylor *et al.*, 1991; AbuHammad and Zihlif, 2013;). In addition to that, doxorubicin resistance

leads to an unsuccessful outcome in nearly 50% of treated patients. Therefore, there is a need for new strategies to empower the anticancer effect of doxorubicin and to decrease its side effect.

3-Hydroxy-3-methylgutarylCoA(HMG-CoA) reductase inhibitors, commonly referred to as the statins have therapeutic and preventative effects in different diseases (Chan *et al*., 2003). Interestingly, statins exert anti-proliferative and anti-cancer effect against a range of types of tumour (Tsuboi *et al*., 2009; Tu *et al*., 2011; Yang and Chen, 2011). The present study, therefore, explored the *in vitro* efficacy of a combined treatment of doxorubicin with pitavastatin in human breast cancer cells. The results of the present study provide several lines of evidence to suggest that pitavastatin may synergistically improve the anti-cancer activities of doxorubicin. The inhibitory concentration 50% (IC_{50}) of doxorubicin in MCF7 ranges between 0.3 to 0.6 µM as reported by previous studies (Osman *et al*., 2012; Buranrat *et al*., 2017). This is close to the results of the current study where doxorubicin inhibited MCF7 growth with an IC50 of 0.29µM. On the other hand, previous studies showed that pitavastatin has a potent cytotoxic effect against MCF7 cells with IC50 around 10 µM (Wang and Kitajima, 2007). The results of our study showed that pitavastatin inhibits MCF7 cells with IC50 of 3.38µM. The difference between the two IC50s might be ascribed to the different techniques used in the two studies. The present study further demonstrated that cancer cells pre-treated with pitavastatin (1µM) are sensitised to doxorubicin resulting in ~50% cell death at doxorubicin dose less than 0.1µM.

Furthermore, the present study revealed that the mechanism of action by which pitavastatin-doxorubicin combined treatment inhibits cancer growth involves cell cycle arrest and intrinsic apoptosis. P53 is major anticancer transcription factor which induces growth arrest and or apoptosis in cells exposed to chemotherapies. Previous studies provided evidence that doxorubicin mediated cytotoxicity depends at least partially on its ability to activate of p53 protein (Kotamraju *et al*., 2000; Wang *et al*., 2004). Similarly, other studies have indicated that doxorubicin treatment results in cell cycle arrest at different phases, and this was accompanied with increasing levels of p53 and p21 proteins (Vali *et al*., 2015; Buranrat *et al*., 2017). The current study showed similar results, as doxorubicin treatment induced slightly increasing level of p53 and p21. The increase in the cycle regulator p21 is usually considered a marker of cell cycle arrest at G1 phase (Aliwaini *et al*., 2015). These data confirm previous data that doxorubicin treatment stops breast cancer cell cycle at G1 stage. Furthermore, doxorubicin has been shown to induce a high level of active caspase 3, an established marker of apoptosis (Buranrat *et al*., 2017). The same study showed that doxorubicin induces intrinsic apoptosis mainly as evident by the release of cytochrome c from mitochondria of breast cancer cells. Similar data was also recorded by our study, as doxorubicin induced high level of active caspase 7 and 9 which are documented markers of intrinsic apoptosis (Aliwaini *et al*., 2015).

Notably, pitavastatin was also demonstrated to inhibit proliferation of breast cancer cells in a dose-dependent manner and to inhibit NF-κB pathway (Wang and Kitajima, 2007). However, there is no adequate data in literature whether pitavastatin induces cell cycle arrest and/or apoptosis and what the exact mechanism behind its inhibitory effect is. The current study provides evidence that pitavastatin treatment mainly increases p53 and p21 proteins and induces cell cycle arrest. This effect is significantly increased when breast cancer cells are treated with both pitavastatin and doxorubicin.

Furthermore, the present study demonstrated that the cytotoxic effect of pitavastatin-doxorubicin includes the induction of intrinsic apoptosis. Notably, whilst doxorubicin treatment induced low level apoptosis, as evident by PARP cleavage and caspases level, combined pitavastatin-doxorubicin treatment resulted in significant levels of apoptosis as evidenced by the increased level of apoptosis markers.

5. Conclusions

The presented results suggest that the combined treatment of pitavastatin-doxorubicin provides a synergistic anti-cancer effect through cell cycle arrest and apoptosis. While the study was performed in vitro, there is a need to determine if pitavastatin would protect against Dox-induced chronic cytotoxicity, and enhance Dox anticancer activities against breast cancer in vivo. The strategy of combined treatment may potentially be applied in future clinical trials and, if successful, could help to improve chemotherapy selection for the benefit of breast cancer patients.

References

AbuHammad S and Zihlif M. 2013. Gene expression alterations in doxorubicin resistant MCF7 breast cancer cell line. *Genomics*, **101(4):** 213-220.

Aliwaini S, Swarts AJAJ, Blanckenberg A, Mapolie S and Prince S. 2013. A novel binuclear palladacycle complex inhibits melanoma growth in vitro and in vivo through apoptosis and autophagy. *Biochem Pharmacol*, **86(12):** 1650-1663.

Aliwaini S, Peres J, Kröger WL, Blanckenberg A, de la Mare J, Edkins AL, *et al*. 2015. The palladacycle, AJ-5, exhibits anti-tumour and anti-cancer stem cell activity in breast cancer cells. *Cancer Lett*, **357(1):** 206-218.

Al-Qatati A and Aliwaini S. 2017. Combined pitavastatin and dacarbazine treatment activates apoptosis and autophagy resulting in synergistic cytotoxicity in melanoma cells. *Oncol Lett*, **14(6):** 7993-7999.

Barni S and Mandala M. 2005. Chemotherapy for metastatic breast cancer. *Ann of Oncol*, **16(Suppl 4):** 23-27.

Buranrat B, Suwannaloet W and Naowaboot J. 2017. Simvastatin potentiates doxorubicin activity against MCF-7 breast cancer cells. *Oncol Lett*, **14(5):** 6243-6250.

Chan KKW, Oza AM and Siu LL. 2003. The statins as anticancer agents. *Clin Cancer Res*, **9(1):**10-19.

Cheng HD, Lui YM and Freimanis RI. 1998. A novel approach to microcalcification detection using fuzzy logic technique. *IEEE Trans Med Imaging*, **(3):** 442-450.

Fujino M, Miura S, Matsuo Y, Tanigawa H, Kawamura A and Saku K. 2006. Pitavastatin-induced downregulation of CCR2 and CCR5 in monocytes is associated with the arrest of cell-cycle in S phase. *Atherosclerosis*, **187(2):** 301-308.

Garwood ER, Baehner FL, Moore DH, Hylton N and Flowers CI. 2010. Fluvastatin reduces proliferation and increases apoptosis in women with high grade breast cancer. *Breast Cancer Res Treat*, **119(1):** 137-144.

Gopalan A, Yu W, Sanders BG and Kline K. 2013. Simvastatin inhibition of mevalonate pathway induces apoptosis in human breast cancer cells via activation of JNK/CHOP/DR5 signaling pathway. *Cancer Lett*, **329(1):** 9-16.

Kotamraju S, Konorev EA, Joseph J and Kalyanaraman B. 2000. Doxorubicin-induced apoptosis in endothelial cells and cardiomyocytes is ameliorated by nitrone spin traps and ebselen. Role of reactive oxygen and nitrogen species *J Biol Chem*, **275(43)**: 33585-33592.

Lee Y-P, Wang C-W, Liao W-C, Yang C-RC-C, Yeh C-T, Tsai C-H, *et al*. 2012. *In vitro* and in vivo anticancer effects of mevalonate pathway modulation on human cancer cells. *Anticancer Res*, **8(32):** 2735–2745.

Malki A, El-Saadani M and Sultan AS. 2009. Garlic constituent diallyl trisulfide induced apoptosis in MCF7 human breast cancer cells. *Cancer Biol Ther*, **8(22)**: 2174-2184.

Massarweh S and Schiff R. 2006. Resistance to endocrine therapy in breast cancer: exploiting estrogen receptor/growth factor signaling crosstalk. *Endocr Relat Cancer*, **13(Suppl 1):** S15-24.

McFarland AJ, Anoopkumar-Dukie S, Arora DS, Grant GD, McDermott CM, Perkins A V, *et al*. 2014. Molecular mechanisms underlying the effects of statins in the central nervous system. *Int J Mol Sci*, **15(11):** 20607-20637.

Osman AMM, Bayoumi HM, Al-Harthi SE, Damanhouri ZA and ElShal MF. 2012. Modulation of doxorubicin cytotoxicity by resveratrol in a human breast cancer cell line. *Cancer Cell Int*, **12(1):** 47.

Taylor CW, Dalton WS, Parrish PR, Gleason MC, Bellamy WT, Thompson FH, *et al*. 1991. Different mechanisms of decreased drug accumulation in doxorubicin and mitoxantrone resistant variants of the MCF7 human breast cancer cell line. *Br J Cancer*, **63(6):** 923.

Tsuboi Y, Kurimoto M, Nagai S, Hayakawa Y, Kamiyama H, Hayashi N, *et al*. 2009. Induction of autophagic cell death and radiosensitization by the pharmacological inhibition of nuclear factor-kappa B activation in human glioma cell lines. *J Neuosurg*, **110(3):** 594-604.

Tu Y-SS, Kang X-LL, Zhou J-GG, Lv X-FF, Tang Y-BB and Guan Y-YY. 2011. Involvement of Chk1–Cdc25A-cyclin A/CDk2 pathway in simvastatin induced S-phase cell cycle arrest and apoptosis in multiple myeloma cells. *Eur J Pharmacol*, **670(2-3):** 356-364.

Vali F, Changizi V and Safa M. 2015. Synergistic apoptotic effect of crocin and paclitaxel or crocin and radiation on MCF-7 cells, a type of breast cancer cell line. *Int J Breast Cancer;* **2015**. Article ID 139349, 7 pages.

Wang J, Centut J, Tokoro T, Higa S and Kitajima I. 2006. Anti-inflammatory effect of pitavastatin on NF-kappa B activated by TNF-alpha in hepatocellular carcinoma cells. *Biol Pharm Bull*, **29(4):** 634–639.

Wang J and Kitajima I. 2007. Pitavastatin inactivates NF-κB and decreases IL-6 production through Rho kinase pathway in MCF-7 cells. *Oncol Rep*, **17(5):** 1149-1154.

Wang S, Konorev EA, Kotamraju S, Joseph J, Kalivendi S and Kalyanaraman B. 2004. Doxorubicin induces apoptosis in normal and tumor cells via distinctly different mechanisms: Intermediacy of H2O2- and p53-dependent pathways. *J Biol Chem*, **279(24):** 25535-25543.

Warita K, Warita T, Beckwitt CH, Schurdak ME, Vazquez A, Wells A, *et al*. 2014. Statin-induced mevalonate pathway inhibition attenuates the growth of mesenchymal-like cancer cells that lack functional E-cadherin mediated cell cohesion. *Sci Rep*, **4**: 7593.

Westbrook K and Stearns V. 2013. Pharmacogenomics of breast cancer therapy: an update. *Pharmacol Ther*, **139(1):** 1-11.

Yang P-M and Chen C-C. 2011. Life or death? Autophagy in anticancer therapies with statins and histone deacetylase inhibitors. *Autophagy*, **7(1):** 107-108.

JJBS

Jordan Journal of Biological Sciences

Volume 13, Number 1,March 2020
ISSN 1995-6673
Pages 107 - 115

Effect of Cyper-diforce® Application and Variety on Major Insect Pests of Watermelon in the Southern Guinea Savanna of Nigeria

Okrikata Emmanuel[1*], Ogunwolu E. Oludele[2] and Odiaka N. Ifeoma[3]

[1]*Department of Biological Sciences, Federal University Wukari,* [2]*Department of Crop and Environmental Protection,* [3]*Department of Crop Production, University of Agriculture, Makurdi, Nigeria*

Received May 2, 2019; Revised June 6, 2019; Accepted June 18, 2019

Abstract

In order to evaluate the inherent potentials of common watermelon varieties to withstand natural pest pressure and to identify potential sources of resistance for breeding programs, a 2-year field study was conducted in the research farm of Federal University Wukari, Nigeria in the early- and late-cropping seasons of 2016 and 2017. The experimental design was a 4 replicated Randomized Complete Block Design with split-plot arrangement of treatments in which main plots were synthetic insecticide (Cyper-diforce®) sprayed and unsprayed ones. The subplot treatments comprised of 5 watermelon commercial varieties namely; Charleston gray, Grey bell, Kaolack, Koloss F_1 and, Sugar baby (Kaolack; the most extensively cultivated variety in the study area was used as a standard for comparison). Kaolack and Koloss F_1, the more recently developed varieties, were observed to be better adapted as their growth were more prolific resulting to higher yields than other varieties. Across years and seasons, the major leaf-feeding beetles [*Aulacophora africana* (Weise), *Asbecesta nigripennis* (Weise), *Asbecesta transversa* (Allard), *Monolepta nigeriae* (Bryant), and *Epilachna chrysomelina* (Fabricius)]; sap-sucking insects [Aphid - *Aphis gossypii* (Glover) and whitefly - *Bemisia tabaci* (Gennadius)] and fruit feeding insects [african bollworm – *Helicoverpa armigera* (Hübner) and fruit fly – *Bactrocera cucurbitae* (Coquillett)] were significantly ($P < 0.0001$) more abundant in the unsprayed plots. Charleston gray, Grey bell and Sugar baby were more susceptible to leaf-feeding beetles but less susceptible to aphid, whitefly, african bollworm and fruit fly. The opposite was observed with Kaolack and Koloss F_1. Therefore, the newest variety (Koloss F_1) is recommended for cultivation in the study area as it produced higher yield. However, a further study is required to determine the mechanisms of resistance and their heritability to enable development of watermelon varieties with resistance to all the major insect pests.

Keywords: *Aphis gossypii* (Glover), Damage, *Helicoverpa armigera* (Hübner), Infestation, Insecticide application, Insect pests, *Monolepta nigeriae* (Bryant), Watermelon varieties.

1. Introduction

Watermelon, *Citrullus lanatus* Thunb. (Cucurbitaceae), is an economically important fruit vegetable crop cultivated in most regions of the world (Adeoye *et al.,* 2011). It has high health, nutritional benefits, and return on investment (Ajewole, 2015). Leaf feeding beetles such as *Aulacophora africana* (Weise), *Asbecesta nigripennis* (Weise), *Asbecesta transversa* (Allard), *Monolepta nigeriae* (Bryant), *Phyllotreta cruciferae* (Goeze) [Coleoptera: Chrysomelidae]; *Epilachna chrysomelina* (Fabricius) [Coleoptera: Coccinellidae]; Sap sucking insects such as Aphid [*Aphis gossypii* (Glover) (Hemiptera: Aphididae)] and Whitefly [*Bemisia tabaci* (Gennadius) (Hemiptera: Aleyrodidae)] and, Fruit feeding insects such as African bollworm [*Helicoverpa armigera* (Hübner) (Lepidoptera, Noctuidae)] and Fruit fly [*Bactrocera cucurbitae* (Coquillett) (Diptera: Tephritidae)] have been reported to infest the crop in different parts of the world and particularly, across different agro-ecological zones of Nigeria (Ogunlana, 1996; Bamaiyi *et al.,* 2010; Burabai *et al.,* 2011; Souza *et al*., 2012; Lima *et al*., 2014; Okrikata *et al*., 2019). Except those who could not afford, watermelon farmers in Nigeria and specifically across the Southern Guinea Savanna Zone depend almost entirely on synthetic insecticides for insect pest control - which are largely applied indiscriminately (Okrikata and Ogunwolu, 2017). Although synthetic insecticides have been found to be effective to a reasonable extent, many health, environmental and economic related challenges have been associated with their usage.

The majority of the documented watermelon varieties worldwide are cultivated in Africa (Yakubu *et al*., 2018). Though most of the farmers in the study area cultivate the variety "Kaolack" popularly called "*Mai Yashi*" - in Hausa language primarily due to its accessibility and market value/customer demand (Okrikata and Ogunwolu, 2017), it is very important to recognize the role morphological and/or physiological differences among varieties can play in influencing crop damage by insect pest. Available literature, however, indicates that while many watermelon varieties have varying levels of resistance to some pathogens, there is rarely such well known and/or well documented information with respect to insect pest

* Corresponding author e-mail: eokrikata@gmail.com.

infestation (Department of Agriculture, Forestry and Fisheries, 2011).

Planting a variety that is not suited for the available market and the particular production situation leads to lower profits or possibly crop failure. In addition, a variety must have acceptable yield and the highest level of pest resistance and such information are useful in breeding programs. There is, however, very little empirically based documented report on relative performance of watermelon varieties exposed to natural insect pest infestation. This study was designed to bridge these knowledge gaps.

2. Materials and Methods

2.1. Study Site

The study was carried out on the experimental farm of Federal University Wukari, Nigeria (N7º50'37", E9º46'31" and 187m altitude), which lies within the Nigerian southern guinea agro-ecological zone [it is characterized by a warm tropical climate with distinct wet and dry seasons - the wet season commences in April and ends in October with June and September being the peak months (Okrikata and Yusuf, 2016)] during 2016 and 2017 early- and late-planting seasons (planting dates: May 14th and August 23rd in 2016 and May 10th and August 15th in 2017).

2.2. Study Design

The experimental design was a Randomized Complete Block Design (RCBD) with split plot arrangement of treatments replicated 4 times. The main plot treatments were 0.5 % Cypermethrin 30g/L + Dimethoate 250g/L EC (Cyper-diforce®) sprayed - maximum of 3 times at each crop growth stage at weekly interval and unsprayed plots. Subplot (subplot size: 5m long, 8m wide) treatments were 5 commercial varieties of watermelon; namely Charleston gray, Grey bell, Kaolack, Koloss F_1 and, Sugar baby. Kaolack variety, popularly called in Hausa language "*Mai yashi*", was the most extensively cultivated variety in the study area largely due to seed accessibility and consumer acceptability/market value (Okrikata and Ogunwlu, 2017) and was therefore used as a standard for comparison in the current study.

2.3. Data Collection

2.3.1. Sampling and Assessment of Insect Pest Population

Sampling of leaf feeding beetles predominated by *Aulacophora africana* (Weise), *Asbecesta nigripennis* (Weise), *Asbecesta transversa* (Allard), *Monolepta nigeriae* (Bryant) [chrysomelidae] and *Epilachna chrysomelina* (Fabricius) [coccinellidae] commenced at 70 % emergence stage (2 weeks after planting - WAP) and proceeded at weekly intervals until fruit maturity. Collection was made between 16:00 and 18:00h using a shoulder mounted motorized suction sampler (Burkard Scientific Ltd., Uxbridge, UK) with a 10 cm diameter inlet cone swept through 5 m length of the middle row at an approximate walking speed of 1 m/sec. The mean population of the insects was computed as number/5 m length of row.

Sampling of sap sucking insects predominated by hemipterous *Aphis gossypii* (Glover) and *Bemisia tabaci* (Gennadius) commenced at the vegetative stage of the crop (3 WAP) and proceeded at weekly intervals till crop maturity. For *A. gossypii*, estimates of population density was made by assessing the colony size on 12 r andomly selected leaves/plot, using a scale of **0** – **5** scale, where: **0** = no aphids; **1** = 1 – 4 aphids; **2** = 5 – 20 aphids; **3** = 21 – 100 aphids; **4** = 101 – 500 aphids and **5** = > 500 aphids modified after Egho (2011). For *B. tabaci*, a 15 x 15 c m yellow sticky board was waved across the 5 m length of the middle row of each subplot on s haking the plants therein and the insects trapped were counted as described by Anaso (1999).

The major fruit feeding pests were *Bactrocera cucurbitae* (Coquillett) [Diptera: Tephritidae] and *Helicoverpa armigera* (Hübner) [Lepidoptera: Noctudae]. Larvae of *B. cucurbitae* (fruit fly) were sampled at harvest in which case infested fruits were isolated and counted in each plot. They were split open and the number of *B. cucurbitae* larvae therein counted and expressed as number/fruit using the formula described by Barma *et al*. (2013):

$$\text{No. of } B.\ cucurbitae \text{ larvae/fruit} = \frac{\text{No. of infested fruits x No. of larvae per infested fruit}}{\text{No. of fruits per plot}}$$

However, sampling of *H. armigera* larvae commenced at mid-flowering stage (6 WAP) using the suction sampler and following the method used for sampling leaf feeding beetles as described above.

2.3.2. Identification of Insect Pest

Samples of dominant insects collected were killed in ethyl acetate in a killing jar and then preserved in 70% ethanol. Moths were dried and preserved in an airtight container containing silica gel. Immature stages were reared to adult in the laboratory for identification. The insects were all identified at the insect museum of Institute of Agricultural Research (IAR), Ahmadu Bello University Zaria, Nigeria.

2.3.3. Assessment of Leaf Injury and Growth Parameters

At 3, 6 a nd 9 W AP, a random sample of 15 leaves/subplot was taken and the proportion damaged was recorded. The leaves were also scored for severity of injury on a scale of **0** – **4**, following the method described by Trusca *et al.* (2013) where:

0 = 0 % leaf area injured
1 = 1 – 25 % leaf area injured
2 = 26 – 50 % leaf area injured
3 = 51 – 75 % leaf area injured
4 = 76 - 100 % leaf area injured.

The individual scores obtained per subplot were converted to attack severity (%) using the equation described by Okrikata and Anaso (2008):

$$\text{Attack severity (\%)} = \sum n \times 100/N \times 4$$

Where; $\sum n$ = summation of individual injury scores/plot, N = number of scores taken/plot (= 15), and4 = highest score on the scale.

Also, at 9 WAP, 3 plants were randomly selected per subplot from which the main vine length (cm) was measured with a flexible tape and the average number of lateral and secondary branches computed.

2.3.4. Evaluation of Fruit Yield

Fruits in each subplot were harvested twice at 10 days interval, weighed, and sorted into marketable and unmarketable categories. The latter comprised of fruits that

were discolored, misshapen, cracked, insect damaged, and infected with blossom end rot. The proportion of the marketable fruits was computed.

2.4. Data Analysis

Numerical data was transformed to $\sqrt{x} + 0.5$ while data in percentages transformed to arcsine before variance analysis. Significantly, different treatment means were separated by Students Newman Keul's (SNK) test at 5 % level of probability using SAS statistical software, version 9.2.

3. Results

3.1. Effect of Chemical Treatment and Variety on Major Insect Pests of Watermelon

Across years and seasons, the major leaf-feeding beetles (*A. africana, A. nigripennis, A. transversa, M. nigeriae* and *E. chrysomelina*) were significantly ($P < 0.0001$) more abundant in the unsprayed plots (Table 1). The most common was *A. nigripennis* followed by *M. nigeriae*. The least was *E. chrysomelina*. Charleston gray variety consistently attracted more beetles followed by Sugar baby. Kaolack variety had the least beetle density followed by Koloss F_1 in both early- ($P < 0.0001$) and late-sown ($P = 0.6399$) crops of 2016. Corresponding probability values for 2017 cropping year were (0.0373 and < 0 .0001), respectively. The interaction between synthetic chemical insecticide (Cyper-diforce®) application (C) and variety (V) in 2016 cropping year was significant ($P < 0.001$) in the early-sown but not ($P = 0.7621$) in the late-sown. Corresponding p-values for 2017 cropping year were 0.3107 and < 0.001, respectively.

Density of *A. gossypii* was 67.2 % ($P < 0.0001$) higher in the unsprayed than sprayed plots of the early-sown crop of 2016 cropping year and correspondingly 460.5 % in the late-sown. In 2016 early-sown crop, Charleston gray had significantly ($P < 0.0001$) the least infestation while Kaolack, the highest. Grey bell, Sugar baby and Koloss F_1 had statistically comparable infestation level. In the late-sown, however, Charleston gray and Sugar baby varieties had significantly ($P < 0.0001$) lower and comparable infestation while Kaolack and Koloss F_1 had higher. Interaction effect was significant in the early- ($P < 0.0001$) and insignificant in the late- ($P = 0.1648$) sown crops. A similar trend in *A. gossypii* infestation was observed in 2017 early- and late-crop, respectively, except that interaction effect was significant ($P < 0.05$) in both. Tables 2a and b reveal that infestation by *B. tabaci* follows a trend similar to that of *A. gossypii*. Insecticide application reduced infestation by 24.5 and 39.6 % (in the early- and late-sown crop of 2016) and correspondingly by 5.7 and 35.2 % in 2017. Across years and seasons, differences among varieties were significant ($P < 0.05$) with Kaolack and Koloss F_1 varieties having higher infestations and, Charleston gray and Sugar baby, lower and interaction effects consistently insignificant ($P > 0.05$).

Tables (3a and b) revealed that *B. cucurbitae* density was 5-fold higher in the unsprayed than in the sprayed early-sown crop of 2016; on the late-sown, differential was 10-fold ($P < 0.0001$). In 2017, the differentials were approximately 4 and 9-folds, respectively. In both the early- and late-sown crops of 2016, the density of *B. cucurbitae* larvae per fruit was significantly ($P < 0.0001$) higher in Kaolack, followed by Koloss F_1 than in Charleston gray and Sugar baby varieties. Differences among varieties in 2017 trials followed a somewhat similar trend with interaction effects across years and seasons being significant ($P < 0.0001$). *H. armigera* infestation was rare on the early-crop of both years. However, it was predominant on late-crops with trends in infestation among varieties following a trend similar to that of *B. cucurbitae* in both years except for the insignificant interactions ($P > 0.05$) between insecticide application and variety (Tables 3a, b).

3.2. Effect of Chemical Treatment and Variety on Leaf Injury of Watermelon

In all the trials, the proportion and severity of leaf injury was significantly ($P < 0.0001$) higher on unsprayed than on sprayed crops. Sugar baby and Charleston gray had significantly ($P < 0.0001$) more proportions of leaves injured with a higher severity of leaf injury than the other varieties. Kaolack had the lowest proportion of leaves injured and severity, followed by Koloss F_1. Interaction between insecticide application and variety were consistently insignificant ($P > 0.05$) for both parameters across years and seasons (Tables 4a and b).

3.3. Effect of Chemical Treatment and Variety on Growth of Watermelon

In 2016, insecticide treatment significantly ($P < 0.001$) increased main vine length by 148.2 and 149.3 % in the early- and late-sown crops, respectively (Table 5a). Varieties differed significantly ($P < 0.0001$) with Sugar baby having the longest main vine length and Grey bell having the shortest. With respect to the number of lateral branches, an increase of 161.8 and 160.9 % due to insecticide treatment in the early- and late-sown crops respectively was observed. Generally, Kaolack, Charleston gray and Koloss F_1 produced more lateral branches ($P < 0.0001$) than Grey bell and Sugar baby in both early- and late-sown crops. Insecticide treatment resulted in significantly increased ($P < 0.0001$) number of secondary branches by 2.8 X in each of the early- and late-sown crop. Koloss F_1 and Kaolack were statistically comparable and both were significantly ($P < 0.0001$) different from the other varieties in the number of secondary branches produced in both early- and late-sown crops. Interaction was significant ($P < 0.05$) for both early- and late-sown crops for main vine length, number of lateral branches and number of secondary branches. A somewhat similar trend was observed in 2017 cropping year (Table 5b).

3.4. Effect of Chemical Treatment and Variety on Fruit Yield of Watermelon

With respect to marketable fruit yield, sprayed plots were observed to be > 240-fold more productive (tha^{-1}) than unsprayed plots in 2016 cropping year. Charleston gray and Sugar baby were statistically comparable in the early- as well as in the late-sown crops. From these 2, the remaining 3 varieties were significantly different. They were significantly different one from another as well with Koloss F_1 being the most productive. Interactions between insecticide application and variety were significant ($P < 0.0001$). A similar trend was observed in 2017 cropping year (Table 6).

Table 1. Effects of insecticide application and variety on abundance (Mean±SE) of major leaf-feeding beetles in early- and late-sown watermelon varieties in Wukari.

Treatment	Leaf-feeding beetles collected/5m length of row[1]			
	2016 cropping year		2017 cropping year	
	Early-sown[2]	Late-sown[2]	Early-sown[2]	Late-sown[2]
Chemical treatment (C)				
Sprayed (0.5 % cyper-diforce®)	2.83±0.11^{b}	1.23±0.04^{b}	2.89±0.21^{b}	1.28±0.05^{b}
Un-sprayed (0 % cyper-diforce®)	21.16±0.39^{a}	10.88±0.22^{a}	23.76±2.45^{a}	11.11±0.25^{a}
P value	<0.0001	<0.0001	<0.0001	<0.0001
Variety (V)				
Kaolack	10.62±3.10^{c}	5.36±1.62^{a}	10.77±3.14^{b}	5.48±1.65^{c}
Charleston gray	13.43±3.77^{a}	6.89±2.01^{a}	19.38±8.02^{a}	6.95±2.05^{a}
Grey bell	11.88±3.45^{c}	5.93±1.79^{a}	12.07±3.50^{ab}	6.06±1.83^{c}
Sugar baby	12.89±3.65^{b}	6.57±1.96^{a}	13.08±3.70^{ab}	6.71±1.99^{b}
Koloss F_1	11.13±3.36^{d}	5.63±1.74^{a}	11.32±3.40^{b}	5.75±1.78^{d}
P value	<0.0001	ns	0.0373	<0.0001
Interaction				
C x V	***	ns	ns	***

[1]Means (±SE) of Aulacophora africana, Asbecesta nigripennis, Asbecesta transversa, Monolepta nigeriae and Epilachna chrysomelina.

[2] Means are values of four replications; Means (±SE) followed by the same superscript letter(s) within a column are not significantly different using Student-Newman Keul's (SNK) test (P ≤ 0.05); * = significantly different (P ≤ 0.05); ** = significantly different (P ≤ 0.01); *** = significantly different (P ≤ 0.001); ns = not significantly different (P > 0.05).

Table 2a. Effects of insecticide application and variety on abundance (Mean±SE) of major sap-sucking insects in early- and late-sown watermelon in Wukari in 2016.

Treatment	***Aphis gossypii* score**		***Bemisia tabaci***	
	Early-sown[1]	**Late-sown[1]**	**Early-sown[1]**	**Late-sown[1]**
Chemical treatment (C)				
Sprayed (0.5 % cyper-diforce®)	1.19±0.02^{b}	0.81±0.05^{b}	13.90±0.29^{b}	23.52±0.79^{b}
Un-sprayed (0 % cyper-diforce®)	1.99±0.07^{a}	4.54±0.12^{a}	17.31±0.39^{a}	32.84±0.96^{a}
P value	<0.0001	<0.0001	<0.0001	<0.0001
Variety (V)				
Kaolack	1.90±0.22^{a}	3.14±0.78^{a}	17.12±0.84^{a}	31.97±2.15^{a}
Charleston gray	1.35±0.09^{c}	2.29±0.62^{c}	14.33±0.60^{c}	25.57±2.01^{b}
Grey bell	1.57±0.15^{b}	2.63±0.73^{b}	15.53±0.81^{bc}	27.64±2.15^{b}
Sugar baby	1.56±0.15^{b}	2.40±0.65^{bc}	14.39±0.77^{c}	24.76±1.96^{b}
Koloss F_1	1.57±0.15^{b}	2.93±0.77^{a}	16.66±0.70^{ab}	30.95±1.74^{a}
P value	<0.0001	<0.0001	<0.0001	<0.0001
Interaction				
C x V	***	ns	ns	ns

[1]Means are values of four replications; Means (±SE) followed by the same superscript letter(s) within a column are not significantly different using Student-Newman Keul's (SNK) test (*P* ≤ 0.05); * = significantly different (*P* ≤ 0.05); ** = significantly different (*P* ≤ 0.01); *** = significantly different (*P* ≤ 0.001); ns = not significantly different (*P* > 0.05)

Table 2b. Effects of insecticide application and variety on abundance (Mean±SE) of major sap-sucking insects in early- and late-sown watermelon in Wukari in 2017.

Treatment	***Aphis gossypii* score**		***Bemisia tabaci***	
	Early-sown[1]	**Late-sown[1]**	**Early-sown[1]**	**Late-sown[1]**
Chemical treatment (C)				
Sprayed (0.5 % cyper-diforce®)	2.22±0.01^{b}	2.74±0.11^{b}	11.01±0.23^{b}	27.13±0.81^{b}
Un-sprayed (0 % cyper-diforce®)	4.02±0.06^{a}	3.36±0.15^{a}	11.64±0.24^{a}	36.67±0.98^{a}
P value	<0.0001	<0.0001	0.0372	<0.0001
Variety (V)				
Kaolack	3.30±0.39^{a}	3.67±0.17^{a}	12.25±0.30^{a}	35.79±2.20^{a}
Charleston gray	2.96±0.30^{d}	2.42±0.10^{c}	10.53±0.26^{b}	29.23±2.06^{b}
Grey bell	3.12±0.35^{c}	3.05±0.12^{b}	11.59±0.36^{ab}	31.35±2.20^{b}
Sugar baby	3.00±0.31^{d}	2.43±0.10^{c}	10.60±0.26^{b}	28.39±2.01^{b}
Koloss F_1	3.22±0.37^{b}	3.67±0.15^{a}	11.64±0.39^{ab}	34.75±1.78^{a}
P value	<0.0001	<0.0001	0.0029	<0.0001
Interaction				
C x V	<0.0001	0.0006	ns	ns

[1]Means are values of four replications; Means (±SE) followed by the same superscript letter(s) within a column are not significantly different using Student-Newman Keul's (SNK) test (*P* ≤ 0.05); * = significantly different (*P* ≤ 0.05); ** = significantly different (*P* ≤ 0.01); *** = significantly different (*P* ≤ 0.001); ns = not significantly different (*P* > 0.05)

Table 3a. Effects of insecticide application and variety on abundance (Mean±SE) of major fruit-feeding insects in early- and late-sown watermelon in Wukari in 2016.

	Early-sown[1]	Late-sown[1]	
Treatment	*Bactrocera cucurbitae* larvae/fruit	*Bactrocera cucurbitae* larvae/fruit	*Helicoverpa armigera* larvae/5m row
Chemical treatment (C)			
Sprayed (0.5 % cyper-diforce®)	4.62±0.20^{b}	0.83±0.13^{b}	4.64±0.23^{b}
Un-sprayed (0 % cyper-diforce®)	21.40±0.72^{a}	8.17±0.30^{a}	9.23±0.03^{a}
P value	<0.0001	<0.0001	<0.0001
Variety (V)			
Kaolack	15.60±3.97^{a}	5.55±1.73^{a}	8.09±0.94^{a}
Charleston gray	11.19±2.63^{d}	3.72±1.04^{c}	6.11±0.93^{bc}
Grey bell	13.13±3.27^{c}	4.62±1.45^{b}	6.58±0.84^{b}
Sugar baby	11.26±2.68^{d}	3.80±1.17^{c}	5.72±0.85^{c}
Koloss F_1	13.88±3.36^{b}	4.79±1.46^{b}	8.16±0.92^{a}
P value	<0.0001	<0.0001	<0.0001
Interaction			
C x V	***	***	ns

[1]Means (±SE) are values of four replications; Means (±SE) followed by the same superscript letter(s) within a column are not significantly different using Student-Newman Keul's (SNK) test ($P \leq 0.05$); * = significantly different ($P \leq 0.05$); ** = significantly different ($P \leq 0.01$); *** = significantly different ($P \leq 0.001$); ns = not significantly different ($P > 0.05$)

Table 3b. Effects of insecticide application and variety on abundance (Mean±SE) of major fruit-feeding insects in early- and late-sown watermelon in Wukari in 2017.

	Early-sown[1]	**Late-sown[1]**	
Treatment	***Bactrocera cucurbitae* larvae/fruit**	***Bactrocera cucurbitae* larvae/fruit**	***Helicoverpa armigera* larvae/5m row**
Chemical treatment (C)			
Sprayed (0.5 % cyper-diforce®)	5.72±0.10^{b}	0.86±0.03^{b}	6.61±0.23^{b}
Un-sprayed (0 % cyper-diforce®)	23.18±0.74^{a}	8.34±0.31^{a}	11.14±0.30^{a}
P value	<0.0001	<0.0001	<0.0001
Variety (V)			
Kaolack	17.15±4.13^{a}	5.68±1.76^{a}	10.02±0.93^{a}
Charleston gray	12.55±2.74^{d}	3.81±1.16^{c}	8.06±0.92^{bc}
Grey bell	14.58±3.40^{c}	4.74±1.48^{b}	8.52±0.83^{b}
Sugar baby	12.63±2.78^{d}	3.89±1.20^{c}	7.68±0.84^{c}
Koloss F_1	15.35±3.50^{b}	4.91±1.49^{b}	10.09±0.91^{a}
P value	<0.0001	<0.0001	<0.0001
Interaction			
C x V	***	***	ns

[1]Means (±SE) are values of four replications; Means (±SE) followed by the same superscript letter(s) within a column are not significantly different using Student-Newman Keul's (SNK) test ($P \leq 0.05$); * = significantly different ($P \leq 0.05$); ** = significantly different ($P \leq 0.01$); *** = significantly different ($P \leq 0.001$); ns = not significantly different ($P > 0.05$).

Table 4a. Effects of insecticide application and variety on leaf injury in early- and late-sown watermelon in Wukari in 2016.

	Mean proportion of leaves injured (%)		**Mean severity of leaf injury (%)**	
Treatment	**Early-sown[1]**	**Late-sown[1]**	**Early-sown[1]**	**Late-sown[1]**
Chemical treatment (C)				
Sprayed (0.5 % cyper-diforce®)	17.51±1.55^{b}	16.63±1.49^{b}	7.15±0.62^{b}	6.83±0.59^{b}
Un-sprayed (0 % cyper-diforce®)	66.86±3.28^{a}	64.66±2.70^{a}	46.45±0.90^{a}	45.24±0.70^{a}
P value	<0.0001	<0.0001	<0.0001	<0.0001
Variety (V)				
Kaolack	33.17±9.17^{b}	31.67±8.70^{c}	24.38±7.50^{c}	23.53±7.26^{b}
Charleston gray	50.24±11.65^{a}	48.04±11.10^{a}	27.74±7.04^{ab}	28.15±7.17^{a}
Grey bell	43.06±8.55^{a}	40.11±7.95^{ab}	26.35±7.60^{bc}	25.46±7.35^{b}
Sugar baby	50.65±11.17^{a}	48.59±10.72^{a}	29.95±7.78^{a}	28.60±7.44^{a}
Koloss F_1	37.28±8.08^{b}	34.80±8.13^{bc}	25.58±7.55^{bc}	24.62±7.27^{b}
P value	<0.0001	<0.0001	0.0019	0.0003
Interaction				
C x V	ns	ns	ns	ns

[1]Means (±SE) are values of four replications; Means (±SE) followed by the same superscript letter(s) within a column are not significantly different using Student-Newman Keul's (SNK) test ($P \leq 0.05$); ns = not significantly different ($P > 0.05$).

Table 4b. Effects of insecticide application and variety on leaf injury in early- and late-sown watermelon in Wukari in 2017.

Treatment	Mean proportion of leaves injured (%)		Mean severity of leaf injury (%)	
	Early-sown[1]	Late-sown[1]	Early-sown[1]	Late-sown[1]
Chemical treatment (C)				
Sprayed (0.5 % cyper-diforce®)	21.66±1.19^{b}	21.66±1.27^{b}	8.01±0.69^{b}	7.97±0.69^{b}
Un-sprayed (0 % cyper-diforce®)	72.33±2.50^{a}	69.22±2.64^{a}	53.58±0.81^{a}	52.41±0.84^{a}
P value	<0.0001	<0.0001	<0.0001	<0.0001
Variety (V)				
Kaolack	37.78±9.02^{c}	36.39±8.54^{c}	27.86±8.63^{b}	27.13±8.36^{b}
Charleston gray	53.89±11.51^{a}	52.50±11.20^{a}	33.04±8.47^{a}	32.61±8.32^{a}
Grey bell	46.94±8.37^{b}	45.27±7.75^{b}	30.08±8.70^{b}	29.34±8.46^{b}
Sugar baby	54.16±11.06^{a}	53.05±0.69^{a}	33.84±8.83^{a}	33.37±8.67^{a}
Koloss F_1	42.22±8.65^{bc}	39.99±7.86^{bc}	29.16±8.66^{b}	28.50±8.42^{b}
P value	<0.0001	<0.0001	0.0003	0.0002
Interaction				
C x V	ns	ns	ns	ns

[1]Means (±SE) are values of four replications; Means (±SE) followed by the same superscript letter(s) within a column are not significantly different using Student-Newman Keul's (SNK) test ($P \leq 0.05$); ns = not significantly different ($P > 0.05$).

Table 5a. Effects of insecticide application and variety on main vine length and number of branches in early- and late-sown watermelon in Wukari in 2016.

Treatment	Main vine length at 9 WAP (cm)		Number of lateral branches at 9 WAP		Number of secondary branches at 9 WAP	
	Early-sown[1]	Late-sown[1]	Early-sown[1]	Late-sown[1]	Early-sown[1]	Late-sown[1]
Chemical treatment (C)						
Sprayed[2]	309.11±3.81^{a}	329.26±4.31^{a}	4.53±0.29^{a}	4.54±0.36^{a}	38.68±3.93^{a}	40.62±4.21^{a}
Un-sprayed[3]	124.54±1.91^{b}	132.06±2.06^{b}	1.73±0.13^{b}	1.74±0.25^{b}	13.58±1.26^{b}	14.28±1.33^{b}
P value	<0.0001	<0.0001	<0.0001	<0.0001	<0.0001	<0.0001
Variety (V)						
Kaolack	216.77±34.87^{c}	230.77±36.89^{c}	3.54±0.78^{a}	3.56±0.88^{a}	36.16±9.12^{a}	38.30±8.78^{a}
Charleston gray	213.57±36.57^{d}	228.33±39.81^{d}	3.41±0.62^{a}	3.49±0.62^{a}	14.28±3.17^{c}	14.94±3.31^{b}
Grey bell	196.92±31.12^{e}	208.10±32.97^{e}	2.28±0.37^{b}	2.29±0.47^{b}	18.16±2.88^{bc}	18.96±3.01^{b}
Sugar baby	232.58±36.78^{a}	246.86±39.49^{a}	2.52±0.50^{b}	2.53±0.60^{b}	24.40±3.80^{b}	25.68±3.96^{b}
Koloss F_1	224.28±34.78^{b}	239.26±37.21^{b}	3.90±0.64^{a}	3.91±0.77^{a}	37.65±6.00^{a}	39.38±7.36^{a}
P value	<0.0001	<0.0001	0.0003	<0.0001	<0.0001	<0.0001
Interaction						
C x V	***	***	*	*	**	**

[1]Means (±SE) are values of four replications; Means (±SE) followed by the same superscript letter(s) within a column are not significantly different using Student-Newman Keul's (SNK) test ($P \leq 0.05$); [2]Sprayed - (0.5 % cyper-diforce®); [3]Un-sprayed - (0 % cyper-diforce®)

* = significantly different ($P \leq 0.05$); ** = significantly different ($P \leq 0.01$); *** = significantly different ($P \leq 0.001$).

Table 5b. Effects of insecticide application and variety on main vine length and number of branches in early- and late-sown watermelon in Wukari in 2017.

Treatment	Main vine length at 9 WAP (cm)		Number of lateral branches at 9 WAP		Number of secondary branches at 9 WAP	
	Early-sown[1]	Late-sown[1]	Early-sown[1]	Late-sown[1]	Early-sown[1]	Late-sown[1]
Chemical treatment (C)						
Sprayed[2]	296.91±3.47^{a}	332.67±4.22^{a}	4.48±0.28^{a}	4.50±0.38^{a}	37.88±3.85^{a}	39.15±3.80^{a}
Un-sprayed[3]	129.17±1.74^{b}	139.42±2.06^{b}	1.72±0.14^{b}	1.73±0.23^{b}	13.30±1.23^{b}	14.01±1.30^{b}
P value	<0.0001	<0.0001	<0.0001	<0.0001	<0.0001	<0.0001
Variety (V)						
Kaolack	219.82±31.61^{b}	244.47±36.46^{b}	3.51±0.77^{a}	3.88±0.64^{a}	35.41±8.94^{a}	37.72±5.69^{a}
Charleston gray	210.09±33.50^{d}	233.76±39.01^{d}	3.37±0.62^{a}	3.38±0.72^{a}	17.78±2.82^{bc}	14.64±3.25^{c}
Grey bell	194.95±28.28^{e}	213.94±32.31^{e}	2.51±0.49^{b}	2.27±0.26^{b}	13.99±2.10^{c}	18.58±2.95^{bc}
Sugar baby	227.36±33.42^{a}	251.92±38.70^{a}	2.26±0.36^{b}	2.51±0.59^{b}	23.90±3.72^{b}	25.17±3.87^{b}
Koloss F_1	212.99±31.69^{c}	236.15±36.16^{c}	3.86±0.63^{a}	3.52±0.87^{a}	36.86±6.86^{a}	36.78±8.99^{a}
P value	<0.0001	<0.0001	0.0004	<0.0001	<0.0001	<0.0001
Interaction						
C x V	***	***	*	*	**	**

[1]Means (±SE) are values of four replications; Means (±SE) followed by the same superscript letter(s) within a column are not significantly different using Student-Newman Keul's (SNK) test ($P \leq 0.05$); [2]Sprayed - (0.5 % cyper-diforce®); [3]Un-sprayed - (0 % cyper-diforce®)

* = significantly different ($P \leq 0.05$); ** = significantly different ($P \leq 0.01$); *** = significantly different ($P \leq 0.001$).

Table 6. Effects of insecticide application and variety on fruit yield/ha in early- and late-sown watermelon in Wukari, cropping years 2016 and 2017,

Treatment	Marketable fruit yield (tha^{-1})			
	2016		2017	
	Early-sown[1]	Late-sown[1]	Early-sown[1]	Late-sown[1]
Chemical treatment (C)				
Sprayed (0.5 % cyper-diforce®)	39.87±2.49[a]	45.76±2.73[a]	38.41±2.41[a]	44.16±2.93[a]
Un-sprayed (0 % cyper-diforce®)	0.15±0.02[b]	0.19±0.02[b]	0.11±0.01[b]	0.14±0.08[b]
P value	<0.0001	<0.0001	<0.0001	<0.0001
Variety (V)				
Kaolack	23.45±8.79[b]	26.70±10.01[b]	22.61±9.50[b]	25.73±9.66[b]
Charleston gray	13.48±5.14[d]	15.70±5.94[d]	12.97±4.96[d]	15.11±5.77[d]
Grey bell	19.77±7.50[c]	22.80±8.60[c]	19.02±7.21[c]	21.94±8.35[c]
Sugar baby	15.42±5.82[d]	17.97±6.85[d]	14.81±5.60[d]	17.33±6.66[d]
Koloss F_1	27.92±10.49[a]	31.71±11.88[a]	26.90±10.13[a]	30.63±11.55[a]
P value	<0.0001	<0.0001	<0.0001	<0.0001
Interaction				
C x V	***	***	***	***

[1]Means (±SE) are values of four replications; Means (±SE) followed by the same superscript letter(s) within a column are not significantly different using Student-Newman Keul's (SNK) test ($P \leq 0.05$); *** = significantly different ($P \leq 0.001$)

4. Discussion

Results obtained show vulnerability of watermelon varieties to insect pest damage as reported by Gichimu *et al*. (2008) and that effective protection against insect pests of watermelon is necessary for meaningful yield in the study area. The insecticide used (Cyper-diforce®) is a mixture of Cypermethrin 30g/L and Dimethoate 250g/L EC. Cypermethrin is a broad-spectrum, neurotoxic, contact synthetic pyrethroid, while Dimethoate is a widely used systemic organophosphate insecticide that interferes with nerve impulse transmission in arthropods (Cox, 1996; Qayoom *et al*., 2016). The choice of cyper-diforce® insecticide is apt as it has the ability of suppressing both chewing and sap sucking insects, and the results obtained indicates that it was significantly effective in managing all the major insect pests of watermelon.

Recommending a variety most suitable to an agro-ecological zone requires using common varieties in the area for performance trial. None of the varieties tested in the current trials exhibited resistance to all the major insect pests of watermelon. While Charleston gray, Sugar baby and Grey bell had relatively higher infestation by leaf-eating beetles and lower infestation by aphid (*A. gossypii*), whitefly (*B. tabaci*), African bollworm (*H. armigera*) and fruit fly (*B. cucurbitae*), Kaolack and Koloss F_1 had higher infestation by aphid, whitefly, African bollworm and fruit fly and lower infestation by leaf-eating beetles. A number of studies have shown that different varieties/genotypes of the same plant species could respond significantly differently to different insect pests (Simmons *et al*., 2010; Haldhar *et al*., 2015). These differences may be attributed to differences in biochemical and/or morphological traits.

Attractiveness of chrysomelid beetles to cucurbits (watermelon, inclusive) had been linked to higher cucurbitacin content (Gichimu *et al*., 2009). This is said to be due to the co-evolutionary relationship between cucurbits and luperine chrysomelid beetles (Metcalf and Lampman, 1989). At the same time, cucurbitacin has been linked to protection against herbivory by other insect pests other than the luperine chrysomelid beetles (Koul *et al*., 2008). The results obtained in this study suggest that Charleston gray, Sugar baby and Grey bell which were developed well over half a century ago (1954, 1956 and 1963, respectively) may contain higher cucurbitacin and hence were more attractive to chrysomelid beetles and resistant to other major pests - aphids, whiteflies, African bollworm and fruit flies. Kaolack and Koloss F_1 are comparatively recently developed varieties and may have been selected for much lower cucurbitacin [cultivated cucurbits have been selected over time for lower amounts of cucurbitacins as a result of their toxicity and bitterness (Recio *et al*., 2012)] and higher yields. The trade-off is such that, lower cucurbitacin implies lesser beetle infestation and higher infestation by other major pests of watermelon.

The ability of leaf eating beetles to weaken seedlings and/or bring about loss of plant stands resulting to yield loss has been shown by Kemble *et al*., (2005). Leaf injury has also been shown to have serious implication on the quantity and quality of fruits produced by watermelon plants as the leaves play a key role in synthesizing sugar and accumulating water in the fruits (Nath, 2002). This implies that the higher the proportion and/or intensity of leaf injury, the lower the quality and/or quantity of fruits produced. Such trend was observed in the present study as Kaolack and Koloss F_1 which had lesser proportion and intensity of leaf injury had higher fruit yields. Of the 5 dominant leaf feeding beetles, *A. nigripennis* followed by *M. nigeriae* were more common. The least common was *E. chrysomelina.* Since the leaf feeding beetles have largely similar pattern of injury on the crop leaves, it was difficult to mention which species of them was most harmful. Therefore, their relative abundance indicates their relative harmfulness on the crop.

Though, the impacts of the major sap-sucking pests (*A. gossypii* and *B. tabaci*) were difficult to estimate on the

field, the negative effect of their infestation on growth and yield cannot be ruled out. Throughout the 2 years research, occurrence of *H. armigera* (a fruit feeding insect) in the early-season was sporadic, which may be attributed to unfavorable weather conditions – increased frequency and intensity of rainfall. However, its effect (along with *B. cucurbitae*) in reducing the marketability of the fruits was very obvious.

The higher yields of Kaolack and Koloss F_1 relative to the other varieties could be attributed to lower infestation and damage by leaf-feeding beetles, higher survival rate, more prolific growth evidenced by longer vine length and more lateral and secondary branches. Gichimu *et al*. (2008) reported an association between prolific growth and high yield of watermelon. The current information on variable response by watermelon varieties to major insect pests could be useful for watermelon breeding programs.

5. Conclusion

Koloss F_1, the more recently developed variety, was better adapted and its growth more prolific producing higher yields than other varieties except, Kaolack. Charleston gray, Grey bell and Sugar baby, which were more susceptible to leaf-eating beetles, were less than aphid, whitefly, African bollworm and fruit fly. The opposite was observed with Kaolack and Koloss F_1. A further study is, therefore, recommended to determine the mechanisms of resistance and their heritability to enable development of commercially acceptable watermelon variety with better resistance to the major insect pests and higher yields.

Acknowledgements

Thanks go to the Management of Federal University Wukari, Nigeria for permission to undertake a s tudy towards Ph.D. degree in Economic Entomology. Many thanks also go to Mr. Ernest Ekoja of Department of Crop and Environmental Protection, Federal University of Agriculture Makurdi for his support in statistical analyses and to Mr. Ishaku Musa of the Insect Museum of Institute of Agricultural Research (IAR), Ahmadu Bello University, Zaria, Nigeria who identified the insects collected on watermelon. The assistance of the Management and Staff of National Horticultural Institute (NIHORT), Kano Sub-station, Nigeria in providing seeds of some of the varieties of watermelon used for the research is appreciated.

References

Adeoye IB, Olayide–Tawo FB, Adebisi–Adelan O, Usman JM, and Badmus MA. 2011. Economic analysis of watermelon based production system in Oyo State. *Nig J Agric Biol Sci.,* **6(7)**: 53-59.

Ajewole OC. 2015. Income analysis of watermelon production in Ekiti State, Nigeria. *J Econs Sus Dev.*, **6(2)**: 67-72.

Anaso CE. 1999. Evaluation of Neem Extracts for Control of Major Insect Pests of Okro (*Abelmoschus esculentus*) Ph.D. Thesis. University of Maiduguri. 131pp.

Bamaiyi LJ, Alao SEL, and Amans E. 2010. Optimum sprays required for insect pest management on rain-fed watermelon. Horticultural Crop Research Programme, Cropping Scheme Reports. IAR, ABU, Zaria. February, 23 – 24, 2010. Pp 33–35.

Barma P, Jha S, and Banerjee S. 2013. Prediction of population development of melon fruit-fly (*Bactrocera cucurbitae* Coquillett) on Pionted Gourd (*Trichosanthes dioica* Roxb.). *Afri J Agric Res.*, **8(38):** 4740–4747.

Burabai W, Etekpe GW, Ambah B, and Angaye PE. 2011. Combination of garlic extract and some organophosphate insecticides in controlling Thrips (*Thrips palmi*) in Watermelon. *Int J Appl Sci Eng.*, **9(1)**: 19–23.

Cox C. 1996. Insecticide factsheet: Cypermethrin. *J Pes Ref.,* **16(2):** 15 – 20.

Department of Agriculture, Forestry and Fisheries. 2011. **Production guidelines: Watermelon (*Citrullus lanatus*)**. Compiled by Directorate of Plant Production, Pretoria, South Africa. 32pp.

Egho EO. 2011. Management of major field insect pests and yield of cowpea (*Vigna unguiculata* (L.)Walp) under calendar and monitored application of synthetic chemicals in Asaba, Southern Nigeria. *Am J Sci Indus Res.*, **2(4)**: 592–602.

Gichimu BM, Owuor BO, and Dida MM. 2008. Assessment of four commercial watermelon cultivars and one local landrace for their response to naturally occurring disease, pests and non-pathogenic disorders in sub-humid tropical conditions. *J Agric Biol Sci.*, **3(5 and 6)**: 32–43.

Gichimu BM, Owuor BO, Mwai GN, and Dida MM. 2009. Morphological characterization of some wild and cultivated watermelon (*Citrullus* sp.) accession in Kenya. *J Agric Biol Sci.*, **4(2)**: 10-18.

Haldhar SM, Choudhary BR, Bhargava R, and Meena SR. 2015. Antixenosis and allelochemical resistance traits of watermelon against Bactrocera cucurbitae in a hot arid region of India. *Flor Entomol.,* **98(3):** 827-834.

Kemble JM, Sikora EJ, Patterson MG, Zehnder GW, and Buske E. 2005. Guide to commercial summer squash production. Alabama Cooperative Extension System. Alabama A and M University and, Auburn University. PubID: 1014.

Koul O. 2008. Phytochemicals and insect control: An antifeedant approach. *Crit Rev Plant Sci.*, **27**: 1 – 24.

Lima CHO, Sarmento RA, Rosado JF, Silveira MCAC, Santos GR, Pedro-Neto M, Erasmo EAL, Nascimento IR, and Picanço MC. 2014. Efficiency and economic feasibility of pest control systems in watermelon cropping. *J of Econ Entomol.*, **107(3)**: 1118–1126.

Metcalf RL, and Lampman RL. 1989. The chemical ecology of diabroticites and cucurbitaceae. *Experentia*, **45**: 240–247.

Nath P, Sundari P, and Singh DP. 2002. Vegetables for the Tropical Region. Indian Council of Agricultural Research, New Delhi. 420pp.

Ogunlana MO. 1996. Insect pests of watermelon *Citrullus lanatus* in Samaru Zaria. Research Programmes Reports (1995 – 1996) of Institute of Agricultural Research, Ahmadu Bello University Zaria. Pp.171–172.

Okrikata E, Ogunwolu EO, and Ukwela MU. 2019. Diversity, spatial and temporal distribution of above-ground arthropods associated with watermelon in the Nigerian Southern Guinea Savanna. *J Insect Biod Syst.*, **5(1)**: 11–32.

Okrikata E, and Yusuf OA. 2016. Diversity and abundance of insects in Wukari, Taraba State, Nigeria. *Intl Biol Biomed J.*, **2(4)**: 156–166.

Okrikata E, and Ogunwolu EO. 2017. Farmers' perceptions on arthropod pests of watermelon and their management practices in the Nigerian Southern Guinea Savanna. *Int J Agric Res.*, **12(4)**: 146–155.

Okrikata E, and Anaso CE. 2008. Influence of some inert diluents of neem kernel powder on protection of sorghum against pink stalk borer (*Sesamia calamistis,* Homps) in Nigerian Sudan Savanna. *J Plant Protec Res.*, **48(2)**: 161–168.

Qayoom I, Shah FA, Mukhtar M, Balkhi MH, Bhat FA, and Bhat BA. 2016. Dimethoate induced behavioural changes in juveniles of *Cyprinus carpio* var. communis under temperate conditions of Kashmir, India. *The Sci World J.*, Article ID 4726126, http://dx.doi.org/10.1155/2016/4726126.

Recio MC, Andujar I, and Rios JL. 2012. Anti-inflammatory agents from plants: Progress and potential. *Curr Med Chem.,* **19**: 2088–2103.

Simmons AM, Kousik CS, and Levi A. 2010. Combining reflective mulch and host plant resistance for sweetpotato whitefly (Hemiptera: Aleyrodidae) management in watermelon. *Crop Protec.*, **29:** 898-902.

Souza CR, Sarmento RA, Venzon M, Barros EC, Santos GR, and Chaves CC. 2012. Impact of insecticides on non-target arthropods in watermelon crop. *Ciėncias Agrårias*, **33(5)**: 1789–1802.

Trusca R, Grozea I, and Stef R. 2013. Attractiveness and injury levels of adults by *Diabrotica virgifera virgifera* (Le Conte) on different host plant. *J Food Agric Environ.*, **2(3 and 4)**: 773–776.

Yakubu VA, Salifu A, Moses KAM, and Ibrahim NI. 2018. Means of transportation of watermelon (*Citrullus lanatus* [Thunb.]) fruit within the Tamale Metropolis in the Northern Region of Ghana. *J Biol Agric Healthcare*, **8(4)**: 50–59.

JJBS

Volume 13, Number 1,March 2020
ISSN 1995-6673
Pages 117 - 122

Jordan Journal of Biological Sciences

Yield and Nutrient Content of Sweet Potato in Response of Plant Growth-Promoting Rhizobacteria (PGPR) Inoculation and N Fertilization

Farzana Yasmin[1], Radziah Othman[2] and Mohammad Nazmul Hasan Maziz[3*]

[1]Faculty of Science, Lincoln University College, No. 2, Jalan Stadium, SS 7/15, 47301, Petaling Jaya;[2]Faculty of Agriculture, Universiti Putra Malaysia, 43400 UPM Serdang, [3]Graduate School of Medicine, Perdana University, Jalan MAEPS Perdana, Serdang, 43400 Selangor, Malaysia

Received March 21, 2019; Revised May 25, 2019; Accepted June 25, 2019

Abstract

This study was carried out to determine the effects of selected beneficial bacterial isolates with N fertilizer application on yield and nutrient content of sweet potato under field condition. A factorial experiment with two factors (Plant growth-promoting rhizobacteria inoculation and N fertilizer) was positioned with three replications in a Randomized Complete Block Design (RCBD). Three stages of N fertilizer (0, 33, and 100 k g N ha^{-1}) and five strains of bacteria (*Bacillus sphaericus* UPMB10, *Erwinia* sp. UPMSP10, *Klebsiella* sp. UPMSP9, *Azospirillum brasilense* SP7 and Uninoculated control) were used for treatments. Plants were grown on sandy clay soil at the Universiti Putra Malaysia experimental plot. The effect of bacterial population in the soil at different phases of plant growth was significantly stimulated by bacterial inoculation and N fertilization. The soil inoculated with *Klebsiella* sp. applied with 33 kg N ha^{-1} showed highest population of $2.63X10^7$ CFU g (dry wt.)$^{-1}$ soil. However, after the 2nd and 3rd month of inoculation, the number of bacteria in soil dropped. The results of inoculated plants showed significant differences in sweet potato yield, N, P, K, Ca and Mg contents of storage root compared to control. After the field experiment, it was found that plants inoculated with *Klebsiella* sp. applied with 33 kg N ha^{-1} showed the highest storage root yield. Substantial relations among PGPR inoculation and N fertilization was detected on nutrient content of sweet potato storage roots. *Klebsiella* and application of 33kg N ha-^{1} demonstrated the highest N, P, K, Ca, Mg content of storage roots. These results recommended that *Klebsiella* sp. can be used as biofertilizer of sweet potato for decreasing the rates of N fertilizers and giving a stage forward for sustainable agriculture.

Keywords: Sweet potato, Plant growth-promoting rhizobacteria, Nitrogen fertilizer, Yield, Nutrient content

1. Introduction

Sweet potato (*Ipomoea batatas* L.) is one of the major staple foods in several countries including Asia and the Pacific Islands. In Malaysia, sweet potato is the second most important root crop after cassava. It is also a good source of carbohydrate, beta-carotene, thiamine, riboflavin, folic acid, ascorbic acid and minerals. There are many nutritious food items like noodles, bakery products, snacks, breakfast cereals and beverages where the storage root is widely used (O' Sullivan *et al.,* 1997; Zhang *et al*., 2009; Santra Kumawat,2014). The sweet potato production in Malaysia is currently less due to non-availability of land and conversion of agricultural land to industrial uses, labor costs, marketing issues, outbreak of diseases and high input namely fertilizer (Tan *et al*., 2005; Loebenstein, 2009). Excessive nitrogen is not only wasteful but can lead to environmental pollution and increase the cost of crop production. One of the methods to sustain production is through the application of beneficial microorganisms such as plant growth-promoting rhizobacteria (PGPR). These microbes can produce phytohormones. These phyto-hormones improve plant growth by increased uptake of nutrients. Indole-acetic acid (IAA) is regarded as the most important hormone synthesized by PGPR, (Glick*.,* 2012; Umair *et al*.,2018). The IAA produced by bacteria is involved in several types of microorganism-plant interaction. IAA may induce the plant either to grow faster or better due to the stimulation on cell division and differentiation. The excreted IAA can positively influence development of root system (Hagen, 1990; Chaiharn, 2011). The promotion of growth and development of sweet potato by PGPR is probable through secretion of plant growth hormones and increased mineral uptake and mineral accumulation through efficient rooting system (Dawwam *et al.,* 2013). Most soils lack nitrogen, and application of nitrogen fertilizer is essential for good yield. Nitrogen supply plants show elaborate responses at both physiological and morphological dimensions to change their development and improvement. Nitrogen is significant for metabolic activities of bacteria. Presumably, it could positively affect IAA biosynthesis (Frankenberger and Arshad, 1995; Spaepen *et al.,* 2007, Moshira, *et al.,*

* Corresponding author e-mail: poorpiku@yahoo.com.

2015). Earlier studies demonstrated that banana and sweet potato inoculated with PGPR and applied 1/3Ni fertilizer produced the highest root yield and shoot growth under field conditions (Radziah and Zulkifli, 2003, Mia *et al.,* 2013). This demonstrates a potential saving on fertilizer cost. Therefore, the following study aimed to assess the beneficial effects of four strains of PGPR and three levels of nitrogen fertilizer on yield and nutrient content of sweet potato under field condition.

2. Materials and Methods

The experiment was conducted at UPM experimental plot (Ladang kongsi). The area was located at $3^0 02'$ N latitude, 101^0 42′ E longitude and about 31 m above sea level. The soil was sandy clay. The land was ploughed with a rotovator, and ridges at 1.0 m apart were then built using a tractor mounted ridge. The size of ridge was 30 cm high and 60 cm wide at the base. Each unit plot measured 3.2 m X 2 m. A factorial experiment with two factors (PGPR inoculation and N fertilizer) was laid out in a Randomized Complete Block Design (RCBD) with three replications. The treatments consisted of five bacterial strains (*Klebsiella* sp. UPMSP9*, Erwinia* sp. UPMSP10, *Azospirillum brasilense* SP7*, Bacillus sphaericus* UPMB10 and uninoculated control) and three levels of N fertilizer (0, 33, and 100 kg N ha^{-1}). Prior to planting, cuttings of sweet potato shoot variety Sepang Oren (30 cm in length with 8 nodes) were soaked in 48 hr old rhizobacterial solution for six hours. Each plant was inoculated with the respective inoculum at planting and one month after planting with 20 mL inoculum per plant (approximately 10^9 CFU mL^{-1}). Control plant received the same volume of sterile media without bacteria.

The field was irrigated regularly by a sprinkler system. Plants were harvested after 3 months of planting. Storage roots were collected for nutrient analysis. The dried storage roots were ground and digested with H_2SO_4 and H_2O_2 using block digestion following the micro-kjeldahl method (Thomas *et al.,* 1967). The clear digested sample was then cooled, diluted to 100ml with distilled water. Approximately 20ml of the sample was kept in test tubes for N, P, K concentration determined by auto-analyzer (Technicon II, Technicon Ltd.). The remaining sample was diluted with Lithium Chloride and analyzed for Ca and Mg using Atomic Absorption Spectrophotometer (Perkin-Elmer, 5100 PC, Perkin Elmer).

The storage root starch content and crude protein were determined according to method of Truong (1992) and Woolfe (1992) respectively. Fresh soil samples from area around plant roots were collected for bacterial counts by using total plate count technique (Parkinson *et al.,* 1971). All data was statistically analyzed by Statistical Analysis System (SAS, version 6.12, 1989). Following the analysis of variance procedure (ANOVA), differences among treatment means were determined using Tukey's Studentized Range test (HSD) comparison method at p=0.05.

3. Results

3.1. Sweet potato Yield

There was significant (P<0.05) effect of PGPR inoculation and nitrogen fertilization on the percentage of sweet potato yield and storage root number (Table 1). There was no significant increase in yield at the highest N rate of 100 kg. *Klebsiella* sp. inoculation and N application of 33 s howed higher percentage of sweet potato yields compared to the same N rate of the uninoculated treatment.

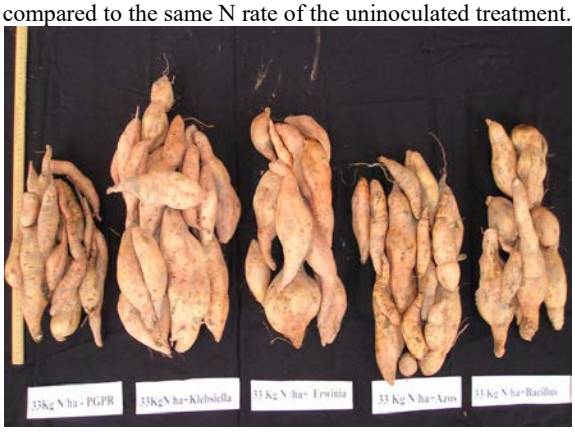

Figure 1. Storage root yield of sweet potato in 33 kg N fertilizer rate with PGPR.

Table 1. Effect of Rhizobacterial Inoculation and N Fertilization on Total Storage Root Number and Yield

Treatments		Storage root yield (%)	Storage root number ($Plot^{-1}$)
Control	0 kg	48.99e	17def
	33 kg	79.93abc	16efg
	100 kg	73.59bcd	16efg
Klebsiella sp.	0 kg	72.53.bcd	14fgh
	33 kg	89.91 a	26b
	100 kg	88.20a	25b
Erwinia sp.	0 kg	71.59bcd	17def
	33 kg	82.63 ab	25b
	100 kg	84.4 8ab	20cd
Azospirillum sp.	0 kg	64.68d	12h
	33 kg	81.47abc	21c
	100 kg	78.21abcd	18cde
Bacillus sp.	0 kg	68.36cd	20cd
	33 kg	81.10abc	32a
	100 kg	74.45bcd	13gh
Significance due to PGPR		* (0.0001)	*(0.0002)
N Fert.		*(0.0001)	*(0.0001)
PGPR * N Fert		*(0.0209)	*(0.0022)

Note: *Significant (P<0.05), Means the values followed with same letter (s) are not significantly different (P>0.05).

3.2. Starch and crude protein concentrations of storage root

PGPR inoculation and nitrogen application significantly (P<0.05) influenced the storage root starch and crude protein contents which increased with the application of 33 kg N ha^{-1} fertilizer (Table 2). There was significant interaction effect of PGPR inoculation and N fertilization on crude protein contents of storage root.

Table 2. Effect of Rhizobacterial Inoculation and N Fertilization on Starch and Crude Protein Content of Storage Root.

Treatments Bacterial Fertilizer	N Isolates (Nha^{-1})	Starch Content (%)	Crude Protein (%)
Control	0 kg	17.09	1.08f
	33 kg	19.88	1.67cde
	100 kg	18.52	1.56de
Klebsiella sp.	0 kg	19.49	1.60cde
	33 kg	22.25	2.23a
	100 kg	21.89	2.13ab
Erwinia sp.	0 kg	20.03	1.51de
	33 kg	20.86	2.22a
	100 kg	20.57	1.68cde
Azospirillum sp.	0 kg	20.09	1.38ef
	33 kg	21.41	2.29a
	100 kg	20.90	1.88bc
Bacillus sp.	0 kg	19.62	1.61cde
	33 kg	21.02	2.13ab
	100 kg	20.06	1.82bcd
Significance due to PGPR		*(0.0001)	*(0.0001)
N Fert.		*(0.0001)	*(0.0001)
PGPR * N Fert		NS (0.2242)	*(0.0027)

Note: *Significant (P<0.05), Means the values followed with same letter (s) are not significantly different (P>0.05).

3.3. Nutrient content of storage root

Nutrient uptake by storage roots were greatly enhanced by PGPR inoculation and N fertilizer. Higher contents of the nutrients were observed in *Klebsiella* inoculated plants. Meanwhile the interaction effect of PGPR inoculation and N fertilization significantly (P<0.05) influenced storage root of N, P, K, Ca and Mg contents. *Klebsiella* and N application of 33 kg N ha^{-1} showed the highest N content of storage root (Table 3).

3.4. Total bacterial population in soil

PGPR inoculation and N fertilization affected the total bacterial population in soil (Figure 2 a, b, c). There was a significant (P≤0.05) interaction effect of PGPR and N fertilization on bacterial population. There were changes in bacterial population during different plant growth stages. In general, the population was high at 30 days after planting and decreased at 60 and 90 days after planting. Inoculated treatments showed higher bacterial population compared to uninoculated control. Highest population (7.42log$_{10}$ CFU g^{-1} soil) was observed with *Klebsiella sp.* inoculation at 33kg N ha^{-1} fertilization rate.

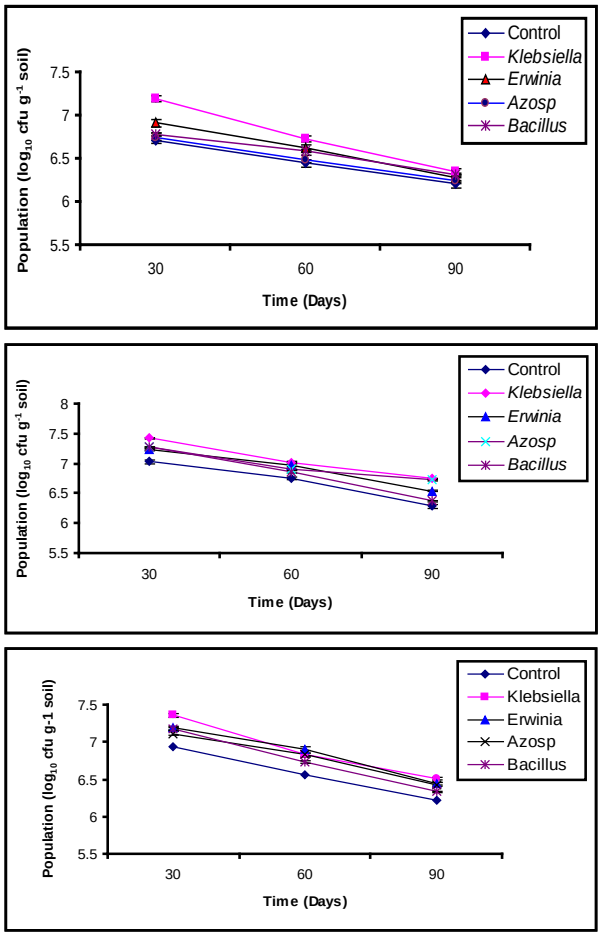

Figure 2. Effect of Rhizobacterial Inoculation and Nitrogen on Soil Bacterial Population at Different Sweet potato Growth Stages; (a) 0 kg Nitrogen, (b) 33 kg Nitrogen and (c) 100 kg Nitrogen.

Table 3. Effect of Rhizobacterial Inoculation and N Fertilization on Nutrient Content of Sweet potato Storage Roots.

Bacterial Treatments	N Isolates	Nutrient Content (mg plant^{-1})				
	Fertilizer (N ha^{-1})	N	P	K	Ca	Mg
Control	0 kg	110.55g	63.87i	623.89i	312.41f	114.91f
	33 kg	304.22c	182.59e	1377.93de	608.67bc	258.52bc
	100 kg	198.67ef	113.76gh	959.60fgh	406.81de	156.07ef
Klebsiella sp.	0 kg	226.74de	132.59fg	1071.41fgh	423.67de	232.74bc
	33 kg	502.89a	310.19a	2329.11a	751.44a	404.11a
	100 kg	447.99b	271.22b	1962.96b	653.72b	394.50a
Erwinia sp.	0 kg	193.01ef	103.50h	1003.56fgh	414.04de	215.02cd
	33 kg	434.60b	215.05cd	1946.49b	639.59bc	403.22a
	100 kg	306.55c	194.44de	1583.35cd	595.70bc	262.37b
Azospirillum sp.	0 kg	152.17fg	104.11h	858.80hi	343.91ef	161.37e
	33 kg	436.28b	196.83de	1815.89bc	602.50bc	265.07b
	100 kg	267.44cd	142.77f	1188.74efg	458.33d	266.93b
Bacillus sp.	0 kg	191.81ef	106.97gh	908.09ghi	380.63def	179.22de
	33 kg	401.08b	226.74c	1889.54b	561.65c	405.06a
	100 kg	257.89cd	143.19f	1234.62ef	451.68d	268.78b
Significance due to PGPR N Fert. PGPR * N Fert		*(0.0001)	*(0.0001)	*(0.0001)	*(0.0001)	*(0.0011)
		*(0.0001)	*(0.0011)	*(0.0021)	*(0.0023)	*(0.0002)
		*(0.0002)	*(0.0021)	*(0.0011)	*(0.0031)	*(0.0022)

Note: NS: non significance, and *: significant difference at (P<0.05). Means the values followed with same letter (s) are not significantly different (P>0.05).

4. Discussion

The PGPR inoculation and N fertilization rates significantly influenced sweet potato storage root yield. Plants inoculated with *Klebsiella sp.* and 33 k g N ha^{-1} fertilizer showed highest yield of sweet potato. The increase could be due to the ability of *Klebsiella* sp. to produce high level of IAA that stimulated plant and root growth. Kloepper *et al*., (1989), Martinez-Viveros *et al*., (2010) and Jordan *et al*., (2013) had recommended that rhizobacteria produced plant growth regulators including IAA that may establish a system for direct plant and root growth promotion by rhizobacterial inocula.

Storage root yield increased with PGPR inoculation compared to the uninoculated control without N fertilizer. This indicated that inoculation and N fertilizer produced a synergistic effect on plant growth and storage root yield. Chela *et al.,* (1993), Saad *et al*., (1999) and Vosawai*et al*., (2015) observed that the use of nitrogen in combinations with PGPR produced significantly higher plant growth and yield than those from fertilization alone under field condition. Also, Helaly *et al*, (2009) found that effect of bio-and mineral fertilizers on yield and tuber quality of potato plants.

PGPR inoculation and N fertilization positively influenced the uptake of nutrients into the storage root. The increase in plant growth could be attributed to the increased uptake of plant nutrients as shown by the higher uptake of N, P, K in storage root of *Klebsiella* inoculated plants. Morphological and physiological changes of plant and enhancement of nutrient content were significantly increased by growth promoting effects of PGPR (Amir *et al.*, 2005; Mia *et al.* 2010; Noor *et al*., 2013). IAA producing PGPR are believed to increase root growth and root length, resulting in greater root surface area which enables the plant to access more nutrients from the soil (Vessey, 2003; Chaiharn, 2011). Nitrogen (N) was considered to be an important factor in determining the production and nutrient composition of root tubers. N may often limit the plant growth and yield among the mineral nutrient elements. For plant development and advancement, N is the most essential mineral nutrient. Therefore, the appropriate management is necessary in an intensive agriculture for plant production and nutrient composition of root tubers (Loebenstein, 2009; Bajshya *et. al*., 2013). The starch and crude protein components of sweet potato appeared to increase by application of Nitrogen. Genotypic and environmental variations are some of the factors that impact the reaction of sweet potato towards Nitrogen fertilizer application (Zhang *et. al*, 2009; Kareem, 2013).

Five sweet potato varieties and four stages of nitrogen fertilizer (N) had been assessed in UPM to examine the yield and nutrient composition of these varieties at estimated optimum N.

Earlier reports have shown that application of nitrogen fertilizer can increase crude protein and starch content in tuber crops. (Ozturk *et al*., 2010; Biruk *et al*., 2014; Vosawai *et al*., 2015).

During plant growth, microbial population density in soil near plant roots was significantly influenced by PGPR inoculation and N fertilizer application. In general, total bacterial population was high at 30 days after planting and reduced with plant age. In the present study, treatment with *Klebsiella* inoculation at 33 kg N ha^{-1} fertilization rate had the highest population of total bacteria in the soil. The inoculated rhizobacteria probably induced the plant growth hormones and other metabolites that encouraged proliferation of other indigenous bacteria. *Klebsiella* inoculation may probably been enhanced root's growth and increased the secretion of root exudates. Kennedy, (1997) and Xing *et al*., (2014) suggested that root exudates contain sugars, amino acids, vitamins, tannins, alkaloids, phosphatides and other unidentified substances. The root exudate sugars give readily available sources of carbon

and energy for the bacterial community in soil. The application of N fertilizer in the soil gives the nitrogen source for bacteria, which improved development.

Liljeroth *et al.,* (1990) and Bashan *et al.,* (2014) observed a significant effect of nitrogen fertilization and PGPR inoculation on microbial populations in rhizosphere soil of barley plants. The decreased population at 60 and 90 days of plant growth could be due to competitions for nutrients and space among the inoculants and other indigenous bacteria in soil. The rhizobacteria probably compete for carbon and energy sources and colonizing space in the rhizosphere.

5. Conclusion

Based on the results obtained in present study, it might be concluded that the application of PGPR and Nitrogen fertilizer improved the yield, microbial population, and also increased the available nutrients (N,P,K) content and quality properties in sweet potato under field condition. Application of 33 kg N ha-1 generally increased yield but at higher application of 100 kg N ha-1 yield was decreased. Field inoculation of *Klebsiella* with 33 kg N ha-1 improved storage root yield which was significantly superior to other treatments, but this treatment reduced the Nitrogen fertilizer rate. Hence, *Klebsiella* has great prospects to be used as biofertilizer for sweet potato production and to sustain soil health under field condition.

References

Amir HG, Shamsuddin ZH, Halimi MS, Ramlan MF and Marziah M. 2005. Enhancement in nutrient accumulation and growth of oil palm seedlings caused by PGPR under field nursery conditions. *Communications in Soil Sci Plant Analysis*, **36**:2059–2066.

Bajshya, LK, Kumar M., Ghosh M and Gosh DC. 2013. Effect of integrated nutrient management on growth, productivity and economics of rainfed potato in meghalya hills. *Inter J Agri Environ Biotechnol.*, **6**: 2013.

Bashan Y, Bashan L E, Prabhu S R and Hernandez J B. 2014. Advances in plant growth-promoting bacterial inoculant technology: formulations and practical perspectives. *Plant Soil*, **378**: 1–33.

Biruk-Masrie Z, Nigussie-Dechassa R, Bekele A, Yibekal A. and Tamado T. 2014. Influence of combined application of inorganic n and p fertilizers and cattle manure on quality and shelf-life of potato (*Solanum tuberosum* L.) Tubers. *J Postharvest Technol.,* **2 (3):** 152-168.

Chaiharn M and Lumyong S. 2011. Screening and optimization of indole-3-acetic acid production and phosphate solubilization from rhizobacteria aimed at improving plant growth. *Curr Microbiol*., **62 (1):**173-81.

Chela G S, Tiwana M S, Thind I S, Puri K P and Kur K. 1993. Effect of bacterial cultures and nitrogen fertility on the yield and quality of maize folder (*Zea mays* L.). *Annual Biol.,* **9**: 83-86.

Dawwam GE, Elbeltagy A, Emara HM, Abbas IH and Hassan MM. 2013. Beneficial effect of plant growth promoting bacteria isolated from the roots of potato plant. *Annals Agri Sci.,* **58 (2)**:195-201.

Frankenberger Jr. W T and Arshad M. 1995. **Phytohormones in soils. Microbial Production and Function**, Marcel Dekker, Inc. New York.

Glick BR. 2012. Plant growth-promoting bacteria: mechanisms and applications," Scientifica, **15**.

Hagen G. 1990. The control of gene expression by auxins. *In*: **Plant Hormones and their Role on Plant Growth and Development**. Davies P J.(Ed.) K luwar Academic Publishers, Netherlands. pp. 149-163.

Helaly MN, Fouda RA and Ramadan EA. 2009. Effect of bio-and mineral fertilizers on growth, yield and tuber quality of potato plants. *J Agri*, *Mansoura University*, **34**: 3547-3579.

Jordan V, Guilhem D, Marie L B, Bruno T, Yvan ML, Daniel M, Laurent L, Florence WD and Claire PC. 2013. Plant growth-promoting rhizobacteria and root system functioning. *Front Plant Sci*., **4**: 356.

Kareem I. 2013. Fertilizers treatment effects on yield and quality parameters of sweet potato (*Ipomoea batatas*). *Res J Chem Environ Sci.,* **1**: 40-49.

Kennedy A C. 1997. The rhizosphere and spermosphere. *In:* **Principles and Application of Soil Microbiology**. Sylvia DM, Fuhrmann JJ, Harter PG and Zuberer DA (Eds). Prentice Hall Inc. pp. 389–407

Kloepper JW, Lifshitz R and Zablotowicz RM. 1989. Free-living bacterial inoculation for enhancing crop productivity, *Trends Biotechnol.,* **7**: 39-44.

Liljeroth E, Baath E, Mathiasson I and Lundborg T. 1990. Root exudation and rhizoplane bacterial abundance of barley (*Hordeum vulgare* L.) in relation to nitrogen fertilization and root growth. *Plant Soil,* **127**: 81-89.

Loebenstein G. 2009. The Sweet Potato: Origin distribution and economic importance. *In: Loebenstein G, et al. editors. Springer; 9–12.*

Martínez-Viveros O, Jorquera MA, Crowley DE, Gajardo G and Mora ML. 2010. Mechanisms and practical considerations involved in plant growth promotion by rhizobacteria . *Soil Sci. Plant Nutr.,* **10 (3):** 293 - 319.

Mia AB, Motaher H, Shamsuddin ZH and Tofazzal I. 2013. Plant-associated bacteria in nitrogen nutrition in crops, with special reference to rice and banana. **Bacteria in Agrobiology: Crop Productivity**. Springer. pp 97-126.

Mia MAB, Shamsuddin ZH, Zakaria W and Marziah M. 2010. Rhizobacteria as bioenhancer for growth and yield of banana (*Musa* spp. cv. "Berangan"). *Scientia Horticult*., **126 (2):** 80-87.

Moshira AES, Tamer I A W, Sherif I AW and Samuel B R. 2015. Advantages of intercropping soybean with maize under two maize plant distributions and three mineral nitrogen fertilizer rates. *Advances in Biosci Bioengin.,* **3(4):** 30-48.

Noor Ai'shah O, Tharek M, Keyeo F, Chan L K, Zamzuri I, Ahmad Ramli M Y and Amir H G. 2013. Influence of Indole-3-Acetic acid (IAA) produced by diazotrophic bacteria on root development and growth of in vitro oil palm shoots (*Elaeis guineensis* Jacq.). *J Oil Palm Res*., **25 (1)**:100-107.

O'Sullivan JN, Asher C J and Blamey FPC. 1997. Nutrient disorders of sweetpotato. ACIAR Monograph No. 48, Canberra.

Öztürk E, Kavurmac Z, Kara K and Polat T. 2010. The effects of different nitrogen and phosphorus rates on some quality traits of potato. *Potato Res.*, **53**:309-312.

Parkinson D T, Gray R G and Williams S T. 1971. **Methods for studying the Ecology of soil Microorganisms** IBP handbook no. 19.

Radziah O and Zulkifli H S. 2003. Utilization of rhizobacteria for increased growth of sweet potato. *In:* **Investing Innovation, vol.1: Agriculture, Food and Forestry,** Zaharah A.R. (Ed), University Putra Malaysia Press, Serdang, Malaysia. pp 255-258

Saad M S, Shabuddin A S A, Yunus A G and Shamsuddin Z H. 1999. Effects of *Azospirillum* inoculation on sweet potato grown on sandy tin-tailing soil. *Comm Soil Sci Plant Analysis,* **30 (11-12)**: 1583-1592.

Santra K. 2014. Effect of Integrated Nutrient Management in Sweet Potato. Master's thesis.Faculty of AgricultureSwami Keshwanand Rajasthan Agricultural University, Bikaner.

SAS Version 6.12. 1989. SAS/ STAT. Guide to Personal Computers. SAS Institute Inc., Cary, North Carolina.

Spaepen S, Vanderleyden J, Remans R. 2007.Indole-3-acetic acid in microbial and microorganism-plant signaling. *FEMS Microbiol Rev*., **31 (4)**: 425–448.

Tan S L, Abdul Aziz AM and Zaharah A. 2005. Selection of sweet potato clones with high starch content in Malaysia. Concise papers of the second international symposium on sweet potato and cassava. 77-78.

Thomas R L, Sheard R W and Moyer J R. 1967. Comparison of conventional and automated procedures for nitrogen, phosphorus and potassium analysis of plant material using a single digestion. *Agronomy J.,* **59**: 240-243.

Truong Van Den. 1992. Evaluation of sweet potato varieties for processing. Paper presented during the second international training on sweet potato production, processing and utilization. May 1992, AES Albay.

Umair M, Muhammad I U H, Muhammad S, Adeela A and Farooq A. 2018. A brief review on plant growth promoting Rhizobacteria (PGPR): A key role in plant growth promotion. *Plant Protect.,***2 (2):** 77-82.

Vessey JK. 2003. Plant growth-promoting rhizobacteria as biofertilizers. *Plant Soil* **255**: 571-586.

Villargarcia OMR. *1996.* Analysis of sweet potato growth under differing rates of nitrogen fertilization. *Raleigh, USA: North California State University.* **62 (1)**, 173–181.

Vosawai P, Halim RA, Shukor AR. 2015. Yield and nutritive quality of five sweet potato varieties in response to nitrogen levels. *Adv Plants Agric Res.* **2(5):**231–237.

Woolfe J A. 1992. **Sweet potato: An untapped Food Resource**. Cambridge University Press. Cambridge, 643 pages.

Xing F H, Jacqueline M C, Kenneth F R, Ruifu Z, Qirong S and Jorge M V. 2014. Rhizosphere interactions: root exudates, microbes, and microbial communities. *Botany*, **92 (4):** 267-275.

Zhang L, Wang Q, Liu Q and Wang Q. 2009. Sweet potato in China. *In*: G. Loebenstein and G. Thottappilly (Eds.) **The Sweet potato**. Springer Dordrecht, The Netherlands.

JJBS

Volume 13, Number 1,March 2020
ISSN 1995-6673
Pages 123 - 126

Jordan Journal of Biological Sciences **Short Communication**

Evaluation of Antimicrobial and Genotoxic Activity of *Ephedra foeminea* Ethanolic and Aqueous Extracts on *Escherichia coli*

Shurooq M. Ismail*, Ghaleb M. Adwan, and Naser R. Jarrar

Department of Biology and Biotechnology, An-Najah National University,P.O. Box (7)-Nablus, Palestine

Received February 21, 2019; Revised April 23, 2019; Accepted May 7, 2019

Abstract

This study was conducted to evaluate the antimicrobial activity and the genotoxic effects of ethanolic and aqueous extracts of aerial parts of *Ephedra foeminea* (*E. foeminea*) plant on *Escherichia coli* (*E. coli* ATCC 25922). Antimicrobial activity was investigated using microbroth dilution method, while the genotoxic effect was determined using enterobacterial repetitive intergenic consensus (ERIC)-PCR. MIC value of both ethanolic and aqueous extracts of *E. foeminea* plant was found to be 50 mg/ml. Genotoxic effects of both extracts, showed an alteration in (ERIC)-PCR profiles of *E. coli* strain treated with extracts compared to untreated control. These alterations included a decreased intensity or absence of some amplified fragments. Such findings strongly indicate the genotoxic effects of both ethanolic and aqueous extracts from *E. foeminea* plant on *E. coli*. The findings draw attention to the unsafe, use of *E. foeminea* plant in folkloric medicine and point out the capability of using *E. foeminea* to treat bacterial infections. Future studies are required to know the exact molecules as well as the mechanisms responsible for the genotoxicity of this plant. *In vivo* genotoxicity studies are recommend for assessment of the safety of using *E. foeminea* plant for therapeutic purposes.

Keywords: *Ephedra foeminea*, Genotoxicity potential, Plant extracts, Antimicrobial activity.

1. Introduction

The family Ephedraceae consists of only one genus called *Ephedra* L. It has a group of approximately fifty species of perennials, evergreen, and dioecious sub-shrubs species growing up to four feet tall, with slender and joined stems. In general, species of this genus adapted to grow wild in arid and semiarid conditions and disseminated mainly in the moderate zones of Asia, Europe and North America (O'Dowd *et al*., 1998; Pirbalouti *et al*., 2013). Approximately 25 species of *Ephedra* are found in the drier regions of the Old World covering the area westwards from Central Asia across southwest Asia and into North Africa and Mediterranean Europe (Caveney *et al*., 2001). In the New World, about 24 species of *Ephedra* are found ranging from the southwestern United States to the central plateau of Mexico, and in South America occur in an area from Ecuador to Patagonia (Caveney et al., 2001). *Ephedra* grows widely in Palestine. In the flora Palestina, 5 species of *Ephedra* has been reported, included *E. foeminea*, *E. alata*, *E. aphyla*, *E. ciliata* and *E. fragilis* (Danin, 2018).

Approximately, all commercial applications of *Ephedra* extracts derived from the ephedrine alkaloids found in the stems in many Eurasian *Ephedra* species. These extracts are used in traditional medicine to treat several diseases such as bronchial asthma, coughs, chills, allergies, colds, edema, headaches, fever, flu and gastric disorders. In addition, *Ephedra* shows anticancer and antimicrobial activities (Parsaeimehr *et al*., 2010; Pirbalouti *et al*., 2013; Dehkordi *at al*., 2015; Dosari *et al*., 2016; Al-Rimawi *et al*., 2017; Mendelovich *et al*., 2017). Besides, it was shown that hydro-alcoholic extract of *E. pachyclada* was effective in experimentally healing rat ulcers (Pirbalouti *et al*., 2013).

Ephedra possesses a high antioxidant potential since it has been considered as a source of different phenolic compounds, as well as, a natural source of alkaloids such as ephedrine, pseudoephedrine, and other related compounds. (Eberhardt *et al*., 2000; Parsaeimehr *et al*. 2010; Amakura *et al*., 2013; Dehkordi *et al*., Ibragic and Sofić 2015; Al-Rimawi *et al*., 2017). The studies conducted on the cytotoxicity of *Ephedra* showed that ephedrine derivatives and ground ma-huang extracts were more cytotoxic than those of the whole herb extracts. A study on Neuro-2a cell line showed the cell line was more sensitive to the cytotoxicity (Lee *et al*., 2000). Ethanolic leaf extract and fruit juice of *E. foeminea* reduced viability of cancer cells *in vitro*, whereas the aqueous extract reduced the cytotoxicity in all cell lines (Mendelovich *et al*., 2017). Since there is no scientific report to date about the genetoxicity of *E. foeminea* on prokaryotes, the current study was performed to determine the antimicrobial effect of ethanolic and aqueous extracts from *E. foeminea* plant growing wild in Palestine as well as evaluate the genotoxic effect of these extracts on *E. coli* strain using enterobacterial repetitive intergenic consensus (ERIC)-PCR.

* Corresponding author e-mail: shurooq.ismail@najah.edu.

2. Materials and Methods

2.1. Plant collection and identification

The aerial parts of *E. foeminea* were collected from a natural habitat in Tulkarm province, West Bank-Palestine, during September, 2018. Identification of the plant was carried out by the plant taxonomist Dr. Ghadeer Omar, Department of Biology and Biotechnology, An-Najah National University, Palestine.

The collected aerial parts of *E. foeminea* were washed with water to remove soil and dust particles then dried. Exposure to light was avoided to prevent possible loss of effective ingredients. The dried aerial parts were powdered finely using a blender to make them ready for ethanolic and aqueous extract preparation.

2.2. Plant extract preparation

2.2.1. Ethanolic extract

Approximately 50 g of dried aerial parts powder were mixed thoroughly using magnetic stirrer in 200 mL of 80% ethanol. The ethanol-aerial parts mixture was incubated on a shaker at room temperature for 48h. The mixture was filtered using muslin cloth to remove large insoluble particles. After that, the mixture was centrifuged at 5,000 rpm for 15 min at 4°C to remove fine particles. Then, the supernatant extract was dried and concentrated by using rotary evaporator at 50°C. The obtained dried plant extract powder was stored in refrigerator at 4°C. Before starting the experiments, this material was dissolved in 10% Dimethyl Sulfoxide (DMSO) to obtain a concentration of 200 mg/mLand stored at 4ºC for further assays.

2.2.2. Aqueous extract

Aqueous aerial parts extract was prepared by mixing approximately 50 g of dried aerial parts powder thoroughly using magnetic stirrer in 200 ml of cold (room temperature) sterile distilled water. The water-aerial parts mixture was incubated on a shaker at room temperature for 48h. The mixture was filtered using muslin cloth to remove large insoluble particles. After that, the mixture was centrifuged at 5,000 rpm for 15 min at 4°C to remove fine particles. Then the supernatant extract was dried and concentrated by freeze dryer (lyophilizer). The obtained dried plant extract powder was stored in refrigerator at 4°C. Before starting the experiments, this dried plant extract powder was dissolved in a sterile distilled water to obtain a concentration of 200 mg/mL and stored at 4ºC for further assays.

2.3. Determination of MIC for plant extracts by broth microdilution method

MIC of plant extracts was determined by the broth microdilution method in sterile 96- wells microtiter plates according to the CLSI instructions (CLSI, 2017). The plant extract (200 mg/mL of 10% DMSO) and 10% DMSO (negative control) were two fold-serially diluted in nutrient broth directly in the wells of the plates in a final volume of 100µL. After that, a bacterial inoculum size of 10^4 CFU/mL was added to each well. Negative control wells containing either 100µL nutrient broth only, or 100µL DMSO with bacterial inoculum, or plant extracts and nutrient broth without bacteria were included in this experiment. Each plant extract was run in duplicate. The microtiter plate was then covered and incubated at 37°C for 24h. The MIC was taken as the minimum concentration of the dilutions that inhibited the growth of the test microorganism. MIC was determined by visual inspection.

2.4. Evaluation of the genotoxic potential of Ephedra foeminea aerial extracts on E. coli

Few colonies from a 24 hour old *E. coli* strain growth culture plated on EMB agar medium were sub-cultured under sterile conditions into a bottle containing 20-mL of nutrient broth, then incubated at 37°C for 1 hour with continuous shaking. After that, aseptically, 1 mL of one hour old *E. coli* culture was added to each of eight sterile bottles each containing 25 mL broth medium. These bottles were incubated at 37°C for 1 hour with continuous shaking. Then three different concentrations of ethanolic extract (3.5 mg/mL, 1.75 mg/mL and 0.875 mg/mL of 10% DMSO), and other three different concentrations of aqueous extract (3.5 mg/mL, 1.75 mg/mL and 0.875 mg/mL of distilled water) were added into six bottles of the *E. coli* broth culture. The other two bottles were considered as a negative or untreated control by adding a specific volume of 10% DMSO and distilled water into each bottle.

Genome of *E. coli* was prepared for enterobacterial repetitive intergenic consensus (ERIC) PCR according to the method described previously (Adwan *et al*., 2013). Three mL samples were taken from the *E. coli* growth culture after 2 hours, 6 hours, and 24 hours, centrifuged for five minutes at 14,000 rpm where the supernatant of each sample was discarded. Then, each bacterial sample pellet was re-suspended in 0.8 mL of Tris-EDTA (10 mM Tris-HCl, 1 mM EDTA [pH 8]), centrifuged for five minutes at 14,000 rpm; after that, the supernatant was discarded. The pellet of each bacterial sample was re-suspended in a 300 µL of sterile distilled water and boiled for 15 minutes. Then the mixture was incubated in ice for 10 minutes. The samples were pelleted by centrifugation at 14,000 rpm for five minutes, and each sample supernatant was transferred into a new Eppendorf tube. The DNA concentration for each sample was determined by using nanodrop spectrophotometer (GenovaNano, Jenway) and the DNA samples were stored at -20ºC for ERIC-PCR analysis. The ERIC-PCR was performed using Primer ERIC1: 5`-ATG TAA GCT CCT GGG GAT TCA C-3` and Primer ERIC2: 5-AAG TAA GTG ACT GGG GTG AGC G-3`. Each PCR reaction mix (25 µL) was composed of 10 mM PCR buffer pH 8.3; 3 mM $MgCl_2$; 0.4 mM of each dNTP; 0.8 µM primer; 1.5U of Taq DNA polymerase and fixed amount of DNA template (60 ng). Then, DNA amplification was carried out using the thermal cycler (Mastercycler personal, Eppendorf, Germany) according to the following thermal conditions: initial denaturation for 3 min at 94 ºC; followed by 40 cycles of denaturation at 94 ºC for 50 s, annealing at 50 ºC for 1 min and extension at 72 ºC for 1 min, followed by a final extension step at 72ºC for 5 min. The PCR products were analyzed by electrophoresis through 1.8% agarose gel. The ERIC-PCR profile was visualized using UV trans-illuminator and photographed. Changes in ERIC-PCR banding pattern profiles following plant extracts treatments, including variations in band intensity as well as gain or loss of bands, were taken into consideration (Lalrotluanga *et al*., 2011; Atienzar *et al*., 2002).

3. Results

Results of this study showed that both aqueous and ethanolic aerial parts extracts of *E. foeminea* had an antibacterial activity. The MIC value of both aqueous and ethanolic aerial parts extracts of *E. foeminea* on *E. coli* strain were found to be 50 mg/ml.

DNA genome which was extracted from each *E. coli* strain which was treated with different concentrations of both aqueous and ethanolic aerial parts extracts of *E. foeminea* at various time intervals. Changes in extracted DNA genome from *E. coli* strain were evaluated and compared with untreated controls at the same time intervals.

The effect of aqueous aerial parts extract on genome of *E. coli* strain was evaluated by using ERIC-PCR. ERIC-PCR profile showed that a band with an amplicon length of about 800-bp was less intense in *E. coli* strain treated with 3.5 mg/mL and 1.75 mg/mL (Figure 1A, lanes 1 and 2) of aqueous aerial parts extract for 2h. Besides, this band disappeared in *E. coli* strain treated with 0.875 mg/ml of the same extract (Figure 1A, lane 3), in comparison with the same band appeared in un-treated control. Moreover, all bands disappeared after 6h in the *E. coli* strain treated with 3.5 mg/mL aqueous aerial parts extract (Figure 1A, lane 4). The band with an amplicon length of about 800-bp was less intense in *E. coli* strain treated with 1.75 mg/mL (Figure 1A, lane 5) disappeared in *E. coli* strain treated with 0.875 mg/mL of the same extract for 6h (Figure 1A, lane 6), in comparison with the same band appeared in the un-treated control. The band with an amplicon length of about 800-bp disappeared in *E. coli* strain treated with 3.5 mg/ml, 1.75 mg/mL and 0.875 mg/mL aqueous aerial parts extract for 24h (Figure 1A, lanes 7,8 and 9). Moreover, the band with an amplicon length of about 300-bp was less intense (Figure 1A, lanes 7, 8 and 9) in comparison with the same band appeared in un-treated control. It was observed that in lane number four most bands disappeared when treated with aqueous aerial parts extract of *E. foeminea* of 3.5 mg/mL concentration. ERIC-PCR profiles for *E. coli* strain untreated and treated with different concentrations of aqueous aerial parts extract of *E. foeminea* at the different time intervals are shown in Figure 1A.

Comparing the ERIC-PCR profile of untreated control samples with the profile of the *E. coli* treated with ethanolic aerial parts extract showed decreasing of intensity or loss of some bands from the profile. ERIC-PCR profile showed that a band with an amplicon length of about 800-bp was less intense in *E. coli* strain treated with 3.5 mg/mL (Figure 1B, lane 2 and 5) and disappeared in *E. coli* strain treated with 1.75 mg/mL (Figure 1B, lane 3 and 6) of ethanolic aerial parts extract for 2h and 6h. The band with an amplicon length of about 800-bp was less intense in *E. coli* strain treated with 3.5 mg/mL (Figure 1B, lane 7), and disappeared in *E. coli* strain treated with 1.75 mg/mL and 0.875 mg/mL (Figure 1B, lane 8 and 9) aqueous aerial parts extract for 24h. In addition, the band with an amplicon length of about 300-bp was less intense (Figure 1B, lanes 8 and 9) in comparison with the same band appeared in untreated control. ERIC-PCR profiles for *E. coli* strain untreated and treated with different concentrations of ethanolic aerial parts extract of *E. foeminea* at the different time intervals are shown in Figure 1A.

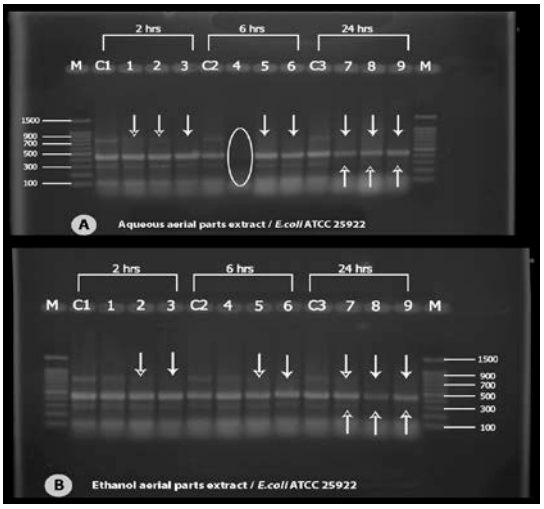

Figure 1. ERIC-PCR profile of *E. coli* strain untreated and treated with different aerial parts extract concentrations. A: aqueous aerial parts extract, B: ethanolic aerial parts extract of *E. foeminea* at different time intervals. Lanes C1, C2 and C3 are untreated (negative controls); lanes 1, 4 and 7 treated with 3.5 mg/ml; Lanes 2, 5 and 8 treated with 1.75 mg/ml; Lanes 3, 6 and 9 treated with 0.875 mg/ml of plant extract.

4. Discussion

In the present study broth microdilution method was used to examine the potential antimicrobial activity of both aqueous and ethanolic aerial parts extracts of *E. foeminea* against *E. coli*. The results confirmed that both aqueous and ethanolic aerial parts extracts of *E. foeminea* exhibited antibacterial activity against *E. coli* strain. Antimicrobial activity of some *Ephedra* species has been reported using different types of extracts (Al-Khalil *et al*., 1998; Feresin *et al*., 2001; Cottiglia *et al*., 2005; Parsaeimehr *et al*., 2010; Rustaiyan *et al*., 2011; Dehkordi *et al*., 2015; Dosari *et al*., 2016). According to previously conducted studies, phenolic compounds are the active ingredients of *Ephedra* plant (Dehkordi *et al*., 2015; Dosari *et al*., 2016).

In this study, the potential genotoxic effect of the aqueous and ethanolic aerial parts extracts of *E. foeminea* against *E. coli* was examined using ERIC-PCR technique. Reviewing the scientific literature showed that this study is the first of its kind that studied the genetoxicity of *E. foeminea* extracts on prokaryotes using ERICPCR technique. Besides, many plants were previously tested to detect their genotoxicity potential by different techniques (Basaran *et al*., 1996; Lalrotluanga *et al*., 2011; El-Tarras *et al*., 2013; Hajar and Gumgumjee, 2014; Ciğerci et al., 2016; Abu-Hijleh *et al*., 2018). ERIC-PCR profiles showed significant differences between the treated and untreated *E. coli* strain used in this study. The changes in the treated *E. coli* strain with both aqueous and ethanolic aerial parts extracts included the disappearance of certain bands as well as the change in the band intensity in comparison with untreated control. The changes in the profile of the treated *E. coli* strain in comparison with the untreated control samples could be explained due to the effect of the genotoxic molecules that were present in the plant extracts. These molecules can induce different

changes such as breakdown in DNA strands, point mutations and/or rearrangements in chromosomes. These changes in the DNA might have a potential effect on the primer binding sites and/or inter-priming distances (Abu-Hijleh *et al*., 2018). DNA sequencing or probing and other techniques can help in understanding the proposed mechanisms that lead to such differences in ERIC-PCR profiles (Lalrotluanga et al., 2011). Ma-huang is a traditional Chinese medicinal preparation derived from *Ephedra sinica* Stapf and other *Ephedra* species that are used to treat different diseases. Studies on cytotoxity of the ma-huang extracts showed that, cytotoxicity of all ma-huang extracts could not be totally accounted for by their ephedrine contents, suggesting the presence of other toxins in the extracts which may modify its pharmacological and toxicological activities (Lee *et al*., 2000).

5. Conclusion

The results of this study showed that aqueous and ethanolic aerial parts extracts of *E. foeminea* possess genotoxic and mutagenic potential against *E. coli*. In addition, the results also point out the capability of using *E. foeminea* to treat infections caused by *E. coli*. More studies are recommended to reveal the exact molecules that are responsible for *E. foeminea* genotoxicity as well as the mechanisms responsible for that genotoxicity.

Competing Interests

Authors have declared that no competing interests exist.

References

Abu-Hijleh A, Adwan G and Abdat W. 2018. Biochemical and molecular evaluation of the plant *Ecballium elaterium* extract effects on *Escherichia coli*. *J Adv Biol Biotechnol*., **9** (**2**): 1-11.

Adwan G, Adwan K, Jarrar N, Salama Y and Barakat A. 2013. Prevalence of *seg*, *seh* and *sei* genes among clinical and nasal *Staphylococcus aureus* isolates. *Br Microbiol Res J.*, **3**(**2**):139-149.

Al-Khalil S, Alkofahi A, El-Eisawi D and Al-Shibib A. 1998. Transtorine, a new quinoline alkaloid from Ephedra transitoria. *J Nat Prod*., **61**(**2**):262-263.

Al-Rimawi F, Abu-Lafi S, Abbadi J, Alamarneh AAA, Sawahreh RA and Odeh I. 2017. Analysis of phenolic and flavonoids of wild *Ephedra alata* plant extracts by LC/PDA and LC/MS and their antioxidant activity. *Afr J Tradit Complement Altern Med*., **14**(**2**): 130-141.

Amakura Y, Yoshimura M, Yamakami S, Yoshida T, Wakana D, Hyuga M, Hyuga S, Hanawa T and Goda Y.2013. Characterization of phenolic constituents from ephedra herb extract. *Molecules*, **18**(**5**):5326-5334.

Andrews, J. M. 2006. BSAC standardized disc susceptibility testing method (version 5). *J Antimicrob Chemother*., **58**(**3**): 511-529.

Atienzar FA, Venier P, Jha AN and Depledge MH. 2002. Evaluation of the random amplified polymorphic DNA (RAPD) assay for the detection of DNA damage and mutations. *Mutation Research/Genetic Toxicol and Environ Mutagen*., **521**(**1-2**): 151-163.

Basaran AA, Yu TW, Plewa MJ and Anderson D. 1996. An investigation of some Turkish herbal medicines in *Salmonella typhimurium* and in the COMET assay in human lymphocytes. *Teratogen, Carcinogen, and Mutagen*., **16**(**2**):125-138.

Caveney S, Charlet DA, Freitag H, Maier-Stolte M and Starratt AN. 2001. New observations on the secondary chemistry of world Ephedra (Ephedraceae). *Am J Bot*., **88**(**7**):1199-1208.

Ciğerci IH., Cenkci S, Kargıoğlu M and Konuk M. 2016. Genotoxicity of *Thermopsis turcica* on *Allium cepa L.* roots revealed by alkaline comet and random amplified polymorphic DNA assays. *Cytotechnol*., **68**(**4**):829-838.

Clinical and Laboratory Standards Institute (CLSI). 2017. **Performance Standards for Antimicrobial Susceptibility Testing**. 27th ed. CLSI supplement. M100S. Wayne, PA, USA.

Cottiglia F, Bonsignore L, Casu L, Deidda D, Pompei R, Casu M and Floris C. 2005. Phenolic constituents from *Ephedra nebrodensis*. *Nat Prod Res*., **19**(**2**):117-23.

Danin A. 2018. Flora of Israel on line. http://flora.huji.ac.il/browse asp. Accessed (Dec. 10, 2018).

Dehkordi NV, Kachouie MA, Pirbalouti AG, Malekpoor F and Rabei M. 2015.Total phenolic content, antioxidant and antibacterial activities of the extract of *Ephedra procera* fisch. et mey. *Acta Pol Pharm*., **72**(**2**):341-345.

Dosari AS, Amin Norouzi A, Moghadam MT and Satarzadeh N. 2016. Antimicrobial activity *of Ephedra pachyclada* methanol extract on some enteric gram negative bacteria which causes nosocomial infections by agar dilution method. *Zahedan J Res Med Sci.*, **18**(**11**):1-4.

El-Tarras AA, Hassan MM and El-Awady MA. 2013. Evaluation of the genetic effects of the *in vitro* antimicrobial activities of *Rhazya stricta* leaf extract using molecular techniques and scanning electron microscope. *Afr J Biotechnol*., **12**(**21**):3171-3180.

Eberhardt MV, Lee CY and Liu RH 2000. Antioxidant activity of fresh apples. *Nature* **405**:903–904.

Feresin GE, Tapia A, López SN and Zacchino SA. 2001. Antimicrobial activity of plants used in traditional medicine of San Juan province, Argentine. *J Ethnopharmacol.*, **78**(**1**):103-107.

Hajar AS and Gumgumjee NM. 2014. Antimicrobial activities and evaluation of genetic effects of *Moringa peregrina* (forsk) fiori using molecular techniques. *Inter J Plant and Animal Environ Sci.*, **4**(**1**):65-72.

Ibragic S and Sofić E. 2015. Chemical composition of various *Ephedra* species. *Bosn J Basic Med Sci.*, **15**(**3**): 21-27.

Lalrotluanga, Kumar NS and Gurusubramanian G. 2011. Evaluation of the random amplified polymorphic DNA (RAPD) assay for the detection of DNA damage in mosquito larvae treated with plant extracts. *Science Vision*, **11**(**3**): 155-158.

Lee MK, Cheng BW, Che CT and Hsieh DP. 2000. Cyto-toxicity assessment of Ma-huang (*Ephedra*) under different conditions of preparation. *Toxicol Sci*., **56**(**2**):424-430.

Mendelovich M, Shoshan M, Fridlender M, Mazuz M, Namder D, Nallathambi R, Selvaraj G, Kumari P, Ion A, Wininger S, Nasser A, Samara M, Sharvit Y, Kapulnik Y, Dudai N and Koltai H. 2017. Effect of *Ephedra foeminea* active compounds on cell viability and actin structures in cancer cell lines. *J Med Plants Res.*, **11**(**43**): 690-702.

O'Dowd NA, McCauley G, Wilson JAN, Parnell TAK and Kavanaugh D. 1998. *In vitro* culture, micropropagation and the production of ephedrine and other alkaloids. *In*: **Biotechnology in Agriculture and Forestry**; Bajaj YPS. (Ed.), p. 41, Springer, Berlin.

Parsaeimehr A, Sargsyan E and Javidnia K. 2010. A comparative study of the antibacterial, antifungal and antioxidant activity and total content of phenolic compounds of cell cultures and wild plants of three endemic species of *Ephedra*. *Molecules*, **15**(**3**): 1668-1678.

Pirbalouti AG, Azizi S, Amirmohammadi M and Craker L. 2013. Healing effect of hydro-alcoholic extract of *Ephedra pachyclada* Boiss. in experimentally gastric ulcer in rat. *Acta Pol Pharm*., **70** (**6**):1003-1009.

Subscription

Jordan Journal of Biological Sciences

An International Peer – Reviewed Research Journal

Published by the Deanship of Scientific Research, The Hashemite University, Zarqa, Jordan

Name: ..... الاسم:

Specialty: ..... التخصص:

Address: ..... العنوان:

P.O. Box: ..... صندوق البريد:

City &Postal Code:..... المدينة: الرمز البريدي:

Country: ..... الدولة:

Phone: ..... رقم الهاتف

Fax No.: ..... رقم الفاكس:

E-mail: ..... البريد الإلكتروني:

Method of payment: ..... طريقة الدفع:

Amount Enclosed: ..... المبلغ المرفق:

Signature: ..... التوقيع:

Cheque should be paid to Deanship of Research and Graduate Studies – The Hashemite University.

I would like to subscribe to the Journal

For

- ☐ One year
- ☐ Two years
- ☐ Three years

One Year Subscription Rates

	Inside Jordan	Outside Jordan
Individuals	JD10	$70
Students	JD5	$35
Institutions	JD 20	$90

Correspondence

Subscriptions and sales:

The Hashemite University
P.O. Box 330127-Zarqa 13115 – Jordan
Telephone: 00 962 5 3903333
Fax no. : 0096253903349
E. mail: jjbs@hu.edu.jo

المجلة الأردنية للعلوم الحياتية
Jordan Journal of Biological Sciences (JJBS)

http://jjbs.hu.edu.jo

المجلة الأردنية للعلوم الحياتية: مجلة علمية عالمية محكمة ومفهرسة ومصنفة، تصدرعن الجامعة الهاشمية وبدعم من صندوق دعم البحث العلمي والإبتكار – وزراة التعليم العالي والبحث العلمي.

ترسل البحوث الى العنوان التالى:

رئيس تحرير المجلة الأردنية للعلوم الحياتية

الجامعة الهاشمية

ص.ب , 330127 , الزرقاء, 13115 , الأردن

هاتف: 0096253903333

E-mail: jjbs@hu.edu.jo, Website: www.jjbs.hu.edu.jo

المملكة الأردنية الهاشمية

المجلة الأردنية

للعلوم الحياتية

مجلة علمية عالمية محكمة

تصدر بدعم من صندوق دعم البحث العلمي و الابتكار

http://jjbs.hu.edu.jo/